Further Insights into Oscillation Theory

Nikolai Verichev,
Stanislav Verichev
and Vladimir Erofeev

Further Insights into Oscillation Theory

Further Insights into Oscillation Theory

By

Nikolai Verichev, Stanislav Verichev and Vladimir Erofeev

Cambridge Scholars Publishing

Further Insights into Oscillation Theory

By Nikolai Verichev, Stanislav Verichev and Vladimir Erofeev

This book first published 2021

Cambridge Scholars Publishing

Lady Stephenson Library, Newcastle upon Tyne, NE6 2PA, UK

British Library Cataloguing in Publication Data
A catalogue record for this book is available from the British Library

ISBN (10): 1-5275-7167-X
ISBN (13): 978-1-5275-7167-9

TABLE OF CONTENTS

FOREWORD

The history of understanding of the phenomenon of synchronization begins in 1665, with the famous experiment of H. Huygens with a clock hanging on one beam. Observing the course of a wall clock located on a beam, Huygens noticed an extraordinary coherence of the rhythms of their movement, whereas without a common beam, the coherence of the clock's course disappeared. He made the correct conclusion that the reason for this was the beam, which played the role of a coupling, leading to the interaction of objects and, as a consequence, to the coherence of their movements. Unfortunately, it is not known whether the genius scientist and inventor (among his inventions, there is a pendulum clock with a trigger, invented in 1657) realized the global nature of the phenomenon that he observed and its determining role in animate and inanimate nature.

The next benchmark case in the history of synchronisation is the capture of organ tube vibrations by vibrations of the tuning fork (forced synchronisation), which was observed by D. Raleigh (1878), who later constructed the Theory of Sound (1878).

The systematic character of experimental studies of synchronization is acquired only at the beginning of the 20th century resulting from

the origination and rapid development of new areas of engineering knowledge: radio engineering and radiolocation.

The first experimental work on synchronization of triode generators is the work of E. V. Appleton. In 1922, studying the influence of periodic electromotive force (EMF) on the lamp generator, Appleton found forced synchronization of oscillations of this generator. Since then, radio generators have been an extremely convenient tool for experimental research demonstrating not only the phenomenon of synchronization, but also general properties of dynamic systems.

The lack of an adequate mathematical apparatus at the beginning of the 20th century did not allow generalizing numerous experimental results in the form of mathematical models, analysing them and explaining them analytically. Therefore, the essence of synchronization as a purely nonlinear phenomenon has long been considered terra incognita.

With regard to synchronization (and nonlinear physics in general), a revolutionary event was a creation of the qualitative theory of A. Poincaré's differential equations [1] and A. Lyapunov's theory of stability of motion [2]. The combination of these theories served as a basis for the development of all modern nonlinear dynamics, including the theory of synchronization.

Analytical studies of synchronization of periodic oscillations begin with pioneering papers of Van der Pol (1927) [3], A. A. Andronov and A. A. Vitt (1930) [4]. Van der Pol formulated the problem of forced synchronization of a local oscillator in the form of a non-autonomous nonlinear differential equation of the second order, which is nowadays known as the Van der Pol oscillator and became one of the canonical equations of nonlinear dynamics. Van der Pol also proposed an original method to investigate the equation, motivating his actions (averaging) only by physical considerations of the different orders of magnitude (by a small parameter) of changes of the variables: amplitude and phase of oscillations. For a long time, this method and its results were considered at best as “approximate” and “engineering”. These were considered as such by A. A. Andronov and A. A. Vitt, who proposed a solution to the problem based on the Poincaré method, in a more general statement, with a mathematically rigorous justification of all “details” of the study. It was then surprising that in the particular case of cubic nonlinearity (Van der Pol's nonlinearity), the results of these two studies coincided. Nowadays, when the meaning of Van der Pol's intuitive averaging procedures has long been known, one can only be surprised by its ingenious discovery.

Next in terms of importance and chronology are the works of L. I. Mandelshtam and N. D. Papaleksi [5], K. F. Teodorchik [6, 7], W. V. Lyon and H. E. Edgerton [8], L. D. Goldstein [9] and other authors. An exceptional contribution to the theory of synchronization

of various systems was made by A. A. Andronov's colleagues and students: A. A. Vitt, S. E. Khaikin, N. A. Zheleztsov [10, 11], A. G. Mayer [12], N. N. Bautin, E. A. Leontovich [13], Yu. I. Neimark [14], N. V. Butenin, N. A. Fufaev [15] and subsequent generations of this research school.

A defining event in the development of the theory of dynamical systems in general and synchronization theory in particular, was the discovery of H. M. Krylov and N. N. Bogolyubov of the method of averaging (1934) [16]. As a set of theorems and algorithms, this method did not only justify the procedure of Van der Pol (a side result), but also initiated a whole direction of research of invariant manifolds of dynamical systems directly related to the theory of synchronization [17–20].

The exceptional efficiency of the method of the averaging, as well as its relation to the method of point mappings, together with the simplicity of the interpretation of results, have led to the massive appearance of works on various aspects of synchronization of periodic oscillations. Significant contributions to the theory of synchronization of systems with direct couplings, as well as its practical application were made by the works of N. N. Moiseev [21], I. I. Blekhman [22, 23], R. V. Khokhlov [24], G. M. Utkin [25], P. S. Landa [26], L. V. Postnikova and V. I. Korolev [27], V. V. Migulin [28], I. I. Minakova [29], Yu. M. Romanovsky [30], M.F. Dimentberg [31], L. Cesari [32], N. Levinson [33] and many others.

As for the directly related to the synchronization analytical studies of nonlocal bifurcations, the destruction of invariant tori and the formation on this base of chaotic attractors, the works of the Nizhny Novgorod mathematical school of L. P. Shilnikov [34–36] are fundamental in this area.

The above refers to the case of synchronization of directly coupled dynamical systems.

Simultaneously with the beginning of research on synchronization of directly coupled oscillators (generators) in the field of radio communication, a new direction emerged: systems for automatic frequency tuning of one source (tuneable generator) to the frequency of another (“reference”) oscillator: the automatic frequency control system (AFC); and the same sense of the phase-locked loop system (PLL). Together they are called the systems of phase synchronization (SPS).

The first phase-locked loop system was proposed by B.P. Terent'ev in 1930 [37], while the theory of these systems originates from the works of de Belsiz [38], F. Tricomi [39], and C. Travis [40].

At present, none of the means of television and radio communication can do without systems of phase synchronization, as well as none of the means of remote control of complex technical systems. The modern state of the art of systems of phase synchronization technology is due to the work of a large team of international re-

searchers: the list of references is huge and most of it can be found in monographs [41–44].

For the theory of oscillations as a scientific discipline that studies the dynamics of mathematical models common to various areas of natural science, it is important that PSS models are simultaneously mathematical models of a large number of physical systems. These models will be the subject of study in this monograph: dynamical systems of phase or, in other words, pendulum type

$$I\ddot{\varphi}_i + \lambda_i\left(1 + f_{1i}\left(\varphi_i\right)\right)\dot{\varphi}_i + f_{2i}\left(\varphi_i\right) = \gamma_i + F_i\left(\varphi_j, \dot{\varphi}_j, \psi, \mathbf{x}, \dot{\mathbf{x}}\right),$$

$$\dot{\mathbf{x}} = \mathbf{A}\mathbf{x} + \mu\mathbf{X}\left(\mathbf{x}, \boldsymbol{\varphi}, \dot{\boldsymbol{\varphi}}, \psi\right), \tag{F1}$$

$$\dot{\psi} = \omega_0.$$

Here $i,\ j = \overline{1,n},\ \ \varphi_i \in S,\ \ \psi \in S,\ \ \mathbf{x} \in R^m;\ I,\ \lambda_i,\ \gamma_i$ are the constant parameters, $\mathbf{A}$ is $\left(m \times m\right)$ constant stable Hurwitz matrix; $F_i, \mathbf{X}$ are the functions of couplings. All functions entering (F1) are periodic according to the phase variables. The system is defined in a toroidal phase space $G\left(\boldsymbol{\varphi},\ \dot{\boldsymbol{\varphi}},\ \psi,\ \mathbf{x}\right) = T^{n+1} \times R^{n+m}$.

Among the physical systems that have mathematical models that belong to the (F1) class, there are autonomous and non-autonomous systems of coupled superconducting Josephson junctions [45, 46]; systems of coupled Froude pendulums [47]; coupled electrical ma-

chines [13, 48, 49]; vibrational mechanisms for various purposes [22, 50–52]; unbalanced shafts that are flexible to bending and torsion [50, 53, 54] and many other systems. We call equations of the form (F1) *systems of coupled rotators*.

The development of new and adaptation of existing methods to study specific dynamical systems is an independent problem that presents one of the main tasks of the theory of oscillations. It must be said that the priority of this problem was determined by A. A. Andronov at the beginning of the creation of the theory of oscillations as a new scientific direction. As for systems of the class (F1), analytical and qualitative-numerical methods are most developed for the study of limited motions of pendulum systems. They are developed mainly for solving problems of the systems of phase synchronization and problems of automatic control, which is covered by papers of A. I. Lurie [55], E. A. Barbashin, N. N. Krasovsky, V. A. Tabueva [56, 57], V. M. Popov [58], V. A. Yakubovich, A. H. Gelig, G. A. Leonov [42, 59, 60], V. V. Shakhgildyan [41, 61], Yu. N. Bakaeva [62], V. N. Belykh, V. I. Nekorkin [42, 63–65], V. P. Ponomarenko, V. D. Shalfeev, L. A. Belyustina [42, 65, 66] and other authors. In this monograph, an adaptation of the method of the averaging will be proposed for the effective study of synchronization, dynamical chaos in the class of rotational motions of systems of coupled rotators.

Discovery in 1983 of synchronization of chaotic oscillations for identical (Yamada T. and Fujisaka H. [67]) and, independently in 1986, for non-identical self-oscillating systems with chaotic dynamics (V. S. Afraimovich, N. N. Verichev, M. I. Rabinovich [68]) changed the existing to date understanding of the phenomenon of synchronization to a large extent. In contrast to classical synchronization (synchronization of periodic oscillations), due to its prevalence and familiarity seeming almost obvious, chaotic synchronization, on the contrary, seemed unlikely and even impossible. The reason for this is the prevailing belief at that time that the interaction of internally unstable systems can only generate an increase in the instability of a coupled system. However, it turned out that this is not entirely true: as a result of the “interaction of strange attractors”, a new strange attractor (an image of synchronization) can be born, such that the motions of the individual systems, while remaining chaotic, become synchronized when a coupled system moves on this attractor. In the course of studying the chaotic synchronization (1985), it became clear that the very definition of synchronization, which had previously been reduced to the commensurability of frequencies, needs an updating. At that time, it was already clear that chaotic synchronization, unique in its properties, which can be implemented using simple technical solutions (in particular, radio circuits), will find the widest application, which has been confirmed over time.

One of the areas of application of chaotic synchronization is modern information technology. The first experiments on information transmission based on chaotic synchronization were carried out by A. S. Dmitriev, A. I. Panas, and S. O. Starkov [69]; L. Kocarev, K. S. Halle, K. Eckert, L. Chua, U. Parlitz [70]; H. Dedieu, M. Kennedy, M. Hasler [71]. The use of PLL systems in the transmission of information with chaotic signals was investigated by V. V. Matrosov [72].

The attractiveness of the dynamical chaos and chaotic synchronization for the transmission of information is explained by several reasons. First, by the broadband signal of the carrier, and, consequently, by the large information capacity. Second, by the possibility of confidentiality (secrecy) of information transfer. Communication confidentiality is achieved due to the fact that the “reference” signal generator (oscillator), which determines the chaotic carrier of the information signal, can be synchronized only with the signal generator (oscillator) that has analogous dynamics.

Another area of application is modelling of the biological neural tissues and artificial neuron-like networks. Numerous physiological observations of the activity of various parts of the brain show the chaotic nature of their dynamics. It can be such as a reflection of a normal life activity or arise as a result of a crisis state of the object [73, 74]. Therefore, modelling neural networks in the form of interconnected dynamical systems with chaotic dynamics seems plausi-

ble and provides quite adequate results. The number of publications devoted to modelling of such systems is large. Some of them are covered in reviews [75, 76]. Basically, the classical models of Hodgkin – Hasley [77], Fitz Hugh – Nagumo [78], Kolmogorov – Petrovsky – Piskunov [79] and their modifications are chosen as a base of the networks.

Chaotic synchronization is a complex phenomenon, and research into its various aspects is still ongoing. Significant contributions were made by the studies of L. M. Pecora, T. L. Carroll [80], N. F. Rulkov, A. R. Volkovsky [81], P. Ashwin, J. Buescu, I. Stewart [82], S. C. Venkataramani, B. R. Hunt, E. Ott, D. J. Gaunthier, J. S. Bienfang [83, 84], A. S. Pikovsky, J. Kurths [85], V. S. Anischenko [86], etc. Due to the large number of papers, providing a somewhat complete and ordered list of publications is simply impossible. However, despite the large number of studies, the problem of chaotic synchronization remains relevant to this day, and this primarily relates to research methods. Below we describe in detail both the phenomenon itself and its asymptotic theory.

Another area of application of chaotic synchronization is dissipative structures, the study of which was initiated by I. R. Prigogine [87]. Chaotic synchronization adds a new aspect to the development of this trend, which can be expressed by the phrase “ordered chaos from universal chaos”, which in its meaning complements the dictum fixed in the title of the famous monograph by I. Prigogine and

I. Stengers “Order out of chaos” [88]. In lattices of dynamical systems (oscillators), as discrete analogues of an active continuous medium, such structures are called “cluster” structures. In addition to modelling processes in a continuous medium, there is also an independent interest in the study of cluster structures in lattices of oscillators: a large number of objects of animate and inanimate nature have or may have similar structures [89–93].

It should be noted that most of the results of studies of “cluster” dynamics were obtained by computer simulation of systems. Analytical results are not so numerous and mainly refer to isotropic lattices [94–101]. Our interest will be in ordering the theory of cluster structures in oscillator lattices and bringing the mechanisms of their formation in accordance with generally accepted concepts of the phenomenon of synchronization.

CHAPTER 1

OSCILLATORS AND ROTATORS WITH CHAOTIC DYNAMICS

In this chapter, we discuss classical and well-known oscillators with chaotic dynamics, which we will use as subjects of chaotic synchronization to illustrate analytical results. Here we consider autonomous and non-autonomous models with a cylindrical phase space. Interest in such models has two aspects. First, along with oscillators, they are of interest as subjects of synchronization. Secondly, these systems are much less studied and described in the scientific and technical literature, despite being of considerable interest for their applications.

1.1. Oscillators with chaotic dynamics

Lorenz oscillator. In 1963, while studying convection in a layer of liquid heated from below, E. Lorentz presented a visually simple dynamic system of the form

$$\begin{aligned} \dot{x} &= -\sigma(x - y), \\ \dot{y} &= -y + rx - xz, \\ \dot{z} &= -bz + xy. \end{aligned} \tag{1.1}$$

The system describes the dynamics of a fluid in the form of convective rolls. To construct it from the equations of hydrodynamics, the Galerkin method and the Boussinesq approximation [102] were used. The physical meaning of variables and parameters is as follows: x is the velocity of rotation of rolls; y, z is the temperature of the fluid in horizontal and vertical directions, σ is the Prandtl number, r is the normalized Rayleigh number, and b is the convection cell scale parameter. In a numerical study of equations (1.1), E. Lorentz discovered a complex non-periodic behavior of the system, which corresponds to a nontrivial attracting set in the phase space of the model, called the strange attractor or the Lorentz attractor (Fig. 1.1). Subsequently, the chaotic nature of this attractor was proved in [103].

There exist numerous publications devoted to the study of various properties of this system. The derivation of the Lorentz equations from the Navier – Stokes equations, as well as the properties of this system, can be learned from [104 – 108]. Note that in addition to thermal convection in the layer, the Lorentz system also simulates fluid convection in an annular tube, the dynamics of a single-mode laser, and dynamics of a water wheel [106]. As it will be shown below, this system is also related to the dynamics of vibrational

mechanisms, superconductive junctions, as well as bending vibrations of shafts.

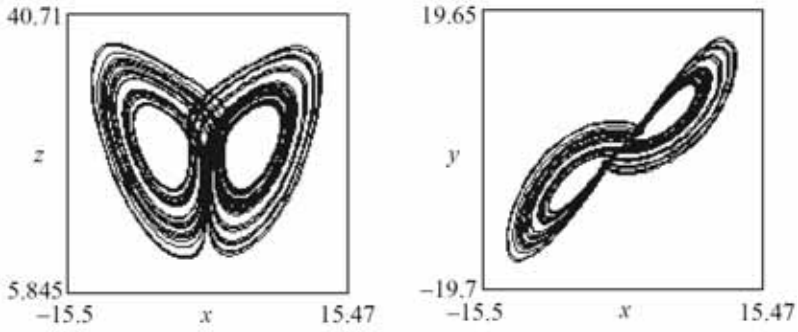

Fig. 1.1. Projections of Lorentz attractor onto coordinate planes for:

$$\sigma = 10,\ r = 25,\ b = 8/3\ .$$

In what follows, let us list certain the properties of the Lorentz system that will be required by us later on.

1. *Dissipativity*. Consider a quadratic form

$$V = \frac{1}{2}\left(x^2 + y^2 + \left(z - \sigma - r\right)^2\right).$$

The derivative of this function, calculated by virtue of system (1.1), has the form

$$\dot{V} = -\sigma x^2 - y^2 - bz^2 + b\left(\sigma + r\right)z$$

and is negative outside the ball $V \le 2(\sigma + r)^2$ (it is assumed that $\sigma > b$). That is, all limit sets of trajectories in the phase space $G(x, y, z)$ of Lorenz system are limited by a dissipation ball. Due to the invariance of the system to a change of the form: $x \to -x$, $y \to -y$, any limit set of trajectories is symmetric with respect to the plane $x = y$ or has a symmetrical "twin".

2. *Equilibria*. In a general case, there exist three equilibria: $O(0, 0, 0)$, $O_1\left(\sqrt{r-1}, \sqrt{r-1}, r-1\right)$ and $O_2\left(-\sqrt{r-1}, -\sqrt{r-1}, r-1\right)$.

a) For $r < 1$, a single equilibrium $O(0, 0, 0)$ is globally asymptotically stable (GAS). This is established using the Lyapunov function

$$V = \frac{1}{2\sigma}x^2 + \frac{1}{2}y^2 + \frac{1}{2}z^2,$$

the derivative of which by virtue of system (1.1)

$$\dot{V} = -x^2 + (r+1)xy - y^2 - bz^2$$

is negative in the entire phase space for $0 < r < 1$.

b) For $r > 1$, equilibrium $O(0, 0, 0)$ represents a saddle with two-dimensional stable and one-dimensional unstable manifolds, $\dim u^s = 2$, $\dim u^u = 1$. For $1 < r < \dfrac{\sigma(\sigma + b + 3)}{\sigma - b - 1}$, equilibria O_1 and

O_2 ("twins") are stable knots or focuses, while for $r > r_c = \frac{\sigma(\sigma + b + 3)}{\sigma - b - 1}$, they represent saddle-focuses with $\dim u^s = 1,\ \dim u^u = 2.$ Loss of stability occurs through the reverse Andronov-Hopf bifurcation ("sticking" into the equilibrium of an unstable limit cycle).

3. For $r = r^* < r_c$, a loop of the saddle separatrix is formed such that for $r = r^* + 0$ a pair of saddle cycles and a strange Lorenz attractor are simultaneously born out of it [103]. For the values $r^* < r < r_c$, either a strange attractor or stable equilibria are realized depending on the initial conditions: the region of "metastable" chaos. For $r > r_c$ (but not too large ones), the chaotic Lorentz attractor is the only attracting limit set of phase trajectories of the system.

4. For large r (for $\sigma = 10,\ b = 8/3,\ r > 300$), a symmetric limit cycle exists in the system. For reduced *r*, this limit cycle loses its stability with the birth of a pair of stable "twin" cycles. With a further decrease of parameter *r*, these cycles undergo a period-doubling cascade with the development of the chaotic Feigenbaum attractor [109] (one of the scenarios).

Generalized Lurie Oscillator. This oscillator describes the dynamics of a nonlinear automatic control system [55] and is governed by differential equations of the form

$$\begin{aligned} \dot{x} &= -f\left(x\right) + \mathbf{a}^T \mathbf{y}, \\ \dot{\mathbf{y}} &= \mathbf{B}\mathbf{y} + \mathbf{b}x. \end{aligned} \tag{1.2}$$

Here $x \in R^1$, $\mathbf{y} = \left(y_1, y_2, ..., y_n\right)^T$, $y_i \in R^1$, $\mathbf{B}$ is the constant stable Hurwitz matrix; **a**, **b** are $\left(n \times 1\right)$ constant vectors.

It must be said that equations (1.2) were not investigated by the author in relation to chaotic dynamics. For this, the system was discovered too early: in 1951. However, at present it represents a generalization of many known models of physical systems with chaotic dynamics.

It is assumed in equations (1.2) that nonlinear function $f\left(x\right)$ is a continuous function and has a form similar to a cubic parabola with three zeros. For this reason, we will assume that the following inequality is fulfilled for all *x*:

$$xf\left(x\right) \geq mx^2 - l, \tag{1.3}$$

where *m*, *l* are some positive constants. The order of their choice will be discussed below. This condition is satisfied for a large number of applied problems (for the case of local oscillators, it is sufficient to recall the form of the current-voltage characteristics (CVC) of tunnel diodes and of other nonlinear active elements).

Of all the properties (1.2), here we point out only the existence of a dissipation ball, and we provide rest of information about the dynamics of the system using an example of another oscillator, which represents a particular case of (1.2).

Let us introduce an auxiliary linear system of the form

$$\dot{\mathbf{u}} = \mathbf{A}\mathbf{u},$$
$$\mathbf{u} = \left(x, \mathbf{y}\right)^T, \quad \mathbf{A} = \begin{pmatrix} -m & \mathbf{a}^T \\ \mathbf{b} & \mathbf{B} \end{pmatrix}. \tag{1.4}$$

With respect to system (1.4), we will assume:

a) equilibrium $\mathbf{u} = 0$ is asymptotically stable;

b) derivative of the Lyapunov function of the form $V = \frac{1}{2}\left(x^2 + \mathbf{y}^T \mathbf{H}\mathbf{y}\right)$, calculated along the trajectories of system (1.4), $\dot{V} = -mx^2 + \left(\mathbf{H}\mathbf{b} + \mathbf{a}\right)^T x\mathbf{y} + \mathbf{y}^T \mathbf{H}\mathbf{B}\mathbf{y} = -Q\left(x, \mathbf{y}\right)$, where $\mathbf{H}$ is a certain positive symmetric matrix, is negative in the entire phase space.

The values of parameter *m* will be chosen as the minimum of those values for which properties of system (1.4) are satisfied. This choice has a simple physical meaning: *m* is the minimum active resistance, replacing the nonlinear element, at which the corresponding linear system acquires the property of absolute stability.

In the language of phase space, such a choice defines a surface without contact for linear system (1.4): $V = \text{const} = V\left(m_{\min}\right)$, which represents the boundary of the dissipation ball of nonlinear system (1.2).

Let us show that under condition (1.3) and conditions of system (1.4), system (1.2) is dissipative.

Consider the following quadratic form: $V = \frac{1}{2}\left(x^2 + \mathbf{y}^T \mathbf{H}\mathbf{y}\right)$. Taking its derivative by virtue of system (1.2) and taking into account inequality (1.3), we obtain the following form and estimate:

$$\dot{V} = -xf\left(x\right) + \left(\mathbf{H}\mathbf{b} + \mathbf{a}\right)^T x\mathbf{y} + \mathbf{y}^T \mathbf{H}\mathbf{B}\mathbf{y} \le -Q\left(x, \mathbf{y}\right) + l.$$

Obviously, the last expression is non-positive outside some ball $x^2 + \left|\mathbf{y}\right|^2 \le r^2$. In turn, the negativity of the derivative outside this ball determines the dissipation ball $x^2 + \mathbf{y}^T \mathbf{H}\mathbf{y} \le R^2$ of system (1.2).

Chua's Oscillator. One of the electric circuit diagrams of a local oscillator of chaotic oscillations, proposed by L. Chua [110], is shown in Fig. 1.2. In this Figure, G^* denotes nonlinear element with current-voltage characteristic $I(V)$.

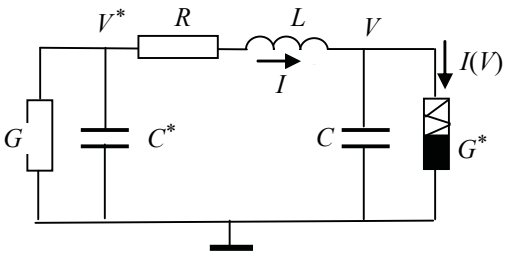

Fig. 1.2. Electric circuit diagram of Chua's oscillator.

This circuit is quite simple as for practical implementation as for a physical experiment. In addition, all the "necessary" properties of this oscillator are found with a piecewise linear volt-ampere characteristic, which makes its mathematical model as simple as possible for analytical research. For these reasons, the dynamics of this local oscillator (and its analogues) has been well studied experimentally, numerically, and analytically [111]. At present, the Chua's oscillator has actually become a classical object of nonlinear dynamics.

In physical variables and parameters, the meaning of which is reflected in Fig. 1.2, the dynamics of the circuit is described by the following equations:

$$C\dot{V} = I - I(V),$$
$$L\dot{I} = -RI + V^* - V,$$
$$C^*\dot{V}^* = -I - GV^*,$$

where $I(V)$ is the volt-ampere characteristic of the nonlinear element with nonlinear conductivity G^*.

By introducing dimensionless time and dimensionless variables and parameters, of the form

$$V = V_0 x,\ I = I_0 y,\ V^* = V_0^* z,\ \frac{R}{L}t = \tau,$$
$$\frac{L}{CR^2} = \alpha,\ \frac{\alpha I(V_0 x)}{I_0} = \alpha h(x),\ \frac{L}{C^* R^2} = \beta,\ \frac{GL}{C^* R} = \gamma,$$

where V_0, I_0, V_0^* are the scale factors, we obtain the following dynamical system:

$$\begin{aligned} \dot{x} &= \alpha\big(y - h(x)\big), \\ \dot{y} &= -y + z - x, \\ \dot{z} &= -\beta y - \gamma z. \end{aligned} \tag{1.5}$$

The idealized volt-ampere characteristic of the nonlinear element has the form

$$h(x) = m_1 x + \frac{m_0 - m_1}{2}\big(|x+1| - |x-1|\big),$$

where m_0, m_1 are the constant parameters. Comparing equations (1.5) with (1.2), we see that the Chua oscillator is a special case of the Lurie oscillator. To pass from (1.5) to (1.2), one should assume that $\mathbf{y} = (y,z)^T$, $f(x) = \alpha h(x)$, $\mathbf{a}^T = (\alpha, 0)$, $\mathbf{B} = \begin{pmatrix} -1 & 1 \\ -\beta & -\gamma \end{pmatrix}$, $\mathbf{b} = (-1,0)^T$.

Fig. 1.3 graphically illustrates the fulfilment of condition (1.3) for the nonlinear function $f(x)=\alpha h(x)$. It follows from the figure that the value of the parameter *m* can also be chosen to be arbitrarily small.

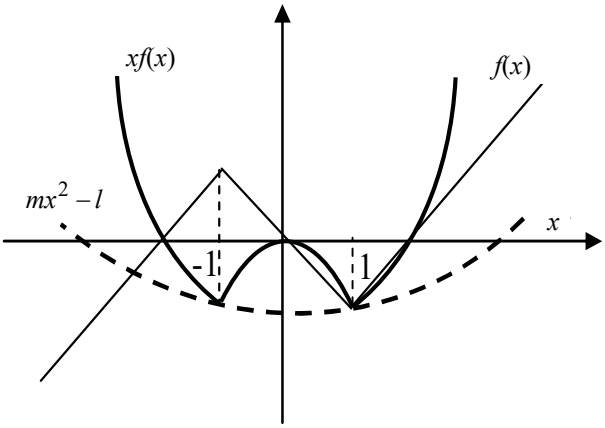

Fig. 1.3. Graphical illustration of the property of a nonlinear function (1.3).

Let us discuss some properties of dynamical system (1.5).

1. *Dissipativity*. Let us show that conditions of system (1.4) are satisfied when its parameters are the parameters of the Chua's oscillator. Let $f(x)=mx.$ In this case, system (1.5) transforms into equations (1.4) and $O(0,0,0)$ is it's only equilibrium. Consider the Lyapunov function of the form $V=\frac{1}{2}x^2+\frac{\alpha}{2}y^2+\frac{\alpha}{2\beta}z^2.$ It's derivative taken along trajectories of system (1.5) has the form

$\dot{V} = -\left(mx^2 + \alpha y^2 + \frac{\alpha\gamma}{\beta} z^2 \right)$. Since the derivative is negative in the entire phase space, the equilibrium $O(0, 0, 0)$ is generally asymptotically stable. In this case $\mathbf{H} = \begin{pmatrix} \alpha & 0 \\ 0 & \alpha/\beta \end{pmatrix}$, and $Q = mx^2 + \alpha y^2 + \frac{\alpha\gamma}{\beta} z^2 \geq 0.$

Let us find a dissipation ball of system (1.5). From Fig. 1.3 and inequality (1.3), we find that maximum $m = \frac{\alpha(m_1 + m_0)}{2}$, wherein $l = \frac{\alpha(m_1 - m_0)}{2}$.

Suppose that $\max(1, \alpha, \alpha/\beta) = \lambda_1$, and $\min(m, \alpha, \alpha\gamma/\beta) = \lambda_2$. In this case $x^2 + \alpha y^2 + \frac{\alpha}{\beta} z^2 \leq \frac{\lambda_1}{\lambda_2} l$ is the dissipation ball.

2. *Equilibria of system (1.5)*. Note that due to oddness of the function $h(x)$, the system is invariant to the change of the variables $x \to -x$, $y \to -y$, $z \to -z$, i.e. possesses central symmetry and all of its limit sets of trajectories inside of the dissipation ball either symmetric with respect to the origin, or have a “twin” symmetric with respect to zero. Naturally, bifurcations of “twins” occur for the same values of parameters.

Depending on the values of parameters, the system has one or three equilibria: $O(0, 0, 0)$, $O_1(x_0, y_0, z_0)$ and $O_2(-x_0, -y_0, -z_0)$ ("twin"), whose coordinates are determined by the equations $f(x) + \left(\mathbf{a}^T \mathbf{B}^{-1} \mathbf{b}\right) x = 0$, $\mathbf{y} = -\mathbf{B}^{-1}\mathbf{b}x$. Solving these equations, we find

$$x_0 = \frac{(\gamma + \beta)(m_1 - m_0)}{\gamma + m_1(\gamma + \beta)}, \quad y_0 = -\frac{\gamma(m_1 - m_0)}{\gamma + m_1(\gamma + \beta)}, \quad z_0 = \frac{\beta(m_1 - m_0)}{\gamma + m_1(\gamma + \beta)}.$$

3. *Bifurcations and chaos*. Let us describe a typical bifurcation scenario when parameter α is varied, while other parameters remain constant.

If $0 < \alpha < \alpha_1$, then equilibrium $O(0, 0, 0)$ is unstable, while equilibria O_1 and O_2 are stable. The value α_1 is determined by the Hurwitz stability conditions. For $\alpha = \alpha_1$, equilibria O_1 and O_2 lose stability with the birth of a limit cycle. Further, the limit cycles undergo a cascade of period-doubling bifurcations with development of two chaotic attractors – "twins" for $\alpha = \alpha_2$ symmetric about the origin (see Fig. 1.4). Parameters of the oscillator are: $(\alpha, \beta, \gamma, m_0, m_1) = (9.0, 14, 0.1, -1/7, 2/7)$.

Attractors have isolated regions of attraction and coexist as independent objects in the interval $\alpha_2 < \alpha < \alpha_3$. For $\alpha = \alpha_3$ the regions of attraction of attractors are merging (so-called crisis of attractors)

and the affix moves on the united attractor, called the double-scroll attractor (see Fig. 1.5). Parameters of the oscillator are: $(\alpha, \beta, \gamma, m_0, m_1) = (9.5, 14, 0.1, -1/7, 2/7)$.

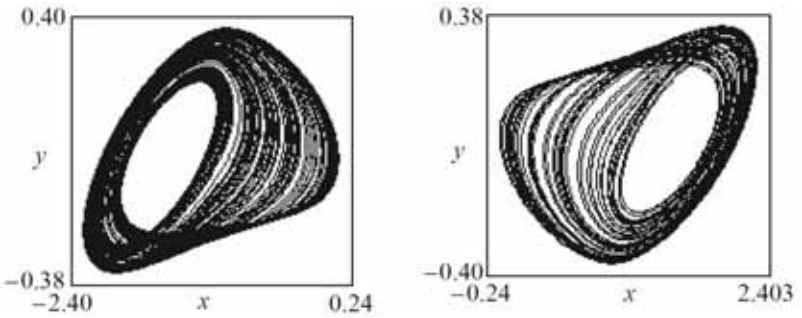

Fig. 1.4. Chaotic attractors - "twins" of the Chua's oscillator.

In the early 1980s, many oscillators with chaotic dynamics have been proposed. The most famous of them is the Kiyashko – Pikovsky – Rabinovich local oscillator [112], whose model can also be reduced to the Lurie oscillator; the Dmitriev – Kislov ring generator [113]; Anishchenko – Astakhov local oscillator with inertial nonlinearity [114], Rössler oscillator [105], etc. With varying degrees of convenience, all of them can also be used for physical or numerical approbation of analytical results that will be discussed in the next sections.

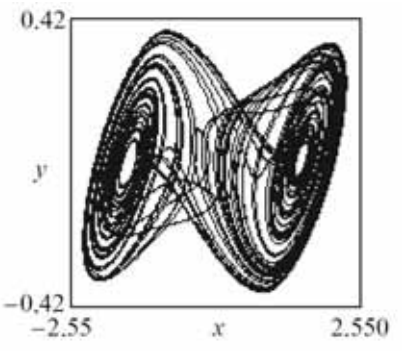

Fig. 1.5. Double-scroll Chua's attractor.

1.2. Synchronization and chaotic rotations of non-autonomous rotator

A non-autonomous rotator is a dynamical system of the form

$$\begin{aligned} &I\ddot{\varphi}+\left(1+F_1(\varphi)\right)\dot{\varphi}+F_2(\varphi)=\gamma+f(\psi),\\ &\dot{\psi}=\omega_0, \end{aligned} \tag{1.6}$$

where $F_1(\varphi)$, $F_2(\varphi)2\pi$ are the periodic functions, $f(\psi)$ is the external periodic excitation (explicit time is "hidden" in the second equation); all functions have zero mean values (the equation is always reducible to this condition); I is the moment of inertia of the rotator, γ is the constant driving moment.

Let us provide examples of physical systems, the dynamics of which is modelled by this dynamical system.

1. Froude pendulum [16] with periodically uneven rotation of the shaft. The pendulum sleeve is mounted on a shaft rotating at variable angular velocity. There is viscous friction between the sleeve and the shaft. The system is shown in Fig. 1.6a.

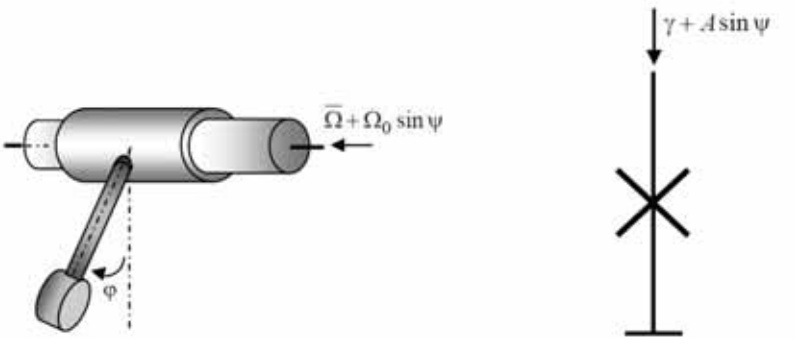

a b

Fig. 1.6. Froude pendulum (a) and schematic representation of a superconductive junction in a microwave field (b).

The equation of motion has the form

$$ml^2\ddot{\varphi} + mgl\sin\varphi = \delta\left(\bar{\Omega} + \Omega_0 \sin\psi - \dot{\varphi}\right),\ \dot{\psi} = \varpi_0,$$

where m, l are the reduced mass and length of the pendulum, δ is the coefficient of viscous friction between the pendulum sleeve and the shaft.

By introducing dimensionless parameters $\frac{m^2 g l^3}{\delta^2} = I$, $\frac{\delta\overline{\Omega}}{mgl} = \gamma$, $\frac{\delta\Omega_0}{mgl} = A$, $\frac{\delta\varpi_0}{mgl} = \omega_0$ and dimensionless time $\frac{mgl}{\delta} t = \tau$, we obtain the form of equations (1.6), where $F_1(\varphi) = 0$, $F_2(\varphi) = \sin\varphi$, $F(\psi) = A\sin\psi$.

2. Superconductive Josephson junction located in a microwave field. This system is shown schematically in Fig. 1.6b. The junction is marked with a cross. Within the framework of the resistive model, using dimensionless variables and parameters [45, 46], the equations of this system have the form (1.6) with functions $F_1(\varphi) = \varepsilon\cos\varphi$, $F_2(\varphi) = \sin\varphi$, $f(\psi) = A\sin\psi$. The physical meaning of variables and parameters is as follows: φ is phase difference of quantum mechanical functions of superconductors, $\dot{\varphi}$ is their potential difference; I is the capacitance of the junction; γ is the constant electric current of the external source; A, ω_0 are the amplitude and frequency of external microwave field.

Dynamical system (1.6) has been investigated for various types of periodic functions by numerical methods in many studies (see, for example, [42, 45, 115] and others). Analytical studies are not so numerous [13, 42, 57, 60, 116, 117], and this “niche” is not fully filled.

For definiteness, we will consider the simplest form of the above nonlinear functions. Here we will provide a brief information on the dynamics of a fully studied autonomous rotator $\left(f\left(\psi\right)=0\right)$ [11, 13, 42, 60], which will be required for us later on.

By changing the time, we transform the equation to the form

$$\ddot{\varphi}+\lambda\left(1+\varepsilon\cos\varphi\right)\dot{\varphi}+\sin\varphi=\gamma, \tag{1.7}$$

where $\lambda=\sqrt{I^{-1}}$, $\left|\varepsilon\right|\le 1$.

Fig. 1.7 shows the bifurcation diagram of parameters of an autonomous rotator. Fig. 1.8 shows phase portraits on the involute of the phase cylinder $\left(\varphi,\dot{\varphi}\right)$ for the parameters of the indicated domains, as well as for the parameters specified on the bifurcation curves. Consider the case of $\left|\varepsilon\right|\le 1$.

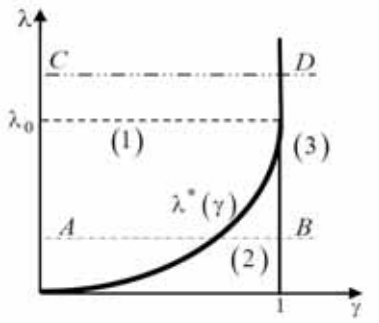

Fig. 1.7. Bifurcation diagram of parameters of an autonomous rotator.

Note that equation (1.6) is invariant under the change of variables $\varphi \to -\varphi,\ \ \gamma \to -\gamma.$ That is, if (1.7) is considered on the whole number line γ, then for completeness of the picture, one should mirror the bifurcation diagram shown in Fig. 1.7 about the axis λ. The phase portraits in the added area will be the same as in Fig. 1.8, if the axes are re-designated as: $\varphi \to -\varphi,\ \ \dot{\varphi} \to -\dot{\varphi}.$

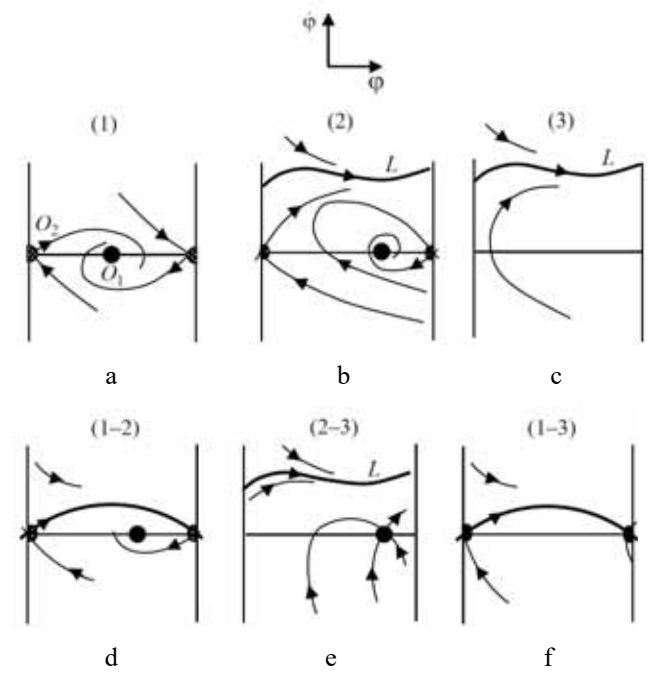

Fig. 1.8. Phase portraits of autonomous rotator on the involute of the phase cylinder.

For $0 < \gamma < 1$, on the phase cylinder $(\varphi, \dot{\varphi})$, there exist two equilibria: stable equilibrium $O_1(\arcsin\gamma, 0)$ and saddle

$O_2\left(\pi - \arcsin\gamma,\, 0\right)$. In domain (1), equilibrium O_1 is globally stable (see Fig. 1.8a). The pendulum reaches the equilibrium for any initial condition. For $\gamma = 1$, equilibria merge to form a saddle-knot (Fig. 1.8e). Equilibria disappear for $\gamma = 1 + 0$. If the equation has a limit cycle, then this cycle enclosing the phase cylinder (sometimes it is called a limit cycle of the second kind) is unique and stable. For $\lambda < \lambda_0$, then the limit cycle is softly (with zero rotation speed) born from a loop of the saddle separatrix (Fig. 1.8d), and for $\lambda > \lambda_0$ it is born from the from the saddle-knot loop (Fig. 1.8f). Bifurcation line of the loop $\lambda = \lambda^*\left(\gamma\right)$ is called the Tricomi curve. For parameters from domain (2), either a stable equilibrium or a stable limit cycle coexist on the phase cylinder that are realized depending on the initial conditions (Fig. 1.8b). For parameters from domain (3), the limit cycle is globally stable (Fig. 1.8c). The rotation speed on the limit cycle increases from zero with increased torque γ, which on the phase cylinder corresponds to its upward motion.

Let us introduce the rotation characteristic of the rotator in the general system (F1) as a dependence of the rotation speed of the rotator on the parameters of the system and its initial conditions. This characteristic will reflect the summary information about the dynamics of the rotator in a coupled system.

Definition 1.2.1. The function $\Omega = \lim\limits_{T\to\infty} \frac{1}{T}\int\limits_0^T \dot{\varphi}(\tau, \tau_0)\, d\tau,$ defined under the parameter space of system (F1) and the space of its initial conditions, is called the rotation characteristic of rotator.

Let us show that $\Omega = \lim\limits_{T^*\to\infty} \frac{1}{T^*}\int\limits_0^{T^*} \dot{\varphi}^*(t, t_0)\, dt,$ where $\dot{\varphi}^*(t,t_0) = \lim\limits_{t\to\infty} \dot{\varphi}(t, t_0)$ is the final solution for $\dot{\varphi}(t, t_0)$.

Any solution of system (A1) for the time derivative of the phase, which represents an instant rotational frequency, can be written in the following form: $\dot{\varphi}(t, t_0) = \tilde{\dot{\varphi}}(t, t_0) + \dot{\varphi}^*(t, t_0),$ where $\tilde{\dot{\varphi}}(t, t_0)$ is a solution that corresponds to the transient process towards the final solution $\dot{\varphi}^*(t, t_0)$. The latter, depending on the initial conditions of the system and its properties, may correspond to equilibria, limit cycles, invariant tori, and chaotic attractors.

Since $\lim\limits_{t\to\infty} \dot{\varphi}(t, t_0) = \dot{\varphi}^*(t, t_0),$ then $\lim\limits_{\tau\to\infty} \tilde{\dot{\varphi}}(t, t_0) = 0.$ According to the above definition, we obtain:

$$\Omega = \lim_{T^*\to\infty} \frac{1}{T^*}\int_0^{T^*} \dot{\varphi}(t,t_0)\, dt = \lim_{T^*\to\infty} \frac{1}{T^*}\int_0^{T^*} \tilde{\dot{\varphi}}(t,t_0)\, dt + \\ + \lim_{T^*\to\infty} \frac{1}{T^*}\int_0^{T^*} \dot{\varphi}^*(t,t_0)\, dt.$$

For simplicity, we assume that stability of the final solution is exponential. At the same time

$$\left\|\tilde{\dot{\varphi}}(t,t_0)\right\| < D\exp(-\lambda t),$$

where D, λ ire the positive constants. Then we obtain:

$$\left\|\lim_{T^*\to\infty}\frac{1}{T^*}\int_0^{T^*}\tilde{\dot{\varphi}}(t,t_0)\,dt\right\| < \lim_{T^*\to\infty}\frac{1}{T^*}\int_0^{T^*}\left\|\tilde{\dot{\varphi}}(t,t_0)\right\|dt <$$

$$< \lim_{T^*\to\infty}\frac{1}{T^*}\int_0^{T^*} D\exp(-\lambda t)\,dt = 0.$$

Which means that

$$\lim_{T^*\to\infty}\frac{1}{T^*}\int_0^{T^*}\tilde{\dot{\varphi}}(t,t_0)\,dt = 0,\ \ \Omega = \lim_{T^*\to\infty}\frac{1}{T^*}\int_0^{T^*}\dot{\varphi}^*(t,t_0)\,dt.$$

In particular if $\dot{\varphi}^*(t,t_0)$ is a periodic solution corresponding to a limit cycle of the second kind, then $\dot{\varphi}^*(t,t_0) = \Omega(\gamma) + R(t)$, where $R(t)$ is a Fourier series with zero mean. As a result, we obtain the speed of rotation of the limit cycle $\Omega = \Omega(\gamma)$.

As one can see, the problem of qualitative study of rotation characteristic is directly related to the classical problem of the theory of

oscillations of splitting the parameter space into areas with qualitatively different trajectory structures in the phase space.

For applied problems, the most interesting is the dependence $\Omega = \Omega(\gamma)$, or the inversed one $\gamma = \gamma(\Omega)$. For the Froude pendulum, this is the dependence of the frequency of rotation of the pendulum on the constant torque, while for a superconductive junction this is the volt-ampere characteristic.

As an example, we will build qualitative forms of rotation characteristic $\gamma = \gamma(\Omega)$ of autonomous rotator in accordance to phase portraits shown in Fig. 1.8.

Suppose that parameter λ corresponds to line *CD* on Fig. 1.7 Let us quasistatically increase parameter γ starting from zero. At all points of domain (1), the equilibrium O_1 is globally stable and therefore $\dot{\varphi}^*(t,t_0) = 0$ for any initial conditions. Rotation characteristic has a vertical section $\Omega = 0, \quad 0 \le \gamma \le 1$ on the plane (Ω, γ) – a "zero step". For $\gamma = 1 + 0$ equilibrium disappears and a limit cycle with the frequency $\Omega = 0 + 0$ is born from the separatrix of the saddle-knot (transition from domain (1) to domain (3), see. Fig. 1.8f). Rotation speed increases from zero as the torque γ increases: the limit cycle moves up on the phase cylinder. The limit cycle corresponds to *L*-branch of rotation characteristic. Bisector $\gamma = \Omega$ is the asymptote of this branch. Due to the invariance of the equation to the change

$\varphi \to -\varphi,\ \ \gamma \to -\gamma$, the same scenario is observed in the lower half-plane (Ω, γ). The complete qualitative form of rotation characteristic is shown in Fig. 1.9a. Let us comment on it.

Suppose that parameter λ corresponds to line *AB* (см. Fig. 1.7). If $\gamma = 0,$ then rotator, starting from any initial condition, in the course of time reaches the sable equilibrium $O_1,$ and at the same time $\Omega = 0.$ For a quasistatic increase of γ, the rotator remains in a stable equilibrium O_1 in the entire interval of its existence by parameter γ: $0 \le \gamma < 1,$ "not noticing" the fact of the birth of the limit cycle, which occurs when $\gamma = \gamma^*.$ For $\gamma = 1 + 0$ (transition from domain (2) into domain (3)) the equilibrium disappears and the rotator jumps into rotation mode – to the limit cycle *L*, the speed of which has already reached the value of $\Omega > 0.$ If γ will keep on growing, the rotator will remain on a stable limit cycle – on the rotational branch of the rotation characteristic. It is obvious that for increased γ, the rotational branch of rotation characteristic has an asymptote $\gamma = \Omega.$

A different scenario is observed when the parameter changes in the opposite direction. For quasi-static reduction of γ, the rotator remains in the rotational regime – on the limit cycle *L* up to its sticking in the loop of the saddle separatrix and turning of its speed to zero. Thus, there is a pronounced hysteretic loop on the rotation

characteristic. A complete qualitative form of the rotation characteristic is shown in Fig. 1.9b.

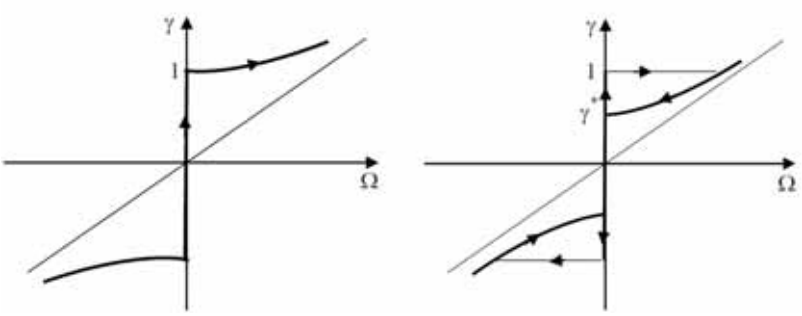

a b

Fig. 1.9. A qualitative form of the rotation characteristic:
a: for variation of γ along *CD*, b: for variation of γ along *AB*.

Let us get back to the non-autonomous rotator. We study its dynamics in the asymptotic case $I^{-1} = \mu \ll 1$. In this case, system (1.6) is quasi-linear and allows application of the method of the averaging. It is known that in the case of a harmonic excitation of a quasi-linear system, only integer harmonic resonances are "strong": $n\omega_0$, with n the integer. The resonance is called "strong" if in the respected parameter domain, the nonlinear properties of a quasi-linear system are realized in the first approximation by a small parameter. Subharmonic resonances are "weak" in this sense.

1) Let us investigate a simple forced synchronization of rotator's rotation (main resonance, $n = 1$) in the case of "moderate" amplitudes of external excitation.

Applying the algorithms for transforming systems of rotators to the standard form [118] (see Appendix), we obtain an equivalent system (1.6) with a fast-spinning phase [20] of the form

$$\begin{aligned}
\dot{\xi} &= \mu\Xi\left(\xi,\varphi,\eta\right),\\
\dot{\eta} &= \mu\Phi\left(\xi,\varphi,\eta\right),\\
\dot{\varphi} &= \omega_0 + \mu\Phi\left(\xi,\varphi,\eta\right),
\end{aligned} \tag{1.8}$$

where $\eta = \varphi - \psi$, $\gamma - \omega_0 = \mu\Delta$ are the phase and the frequency mistunings,

$$\Phi\left(\varphi,\xi\right) = -\varepsilon\sin\varphi + \frac{1}{\omega_0}\cos\varphi - \frac{A}{\omega_0}\cos\psi + \xi,$$

$$\Xi\left(\xi,\varphi,\psi\right) = \Delta - \left(-\varepsilon\sin\varphi + \frac{1}{\omega_0}\cos\varphi - \frac{A}{\omega_0}\cos\psi + \xi\right)\left(1 - \frac{1}{\omega_0}\sin\varphi\right).$$

By averaging system (1.8), we obtain the "truncated" equations:

$$\begin{aligned}
\dot{\xi} &= \mu\left(-\xi + \Delta - \frac{\varepsilon}{2\omega_0} - \frac{A}{2\omega_0^2}\sin\eta\right),\\
\dot{\eta} &= \mu\xi,\\
\dot{\varphi} &= \omega_0 + \mu\xi.
\end{aligned} \tag{1.9}$$

The first two equations in (1.9) are independent of the third one and with respect to the variable η, for a change of time of the form

$\mu\sqrt{\frac{A}{2\omega_0^2}}\tau = \tau_n$ are reduced to the form of equations of the autonomous rotator already known to us:

$$\ddot{\eta} + \lambda_1^r \dot{\eta} + \sin\eta = \gamma_1^r, \tag{1.10}$$

where $\lambda_1^r = \sqrt{\frac{2\omega_0^2}{A}}$, $\gamma_1^r = \left(\Delta - \frac{\varepsilon}{2\omega_0}\right)\frac{2\omega_0^2}{A}$.

Thus, from equation (1.10), we immediately obtain a bifurcation diagram on the plane $\left(\gamma_1^r, \lambda_1^r\right)$ of effective parameters in the main resonance zone (see Fig. 1.10). The fundamental difference between this diagram and the diagram shown in Fig. 1.7 consists in the presence of a "gray" parameter domain (4) located in place of the Tricomi curve (domain (4) is a thick Tricomi curve whose width is $\sim\mu$ In what follows, we explain the appearance of this domain.

To interpret the dynamic properties of system (1.6) in various parameter domains highlighted in Fig. 1.10, let us remind the following fact. If Γ is a the limit set of a certain averaged system with zero characteristic parameters sufficiently separated from the imaginary axis, then for small values of parameter $\mu \in \left(0, \mu^*\right]$ it corresponds to the limit set $\Gamma \times S^1$ of the initial system including the nature of its stability.

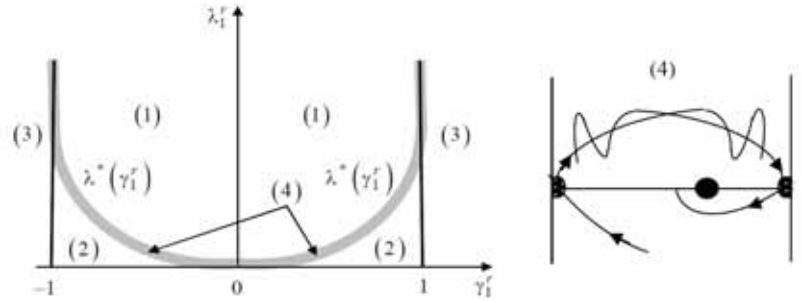

a b

Fig. 1.10. Bifurcation diagram for parameters in the main resonance zone (a) and a homoclinic structure for the domain (4) (b).

In other words, there is a correspondence: an equilibrium in the averaged system corresponds to a limit cycle in the initial system; a limit cycle corresponds to two-dimensional torus, and so on. There is also a topological equivalence of "rough" (structurally stable) phase portraits of the averaged system and structures of discrete trajectories in the space of the Poincaré mapping of the secant plane $\varphi = \text{const}$ into itself through the period of the fast-spinning phase, built for the initial system. In this case, phase portraits shown in Figs. 1.7a-c can be interpreted as portraits of trajectories of the point mapping of the form $(\xi, \eta)_{\varphi} \to (\bar{\xi}, \bar{\eta})_{\varphi+2\pi}$ for system (1.6) [14]. Let us justify the existence of the "gray" domain (4) as a region corresponding to complex limit sets of phase trajectories. First, there is an invariant (non-resonant) torus in domains (2) and (3), but there is no such torus in domain (1). That is, as the parameter γ_1^r

approaches the Tricomi curve of the averaged system, the torus, losing its smoothness, disappears according to one of the scenarios [35]. In most cases, a complex limit set of trajectories is formed in its place. Second, the loop of the averaged system itself cannot be interpreted unambiguously on the initial system. In general, stable and unstable saddle manifolds intersect (Fig. 1.10b), and, as a result, a complex limit set of trajectories – a homoclinic structure [14, 119] arises. In particular, this fact can be established within the framework of the Melnikov criterion [120], considering the second approximation of the averaging method as a perturbation of the truncated system (1.9). Based on the above, one can state that when the parameter is γ_1^r approaches the Tricomi curve of the averaged system from the left-hand side, the resonant torus as a manifold will lose smoothness and collapse, as already noted, with the birth of a nontrivial quasi-hyperbolic set [34, 35]. Thus, there exist three factors to state that instead of the Tricomi curve, there exist domain (4) corresponding to complex limit sets of trajectories of a non-autonomous rotator. Whether these limit sets are chaotic attractors or not will be shown by the numerical experiment.

Rotation characteristic in the zone of resonance. From the definition of rotation characteristic and the change of the variables we obtain

$$\left\langle \dot{\varphi}^* \right\rangle_t = \omega_0 + \left\langle \dot{\eta}^* \right\rangle_t .$$

That is, in its main features, the structure of rotation characteristic in the zone of resonance of parameters is determined by the properties of equation (1.10), and in this way it is similar to the structure of rotation characteristic of the autonomous rotator (see Fig. 1.8). If one would forget about the existence of domain (4), then the "non-autonomous" rotation characteristic in the zone of resonance is, actually, an "autonomous" rotation characteristic shifted along its rotational branch to the point $\Omega = \omega_0$ (Fig. 1.11). The resonance step, for which $\dot{\eta}^* = 0,\ \Omega = \omega_0,$ is determined by inequality $\left|\gamma_1^r\right| \le 1,$ or

$$\omega_0 + \frac{\mu\varepsilon}{2\omega_0} - \mu\frac{A}{2\omega_0^2} \le \gamma \le \omega_0 + \frac{\mu\varepsilon}{2\omega_0} + \mu\frac{A}{2\omega_0^2}.$$

Nevertheless, the presence of domain (4) and, accordingly, of the "gray zones" on the rotation characteristic on both sides of the resonance step is a fundamental property of a non-autonomous rotator. In these areas, the rotation characteristic is infinite-valued and has an extremely complex form. Let us clarify this. We assume that the rotator is in the mode of quasi-periodic beatings and its average rotation frequency $\Omega > \omega_0$ (from the right-hand side from the step). When parameter γ_1^r is decreased and as it "enters" domain (4), the torus loses smoothness with the further birth of a chaotic torus-attractor (in a general case). The rotator switches to the mode of chaotic beatings. The chaotic dynamics is enhanced by "mixing" the aforementioned homoclinic structure with the existing attractor.

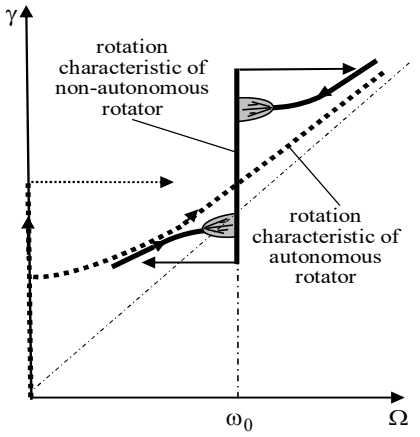

Fig. 1.11. Rotation characteristic of a non-autonomous rotator in the zone of the main resonance.

The same thing happens when approaching the resonance from the left-hand side. We will obtain an understanding of the structure of the rotation characteristic in the "gray" zones if we take into account the following circumstances. First, solution $\dot{\varphi}^*(\tau, \varphi_0)$, which corresponds to a trajectory of the chaotic attractor depends strongly on the initial conditions. This means that when one repeatedly passes through the zone, each time there will be different "branches" of the rotation characteristic. The rotation characteristic in this zone is non-reproducible and contains an infinite number of branches. The presence of natural fluctuations and the finiteness of the averaging time can only increase the effect of rotation characteristics' instability. The described effect is steadily observed in the

dynamics of superconductive junctions and is called the scattering effect of the volt-ampere characteristic [121].

Let's turn to one of the applications of the system under consideration: the dynamics of a superconductive junction in a microwave field. As already noted, the physical meaning of the rotation characteristic is the volt-ampere characteristic of the junction. The presence of a resonance step on the volt-ampere characteristic along with the Josephson ratio is the basis in the idea of a voltage standard design ("standard volt"). The idea is simple. On the one hand, according to the Josephson ratio, $\omega_0 = \frac{2e}{h}V$, where e is the charge of the electron, h is the Planck's constant, ω_0, V are the – generation frequency and potential difference of superconductors. That is, the stability of the frequency of Josephson generation and the stability of the resulting voltage are the same. Ideally, frequency instability can only be related to the instability of an external DC source – of the parameter γ. On the other hand, if the junction is synchronized by a microwave source, the instability of this parameter within a step of current does not affect the stability of the frequency (see Fig. 1.11). In other words, when synchronizing the junction by a microwave source, the voltage stability is determined solely by the stability of the frequency of the microwave source. Of course, dynamical chaos in this system is rather unwanted. However, the need

to know the full picture of the dynamics of the system is also obvious.

2) Now let us consider the dynamics of rotator at large amplitudes of the external excitation $A \sim \mu^{-1} \gg 1$. This case is technically more complicated than the previous case of "moderate" amplitudes. However, in the framework of the method of the averaging, it is possible to study system dynamics in the zone of an arbitrary resonance.

Before applying the known algorithms, let us perform a preliminary transformation of equation (1.6), assuming for simplicity $\varepsilon = 0$.

We make a change of the variables: $\varphi = b\sin(\psi + \psi_0) + \theta$, $\psi + \psi_0 = \psi_n$ (further, subscript n will be omitted), $\psi_0 = \operatorname{arc\,tg}\dfrac{1}{\omega_0 I}$, $b = \dfrac{A}{\omega_0\sqrt{\omega_0^2 I^2 + 1}} \approx \dfrac{A}{\omega_0^2 I}$. As a result, (1.6) reduces to an equivalent equation of the form

$$I\ddot{\theta} + \dot{\theta} + \sin(\theta + b\sin\psi) = \gamma. \tag{1.11}$$

It is known that

$$\sin(\theta + b\sin\psi) = J_0 \sin\theta + \sum_{m=1}^{\infty} J_{2m}\left\{\sin(2m\psi + \theta) - \sin(2m\psi - \theta)\right\} +$$

$$+\sum_{k=0}^{\infty} J_{2k+1}\left\{\sin\left(\left(2k+1\right)\psi+\theta\right)+\sin\left(\left(2k+1\right)\psi-\theta\right)\right\},$$

where $J_l = J_l\left(b\right)$ are the Bessel functions of the first kind with an integer argument.

Now transforming Eq. (1.11) according to the already known rule, we obtain an equivalent system in the standard form:

$$\begin{aligned}
&\dot{\xi} = \mu^{1/2}\left(\gamma - n\omega_0 \pm J_n\left(b\right)\sin\eta\right) - \mu\xi - \mu\xi\frac{\partial\Phi}{\partial\theta} - \mu^{3/2}\left(1+\frac{\partial\Phi}{\partial\theta}\right),\\
&\dot{\theta} = n\omega_0 + \mu^{1/2}\xi + \mu\Phi\left(\theta,\psi\right),\\
&\dot{\psi} = \omega_0.
\end{aligned} \tag{1.12}$$

where notation "+" is used for even numbers n, and "−" for odd numbers, $\eta = \theta - n\psi$.

In this case, an equation that defines function Φ has the form

$$n\omega_0\frac{\partial\Phi}{\partial\theta} + \omega_0\frac{\partial\Phi}{\partial\psi} =$$

$$= -J_0\sin\theta - \sum_{m=1}^{\infty} J_{2m}\left\{\sin\left(2m\psi+\theta\right) - \delta_{n,2m}\sin\left(2m\psi-\theta\right)\right\} -$$

$$-\sum_{k=0}^{\infty} J_{2k+1}\left\{\sin\left(\left(2k+1\right)\psi+\theta\right) + \delta_{n,2k+1}\sin\left(\left(2k+1\right)\psi-\theta\right)\right\}, \tag{1.13}$$

where $\delta_{n,l}=1,$ for $n\neq l,$ and $\delta_{n,l}=0,$ for $n=l.$

By introducing a phase mistuning $\eta=\theta-n\psi$ and averaging system (1.13) up to terms of the order of $\sim\mu$, we obtain the following averaged system:

$$\begin{aligned}\dot{\xi}&=\mu^{1/2}\left(\gamma-n\omega_0\pm J_n(b)\sin\eta\right)-\mu\xi,\\ \dot{\eta}&=\mu^{1/2}\xi,\\ \dot{\theta}&=n\omega_0+\mu^{1/2}\xi.\end{aligned}$$

Implementing a time change $\sqrt{\mu\left|J_n(b)\right|}\,\tau=\tau_n$, we reduce the first two equations of this system to the already known equation:

$$\ddot{\eta}+\lambda_n^r\dot{\eta}\pm\sin\eta=\gamma_n^r, \tag{1.14}$$

where $\lambda_n^r=\sqrt{\dfrac{\mu}{\left|J_n(b)\right|}},\ \gamma_n^r=\dfrac{\gamma-n\omega_0}{\left|J_n(b)\right|}.$

Note that signs in front of function (1.14) are not of fundamental importance. If necessary, one could remove the sign "–" by applying transformation $\eta\to\eta+\pi.$ There is an interesting fact regarding Eq. (1.18): if one would forget that A in this equation is a "large" parameter, then the argument of the Bessel function is sufficiently small and $J_1\left(\dfrac{A}{\omega_0^2 I}\right)\approx\dfrac{A}{2\omega_0^2 I}.$ In this case, Eq. (1.14) turns into Eq.

(1.10). This can be considered as another “miracle of a small parameter”, when a result that has been obtained under certain conditions remains valid for other conditions.

Let us analyse Eq. (1.14). In a general case, for large amplitudes of the external excitation, all the harmonic resonances of the quasilinear rotator are essential. The magnitude of the resonance steps equals $2\left|J_n(b)\right|$. Neighbouring resonance steps on the rotation characteristic can overlap. The overlap value of adjacent resonances $\delta\gamma$ is defined by inequality $(n+1)\omega_0 - \left|J_{n+1}(b)\right| < \delta\gamma < n\omega_0 + \left|J_n(b)\right|$. In this interval, one or another resonance is realized depending on the initial conditions of the system. From this inequality and from the properties of the Bessel functions [122]], it follows that there is no overlap of the resonances for $\omega_0 > 1.2$, and if ω_0 is sufficiently small, then the overlap occurs not only for the neighbouring resonances. Fig. 1.12 exemplifies graphs of several Bessel functions.

It follows from the properties of these functions that hysteretic properties of the rotation characteristic strongly appearing for small n disappear as soon as the number of resonance is increased. A transition to the non-hysteretic rotation characteristics may be non-monotonous. Finally, for the values of amplitudes that correspond to the roots of equation $J_n(b) = 0$, resonance with number n is

just absent. In particular, the main resonance is absent for $A = \nu\omega_0^2 I, \quad \nu \approx 3.9; 7.0; 10.2; \ldots$. For the second resonance $\nu \approx 5.2; 8.4; \ldots$. Thus, by changing the parameter b we can obtain a long gallery of different rotation characteristics with different combinations of values of resonance steps.

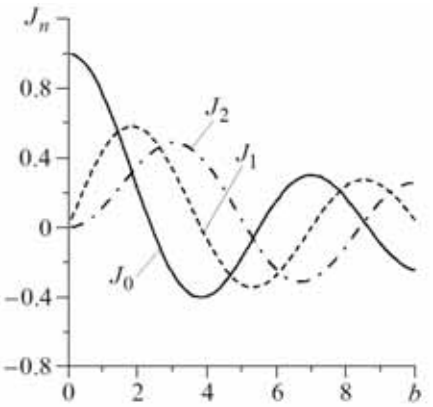

Fig. 1.12. Graphs of Bessel functions.

Fig. 1.13 shows a qualitative example of the rotation characteristic of non-autonomous rotator for high amplitudes of the external excitation (subharmonic resonances are not shown). Rotation characteristic in the vicinity of resonance steps (gray zones) has the same features as described in paragraph 1.

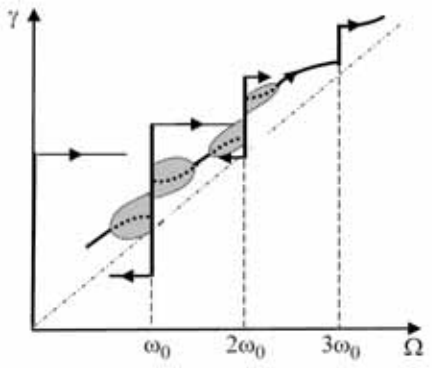

Fig. 1.13. Rotation characteristic of non-autonomous rotator, a "devil's" stairway of resonances. Subharmonic resonances are not shown here.

As an illustration of the analytical results, in what follows, we present results of a *numerical experiment*. For simplicity, we assume that $F_1(\varphi) \equiv 0$. The values of parameters are: $\mu = 0.2$, $A = 3.5$, $\omega_0 = 0.75$. Parameter γ has been varied from the right-hand side to the left-hand side in the interval [1.1177; 1.8248], covering two resonance zones. For simplicity, system (1.6) was written in the form

$$\begin{aligned} \dot{\varphi} &= \gamma + x, \\ \dot{x} &= \mu\left(-x - \sin\varphi + A\sin\psi\right), \\ \dot{\psi} &= \omega_0. \end{aligned} \tag{1.15}$$

Figure 1.14 shows the gallery of projections of trajectories of system (1.19) onto the involute of phase cylinder (bold lines) as well as

trajectories of Poincaré mapping $(\varphi,\xi)_{\psi=\psi_0} \to (\bar{\varphi},\bar{\xi})_{\psi=\psi_0+2\pi}$, constructed for this system (dotted lines).

Starting with $\gamma = 1.8248$ we start to decrease this parameter. Physically, it corresponds to the decrease in torque of the pendulum. For the initial parameter value, the pendulum performs quasi-periodic rotations, whose image is an ergodic torus. This dynamical regime is realized for arbitrary initial conditions (it is globally stable). Fig. 1.14a shows quasi-periodic winding of this torus, while Fig. 1.14b shows invariant curve of the Poincaré mapping (compare to Fig. 1.14c). During the decrease of parameter γ, a subharmonic resonance with rotation number of 11/5 arises on the torus (stable and unstable limit cycles, see Fig. 1.14c). The value of a corresponding resonance step is very small (for this reason, such resonances cannot be "caught" using the method of the averaging). Further, limit cycles move closer to each other and disappear. A new ergodic torus is then formed. In the space of the Poincaré mapping, the scenario of merging of limit cycles is almost the same as a scenario of merging of equilibria with further origination of a limit cycle from the separatrix loop of saddle-knot in the phase space of the autonomous pendulum. The only difference is: before the merging of limit cycles, the "old" torus (as a manifold) loses its smoothness. During such loss of smoothness, an origination of a chaotic attractor may occur. In our case, this effect is so weak that it is almost invisible. At least, the interval of existence of such attractor by parameter γ is

negligibly small. Fig. 1.14d shows a projection of this torus, while Fig. 1.14e shows an invariant curve of the Poincaré mapping. Dark areas shown in this figure correspond to the thickening of trajectories, which represents an inheritance of the disappeared limit cycle. Further, a new fractional resonance with rotation number 15/7 arises at the appeared torus and disappears according to the same scenario. Such scenario is repeated over and over until the rotator jumps from one of such fractional resonances (at the moment of its disappearance) to the resonance with the rotation number of 2, i.e. to the regime of harmonic synchronization (see Fig. 1.14f).

In this case, the chaotic limit set of trajectories from the gray parameter domain is either not an attractor, or the width of this zone is too small. In our experiment, the value of the second harmonic step equals $\delta_2(\gamma) = 0.32$. Just to compare: $b = \dfrac{A}{\omega_0\sqrt{\omega_0^2 I^2 + 1}} = 1.2024,$

$$\delta_2(\gamma) = 2\left|J_2(b)\right| = 2J_2(1.2024) = 0.3198.$$

For $\gamma = 1.35$ the rotator suddenly jumps from the resonance step to the regime of chaotic rotations. At this time, the chaotic attractor is already formed (see Fig. 1.14g). Figure1.14g shows a small time interval of trajectories, since otherwise trajectories would not be distinguishable and the whole square area of a graph would be completely black.

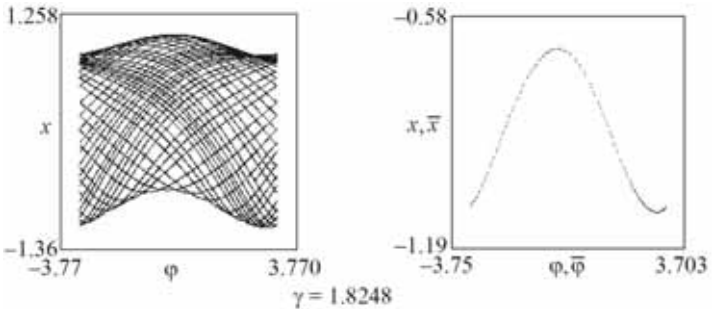

a b

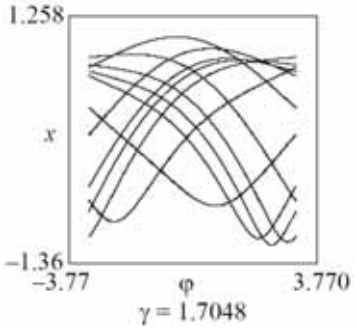

c

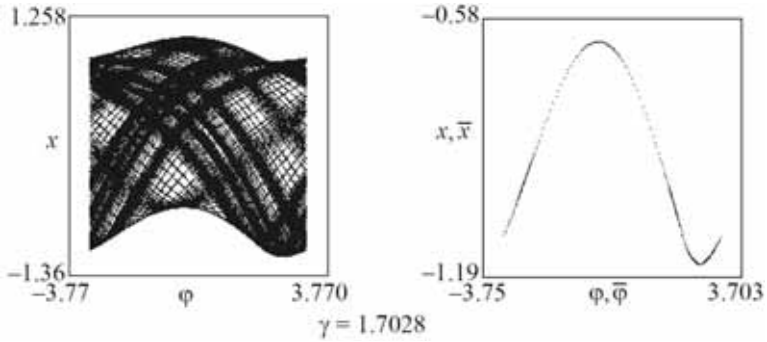

d e

Fig. 1.14. The gallery of qualitatively different phase portraits and Poincaré mappings (continues on pp. 43 – 45).

At the Poincaré plane, there is a torus with a “fold” and “appendices” (see Fig. 1.14h) that indicates a chaotic character of the motion. To clarify types of bifurcations that lead to chaos, parameter γ has been increased with a smaller step. It has been found that the chaotic attractor originates according to the following scenario: “subharmonic resonance at torus $\rightarrow$ torus loses smoothness $\rightarrow$ doubling of the period of stable resonance limit cycle $\rightarrow$ strange attractor” [35].

With further decrease of parameter γ, a stable limit cycle (subharmonic resonance with rotation number 5/3) originates at the chaotic attractor (internal bifurcation, see Fig. 1.14i). Further, as the parameter moves in the gray zone, this resonance experiences a cascade of period doubling with further formation of the Feigenbaum attractor. Fig. 1.14p shows a small interval of phase trajectories, while Fig. 1.14q shows Poincaré mapping. There is an ambiguous branch in the right bottom corner. Further, a chaotic attractor related to homoclinic trajectories of saddle resonance limit cycle (with rotation number 1/1) is mixed with this attractor. A “splash” in the chaotic state of rotations occurs (see Figs. 1.14r,s). Further, the frequency of rotation of the rotator jumps to the value $\Omega = \omega_0 = 0.75$ which means a jump to the regime of simple synchronization (see Figure 1.14t).

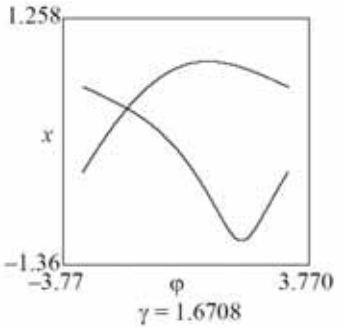

f

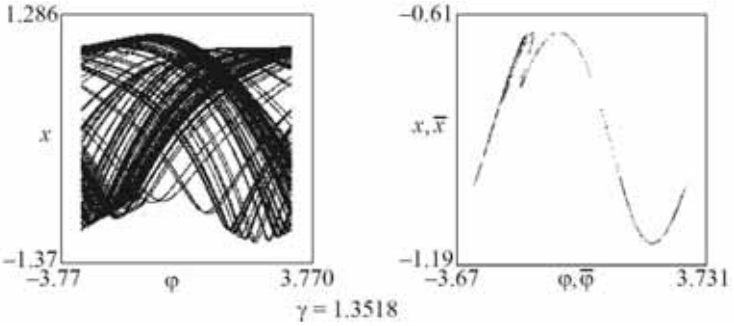

g h

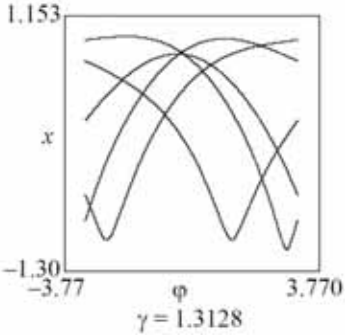

i

Fig. 1.14. Continuation.

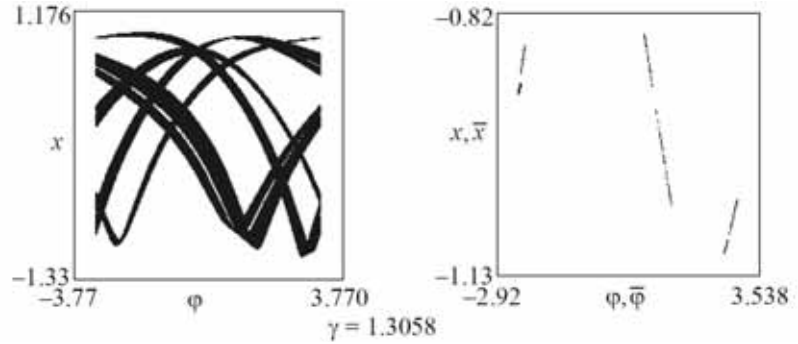

j k

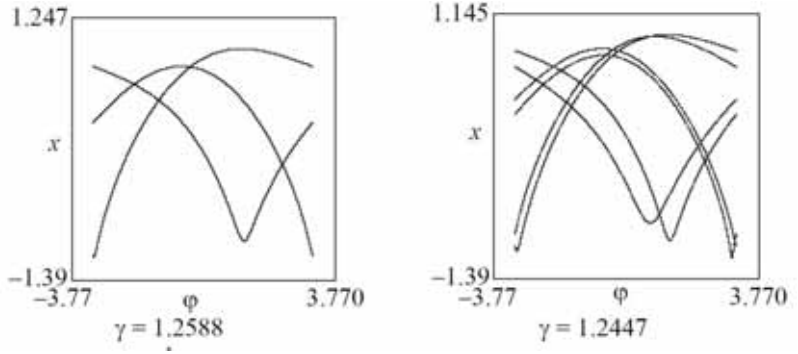

l m

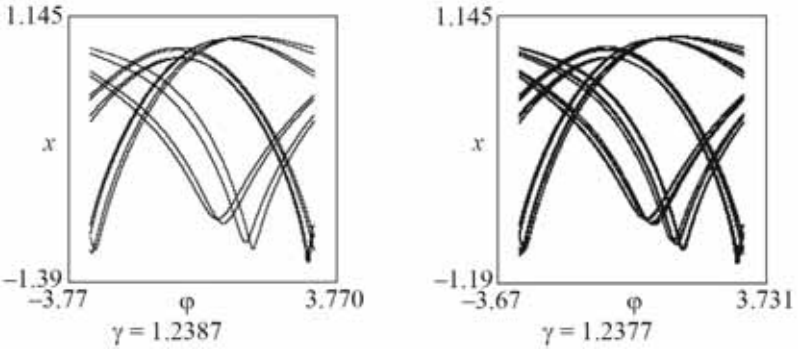

n o

Fig. 1.14. Continuation.

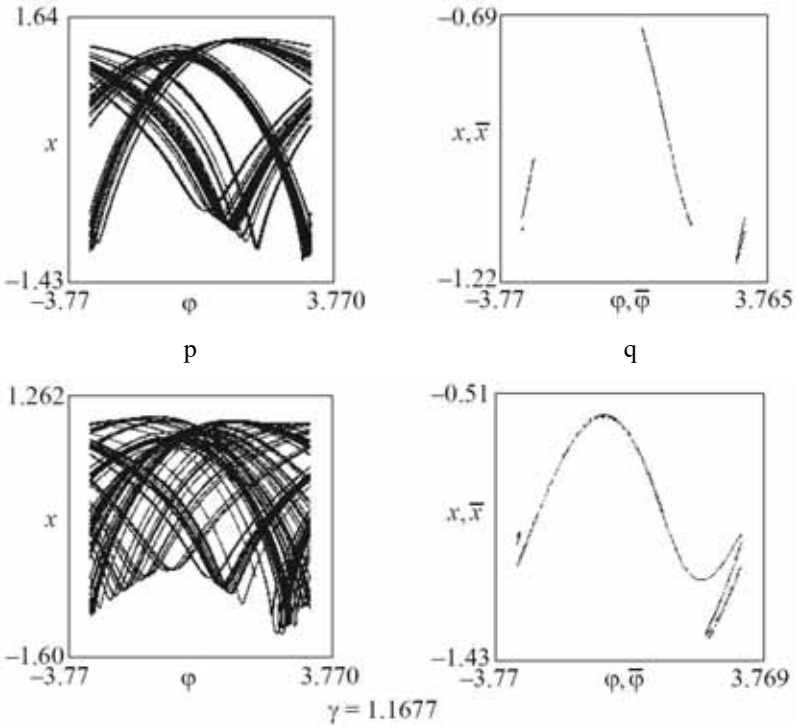

p q

r s

t

Fig. 1.14. Conclusion.

1.3. Dynamics of rotator with aperiodic link

The "rotator with an aperiodic link" is a dynamic system of the form

$$\begin{aligned} &I\ddot{\varphi}+\dot{\varphi}+\sin\varphi=\gamma+J,\\ &\dot{J}+hJ=a\dot{\varphi}+b\left(\sin\varphi-\gamma\right), \end{aligned} \tag{1.16}$$

defined in the cylindrical phase space $G\left(\varphi,\dot{\varphi},J\right)=S^1\times R^2$.

Let us list examples of physical systems modelled by this dynamical system.

1. Froude pendulum with an internal movable sleeve [123]. Fig. 1.15 shows a cross-section of the Froude pendulum by the plane passing through the shaft axis and the centre of the pendulum disk. The sleeve of the pendulum has an additional internal sleeve, which is movable relative to the shaft and the outer sleeve. There is viscous damping in between the sleeves just as in between the shaft and the external sleeve. The shaft rotates with a constant angular speed. The moment of the friction force acting out of the shaft and towards the pendulum has the form $\delta_1\left(\Omega-\dot{\varphi}\right)$. The moment of the friction force acting from the internal sleeve has the form $\delta_2\left(\omega-\dot{\varphi}\right)$, where ω is its instant angular speed. The moment of the gravity force has the form $mgl\sin\varphi$. The moment of the friction force acting from the shaft towards the internal sleeve has the form

$\delta_3(\Omega-\omega)$, while that acting from the external sleeve has the form $\delta_2(\dot{\varphi}-\omega)$. Parameters $\delta_1, \delta_2, \delta_3$ are the constant parameters. The governing equations have the form

$$I_1\ddot{\varphi} = \delta_1(\Omega-\dot{\varphi}) + \delta_2(\omega-\dot{\varphi}) - mgl\sin\varphi,$$
$$I_2\dot{\omega} = \delta_3(\Omega-\omega) - \delta_2(\omega-\dot{\varphi}),$$

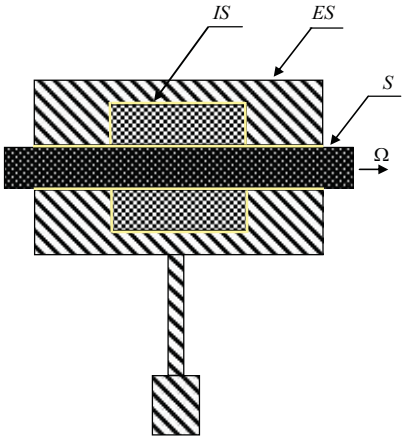

Fig. 1.15. Cross-section of the Froude pendulum with extra internal sleeve. ES is the external sleeve, IS is the internal sleeve, and S is the shaft.

where I_1, I_2 are the normalized moment of inertia of the pendulum and moment of inertia of the internal sleeve, respectively.

Using the transformation of variable $J = \frac{\delta_2}{mgl}(\omega-\dot{\varphi}) - \frac{\delta_2\delta_3}{mgl(\delta_2+\delta_3)}\Omega$ and time $\frac{mgl}{\delta_1}\tau = \tau_n$, we reduce these equations to the form (1.16), with

$$I=\frac{I_1 mgl}{\delta_1^2},\ \ \gamma=\frac{\Omega}{mgl}\left(\frac{\delta_1\delta_2+\delta_1\delta_3+\delta_2\delta_3}{\delta_2+\delta_3}\right),\ \ h=\frac{\delta_1}{mgl}\left(\frac{\delta_1+\delta_2}{I_2}+\frac{\delta_2}{I_1}\right),$$

$$a=\frac{\delta_2}{mgl}\left(\frac{\delta_1}{I_1}-\frac{\delta_3}{I_2}\right),\ \ b=\frac{\delta_1\delta_2}{I_1 mgl}.$$

2. Consider one more system: an asynchronous electric motor of finite power is coupled to an elastic shaft with a rigidly coupled unbalanced disk (see Figure 1.16) [124]. An inertial sleeve is placed over the shaft. There is viscous damping in between the shaft and the sleeve. The latter cannot move along the shaft. Note that such a coupling can play the role of a motor speed stabilizer: when the operational speed of rotation fluctuates towards higher values, the sleeve starts consuming energy of the motor, while for an opposite fluctuation, a part of kinetic energy of the sleeve is transmitted to the shaft. The balancing sleeve plays a role of an integrator (averaging component), which is analogous to properties of a frequency filter in electric engineering.

Let us assume that torque is a linear function of the form $M_d=M_0-\lambda\dot{\varphi},$ where $M_0=\text{const},$ $\lambda\dot{\varphi}$ is the normalized moment of friction forces. Moments that act on the rotor: $mg\varepsilon\sin\varphi$ is the moment of the gravity force of the unbalanced mass, where ε is the eccentricity; $\delta\left(\omega-\dot{\varphi}\right)$ is the moment of forces of viscous damping acting from the sleeve. The moment that acts on the sleeve from the

shaft has the form $-\delta(\omega-\dot{\varphi})$. In this case, the governing equations take the form

$$\begin{aligned} I_1\ddot{\varphi} &= M_0 - \lambda\dot{\varphi} + \delta(\omega-\dot{\varphi}) - mg\varepsilon\sin\varphi, \\ I_2\dot{\omega} &= -\delta(\omega-\dot{\varphi}), \end{aligned} \tag{1.17}$$

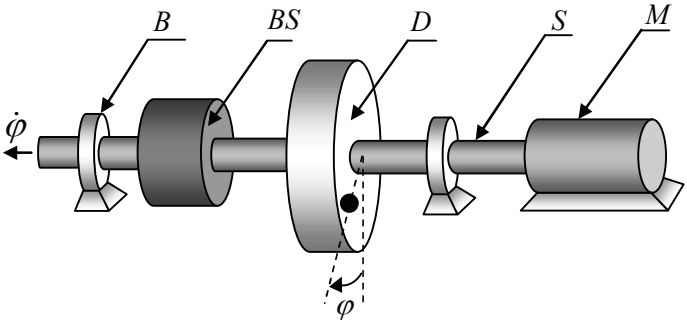

Fig. 1.16. Asynchronous electric motor with unbalanced disk and balancing sleeve. M is the motor, D is the disk, BS is the balancing sleeve, S is the shaft, and B is the bearing.

where I_1, I_2 are the normalized moment of inertia of the pendulum and moment of inertia of the internal sleeve, respectively; λ, δ are the coefficients of viscous damping.

Using the transformation of variable $\frac{\delta}{mg\varepsilon}\omega = J$ and time $\frac{mg\varepsilon}{\lambda+\delta}\tau = \tau_n$ equations (1.17) are reduced to system (1.16) with the following parameters:

$$I = \frac{I_1 mg\varepsilon}{(\lambda+\delta)^2},\ \gamma = \frac{M_0}{mg\varepsilon},\ h = \frac{\delta(\lambda+\delta)}{I_2 mg\varepsilon},\ a = \frac{\delta^2}{I_2 mg\varepsilon}.$$

3. Fig. 1.17a shows a scheme of a superconductive quantum interferometer (R-SQUID), which is used for the measurement of extra-small magnetic fields [45, 46]. Fig. 1.17b shows Its equivalent electric scheme.

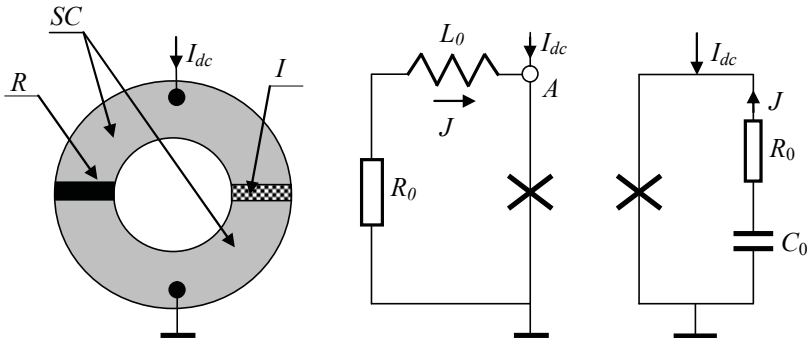

Fig. 1.17. Superconductive quantum interferometer R-SQUID:
a: a scheme of the R-SQUID, where R is the resistor,
SC are the superconductors, I is the isolator; b: equivalent electric scheme;
c: superconductive junction loaded by RC-chain.

We obtain a dynamical model of this system using the Josephson relation and Kirchhoff laws. For dimensionless variables and parameters, the governing equations have the form:

$$C\ddot{\varphi} + \dot{\varphi} + \sin\varphi = \gamma + J,$$
$$\dot{J} + hJ = a\dot{\varphi},$$

where $\frac{I_{dc}}{I_c} = \gamma;\ \frac{r}{l} = h;\ -\frac{1}{l} = a; r, l$ are the dimensionless resistance and inductance of the ring, respectively, C is the capacitance of the junction.

The first equation is obtained from the equations for currents at node A. The second one comes from the equality of voltages at the RL-chain and superconductive junction. One can see that the equations of the aforementioned systems coincide accurate within designations and physical sense of the variables.

You can make sure that the dynamics of the circuit with a superconductive junction shown in Fig. 1.17 is also described by the model (1.16). Note that again there is a dynamic analogy of quantum and mechanical systems.

Let us consider the *dynamical properties* of system (1.16).

This system has two equilibria $O\left(\varphi_0, \dot{\varphi}_0, J_0\right)$: $O_1\left(\arcsin\gamma, 0, 0\right)$ and $O_2\left(\pi - \arcsin\gamma, 0, 0\right)$. Depending on the parameters of the system, equilibrium O_1 is stable throughout the entire domain of existence and is either a knot or a focus. Equilibrium O_2 can either rep-

resent a saddle-knot or a saddle-focus, for which $\dim W^s = 2$, $\dim W^u = 1$, and W^s, W^u are its stable and unstable manifolds.

Oscillatory phase trajectories (bounded by φ) do not exist in the phase space $G(\varphi, \dot{\varphi}, J)$. In particular, if $Ib(h-a)+b-a>0$, (which is valid for the systems under consideration), then this fact can be proven with the help of the periodic Lyapunov function of the form:

$$V = \frac{Ib(h-a)+b-a}{2} I\dot{\varphi}^2 +$$

$$+ \frac{1}{2}J^2 + bI\dot{\varphi}J + \left(b + bhI - a - b^2 I\right) \int_{\varphi_0}^{\varphi} (\sin\varphi - \gamma) d\varphi.$$

Its derivative, taken along the trajectories of system (1.16), has the form

$$\dot{V} = -\left(Ib(h-a)+b-a\right)\dot{\varphi}^2 - (h-b)J^2 \le 0$$

and remains negative in the whole phase space.

Thus, stationary oscillatory motions (oscillatory limit cycles) cannot exist in the system under consideration. Physically, it means that during the change of initial conditions, the Froude pendulum (see Fig. 1.15) and unbalanced disk (see Fig. 1.16) in the course of time reach either equilibrium or a rotary dynamical regime, but never in the oscillatory regime in the vicinity of the equilibrium.

Consequently, the Josephson junction in the course of time enters either a superconductive state or a generation regime. Rotary limit cycles can originate from the separatrix loop of a saddle via bifurcation of a doubled limit cycle that can appear due to the thickening of phase trajectories.

Let us consider structures of rotary trajectories in more detail. Excluding variable J and using the transformation of time, we reduce system (1.16) to the equivalent equation of the third order

$$\beta\dddot{\varphi}+\ddot{\varphi}+\left(\lambda+\alpha\cos\varphi\right)\dot{\varphi}+\sin\varphi=\gamma, \tag{1.18}$$

where $\beta=\sqrt{\dfrac{I^2\left(h-b\right)}{\left(1+hI\right)^3}}$, $\alpha=\dfrac{1}{\sqrt{\left(h-b\right)\left(1+hI\right)}}$, $\lambda=\dfrac{h-a}{\sqrt{\left(h-b\right)\left(1+hI\right)}}$.

First of all, one can note that when $\beta=0$, then Eq. (1.18) is the equation of an autonomous rotator, the dynamics of which is partially described in the previous section. To add to the already known information, we consider the case $\alpha/\lambda>1$ [13, 64]. Under this condition, on the known bifurcation diagram (see Fig. 1.17) there is an extra curve $\lambda=\lambda^0\left(\gamma\right)$ multiple (double) limit cycle (of the second kind) (Fig. 1.18a). This curve together with the Tricomi curve defines area (4). The qualitative structure of the trajectories on the involute of the phase cylinder for parameters defined inside of this area is shown in Fig. 1.18b. The intersection point of the

curves corresponds to the zero saddle value $\sigma_s = \lambda - \alpha\sqrt{1-\gamma^2}$ of equilibrium O_2. below this point $\sigma_s > 0$, while above this point $\sigma_s < 0$.

Asymptotic properties of system (1.16). Let us rewrite this system in a following form

$$\begin{aligned} &\dot{\varphi} = y, \\ &I\dot{y} = -y - \sin\varphi + \gamma + J, \\ &\dot{J} + hJ = a\dot{\varphi} + b\left(\sin\varphi - \gamma\right). \end{aligned} \tag{1.19}$$

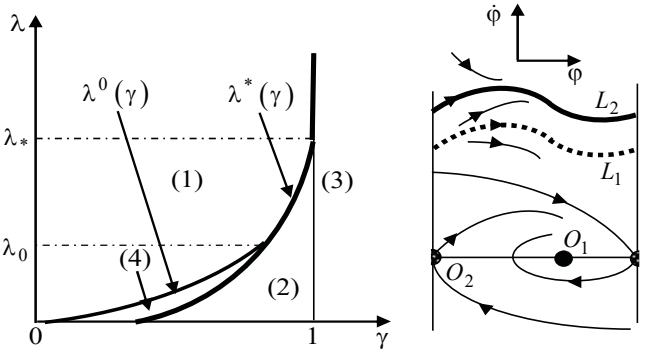

a b

Fig. 1.18. Bifurcation diagram in the case of regular dynamics (a) and two dimensional analogue of the phase portrait for the parameters that belong to domain (4) (b).

If $0 < I \ll 1$ $\left(0 < \beta \ll 1\right)$, then (1.19) is a singularly perturbed system. According to [18] in the interval $I \in \left(0, I^*\right]$ $\left(\beta \in \left(0, \beta^*\right]\right)$ it has a stable integral manifold – the surface of slow motions, which in the zero approximation has the form $y = -\sin\varphi + \gamma + J$. This cylinder is filled with the phase trajectories of equation of the two-dimensional autonomous rotator. In the zero approximation, its equation is equation (1.18) for $\beta = 0$ $\left(I = 0\right)$. Thus, for small β the trajectory structures shown in Fig. 1.8 and in Fig. 1.18b, are two-dimensional analogues of the trajectory structures of equation (1.18) for the respective parameter domains.

To illustrate other properties of equation (1.18), let us turn to research [63, 64]. Consider the case $\alpha > \beta$, corresponding to the aforementioned examples of physical systems. Under this condition, two qualitatively different cases of decomposition of the parameter space are possible: the first one is already described above (see Fig. 1.18), while the second one is shown in Fig. 1.19. The peculiarity of the second case is the existence of a region (5) on the bifurcation diagram. This "gray" region is associated with the bifurcation of the separatrix loop of the saddle-focus and, as a consequence, with the existence of a complex limit set of trajectories associated with the loop containing a countable set of saddle limit cycles [125]. In practice, this is the area of possible strange attractors.

Let us clarify: for parameters that belong to the Tricomi curve below the gray area, the equilibrium O_2 is a saddle with a saddle value of $\sigma_s > 0$. According to [64, 125], in this case, a single unstable limit cycle "sticks" in the saddle separatrix loop (or is born from it). As the parameters along the curve of the loop approach domain (5), a local rearrangement of the trajectory structure on the stable saddle manifold and in domain (5) takes place. Equilibrium O_2 becomes a saddle-focus with a saddle-focus value $\sigma_{sf} > 0$. According to L. P. Shilnikov's theorem, when such a loop is formed and destroyed, there is a countable set of saddle limit cycles in its vicinity. Whether this set is an attractor or not is an open question. The question regarding the border of domain (5) is also open. These questions are answered by carrying out a numerical experiment.

Numerical experiment. Let us discuss the dynamics of the system during the variation of parameters through grey zone from right to left. By decreasing the constant component of the torque of the rotator (parameter γ) and by keeping all other system parameters constant: $\mu = I^{-1} = 0.08$; $h = 0.05524$; $a = -0.0809$; $b = 0.021$. In this case $\lambda = 0.567$.

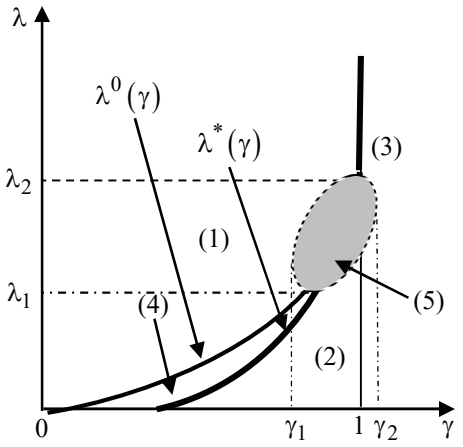

Fig. 1.19. Bifurcation diagram in the case of existence of dynamical chaos.

Fig. 1.20 shows phase portraits and portraits of the point mapping $(x, J)_{\varphi=\varphi_0} \to (\bar{x}, \bar{J})_{\varphi=\varphi_0+2\pi}$, obtained for an equivalent dynamical system of the form

$$\begin{aligned} \dot{\varphi} &= \gamma + x, \\ \dot{x} &= \mu(-x - \sin\varphi + J), \\ \dot{J} &= -hJ + a(\gamma + x) + b(\sin\varphi - \gamma). \end{aligned}$$

For $\gamma = 1.29$ (and for $\gamma > 1.29$), the rotator performs periodic motions (see Fig. 1.20a). For $\gamma = 1.282$ the limit cycle experiences the first bifurcation of doubling of the period (pitchfork bifurcation), see Fig. 1.20b). . Then a cascade of pitchfork bifurcations occurs, see Figs. 1.20c-f), that ends by origination of the Feigenbaum attractor. (Fig. 1.20g). Fig. 1.20h shows the curve of a point mapping

that corresponds to this strange attractor. This is followed by "periodicity windows". With the decrease of γ, a stable rotary-oscillatory limit cycle of a tripled period (with the main period equal to 2π) is born on the chaotic attractor (see Fig. 1.20i). A typical feature of this limit cycle consists of a rotation of the phase at a two-dimensional stable manifold. The motion at the limit cycle occurs in such a way that the aforementioned equilibrium would exist in the phase space of the system (saddle-focus with two-dimensional stable and one-dimensional unstable manifolds). For this reason, this limit cycle can be considered a "legacy" of the complex limit set that occurs when the loop of the saddle-focus is destroyed. With the further decrease of γ, this limit cycle loses stability, and the limit cycle with the period of five becomes stable instead (Fig. 1.20j). Limit cycles of a larger period of the Sharkovsky ordering [126, 127] were not observed in the experiment. After the limit cycle with a period of five, the motions of rotator become chaotic. The form of the attractor shown in Fig. 1.20k, l indicates that the motions occur at a certain combination of the Feigenbaum attractor and the limit set obtained at the place of the collapsed loop of the saddle-focus. This combined set is an attractor. The respective Poincaré mapping is shown in Fig. 1.20l, m. With the further decrease of γ, the rotator breaks from the regime of chaotic rotations mode to stable equilibrium O_1.

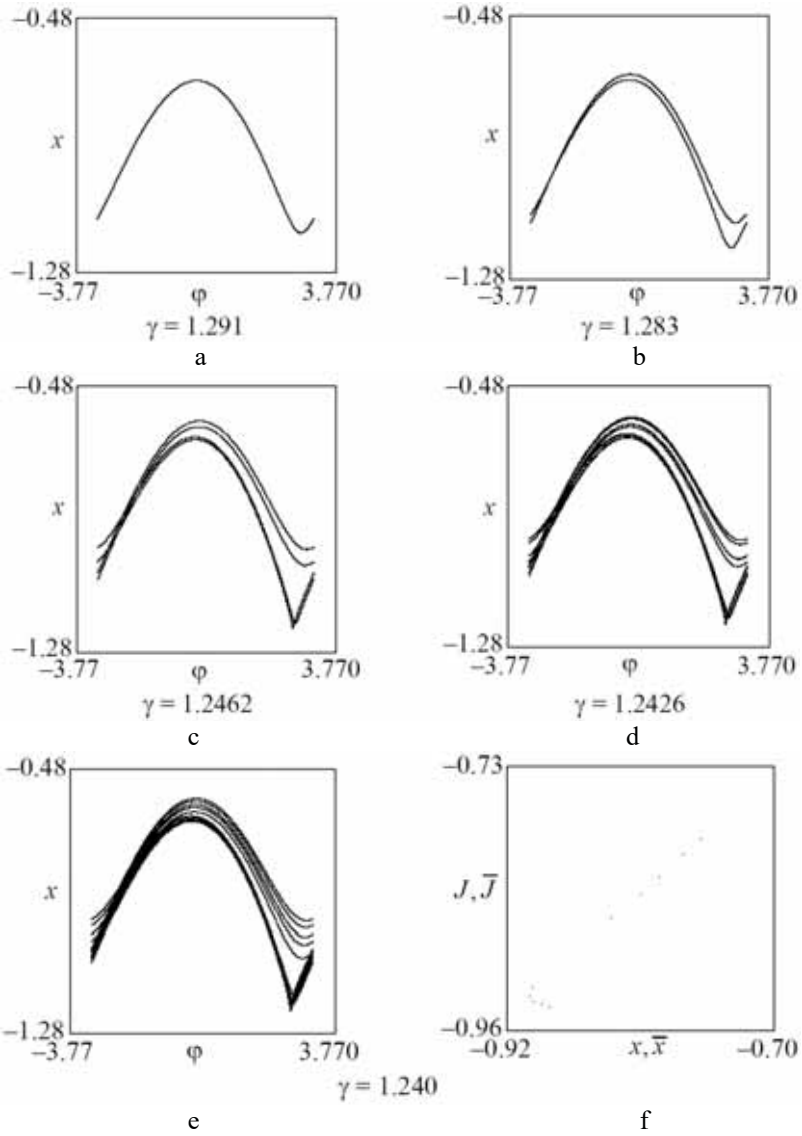

Fig. 1.20. The gallery of qualitatively different phase portraits and Poincaré mappings (continues on the next page).

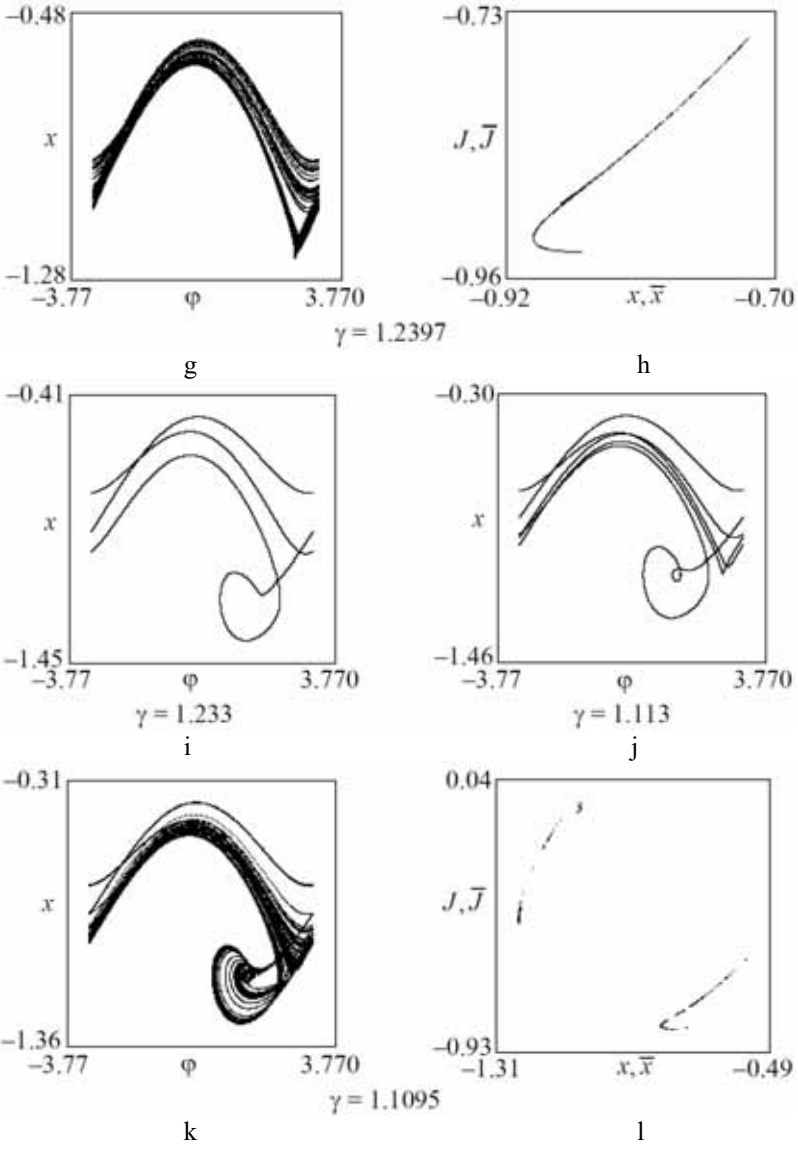

Fig. 1.20. Conclusion.

Rotation characteristic. Let us present qualitative forms of the rotation characteristic based on the results of the study of the dynamical properties of the model.

For $\alpha/\lambda < 1$, the qualitative forms of the rotation characteristic of rotator in system (1.16) do not differ from the rotation characteristic of a two-dimensional autonomous rotator, which are described in section 1.2. We consider cases shown in the bifurcation diagrams (see Figs. 1.18, 1.19).

1^0. Consider the bifurcation diagram shown in Fig. 1.20a using phase portraits for each of the parameter domains. Suppose, $\lambda < \lambda_0$. A qualitative form of the rotation characteristic is shown in Fig. 1.21a. Let us discuss it. We increase parameter γ (quasi-statistically) starting from zero while keeping other system parameters constant. For $\gamma = 0$, the rotator is in a stable equilibrium O_1 (in domain (1), it is globally stable) until it disappears "without noticing" the bifurcations occurring in the phase space. For $\gamma = 1 + 0$, the rotator jumps into rotational motions – to a stable limit cycle, which is globally stable in domain (3). This limit cycle was born earlier by separating from the multiple limit cycle, when parameter γ entered domain (4). The diagonal of the plane is an asymptote of the rotational branch of rotation characteristic. For the decreased γ, when "entering" domain (4), the following happens. The stable limit cycle, on which the rotator is "located" moves down the phase cylin-

der. At the same time, the unstable limit cycle, born from the separatrix loop of the saddle, moves up, towards the stable limit cycle. An unstable branch of rotation characteristic corresponding to an unstable limit cycle, shown in Fig. 1.21 by a dotted line. When parameter γ reaches the curve $\lambda = \lambda^0(\gamma)$, the limit cycles merge and disappear, and the rotator jumps back into equilibrium O_1 – to the zero step.

For $\lambda_0 < \lambda < \lambda_*$, the qualitative form of the rotation characteristic is the same as that for the hysteretic rotation characteristic discussed in section 1.2, while for $\lambda > \lambda_*$, it is the same as the non-hysteretic one.

2^0. Consider the bifurcation diagram shown in Fig. 1.19. We assume that $\lambda_1 < \lambda < \lambda_2$. The rotation characteristic is shown in Fig. 1.21b. When parameter γ is increased, one has the same arrangement of dynamical regimes as in 1^0. A significant difference in characteristics is observed when variation of parameter γ is reversed. Once the parameter gets into the "gray" zone, the rotation characteristic becomes undefined: the scattering effect of the rotation characteristic, already described in section 1.2 takes place. For other values of parameter λ, the qualitative forms of rotation characteristic are discussed in 1^0.

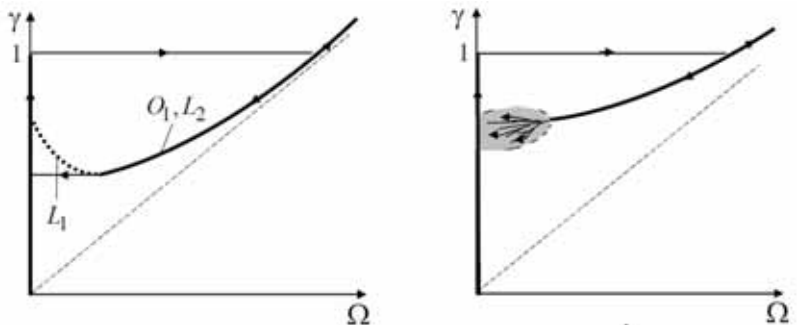

a b

Fig. 1.21. Qualitative forms of the rotation characteristic:
a: for $\lambda < \lambda_0$, b: for $\lambda_1 < \lambda < \lambda_2$.

1.4. Chaotic dynamics of a non-autonomous rotator with aperiodic load

Let us again consider the Froude pendulum with a balancing sleeve (see Fig. 1.15a). We will assume that the shaft of the pendulum rotates with the frequency $\Omega(t) = \Omega_0 + \Omega_s \sin\psi$, $\dot{\psi} = \varpi_0$. In this case, the governing equations have the form [123]

$$\begin{aligned} I_1\ddot{\varphi} &= \delta_1(\Omega_0 - \dot{\varphi}) + \delta_2(\omega - \dot{\varphi}) - mgl\sin\varphi + \delta_1\Omega_s\sin\psi, \\ I_2\dot{\omega} &= \delta_3(\Omega_0 - \omega) - \delta_2(\omega - \dot{\varphi}) + \delta_3\Omega_s\sin\psi, \\ \dot{\psi} &= \varpi_0. \end{aligned} \tag{1.20}$$

Let us transform equations (1.20). First of all, let us remove the periodic function from the second equation by using a change of the variables of the form $\omega = A_s\sin\psi + A_c\cos\psi + y$, where

$$A_s = \frac{\delta_3\left(\delta_2+\delta_3\right)}{\left(I_2\varpi_0\right)^2+\left(\delta_2+\delta_3\right)^2}\Omega_s,\quad A_c = -\frac{I_2\delta_3\varpi_0}{\left(I_2\varpi_0\right)^2+\left(\delta_2+\delta_3\right)^2}\Omega_s.$$

As a result, we obtain a system of the form

$$\begin{aligned} &I_1\ddot{\varphi}+\delta_1\dot{\varphi}+mgl\sin\varphi = \delta_1\Omega_0+\delta_2\left(y-\dot{\varphi}\right)y+B\sin\left(\psi+\psi_0\right),\\ &I_2\left(y-\dot{\varphi}\right)^{\cdot}+\left(\delta_2+\delta_3\right)\left(y-\dot{\varphi}\right)=\delta_3\Omega_0-\delta_3\dot{\varphi}-I_2\ddot{\varphi},\\ &\dot{\psi}=\varpi_0, \end{aligned} \tag{1.21}$$

where $B=\sqrt{\left(\delta_2A_s+\delta_1\Omega_s\right)^2+\left(\delta_2A_c\right)^2}$, $\psi_0=\operatorname{arctg}\dfrac{\delta_2A_c}{\delta_2A_s+\delta_1\Omega_s}$.

Further, similarly to the autonomous case, we transform time in (1.21): $\dfrac{mgl}{\delta_1}\tau=\tau_n$ as well as variables $J=\dfrac{\delta_2}{mgl}\left(y-\dot{\varphi}\right)-$ $-\dfrac{\delta_2\delta_3}{mgl\left(\delta_2+\delta_3\right)}\Omega_0$, and $\psi+\psi_0=\psi_n$. We obtain the following system:

$$\begin{aligned} &I\ddot{\varphi}+\dot{\varphi}+\sin\varphi=\gamma+J+A\sin\psi,\\ &\dot{J}+hJ=a\dot{\varphi}+b\left(\sin\varphi-\gamma-A\sin\psi\right),\\ &\dot{\psi}=\omega_0, \end{aligned} \tag{1.22}$$

where $A=\dfrac{B}{mgl}$, $\omega_0=\dfrac{\delta_1}{mgl}\varpi_0$, and all other parameters are the same as ones in the autonomous case. Subscript "*n*" is omitted here.

Consider dynamics of system (1.22) for the different asymptotic values of parameter *I*.

Asymptotic case I << 1. According to [18], a singularly perturbed system (1.22) has a stable integral surface of "slow motions" in the phase space $G(\varphi,\psi,\dot{\varphi},J)$. Integral curves at this surface represent trajectories of the non-autonomous rotator. Its equation is close (~ *I*) to that obtained from system (1.22) for $I = 0$ [128]. The system is reduced to equation (1.6) with functions $F_1(\varphi)=\varepsilon\cos\varphi$, $F_2(\varphi)=\sin\varphi$. In this case, parameters I, ε, γ, A, ω_0 of equation (1.6) correspond to the following parameter combinations of system (1.22):

$$\frac{h-b}{(h-a)^2},\ \frac{1}{(h-a)},\ \gamma,\ \frac{\sqrt{\omega_0^2+(h-b)^2}}{h-b}A,\ \frac{h-a}{h-b}\omega_0.$$

This case has been already sufficiently investigated in sections 1.2 and 1.3.2.

Asymptotic case $I^{-1} = \mu << 1$. We investigate the main resonance of the system (simple synchronization), considering the parameter domain

$$D_\mu = \left\{ I^{-1} = \mu;\ h = \mu h^*; a = \mu a^*; b = \mu b^*;\ \frac{h-a}{h-b}\left(\frac{h-b}{h-a}\gamma - \omega_0\right) = \mu\Delta \right\}.$$

Domain D_μ corresponds to the zone of a simple master-slave synchronization of rotator with aperiodic load that has low damping.

We apply to (1.22) a change of the variables of the form

$$\begin{aligned} \dot{\varphi} &= \omega_0 + \mu\Phi(\varphi, \psi, \xi), \\ J &= \frac{a-b}{h-b}\ \omega_0 + \mu Y(\varphi, \psi) + \mu y. \end{aligned} \tag{1.23}$$

It reduces (1.22) to an equivalent system in a standard form with a fast-spinning phase:

$$\begin{aligned} \dot{\xi} &= \mu\left(y + Y - \Phi\frac{\partial\Phi}{\partial\varphi} - \Phi + \Delta \right), \\ \dot{y} &= \mu\left(-h^* y - h^* Y - \Phi\frac{\partial Y}{\partial\varphi} + a^*\Phi - b^*\Delta \right), \\ \dot{\eta} &= \mu\Phi(\xi, \varphi, \eta), \\ \dot{\varphi} &= \omega_0 + \mu\Phi(\xi, \varphi, \eta), \end{aligned} \tag{1.24}$$

where $\Phi = \frac{1}{\omega_0}\cos\varphi - \frac{A}{\omega_0}\cos\psi + \xi, \qquad Y = \frac{b^*}{\omega_0}\cos\varphi + \frac{Ab^*}{\omega_0}\cos\psi,$

$\eta = \varphi - \psi$ is the phase mistuning, Δ is the frequency mistuning.

Details of the changes of the variables like (1.23) are provided in the Appendix.

Having averaged system (1.24) over a fast-spinning phase, we obtain a truncated system of the form

$$\begin{aligned}
&\dot{\xi} = \mu\left(-\xi + y - \frac{A}{2\omega_0^2}\sin\eta + \Delta\right),\\
&\dot{y} = \mu\left(-h^* y + a^*\xi + b^*\left(\frac{A}{2\omega_0^2}\sin\eta - \Delta\right)\right),\\
&\dot{\eta} = \mu\xi,\\
&\dot{\varphi} = \omega_0 + \mu\xi.
\end{aligned} \tag{1.25}$$

In system (1.25), we have kept old notations for the averaged variables.

By transforming time $\mu\frac{2\omega_0^2}{A}\tau = \tau_n$ and variable $y = \frac{A}{2\omega_0^2}x$ we reduce the first three equations of system (1.25) to the equivalent system of the form

$$\begin{aligned}
&I_r\ddot{\eta} + \dot{\eta} + \sin\eta = \gamma^r + x,\\
&\dot{x} + h_r x = a_r\dot{\eta} + b_r\left(\sin\eta - \gamma^r\right),
\end{aligned} \tag{1.26}$$

where $I_r = \frac{A}{2\omega_0^2}$, $\gamma^r = \Delta I_r^{-1}$, $h_r = h^* I_r^{-1}$, $a_r = a^* I_r^{-1}$, $b_r = b^* I_r^{-1}$.

Here we meet again with a remarkable fact: the obtained averaged system (1.26), accurate within notations of variables and parameters, coincides with system (2.6). This allows us to obtain important

information about the dynamics of the non-autonomous model (1.22) without doing any further research.

Note that when passing from the system (1.26) to the equivalent third-order equation (1.18), we obtain the following parameters:

$$\beta = \sqrt{\frac{A}{2\omega_0^2}\frac{\left(h^* - b^*\right)}{\left(1+h^*\right)^3}}, \quad \alpha = \sqrt{\frac{A}{2\omega_0^2}\frac{1}{\left(h^* - b^*\right)\left(1+h^*\right)}},$$

$$\lambda^r = \sqrt{\frac{2\omega_0^2}{A}}\frac{h^* - a^*}{\sqrt{\left(h^* - b^*\right)\left(1+h^*\right)}}, \quad \gamma^r = \left(\frac{A}{2\omega_0^2}\right)^{-1}\Delta.$$

Fig. 1.22 shows bifurcation diagrams of the parameters of system as analogues of respective diagrams for the autonomous system shown in Figs. 1.18 and 1.19.

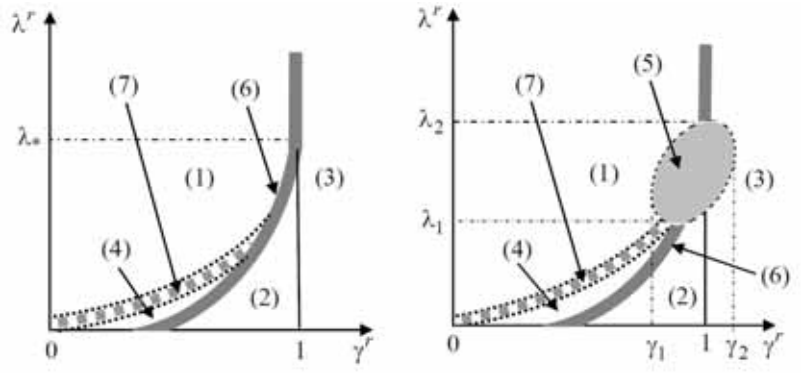

a b

Fig. 1.22. Bifurcation diagrams of effective parameters of system (1.22) in a zone of the main resonance.

Note that Eqs. (1.26) are invariant with respect to the transformation $\eta \to -\eta$, $x \to -x$, $\gamma^r \to -\gamma^r \left(\Delta \to -\Delta\right)$. This means that bifurcation diagrams shall also contain their mirrored reflection with respect to the ordinate axis. On the complete diagram, the left-hand side of each graph will represent transformations of the phase space of Eqs. (1.22) when parameter γ approaches the resonance from the left-hand side (when γ is increased), while the right-hand side would represent that when parameter γ approaches the resonance from the right-hand side (when γ is decreased).

In Fig. 1.22, parameter domain (1) corresponds to the global asymptotic stability (GAS) of a stable limit cycle – the synchronization capture area. Domain (2) corresponds to the existence of stable and saddle limit cycles, as well as a stable invariant torus T^2. Depending on the initial conditions for parameters from this domain, both the synchronization regime and the stable stationary beatings regime are possible. Domain (3) corresponds to the existence of a globally stable invariant torus. For parameters from this area, simple synchronization mode is not possible. Note that in all cases we consider tori as invariant manifolds, not to mentioning structures of trajectories on these tori. These manifolds can have both a quasi-periodic winding and a pair: stable and unstable limit cycles corresponding to a subharmonic resonance.

For parameter domain (4), there exist stable and saddle limit cycles and stable and unstable tori. In contrast to Figs. 1.18 and 1.19, Fig. 1.22 shows the existence of two new domains (domains (6) and (7)). Domain (6) ("bold Tricomi curve") corresponds to the existence of complex limit sets in the phase space that are related to the destruction of a two-dimensional invariant torus and also to the existence of rough homoclinic curves of a saddle resonance limit cycle. For the parameters transition from domain (4) to domain (1), a merging of stable and unstable tori occurs. Such a bifurcation of merging of tori is poorly studied. Probably, before the merging, tori lose their smoothness. Normally, this leads to the origination of a complex limit set. For this reason, we consider domain (7) to be "grey" in the sense that its exact borders are not determined and exact bifurcations leading to the chaotic state of dynamical processes are not known. Domains (6) and (7) are the narrow strips with a width $\sim \mu$, which for $\mu \to 0$ are shrinking to the respective bifurcation curves shown in Figs. 1.18 and 1.19.

Let us discuss the correspondence of chaotic attractors of initial system (1.22) and averaged system (1.16). This applies to the attractors corresponding to domain (5) in Figs. 1.26b and 1.19.

It is clear that if A is a strange attractor of the averaged system, then the attractor of the original system does not represent a formal multiplication $A \times S^1$ due to non-roughness of attractor A (homoclinic trajectories do not have an unambiguous interpretation). On the

other hand, with the decrease of parameter μ, domain (5) shown in Fig. 1.26b shrinks to the corresponding domain shown in Fig. 1.19. It is natural to assume that some of the corresponding bifurcation curves in these domains also converge, in particular the curves of doubling of the period of the limit cycle in system (1.16) and the curves of doubling of the period of the torus in system (1.22). In other words, one can state that for any $\mu = \mu_0$, a chaotic attractor of the initial system contains $N(\mu_0)$ number of tori of saddle type (a "skeleton" of the chaotic attractor). Each of these tori corresponds to a limit cycle of the averaged system and $\lim_{\mu_0 \to 0} N(\mu_0) = \infty$. Due to this reason, hereinafter, we will state that a chaotic attractor of initial system has the same type as a chaotic attractor of the averaged system, keeping in mind that this statement is not entirely correct. In this sense, bifurcations of tori in system (1.22) should take place according to the same scenario as bifurcations of limit cycles in averaged system (1.26). Phase portraits of system (1.16) and forms of trajectories of point mappings for system (1.22) (on the respective planes) should have identical qualitative features.

Numerical study. This study is focused on bifurcations of dynamical regimes of the rotator during the transition from the regime of beatings to the regime of synchronization, which corresponds to the transition of parameter γ (while all other parameters remain fixed) from domain (3) to domain (1).

When parameter γ is varied through domain (6), the character of bifurcations is the same as that for the non-autonomous rotator described in Section 1.2, therefore, this case can be skipped. Let us discuss the case of parameter transition from domain (3) to domain (1) through domain (5), since this is the most interesting case in terms of the demonstration of theoretical results.

In this numerical study, phase portraits and structures of point mapping

$$\left(\varphi, x, J\right)_{\psi=\psi_0} \to \left(\overline{\varphi}, \overline{x}, \overline{J}\right)_{\psi=\psi_0+2\pi},$$

have been analysed. This point mapping has been made for a system which is equivalent to system (1.22):

$$\begin{aligned}
&\dot{\varphi} = \gamma + x,\\
&\dot{x} = \mu\left(-x - \sin\varphi + J + A\sin\psi\right),\\
&\dot{J} = -hJ + a\left(\gamma + x\right) + b\left(\sin\varphi - \gamma - A\sin\psi\right),\\
&\dot{\psi} = \omega_0.
\end{aligned}$$

Experiment 1. The following parameter set has been used: $\mu = h = 0.006$, $a = -0.006$, $b = 0.003$, $A = 5$, $\omega_0 = 0.5$. For these parameters, $\lambda^r = 0.632$. The gallery of phase portraits and their corresponding point mappings are shown in Fig. 1.23. Parameter γ is varied towards the resonance step from the right-hand side.

For $\gamma = 2.0892$, the rotator experiences quasi-periodic beatings (Fig. 1.23a). The left figure shows a torus with quasi-periodic winding. The middle and right figures represent a trajectory of point mapping of this torus (the discreteness of the trajectory is hardly noticeable due to the high density of points). For the decreased γ,

For the decreased values of γ, a bifurcation of doubling of the period of torus (pitchfork bifurcation) occurs, see Fig. 1.23b. Further, the torus changes its configuration with no further pitchfork bifurcations, see Fig. 1.23c). Then an opposite pitchfork bifurcation occurs, see Fig. 1.23d). The obtained torus loses its stability and the rotator suddenly jumps into the synchronization regime, see Fig. 1.23e). Fig. 1.23d shows a trajectory of the limit cycle at the involute of the phase cylinder.

For $\gamma = 1.9412$, the rotator suddenly jumps from the synchronization regime into the regime of quasi-periodic beatings (a jump from the lower end of the resonance step), see the torus of the doubled period shown in Fig. 1.23f) (compare to Fig. 1.23c). If parameter γ would be increased, then the torus would experience an opposite pitchfork bifurcation similar to the transition from Fig. 1.23c to Fig. 1.23d. Further, a loss of the stability of this torus and a jump towards the resonance step from the left-hand side would occur. A slight visual difference of cases shown in Fig. 1.23f and 1.23c 8c is concerned with the choice of a secant plane. For the transition from

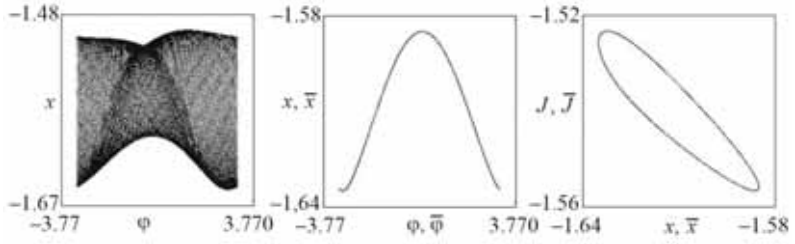

$\gamma = 2.0892$

a

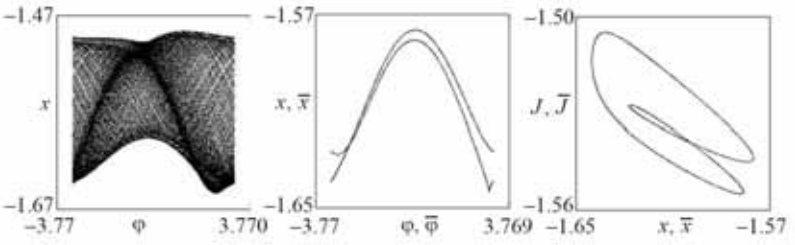

$\gamma = 2.0842$

b

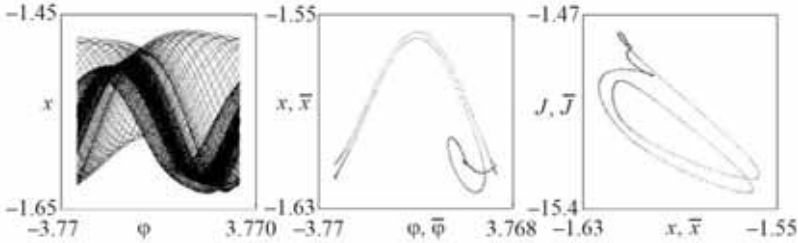

$\gamma = 2.0612$

c

Fig. 1.23. The gallery of qualitatively different phase portraits and Poincaré mappings (continues on the next pages).

Fig. 1.23f to Fig. 1.23h, the torus changes its configuration and then experiences an opposite pitchfork bifurcation, see Fig. 1.23i.

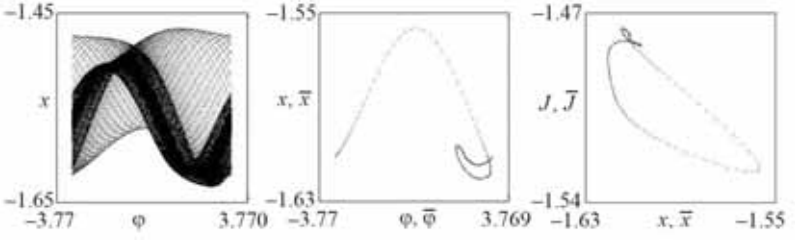

γ = 2.0602

d

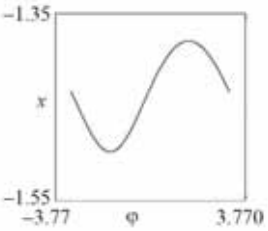

e

γ = 1.9362

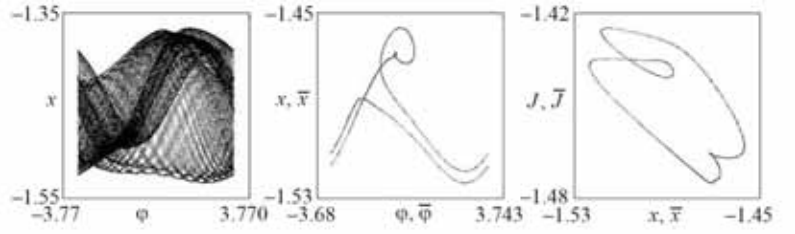

f

Fig. 1.23. Continuation.

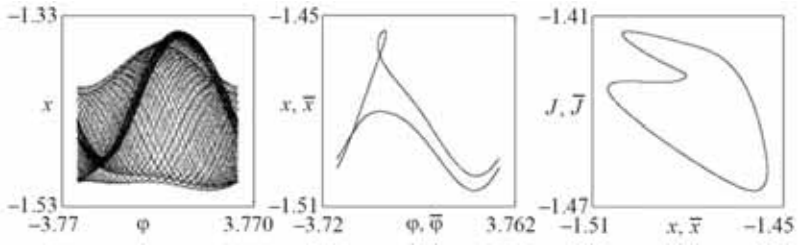

γ = 1.9182

g

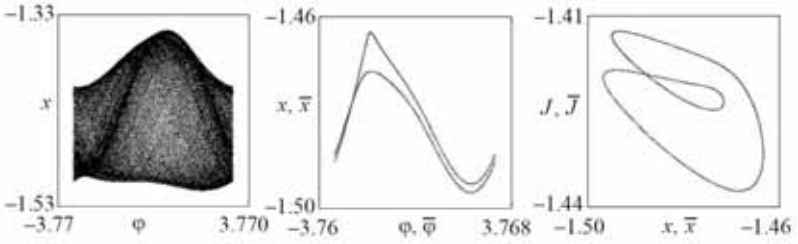

γ = 1.9152

h

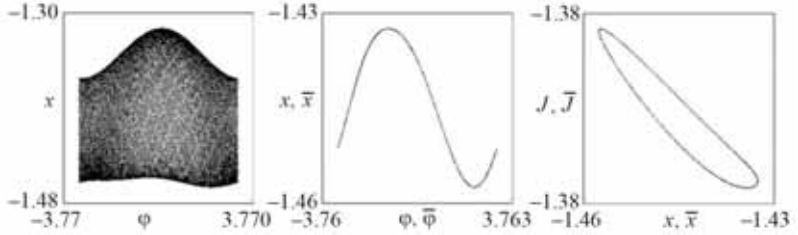

γ = 1.8682

i

Fig. 1.23. Conclusion.

Thus, in this case, dynamics of the rotator during the transition to the synchronization regime is regular. Note that bifurcation scenarios during the transition to the regime of synchronization from the left-hand and from the right-hand sides to the resonance step are the same. This fact is a consequence of the invariance of the averaged system to the applied transformations.

Experiment 2. The following parameter set has been used: $\mu = 0.086,\ h = 0.006,\ a = -0.006,\ b = 0.003,\ A = 2.5.$ In this case, $\lambda^r = 0.517$. The gallery of phase portraits and corresponding point mappings are shown in Fig. 1.24. Parameter γ has been varied from the right-hand side towards the resonance step.

For $\gamma = 3.6091$, a quasi-periodic motion of the rotator occurs, see Fig. 1.24a. For the decreased values of this parameter, the torus experiences two pitchfork bifurcations, while itself remaining ergodic and "smooth", see Figs. 1.24b,c) (compare to Figs. 1.20b,c). After the next pitchfork bifurcation, the torus loses smoothness, see Fig. 1.24d. A chain of pitchfork bifurcations leads to the origination of a strange Feigenbaum attractor, see Fig. 1.24d (compare to Fig. 1.20i). Further, like in an autonomous case, an attractor related to the loop of the saddle-focus of the averaged system merges with this attractor. For the decreased γ, a stable torus of the period four is born at the united attractor, see Fig. 1.24f. Further, the torus experiences a series of the opposite pitchfork bifurcations while itself re-

maining “smooth”, see Figs. 1.24g,h,i. Finally, a torus of the period one loses stability and the rotator suddenly jumps into the synchronization regime, see Fig. 1.24j.

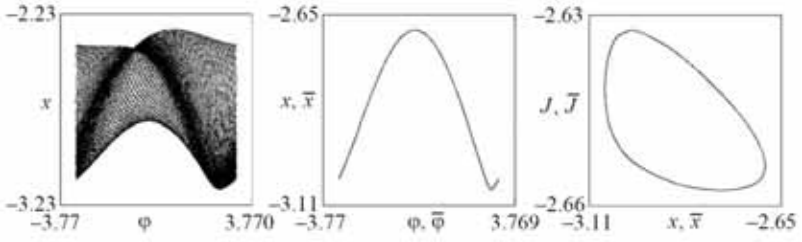

γ = 3.6091

a

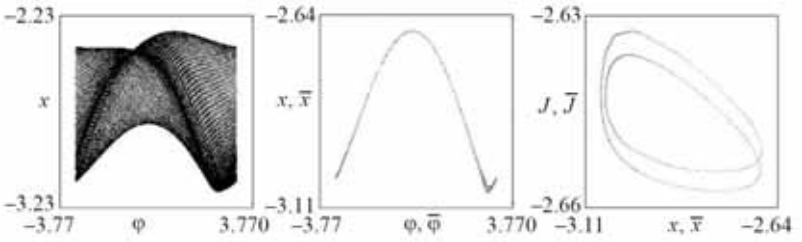

γ = 3.6051

b

Fig. 1.24. The gallery of qualitatively different phase portraits and Poincaré mappings (continues on the next pages).

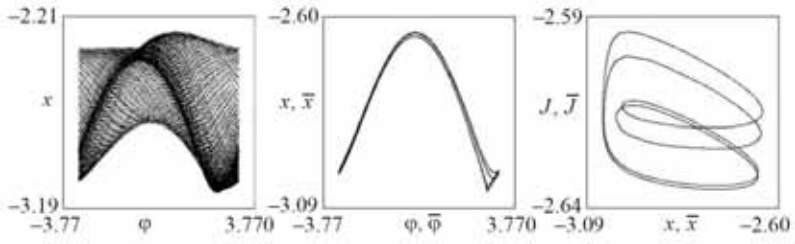

$\gamma = 3.5761$

c

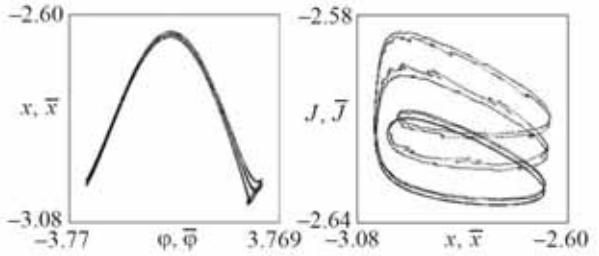

$\gamma = 3.5741$

d

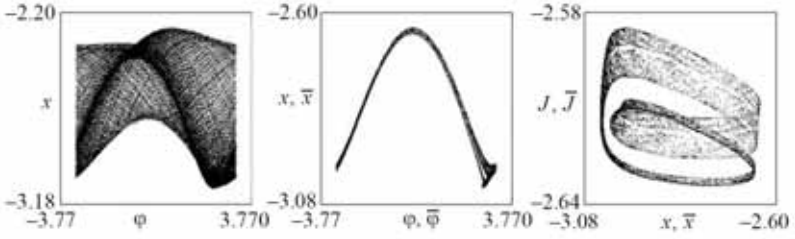

$\gamma = 3.5731$

e

Fig. 1.24. Continuation.

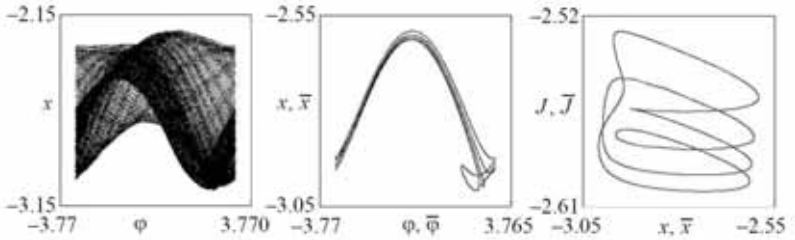

γ = 3.5321

f

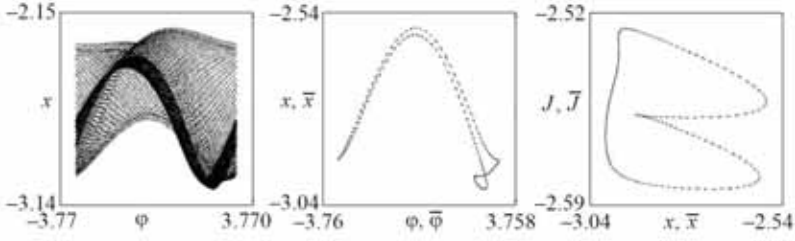

γ = 3.5251

g

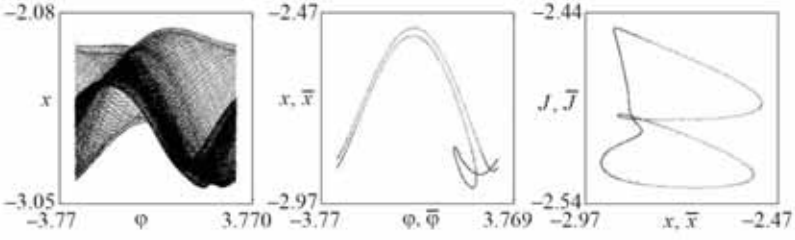

γ = 3.4451

h

Fig. 1.24. Continuation.

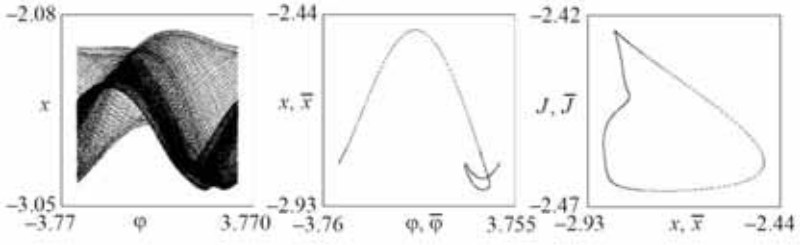

$\gamma = 3.4091$

i

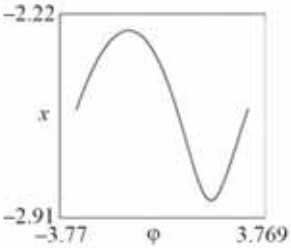

$\gamma = 3.3701$

j

Fig. 1.24. Conclusion.

Experiment 3. In the previous experiment, during a series of pitchfork bifurcations the torus lost its smoothness. The question is: is it a rule or not?

The following parameter set has been used: $\mu = 0.006$, $h = 0.004$, $a = -0.006$, $b = 0$, $A = 5$, $\omega_0 = 0.5$. In this case, $\lambda^r = 0.5$. We move towards the resonance from the left-hand side.

For $\gamma = 1.19534$ (see Fig. 1.25a), there exists a doubled smooth torus. During the increase of γ, the torus experiences a cascade of

pitchfork bifurcations, but does not lose its smoothness, see Figs. 1.25b,c. As a result of doublings of this smooth torus, a Feigenbaum attractor is originated, see Fig. 1.25d (compare to Fig. 1.25i).

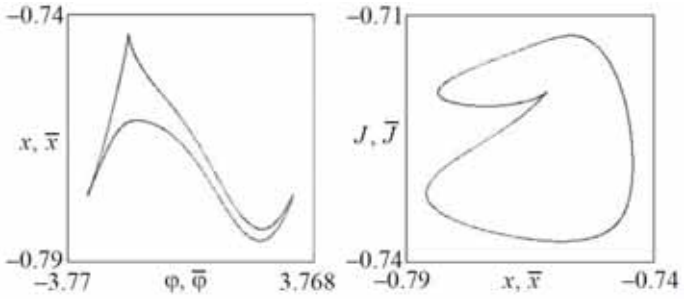

γ = 1.19534

a

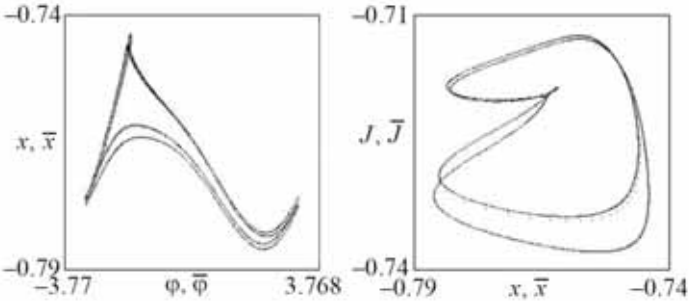

γ = 1.19558

b

Fig. 1.25. The gallery of qualitatively different phase portraits and Poincaré mappings (continues on the next page).

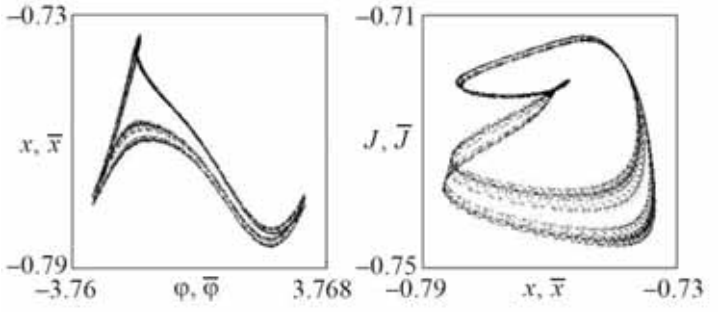

γ = 1.19563

c

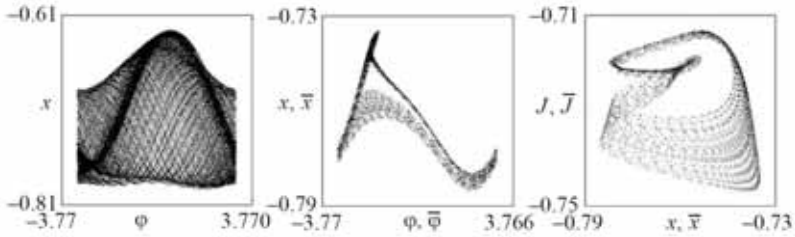

γ = 1.19567

d

Fig. 1.25. Conclusion.

Rotation characteristic. We will obtain a qualitative form of the rotation characteristic of the rotator in the zone of the main resonance from the rotation characteristic of the rotator in the autonomous system (1.16) as a result of the following transformations. Fig. 1.21b is supplemented by its reflection relative to the origin, and as a result, a complete resonance step with its "environment" is obtained. Further, obtained figure is transferred along the autonomous rotation characteristic to the point $\Omega = (h-a)\omega_0/(h-b)$.

Finalizing this section, we would like to draw the reader's attention to how the rotator returns to the "zero" resonance step, i.e. comes from the regime of rotations to the oscillatory regime. Fig. 1.26a shows a trajectory of a complex a rotary-oscillatory limit cycle of a very large period, as illustrated by the point mapping. The dark part of it corresponds to a denser concentration of trajectories. During the decrease of parameter γ, due to the trajectories thickening, a divisible oscillatory limit cycle originates. In the moment of bifurcation, a period of the limit cycle becomes infinite. Such a bifurcation is called the "blue sky catastrophe" [129 – 132]. For further decrease of γ, the aforementioned limit cycle splits into two limit cycles: stable and unstable ones and the rotator moves along the stable oscillatory limit cycle, see 1.26b.

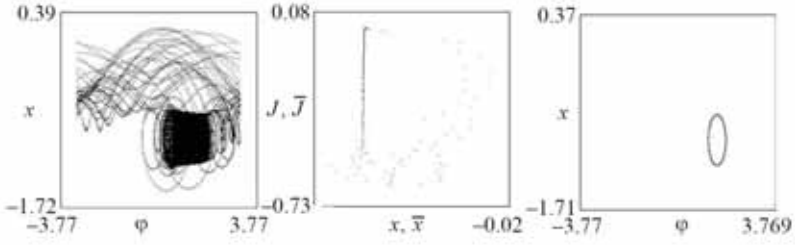

γ = 1.19563 γ = 1.19567

a b

Fig. 1.26. Blue sky catastrophe bifurcation (a) and oscillatory regime of rotator (b) for $\mu = 0.086$, $h = 0.006$, $a = -0.006$, $b = 0.003$, $A = 2.5, \omega_0 = 0.8$.

1.5. Chaotic dynamics of the "rotator – oscillator" system

The "rotator – oscillator" system is a dynamical system of the form [118, 133]

$$\begin{aligned} &I\ddot{\varphi}+\dot{\varphi}+\sin\varphi=\gamma+J,\\ &\ddot{J}+\delta\dot{J}+\omega_0^2 J=d\dot{\varphi}+b\ddot{\varphi}, \end{aligned} \tag{1.27}$$

defined in the phase space $G\left(\varphi,\dot{\varphi},J,\dot{J}\right)=T^1\times R^3$ and in the parameter domain $D=\left\{I>0,\ \gamma\geq 0,\ \delta>0,\ \omega_0>0,\ b,\ d\right\}$, where I, γ moment of inertia and driving moment of the rotator, respectively; δ, ω_0 dissipation coefficient and natural frequency of the oscillator, b, d are the parameters of the coupling.

Let us provide examples of physical systems modelled by equations (1.27).

1. Torsional vibrations of a flexible rotor in a system with an energy source of limited power.

Consider dynamics of a torsional-elastic shaft driven by an energy source of limited power. A scheme of this model is shown in Fig. 1.27a.

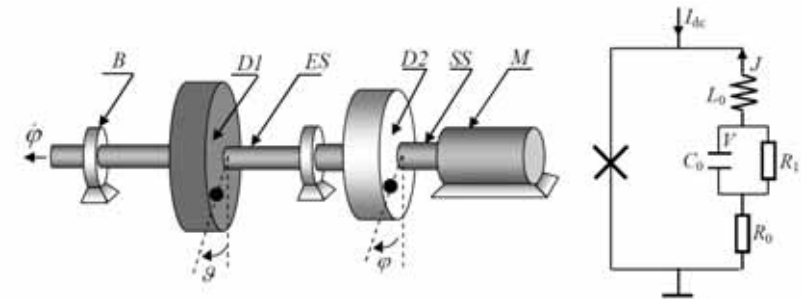

a b

Fig. 1.27. Asynchronous motor with unbalanced disk and adduction disk of the elastic shaft (a): *M* is the motor, *ES* is the elastic shaft, *D1* is the unbalanced disk, *SS* is the solid shaft, *D2* is the adduction disk of elastic shaft, *B* is the bearing; an equivalent scheme of the system "superconductive junction – resonator" (b).

An asynchronous electric motor is taken as an example, but in general an engine of any other type could be chosen. We consider a simple model, when an elastic shaft, (distributed system) including other systems installed on it, is modelled as one disk with known moment of inertia [54]. The disk is placed in the centre of the shaft (one mode model). We will assume that all resistance forces are linear with respect to angular speed and elastic restoring force is linear with respect to the angle of twist.

The Lagrange function for this system has the form

$$L = T + V = \frac{I_1}{2}\dot{\varphi}^2 + \frac{I_0}{2}\dot{\vartheta}^2 + mge\left(1-\cos\varphi\right) + \frac{k}{2}\left(\varphi - \vartheta\right)^2,$$

where φ, ϑ are the angles of rotation of the imbalanced disk and adduction disk, respectively; I_1, I_0 are their moments of inertia, respectively; *m*, *e* are the imbalance and the eccentricity, respectively; *k* is the torsional stiffness of the elastic shaft.

By assumption, the motor driving torque is a linear function of the rotational speed $M_d = M_0 - \lambda\dot{\varphi}$. We also account for the fact that the whole system can operate inside a viscous environment (like electric submersible pumps). We assume that all moments of dissipative forces acting on the imbalanced disk are described by the term $-\lambda\dot{\varphi}$ in the expression for the torque. We also assume that the moment of external forces acting on the adduction disk has the form $-\delta_0\dot{\vartheta}$. Finally, we assume that there exists a hypothetical moment of forces of internal torsional friction $\varepsilon_0\left(\dot{\varphi}-\dot{\theta}\right)$. Under these assumptions, the governing equations have the form:

$$I_1\ddot{\varphi} + mge\sin\varphi + k\left(\varphi-\vartheta\right) = M_0 - \lambda\dot{\varphi},$$
$$I_0\ddot{\vartheta} + k\left(\vartheta-\varphi\right) = -\delta_0\dot{\vartheta} + \varepsilon_0\left(\dot{\varphi}-\dot{\vartheta}\right).$$

Introducing a new variable $\frac{k}{mge}\left(\vartheta-\varphi\right) = J$ and time $\frac{mge}{\lambda}\tau = \tau_n$,

we reduce the system above to the form (1.27), with $I = \frac{I_1 mge}{\lambda^2}$,

$$\gamma = \frac{M_0}{mge}, \quad \delta = \left(\delta_0 + \varepsilon_0\right) I_0^{-1} \frac{\lambda}{mge}, \quad \omega_0^2 = k I_0^{-1} \left(\frac{\lambda}{mge}\right)^2,$$

$$b = -\frac{k}{mge}, \quad d = -\frac{\delta_0}{\lambda}\omega_0^2.$$

2. The "superconductive junction – resonator" system. In one-mode approximation, an equivalent electric scheme is shown in Fig. 1.27b.

Using Kirchhoff laws and Josephson relation, we obtain dimensionless governing equations with dimensionless variables, parameters, and time:

$$c\ddot{\varphi} + \dot{\varphi} + \sin\varphi = \gamma + J,$$
$$l_0 \dot{J} + r_0 J - V = -\dot{\varphi}, J = -c_0 \dot{V} - r_1^{-1} V.$$

By excluding variable V, we obtain system of the form (1.27) with the following parameters:

$$\delta = \frac{c_0 r_0 r_1 + l_0}{c_0 l_0 r_1}, \quad \omega_0^2 = \frac{1}{c_0 l_0}\left(1 + \frac{r_0}{r_1}\right), \quad b = -\frac{1}{l_0}, \quad d = -\frac{1}{c_0 l_0 r_1}.$$

The list of physical systems modelled by equations (1.27) or similar equations is not limited to these examples [134 – 138].

Consider the dynamics of system (1.27) in the following parameter domain:

$$D_\mu = \left\{ I^{-1} = \mu \ll 1,\ \delta = \mu h,\ \gamma + \frac{d}{\omega_0} - \omega_0 = \mu\Delta \right\}.$$

For these conditions, system (1.27) represents a quasi-linear rotator coupled to a high-quality oscillator. The last equation in D_μ determines the mistuning of the normal frequencies of the rotator and the oscillator.

According to the transformation algorithms described in Appendix, the system, which is equivalent to system (1.27)

$$\begin{aligned} &I\ddot{\varphi} + \dot{\varphi} + \sin\varphi = \gamma + J, \\ &\dot{J} = W + b\dot{\varphi} - \mu h J, \\ &\dot{W} = -\omega_0^2 J + d\dot{\varphi} \end{aligned}$$

by applying changes of the variables

$$\begin{aligned} &J = \theta\sin\varphi + \eta\cos\varphi + \frac{d}{\omega_0}, \\ &W = \left(\theta\cos\varphi - \eta\sin\varphi\right)\omega_0 - b\omega_0, \\ &\dot{\varphi} = \omega_0 + \mu\Phi\left(\theta,\eta,\varphi,\xi\right) \end{aligned} \tag{1.28}$$

is reduced to an equivalent system in a standard form with a fast-spinning phase of the form

$$\begin{aligned}
\dot{\theta} &= \mu\Theta(\theta,\eta,\xi,\varphi),\\
\dot{\eta} &= \mu T(\theta,\eta,\xi,\varphi),\\
\dot{\xi} &= \mu\Xi(\theta,\eta,\xi,\varphi),\\
\dot{\varphi} &= \omega_0 + \mu\Phi(\theta,\eta,\xi,\varphi),
\end{aligned} \tag{1.29}$$

where

$$\Theta = \left(\eta + b\sin\varphi + \frac{d}{\omega_0}\cos\varphi\right)\Phi - h\left(\theta\sin\varphi + \eta\cos\varphi\right)\sin\varphi + \frac{d}{\omega_0}\sin\varphi,$$

$$T = \left(b\cos\varphi - \theta - \frac{d}{\omega_0}\sin\varphi\right)\Phi - h\left(\theta\sin\varphi + \eta\cos\varphi\right)\cos\varphi + \frac{d}{\omega_0}\cos\varphi,$$

$$\Xi = \Delta - \left(\frac{\partial\Phi}{\partial\theta}\Theta + \frac{\partial\Phi}{\partial\eta}T + \frac{\partial\Phi}{\partial\varphi}\Phi + \Phi\right),$$

$$\Phi = \frac{1-\theta}{\omega_0}\cos\varphi + \frac{\eta}{\omega_0}\sin\varphi + \xi.$$

By averaging (1.29) by a fast-spinning phase, we obtain a system of the form

$$\begin{aligned}
\dot{\xi} &= \mu\left(-b_1\xi + b_2\theta + b_3\eta + \Delta\right),\\
\dot{\theta} &= \mu\left(-b_4\theta + b_5\eta + \eta\xi + b_6\right),\\
\dot{\eta} &= \mu\left(-b_4\eta - b_5\theta - \theta\xi + b_7\right),\\
\dot{\varphi} &= \omega_0 + \mu\xi
\end{aligned}$$

with parameters

$$b_1 = 1 - \frac{d}{\omega_0^2},\ b_2 = 0,\ b_3 = \frac{1}{2\omega_0^2},\ b_4 = \frac{1}{2}\left(h + \frac{d}{\omega_0^2}\right),\ b_5 = \frac{b}{2\omega_0},$$

$$b_6 = \frac{d}{2\omega_0^2},\ b_7 = \frac{b}{2\omega_0}.$$

Further, a change of the variables of the form

$$x = b_4^{-1}\left(\xi + b_5\right),\ y = \left(b_3\eta + b_2\theta\right)/b_1b_4 - \Lambda,$$

$$z = \left(b_3\theta - b_2\eta\right)/b_1b_4 + R,\ \mu b_4\tau = \tau_{\text{н}} \tag{1.30}$$

reduces the averaged system to a Lorenz type system of the form

$$\begin{aligned}\dot{x} &= -\sigma\left(x - y\right) + \rho,\\ \dot{y} &= -y + Rx - xz,\\ \dot{z} &= -z + xy + \Lambda x,\end{aligned} \tag{1.31}$$

whose parameters are expressed as follows:

$$\sigma = b_1/b_4,\ R = \frac{b_2b_7 - b_3b_6}{b_1b_4^2},\ \Lambda = \frac{b_3b_7 + b_2b_6}{b_1b_4^2},$$

$$\rho = \left(\Delta + \left(b_1b_4b_5 + b_3b_7 + b_2b_6\right)b_4^{-1}\right)b_4^{-2}.$$

Let us discuss some of the dynamical properties of the averaged system (1.31).

1) The system is a dissipative system. This property is justified with the help of quadratic form $V=\frac{1}{2}\left(x^2+\left(y+\Lambda\right)^2+\left(z-\sigma-R\right)^2\right)$, whose derivative taken along the vector field of system (1.31) has the form $\dot{V}=-\sigma x^2-\left(\rho-\sigma\Lambda\right)x-y^2-\Lambda y-z^2+\left(\sigma+R\right)z$. It is obvious that it is negative outside a sphere $V\le L^2$. This means that all limit sets of trajectories remain inside a bounded spherical domain of the phase space $G^*\left(x,y,z\right)=R^3$.

2) Depending on the parameters, this system has up to three equilibria with coordinates:

$$x_0=\omega,\ \ y_0=\left(R\omega-\Lambda\omega^2\right)\Big/\left(1+\omega^2\right),\ \ z_0=\left(R\omega^2+\Lambda\omega\right)\Big/\left(1+\omega^2\right),$$

where $\omega_{1,2,3}$ are the solutions of equation

$$f=\omega+\left(\Lambda\omega^2-R\omega\right)\Big/\left(1+\omega^2\right). \tag{1.32}$$

Parameter ω it has a sense of the mistuning of the normal frequencies of the rotator and oscillator.

3) If system (1.31) has one equilibrium $O\left(x_0,y_0,z_0\right)$, then this equilibrium is globally asymptotically stable. This can be proven with the help of the Lyapunov function $V=\frac{1}{2}\left(mx_1^2+y_1^2+z_1^2\right)$,

where $x_1 = x - x_0$, $y_1 = y - y_0$, $z_1 = z - z_0$. The derivative of this function, taken along the vector field of system (1.31) has the form $\dot{V} = -(\alpha_1 x_1 + y_1)^2 - (\alpha_2 x_1 + z_1)^2 \le 0, \forall (x_1, y_1, z_1)$, where $\alpha_1 = -(\sigma m + R - z_0)/2$, $\alpha_2 = -(y_0 + \Lambda)/2$, m is a positive root of equation $\sigma^2 m^2 + 2\sigma(R - z_0 - 2)m + (R - z_0)^2 + (y_0 + \Lambda)^2 = 0$. It may be proven that conditions of existence of a positive root and conditions of unicity of the equilibrium are the same.

4) Stability of equilibria. A characteristic equation for an arbitrary equilibrium $O(x_0, y_0, z_0)$ of system (1.31) has the form $p^3 + a_0 p^2 + a_1 p + a_2 = 0$, where

$$a_0 = \sigma + 2,$$

$$a_1 = 2\sigma + 1 + \omega^2 + \frac{\sigma(\Lambda\omega - R)}{1 + \omega^2},$$

$$a_2 = \sigma(1 + \omega^2)\left(1 + \left(\frac{R\omega^2 + 2\Lambda\omega - R}{1 + \omega^2}\right)^2\right).$$

If $\omega = 0$ $(\rho = 0)$, then equilibrium $O(0,0,0)$ is stable if $R < 1$. For $\omega \neq 0$ the Hurwitz conditions are equivalent to a set of the following inequalities:

$$a_1 > 0 : f > (<) f_1, \quad a_2 > 0 : f > (<) f_2,$$
$$a_0 a_1 - a_2 > 0 : f > (<) f_3, \quad \omega > 0 (\omega < 0),$$

where $f_1 = -\omega\left(\sigma + 1 + \omega^2\right)/\sigma, \qquad f_2 = -\omega\left(R - 1 + \omega^2\right)/2,$

$f_3 = -\omega\left(\sigma^2 + 4\sigma - \sigma R + 2 + 2\omega^2\right)/\sigma^2$. Therefore, if $\omega > 0 \ (\omega < 0)$, the criterion of stability of any equilibrium of the system consists of a location of a point of the curve (1.32), corresponding to equilibria, above (below) all curves $f_{1,2,3}$. Equations $f = f_{1,2,3}, \ f = \rho/\sigma$ define bifurcation surfaces, which correspond to transformations of structures of trajectories at manifolds of equilibria.

The auxiliary functions have two simple properties that help studying the stability:

– function f_2 crosses f in the positions of extrema and at the origin;

– All curves cross each other at the origin and at three points $\omega_{1,2} = \pm\sqrt{\left(3\sigma - \sigma R + 2\right)/\left(\sigma - 2\right)}$.

Properties of equilibria will be discussed in more detail during the consideration of the rotation characteristic.

5) Chaotic attractors.

a) *Lorenz attractor*. For $\rho = \Lambda = 0$ equations (1.31) represent the Lorenz system (see Section 1.1). It is known that parameter *b* in the Lorentz system is a scale parameter and its value in relation to the properties of the system is not of fundamental importance. In this case, $b = 1$. As stated above, for $\sigma = \sigma^*$, $R = R^* > R_c$, $R_c = \left(\sigma^2 + 4\sigma\right)\Big/\left(\sigma - 2\right)$, strange attractor is a unique attracting limit set of trajectories. According to paragraph 4, the expression for R_c is defined by the condition of the coincidence of the zeros of functions *f* and f_3. This condition corresponds to the loss of stability of the equilibria $O_{2,3}\left(\pm\sqrt{R-1},\ \pm\sqrt{R-1},\ R-1\right)$ caused by the fact that unstable limit cycles get stuck in them. These limit cycles have been earlier born (by varying parameter *R*) from the separatrix loop of saddle $O_1(0,0,0)$. Le us remind that strange attractor begins to exist for $R = R^*$, where R^* is the value of the parameter *R* that corresponds to the separatrix loop of the saddle. In the interval $R^* < R < R_c$, the strange attractor and stable equilibria coexist, having non-overlapping attraction domains. In this interval of values of parameter *R*, depending on initial conditions, either a strange attractor or one of two stable equilibria would be born.

"Deformation" and degeneration of the Lorenz attractor for nonzero parameters ρ and Λ have been studied in a numerical experiment. For $\Lambda = 0$, and by increasing parameter ρ from zero, the attractor

loses its symmetry since the affix remains mostly in the vicinity of the right-hand saddle-focus (for the projection onto (x,z)-plane). Further, this equilibrium becomes stable after the birth of a saddle limit cycle (Andronov-Hopf bifurcation in reversed time). In this case, depending on the initial conditions, either equilibrium or a chaotic attractor may originate. With further increase of parameter ρ, the saddle limit cycle gets "stuck" in the separatrix loop of a saddle and the equilibrium becomes globally stable. Due to invariance of system (1.31) with respect to a change of the variables of the form $(x,y,z)\mapsto(-x,-y,z)$, $\rho\mapsto-\rho$ the same scenario of the degeneration of the Lorenz dynamical chaos occurs with the change of the parameter ρ towards lower values. The only difference is that now the right-hand equilibrium becomes globally stable. The same order of bifurcations also takes place for the small values of $|\Lambda|$. Asymmetric Lorenz attractors are shown in Figs. 1.28a,c. Note that for $\rho\Lambda>0$ and small values of $|\Lambda|$ there exists a value of ρ, for which the attractor loses its visual symmetry (see Fig. 1.28b).

b) *The Feigenbaum attractor and the alternation*. This type of chaotic attractors has been found for $\rho\Lambda>0$ and sufficiently large absolute values of Λ. In the numerical experiment $|\Lambda|\geq 7$. The Feigenbaum attractor is shown in Fig. 1.29a. For $\Lambda\leq -7$ and for increased parameter ρ, the left equilibrium of system (1.31) loses stability when a stable limit cycle is born. Further, this cycle expe-

riences a series of bifurcations of doubling of the period (pitchfork bifurcations). In some interval of values of parameter ρ the chaotic attractor is born and has the attraction domain isolated from the attraction domains of other limit sets. With the further increase of parameter ρ, the attraction domain of the attractor intersects with the attraction domain of another chaotic limit set (it has not been studied, which one exactly, but probably this limit set is an "inheritance" of the asymmetric Lorenz attractor). As a result, a typical alternation [7] is observed, see Fig. 1.29b. Since system (1.31) is invariant with respect to transformation $(x,y,z)\mapsto(-x,-y,z)$, $\rho\mapsto-\rho$, $\Lambda\mapsto-\Lambda$, the same scenario occurs for $\Lambda>0$ and decreased values of parameter ρ.

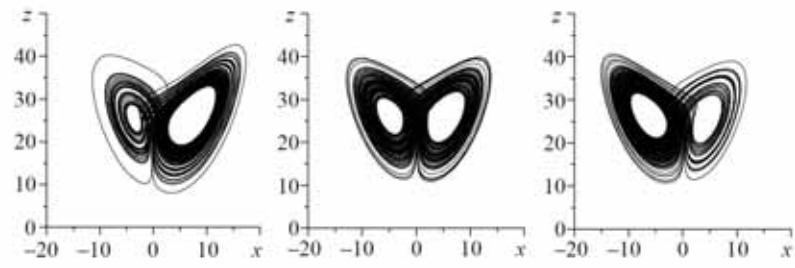

a b c

Fig. 1.28. Asymmetric Lorenz attractors (a: for $\sigma=9.7,\ R=27,\ \Lambda=-1,\ \rho=28.53$, c: for $\sigma=9.7,\ R=27,\ \Lambda=-1,\ \rho=-31.67$) and attractor with a visual symmetry (b: for $\sigma=9.7,\ R=27,\ \Lambda=-1,\ \rho=-3.5$).

For negative values of R and any values of other parameters, no chaotic attractors have been found in system (1.31).

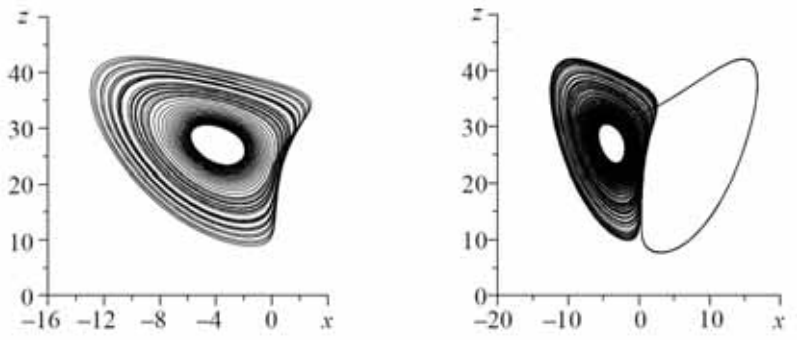

a b

Fig. 1.29. The Feigenbaum attractor: a: for $\sigma = 9.7,\ R = 27,\ \Lambda = -7$; b: for $\sigma = 9.7,\ R = 27,\ \Lambda = -7,\ \rho = -36.27$.

In the previous section, we have discussed the relationship between the properties of the averaged system and the initial system. In this case, the theory guarantees the existence of an arbitrarily large number of saddle-type tori in system (1.31) conditioned that chaotic attractors exist in this system. The same can be said about the bifurcation of doubling of the period of the torus. In other words, phase portraits of system (1.31) and portraits of the point mappings of system (1.27) must contain the same qualitative features. Let us illustrate this using the results of a numerical experiment.

Numerical experiment. For the sake of convenience, the Poincaré mapping $(x,\theta,\eta)_{\varphi=\varphi_0} \to (\bar{x},\bar{\theta},\bar{\eta})_{\varphi=\varphi_0+2\pi}$ for the following system that is equivalent to system (1.27):

$$\begin{aligned}
&\dot{\varphi} = \omega_0 + \mu x,\\
&\dot{x} = -\mu x - \sin\varphi + \theta\sin\varphi + \eta\cos\varphi + \gamma - \omega_0,\\
&\dot{\theta} = \mu x\eta - \delta\left(\theta\sin\varphi + \eta\cos\varphi\right)\sin\varphi + \left(b\sin\varphi + \frac{d}{\omega_0}\cos\varphi\right)\left(\omega_0 + \mu x\right),\\
&\dot{\eta} = -\mu x\theta - \delta\left(\theta\sin\varphi + \eta\cos\varphi\right)\cos\varphi + \left(b\cos\varphi - \frac{d}{\omega_0}\sin\varphi\right)\left(\omega_0 + \mu x\right).
\end{aligned} \tag{1.33}$$

During the transformation to system (1.33) transformation of the form (1.28) has been made for $\Phi \equiv x$.

Experiment 1. The following parameter set has been used: $d = -0.27508$, $\mu = 0.01$, $\delta = 0.0134$, $b = -0.005016$, $\omega_0 = 0.5$. The parameters are chosen such that their combinations are close to the values of parameters in the numerical experiment for averaged system (1.31). Fig. 1.30 shows a gallery of phase portraits and Poincaré mappings. Parameter $b = -0.005016$ is chosen to be small in order to correspond to a small value of parameter Λ of the averaged system. During the variation of parameter γ, the resonance zone is passed from left to right.

For $\gamma = 1.0448906$ and lower values, a periodic motion (limit cycle) is observed in system (1.33), see Fig. 1.30a. Fig. 1.30b shows a transient process of formation of a fixed point of the Poincaré mapping that represents a focus.

Similarly to the dynamics of an average system, for the increased values of parameter γ, the fixed point loses stability via the opposite Andronov-Hopf bifurcation, i.e. due to the sticking of the invariant curve (that corresponds to two-dimensional torus) in the equilibrium. As far as the phase space of system (1.33) is concerned, a sticking of an unstable torus into a limit cycle occurs that is followed by instability "transfer" from the torus to the limit cycle. As a result of this bifurcation, our system suddenly jumps from the regime of periodic motions to the regime of chaotic vibrations. As a result of this bifurcation, the system jumps from the periodic regime to the chaotic oscillation regime. Fig. 1.30c shows a segment of the chaotic phase trajectory on the involute of the phase cylinder, while Fig. 1.30d shows the corresponding segment of the discrete trajectory of the asymmetric Lorentz attractor in the space of the Poincaré point mapping.

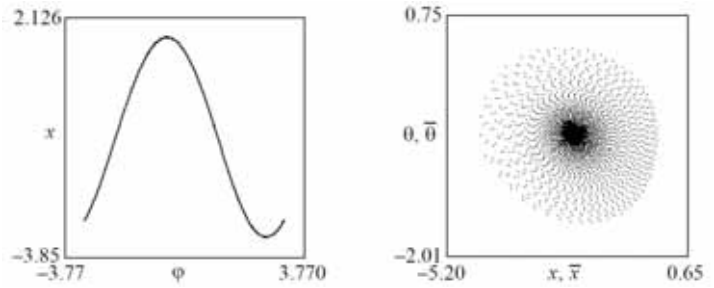

γ = 1.0448906

a b

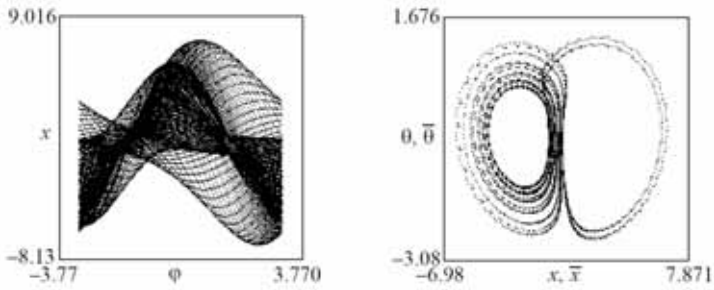

γ = 1.051491

c d

Fig. 1.30. The gallery of qualitatively different phase portraits and Poincaré mappings (continues on the next page).

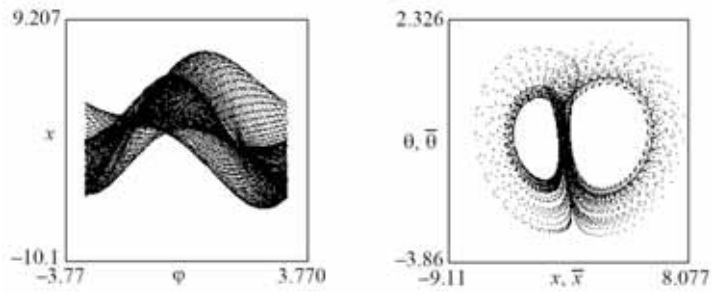

γ = 1.058991

e f

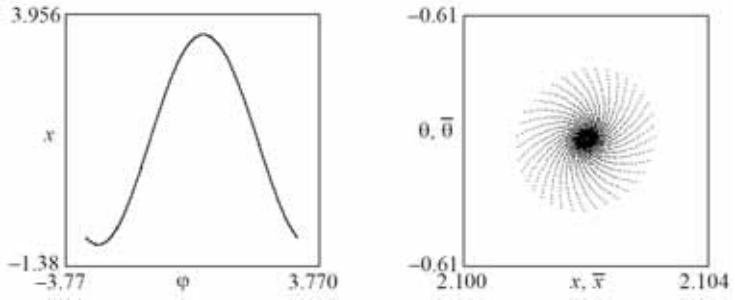

γ = 1.069291

g h

Fig. 1.30. Conclusion.

For the increased values of γ the strange attractor, first, becomes symmetric (see Figs. 1.30e,f), and then becomes asymmetric to the right. Further, the stability of the right fixed point (limit cycle) changes: being unstable, it becomes stable with the separation of an unstable invariant curve (torus) out of it. Further, the fixed point becomes globally stable (see Figs. 1.30g,h). Thus, in this case, the

bifurcation scenario described in paragraph 5a) for the averaged system is observed.

In what follows, let us numerically demonstrate the adequacy and effectiveness of the method of the averaging with respect to the period-doubling bifurcations of the torus.

Experiment 2. The following parameter set has been used: $d = -0.27508, \quad \mu = 0.01, \quad \delta = 0.01252, \quad b = -0.01875, \quad \omega_0 = 0.5.$ Note that parameters of the averaged system are quite "sensitive" to changes of initial parameters, in particular, parameter *b*. For selected parameters of system (1.27), the value of parameter Λ in system (1.31) is large and corresponds to the existence of the Feigenbaum attractor in the averaged system.

Fig. 1.31 shows a gallery of phase portraits and Poincaré mappings. Parameter γ is varied such that it approaches the resonance frequency from the right-hand side. For $\gamma < 1$, a stable limit cycle is observed – a fixed point of the Poincaré mapping. Further, this fixed point loses stability during the origination of a stable invariant curve (torus), see Fig. 1.31a. For increased γ, the torus including the quasi-periodic winding experiences a cascade of pitchfork bifurcations (see Figs. 1.31b-d). The series of bifurcations ends with origination of the strange Feigenbaum attractor, see Figs. 1.31e,f). Further, a crisis occurs that consists of an alternation of the Feigenbaum attractor with "remains" of non-symmetrical Lorenz attractor,

see (Figs. 1.31g,h). In this case, the affix remains most of the time in the vicinity of the Feigenbaum attractor, performing random ejections towards the right-hand fixed point and rapidly coming back again. For a further increase of γ, the same scenario of development and degradation of the dynamical chaos as described in Experiment 1 occurs. Such scenario of appearance and development of the chaos is the same as scenario described in paragraph 5b for the averaged system.

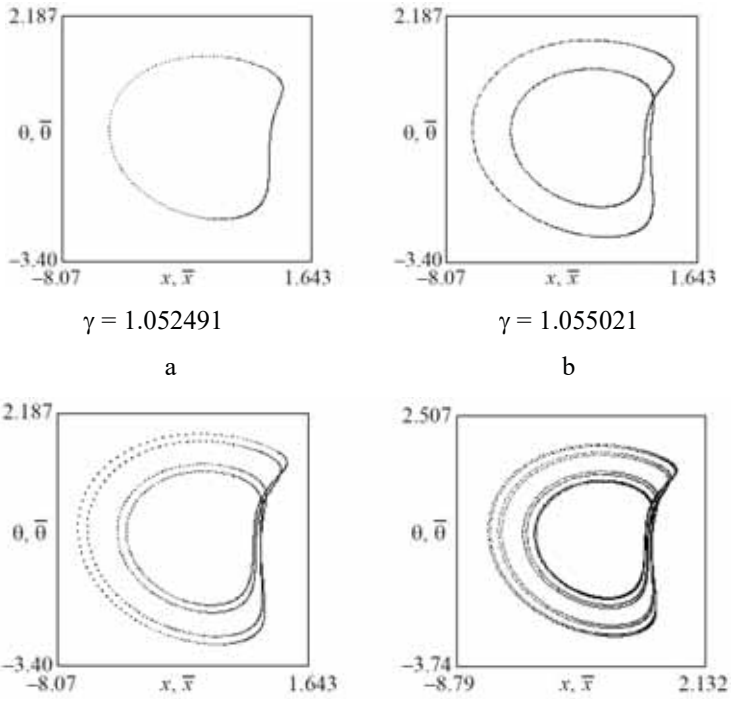

Fig. 1.31. The gallery of qualitatively different phase portraits and Poincaré mappings (continues on the next page).

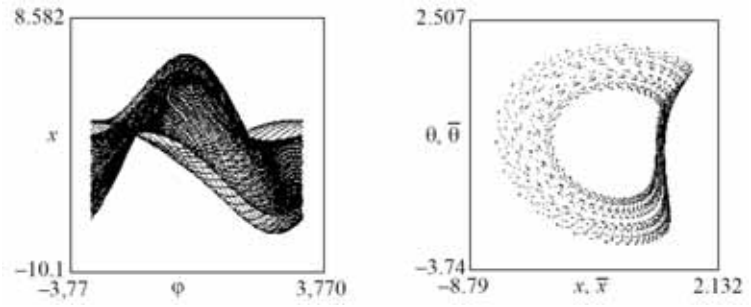

γ = 1.055795

e f

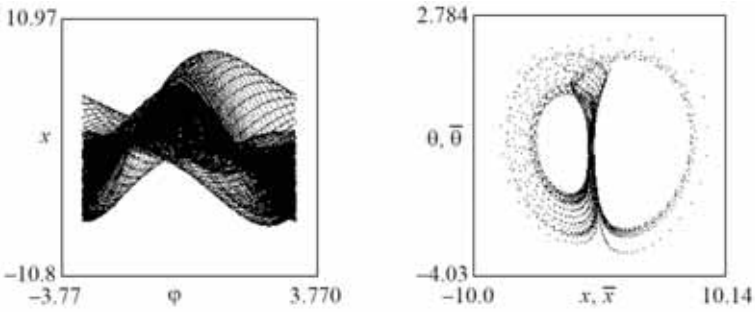

γ = 1.057391

g h

Fig. 1.31. Conclusion.

Using obtained results, let us study qualitative forms of rotation characteristic of rotator's rotations and resonance characteristic of the oscillatory system.

Rotation characteristic. First, we note that from the formulae of transformations of variables and parameters from (1.30) to system (1.31), it follows that $\gamma \sim \Delta \sim \rho$, $\xi(t) \sim x(t)$ (linear rela-

tions), i.e. rotation characteristic $\gamma = \gamma\left(\overline{\xi^*(t,t_0)}\right)$ and curve $\rho = \rho\left(\overline{x^*(t,t_0)}\right)$ have identical qualitative features. For the sake of convenience, we will consider this curve as a rotation characteristic.

Resonance characteristic.

Definition. The function $A(\Omega) = \max_t \left| \lim_{t\to\infty} J(t,t_0) \right|$, defined under parameter space and space of initial conditions in system (1.27) is called the resonance characteristic of oscillations. Since $\lim_{t\to\infty} J(t,t_0) = J^*(t,t_0)$, where $J^*(t,t_0)$ is the final solution for $J(t,t_0)$, then $A(\Omega) = \max_t \left| J^*(t,t_0) \right|$.

In Example 1, physically, the resonance characteristic defines a maximal angle of twist of the flexible rotor with respect to the frequency of rotation of the motor and initial conditions. In particular, if the motor (the energy source) has an unlimited power and its frequency is independent of the loading, then a resonance characteristic represents an amplitude-frequency characteristic of the oscillatory system.

Let us perform simple transformations. From the formulae of transition from Eqs. (1.27) to the system in a standard form, we obtain

$J-\frac{d}{\omega_0}=\sqrt{\theta^2+\eta^2}\sin\left(\varphi+\varphi_0\right)$, i.e. the expression for the amplitude of vibrations $A=\sqrt{\theta^2+\eta^2}$. On the other hand, the formulae of transition to system (1.31), we obtain $\left(y+\Lambda\right)^2+\left(z-R\right)^2=\frac{b_1^2b_4^2}{b_3^2+b_2^2}\left(\theta^2+\eta^2\right)$, i.e. $A=\frac{\sqrt{b_3^2+b_2^2}}{b_1b_4}\times$ $\times\sqrt{\left(y^*+\Lambda\right)^2+\left(z^*-R\right)^2}$, where $y^*\left(t,t_0\right)$, $z^*\left(t,t_0\right)$ is a stationary solution of system (1.31). For equilibria of system (1.31) (limit cycles of initial system (1.27)), we obtain $\left(y^*+\Lambda\right)^2+\left(z^*-R\right)^2=\frac{R^2+\Lambda^2}{1+\omega^2}$, i.e. $A=\frac{\sqrt{b_3^2+b_2^2}\sqrt{R^2+\Lambda^2}}{b_1b_4}\frac{1}{\sqrt{1+\omega^2}}$.

Since we are interested in qualitative forms of the resonance characteristic, let us consider its normalized form:

$$A^*\left(\rho\right)=\frac{1}{\sqrt{1+\left(\omega\left(\rho\right)\right)^2}}. \tag{1.34}$$

It is easy to see that both characteristics are interrelated. Having obtained the rotation characteristic, we also know the resonance characteristic, including the stability of its various sections.

1. For values of parameters Λ and R, satisfying the inequality $|\Lambda| \le \frac{R+8}{3\sqrt{3}}\sqrt{1-R}$, rotation characteristic is a one-to-one (hysteresis-free) curve that is stable at all points. In this case, the behavior of system (1.27) is similar to a linear system, and the resonance characteristic has a form similar to the amplitude-frequency characteristic of a linear oscillator, which follows directly from expression (1.34). The case is of a little interest.

2. Suppose that $\sigma = 10,\ \Lambda = 0$ (for which, system (1.31) takes the form of the Lorenz system), while parameter $R > 1$ and we keep increasing it. The qualitative forms of rotation characteristic and resonance characteristic for $R = 10$ and R = 27 are shown in Fig. 1.32. As usual, bold lines indicate stable sections of rotation and resonance characteristics, while dashed lines indicate the unstable ones. Thin lines indicate graphs of auxiliary functions $f_{1,2,3}$, defining stability of equilibria of system (1.31).

For all $R > 1$, the rotation characteristic in the zone of resonance has a symmetric hysteretic loop. And for all values from the interval $1 < R < (3\sigma + 2)/\sigma$, only the falling section of the rotation characteristic is unstable and, accordingly, the upper section of the resonance characteristic, enclosed between the vertical tangents is also unstable. This follows from the condition of the existence of the intersection point of curves $f_{1,2,3}$ (see properties of the averaged

system). In system (1.31), the only bifurcations are bifurcations of merging and disappearing equilibria that occur at the extrema of the rotation characteristic. Consequently, the frequency jumps of the rotator from the state of resonance to the post-resonant regime and vice versa taking place from the upper and lower extrema. The respective amplitude jumps occur from intersection points with a vertical tangent. This case is not depicted, but it can be restored from the next one.

For $R > (3\sigma + 2)/\sigma$, certain sections of positively sloped rotation characteristic curves become unstable, see Fig. 1.32a. As described above, the limit cycle of (1.27) loses stability due to "sticking" of an unstable torus. As a result, the frequency jumps of the rotator are performed from the points of positively sloped sections as shown in Fig. 1.32a. Accordingly, the jumps of the oscillator's amplitudes occurs from points below the vertical tangent (Fig. 1.32b). The depth of the hysteretic loop decreases to zero as parameter R approaches the value of R_c.

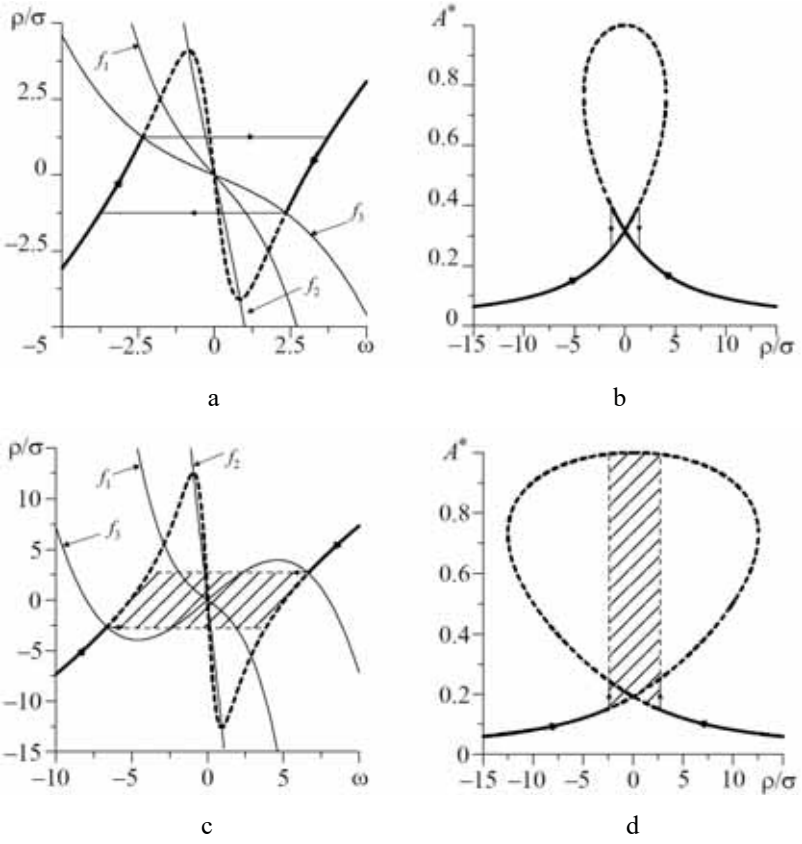

Fig. 1.32. Rotation and resonance characteristics for $\Lambda = 0$ and $R = 10$ (a, b) and $R = 27$ (c, d), respectively.

When parameter R grows above R_c, then a "gray" area that corresponds to chaotic oscillations appears at both rotation and resonance characteristics (Figs. 1.32c,d). In this area, the rotation frequency of the rotator and the amplitude of vibrations of the oscillator make random transitions from the pre-resonant to the post-resonant state. In this case, the average frequency and amplitude

have uncertain values. The forms of rotation and resonance characteristics are uncertain. The reasons for this have already been discussed in the previous sections.

3. The asymmetry of rotation and resonance characteristics, hardly noticeable for small values of Λ, becomes apparent for increased $|\Lambda|$. Fig. 1.33 shows a gallery of rotation and resonance characteristics for $\Lambda = -3$ and various values of *R*. In this case, rotation characteristic is hysteretic including the small values of *R*, while resonance characteristic turns to the right (see Figs. 1.33a,b). As parameter *R* is increased further, unstable sections of rotation and resonance characteristics increase (see Figs. 1.33c,d). The dynamics of the system, as in the previous case, remains regular for all ρ.

For the increased values of *R*, the depth of the hysteresis decreases to zero, and then the uncertainty zone of rotation and resonance characteristics appears, which corresponds to the chaotic dynamics of the system (see Figs. 1.33f,g). The scattering effect of rotation and resonance characteristics discussed above occurs in the shaded areas. The bifurcation scenario for the development of dynamic chaos with a slow increase in the torque of the rotator is explained above in Numerical Experiment 2.

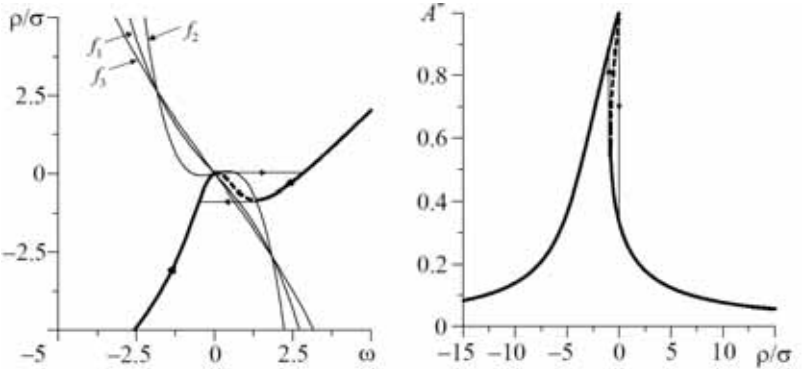

Λ = –3, R = 0.5

a b

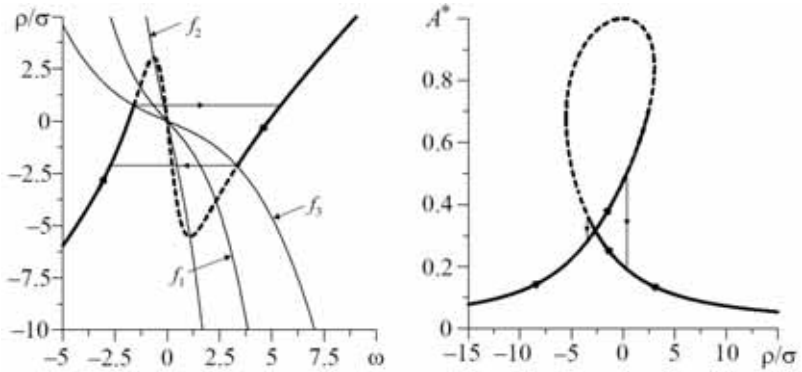

Λ = –3, R = 10

c d

Fig. 1.33. Rotation and resonance characteristics for Λ = –3 and different values of R (continues on the next page).

4. For the increased values of $|\Lambda|$, the zones of uncertainty of both characteristics decrease and disappear for some $|\Lambda^*|$ and given R. In other words, for all “moderate” values of parameter R and large

$|\Lambda|$, the system dynamics is regular for all values of parameter ρ. Fig. 1.34 shows a gallery of rotation and resonance characteristics for $\Lambda = -20$ and different values of R.

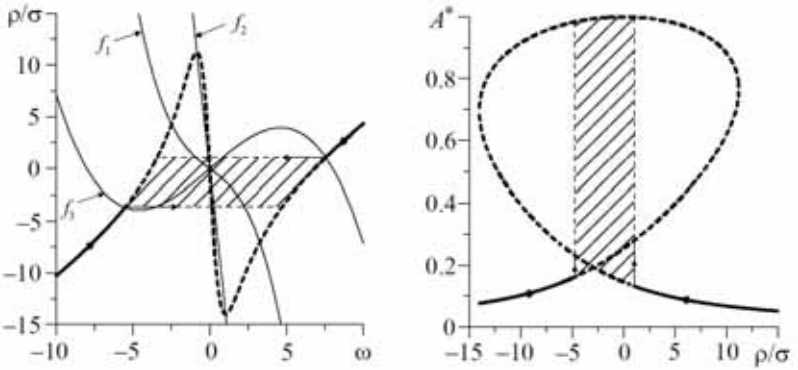

$\Lambda = -3$, $R = 27$

e f

Fig. 1.33. Conclusion.

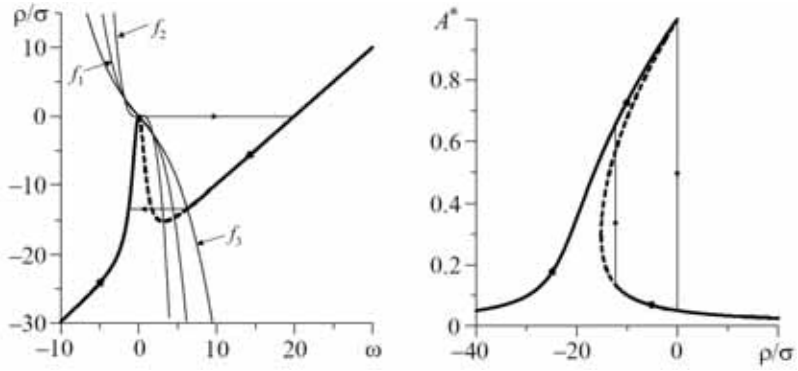

a b

Fig. 1.34. Rotation and resonance characteristics for $\Lambda = -20$ and various R (continues on the next page).

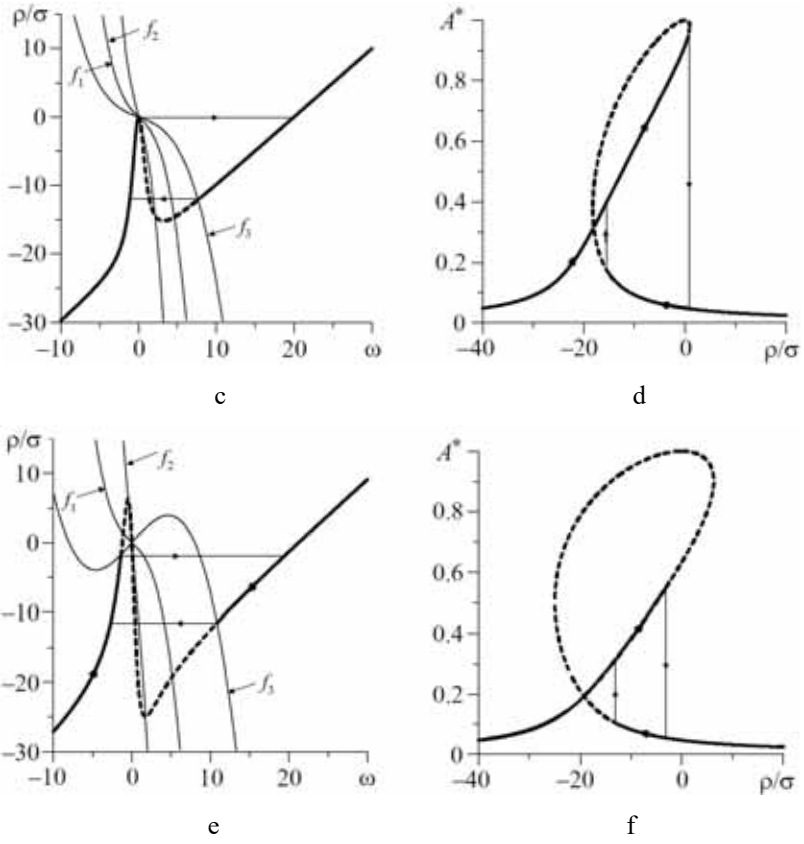

Fig. 1.34. Conclusion.

For the given value of Λ and aforementioned values of R, the dynamics of the system is regular throughout the zone of resonance. Jumps in the frequency of the rotator and in the amplitude of the oscillator's vibration are conditioned by bifurcations of periodic motions of system (1.27) (equilibria of system (1.31)). Figs. 1.34a,b are plotted for $R = 0.5$. The frequency jump towards the right-hand

side takes place from the maximum of the rotation characteristic, which corresponds to the merging of stable and unstable equilibria, followed by the disappearance of a complex fixed point as parameter ρ increases. The frequency jump towards the left-hand side is associated with the loss of stability of the equilibrium due to the "sticking" of an unstable limit cycle. For the increased values of R, a part of the left positively sloped section of rotation characteristic and the respective section of the resonance characteristic become unstable (see Figs. 1.34c-f); $R = 10$ and $R = 27$, respectively.

To interpret dynamical properties of the model onto the physical system "*flexible shaft – asynchronous electric motor*", we remind that parameter ρ is proportional to the torque, while amplitude A^* is proportional to the amplitude of torsional vibrations of the shaft. It is obvious that the regime of chaotic vibrations, which is performed by multiple spontaneous and, at the same time, significant jumps in the rotation frequency and the amplitude of the angle of twist of the shaft, is extremely unfavourable for the system and can lead to its failure. In the case of a "*superconductive junction – resonator*" system, rotational speed of the rotator is proportional to the voltage at the junction; parameter ρ is proportional to the current of the external source; and the amplitude A^* is proportional to the amplitude of the first harmonic of the resonator. Thus, the above types of rotation characteristic are types of volt-ampere characteristic of the superconductive junction. Bifurcations of dynamical re-

gimes of this system (periodic → quasiperiodic with doubling of the period → chaotic) can be identified by the change in the vibration spectrum when it passes from linear to continuous form.

Finally, let us provide expression for the width of the "gray" area l_ρ for $\Lambda = 0$. It is evident that $l_\rho = \sigma\left(f\left(\omega_2\right) - f\left(\omega_1\right)\right)$, where $\omega_{1,2}$ are the roots of equation $f\left(\omega\right) = f_3\left(\omega\right)$. Solving this equation and applying transformations, we obtain the expression for l_ρ:

$$l_\rho = \left(R - 4 - \sqrt{\left(R - 4 - 2\sigma\right)^2 + 8R}\right) \times$$

$$\times \sqrt{\frac{\sigma}{4}\left(R - 4 - 2\sigma + \sqrt{\left(R - 4 - 2\sigma\right)^2 + 8R}\right) - 1}.$$

For instance, for $\sigma = 10$, $R = 27$: $l_\rho / \sigma = 5.3066$, while for $\sigma = 10$, $R = 27$, $\lambda = -3$ (see Figs. 1.34e,f), the width of the area equals 5.8, which has not much difference to the case $\Lambda = 0$.

Note that from the condition $l_\rho > 0$, we obtain already familiar inequality $R > R_c = \left(\sigma^2 + 4\sigma\right) / \left(\sigma - 2\right)$, which determines the condition of existence of Lorenz attractor being a unique attracting limit in the phase space of the system.

1.6. Dynamics of coupled rotators

A model of coupled rotators is governed by a system of differential equations of the form [139]

$$\begin{aligned} I\ddot{\varphi}_1 + \delta_1\dot{\varphi}_1 + \sigma_1 \sin\varphi_1 &= \gamma_1 + a_1\dot{\varphi}_2 + b_1 \sin\varphi_2, \\ I\ddot{\varphi}_2 + \delta_2\dot{\varphi}_2 + \sigma_2 \sin\varphi_2 &= \gamma_2 + a_2\dot{\varphi}_1 + b_2 \sin\varphi_1. \end{aligned} \tag{1.35}$$

This system is defined in a toroidal phase space $G\left(\varphi_{1,2},\ \dot{\varphi}_{1,2}\right) = T^2 \times R^2$ and it will be considered in the following parameter domain:

$$D = \left\{ I > 0,\ \delta_{1,2} > 0,\ \gamma_{1,2} \geq 0,\ \delta_1\delta_2 - a_1a_2 > 0,\ \sigma_{1,2} \geq 0 \right\}.$$

We will be interested in solving the following problems of dynamics of system (1.35):

- determination of parameter domains that correspond to various topologically different motions of the system: oscillatory motions, rotary-oscillatory motions, and rotary motions of rotators;
- study of qualitative forms of trajectories and bifurcations of rotary motions;
- obtaining qualitative forms of rotation characteristics of rotators.

1. Dynamics of rotators and attracting sets of trajectories of system (1.35).

It has been shown in [139], that, in the phase space $G\left(\varphi_{1,2}\,,\ \dot{\varphi}_{1,2}\right)$ of system (1.35), there exists a toroidal absorbing region

$$G^{*}\left(\varphi_{1,2}\,,\ \dot{\varphi}_{1,2}\right)=\left(\forall\varphi_{1,2}\,,\ \omega_{1,2}-\omega_{1,2}^{0}\le\dot{\varphi}_{1,2}\le\omega_{1,2}+\omega_{1,2}^{0}\right),$$

$$\omega_1=\frac{\gamma_1\delta_2+\gamma_2 a_1}{\delta_1\delta_2-a_1a_2},\ \ \omega_2=\frac{\gamma_2\delta_1+\gamma_1 a_2}{\delta_1\delta_2-a_1a_2},$$

such that all trajectories that enter it remain there forever, i.e. for $\tau\to\infty$. It means that for parameters that belong to domain *D*, all limit sets of trajectories of the system under consideration remain in the absorbing region G^{*} of the phase space and any solution $\left(\varphi_1\left(\tau,\tau_0\right),\ \varphi_2\left(\tau,\tau_0\right)\right)$ has finite derivatives $\dot{\varphi}_1\left(\tau,\tau_0\right),\ \dot{\varphi}_2\left(\tau,\tau_0\right)$.

Let us subdivide the limit sets of phase trajectories within domain G^{*} into sub-classes:

- K_{00} is the class of trajectories bounded by φ_1 and φ_2;
- K_{0r} is the class of trajectories bounded by φ_1 and not bounded by φ_2;

- K_{r0} is the class of trajectories not bounded by φ_1 and bounded by φ_2;

- K_{rr} is the class of trajectories not bounded by φ_1 and not bounded by φ_2.

It is evident that $\left\langle \dot{\varphi}_1^* \right\rangle_\tau = 0$, $\left\langle \dot{\varphi}_2^* \right\rangle_\tau = 0$, if $L^* \in K_{00}$; $\left\langle \dot{\varphi}_1^* \right\rangle_\tau \neq 0$, $\left\langle \dot{\varphi}_2^* \right\rangle_\tau = 0$, if $L^* \in K_{r0}$; $\left\langle \dot{\varphi}_1^* \right\rangle_\tau = 0$, $\left\langle \dot{\varphi}_2^* \right\rangle_\tau \neq 0$, if $L^* \in K_{0r}$; $\left\langle \dot{\varphi}_1^* \right\rangle_\tau \neq 0$, $\left\langle \dot{\varphi}_2^* \right\rangle_\tau \neq 0$, if $L^* \in K_{rr}$. Determination of parameter domains that correspond to various classes of non-wandering trajectories will be carried out by the method of two-dimensional comparison systems [42].

For each equation of system (1.35), we introduce comparison systems of the form

$$\begin{aligned} A_1^{\pm} &: I\ddot{\varphi}_1 + \delta_1\dot{\varphi}_1 + \sigma_1 \sin\varphi_1 = \delta_1\omega_1 + \mu_1^{\pm}, \\ A_2^{\pm} &: I\ddot{\varphi}_2 + \delta_2\dot{\varphi}_2 + \sigma_2 \sin\varphi_2 = \delta_2\omega_2 + \mu_2^{\pm}, \end{aligned} \tag{1.36}$$

where

$$\delta_{1,2}\omega_{1,2} + \mu_{1,2}^{+} = \sup_{\forall(\varphi_{1,2},\dot{\varphi}_{1,2})\in G^*} \left(\gamma_{1,2} + a_{1,2}\dot{\varphi}_{1,2} + b_{1,2}\sin\varphi_{1,2}\right),$$

$$\delta_{1,2}\omega_{1,2} + \mu_{1,2}^{-} = \inf_{\forall(\varphi_{1,2},\dot{\varphi}_{1,2})\in G^{*}} \left(\gamma_{1,2} + a_{1,2}\dot{\varphi}_{1,2} + b_{1,2}\sin\varphi_{1,2}\right),$$

$$\mu_{1,2}^{\pm} = \pm\left(\left|a_{1,2}\right|\omega_{1,2}^{0} + \left|b_{1,2}\right|\right).$$

Trajectories of the comparison systems define surfaces that have no contact with the vector field of system (1.35) in the phase space $G\left(\varphi_{1,2}, \dot{\varphi}_{1,2}\right)$. This can be proven by considering the rotation of the vector field of the system on the trajectories of the comparison systems. It means that if both systems $A_k^{\pm}$ ("plus" and "minus") have topologically similar structures of trajectories on the involutes of cylinders $\left(\varphi_k, \dot{\varphi}_k\right)$, then projections of limit sets $K_{(.)}$ onto these involutes turn out to lie between special manifolds of comparison systems (see Fig. 1.35). Fig. 1.35 shows separatrices of saddles and limit cycles of comparison systems. Arrows indicate direction of the component of the vector field of system (1.35) along these trajectories.

Let us introduce the following notations: $D_{(0)k}^{\pm}$, $D_{(0r)k}^{\pm}$, $D_{(r)k}^{\pm}$, $k = 1, 2$ for the parameter domains, for which both comparison systems $A_k^{\pm}$ (separately for each index *k*) have a globally stable equilibrium, a globally stable equilibrium and a limit cycle, and globally stable limit cycle, respectively (see Fig. 1.35, as well as Section

1.2). For parameter planes $\left(\lambda_k, \gamma_k^{\pm}\right)$, where $\lambda_k = \delta_k \left(I\sigma_k\right)^{-\frac{1}{2}}$, $\gamma_k^{\pm} = \dfrac{\delta_k \omega_k + \mu_k^{\pm}}{\sigma_k}$, these domains are separated by line $\gamma_k^{\pm} = 1$ (bifurcation of equilibrium) and Tricomi curve $\lambda_k = \lambda_k^{*}\left(\gamma_k^{\pm}\right)$ (bifurcation of the separatrix loop). Bifurcation diagrams of comparison systems are shown in Fig. 3.12. The hatching shows the projections of the absorbing regions for various classes of trajectories. Bifurcation diagrams of comparison systems are shown in Fig. 1.36. The hatching shows the projections of the absorbing regions for various classes of trajectories.

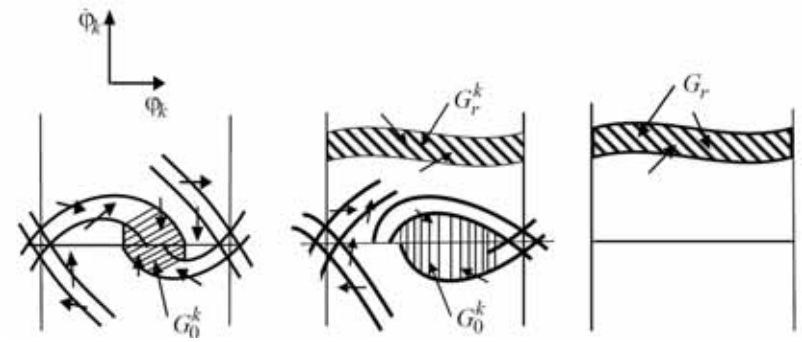

a b c

Fig. 1.35. Qualitative forms of trajectories of comparison systems and orientation of projection of the vector field of system (1.35) on their special trajectories.

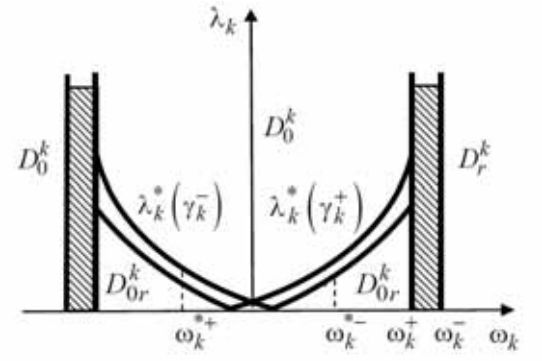

Fig. 1.36. Combined bifurcation diagram for comparison systems.

It is evident that for parameter domains $D_{(.)}^k = D_{(.)k}^+ \bigcap D_{(.)k}^-$, comparison systems $A_k^{\pm}$ have similar structures of trajectories on involutes $(\varphi_k, \dot{\varphi}_k)$. From the aforesaid case, we can make the following statements regarding parameter domains of existence of the aforementioned classes of limit sets of trajectories of system (1.35). For parameter domain $D_{00} = D_0^1 \times D_0^2$, there exists a limit set of trajectories $K_{00} \in G_0^1 \times G_0^2$, which is realized for any initial condition; for parameters $D_{0r} = D_0^1 \times D_r^2$, there exists a globally stable limit set $K_{0r} \in G_0^1 \times G_r^2$, from any initial condition, the system reaches the state when the first rotator experiences oscillatory motion, while the second one is rotating (we are not yet talking about specific forms of movements); for parameter domain $D_{r0} = D_r^1 \times D_0^2$ there exists a globally stable limit set

$K_{00} \in G_0^1 \times G_0^2$, for parameters $D_{0r} = D_0^1 \times D_r^2$, there exists a globally stable limit set $K_{0r} \in G_0^1 \times G_r^2$, Outside of those parameter domains, there exist populations of sets of trajectories of different types that are realized depending on the initial conditions. A mutual distribution of parameter domains is shown in Fig. 1.37.

Let us introduce another form of system of coupled rotators, for which we consider a physical example [140].

Fig. 1.38 shows an electric scheme of two superconductive junctions with a capacitive coupling.

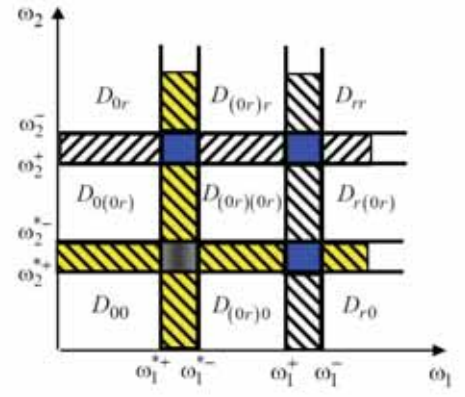

Fig. 1.37. Decomposition of parameter plane into domains that correspond to different classes of trajectories.

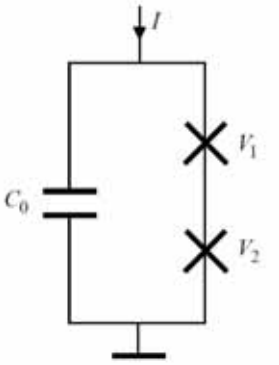

Fig. 1.38. Electric scheme of two superconductive junctions with capacitive coupling.

In physical variables and parameters, the Kirchhoff rules and the Josephson relation result in the following dynamical model of the system under consideration:

$$\begin{aligned} &C_1\frac{dV_1}{dt}+R_1^{-1}V_1+I_{c1}\sin\varphi_1=I-C_0\frac{d\left(V_1+V_2\right)}{dt},\\ &C_2\frac{dV_2}{dt}+R_2^{-1}V_2+I_{c2}\sin\varphi_2=I-C_0\frac{d\left(V_1+V_2\right)}{dt},\\ &\frac{d\varphi_1}{dt}=\frac{2\pi}{\Phi_0}V_1,\qquad \frac{d\varphi_2}{dt}=\frac{2\pi}{\Phi_0}V_2. \end{aligned} \tag{1.37}$$

Here $V_{1,2}$ are the potential differences of superconductors; $C_{1,2}$, $R_{1,2}$, $I_{c1,c2}$ are their capacitances, normal resistances, and values of critical overcurrent, respectively; C_0 is the capacitance of the coupling.

We introduce physical and dimensionless parameters, as well as dimensionless time, as follows:

$$I_c=\frac{I_{c1}+I_{c2}}{2},\ R=\frac{R_1+R_2}{2},\ \frac{2\pi RI_c}{\Phi_0}=\Omega,\ \Omega t=\tau,\ C_{1,2}\Omega R=c_{1,2},$$

$$C_0\Omega R=c_0,\ \ r_{1,2}=\frac{R_{1,2}}{R},\ \ v_{1,2}=\frac{I_{c1,c2}}{I_c},\ \ i=\frac{I}{I_c}.$$

Instead of system (1.37), we obtain a dimensionless system of the form

$$c_1\ddot{\varphi}_1 + r_1^{-1}\dot{\varphi}_1 + v_1 \sin\varphi_1 = i - c_0\left(\ddot{\varphi}_1 + \ddot{\varphi}_2\right),$$
$$c_2\ddot{\varphi}_2 + r_2^{-1}\dot{\varphi}_2 + v_2 \sin\varphi_2 = i - c_0\left(\ddot{\varphi}_1 + \ddot{\varphi}_2\right). \tag{1.38}$$

By solving system (1.38) with respect to higher-order derivatives, we obtain system (1.35). Parameters of these two systems are related to each other as follows:

$$I = \frac{c_1c_2 + c_0\left(c_1 + c_2\right)}{c_0},\ \ \delta_{1,2} = \left(1 + \frac{c_{2,1}}{c_0}\right)\frac{1}{r_{1,2}},\ \ \sigma_{1,2} = \left(1 + \frac{c_{2,1}}{c_0}\right)v_{1,2},$$
$$\gamma_{1,2} = \frac{c_{2,1}}{c_0}i,\ \ a_{1,2} = \frac{1}{r_{2,1}},\ \ b_{1,2} = v_{2,1},\ \ \omega_{1,2} = r_{1,2}i.$$

In what follows, in addition to system (1.35), we consider an equivalent system (1.38). The following statement answers the question on the composition of the limit set of trajectories K_{00}.

System (1.38), as well as system (1.35), has no closed limited phase trajectories (limit cycles of oscillatory type). This property is proven by means of the periodic Lyapunov function

$$V = \frac{1}{2}\sum_{k=1}^{2} c_k c_0^{-1}\dot{\varphi}_k^2 + c_0^{-1}\sum_{k=1}^{2}\int_{\varphi_{0k}}^{\varphi_k}\left(v_k \sin\varphi_k - i\right)d\varphi_k + \frac{1}{2}\left(\dot{\varphi}_1 + \dot{\varphi}_2\right)^2,$$

the derivative of which along the vector field of system (1.38) has the form

$$\dot{V} = -\frac{1}{r_1c_0}\dot{\varphi}_1^2 - \frac{1}{r_2c_0}\dot{\varphi}_2^2.$$

i.e. the derivative is non-positive in the whole phase space $G\left(\varphi_{1,2},\, \dot{\varphi}_{1,2}\right)$.

This means that limit trajectories of limit set K_{00} are (only) the equilibria: stable equilibrium

$$O_1\left(\varphi_1,\, \varphi_2,\, \dot{\varphi}_1,\, \dot{\varphi}_2\right) = O_1\left(\arcsin\frac{i}{\nu_1},\ \arcsin\frac{i}{\nu_2}, 0, 0\right) \text{ (knot or focus)}$$

and saddle-type equilibria: $O_2\left(\pi - \arcsin\frac{i}{\nu_1},\ \arcsin\frac{i}{\nu_2}, 0, 0\right)$,

$$O_3\left(\arcsin\frac{i}{\nu_1},\ \pi - \arcsin\frac{i}{\nu_2},\, 0,\, 0\right),\ O_4\left(\pi - \arcsin\frac{i}{\nu_1}, \pi - \arcsin\frac{i}{\nu_2},\, 0,\, 0\right).$$

The only bifurcation of equilibria is the fusion of the entire four equilibria that is followed by the formation of a complex equilibrium that disappears at $i = \min\left(\nu_1, \nu_2\right) + 0 = i_0 + 0$.

2. Structures of trajectories and bifurcations of rotary motions of rotators.

Let us consider a qualitative structure of the set of rotary motions K_{rr}. We will select parameters of the system from those domains, for which rotary motions of both rotators occur (see Fig. 1.37). This can take place for initial conditions for a part of the phase space if parameters are chosen from domains $D_{(0r)(0r)}$, $D_{(0r)r}$, $D_{r(0r)}$, or

for the whole phase space if parameters are chosen from domain D_{rr}. Let us consider asymptotic case $I \gg 1$.

Using a change of the variables (see Appendix) of the form

$$\dot{\varphi}_1 = \omega_1 + \mu\Phi_1(\varphi_1, \varphi_2, x_1), \quad \dot{\varphi}_2 = \omega_2 + \mu\Phi_2(\varphi_1, \varphi_2, x_2),$$
$$\Phi_1 = \frac{\sigma_1}{\omega_1}\cos\varphi_1 - \frac{b_1}{\omega_2}\cos\varphi_2 + x_1, \quad \Phi_2 = \frac{\sigma_2}{\omega_2}\cos\varphi_2 - \frac{b_2}{\omega_1}\cos\varphi_1 + x_2,$$
$$\mu = I^{-1}$$

we reduce system (1.35) to an equivalent system with fast-spinning phases $\varphi_{1,2}$. In the zone of the main resonance of $\omega_1 \approx \omega_2$, the averaged system has the form

$$\begin{aligned} \dot{x}_1 &= \mu(-\delta_1 x_1 + a_1 x_2 - B_1 \sin\eta), \\ \dot{x}_2 &= \mu(-\delta_2 x_2 + a_2 x_1 + B_2 \sin\eta), \\ \dot{\eta} &= \mu(\Delta + x_1 - x_2). \end{aligned} \tag{1.39}$$

Here $\eta = \varphi_1 - \varphi_2$ is the phase mistuning, $\omega_1 - \omega_2 = \mu\Delta$ is the frequency mistuning, $B_1 = \frac{b_1(\sigma_1 + b_2)}{2\omega_1\omega_2}$, $B_2 = \frac{b_2(\sigma_2 + b_1)}{2\omega_1\omega_2}$. Note that the condition of closeness of normal frequencies of rotators $\omega_{1,2}$ means that, first, parameters of the system are chosen from a small vicinity of the diagonal line of plane (ω_1, ω_2), and, second, closeness of parameters $r_{1,2}$: $\mu\Delta = (r_1 - r_2)i$.

In turn, Eqs. (1.39) for a change of time $\mu\Omega_0\tau=\tau_n$, $\Omega_0=\left(\dfrac{B_1\left(\delta_2-a_2\right)+B_2\left(\delta_1-a_1\right)}{\delta_1+\delta_2}\right)^{\frac{1}{2}}$, are reduced to an already known equation of the third order (see Sections 1.3 and 1.4)

$$\beta\dddot{\eta}+\ddot{\eta}+\alpha\cos\eta\dot{\eta}+\lambda^r\dot{\eta}+\sin\eta=\gamma^r, \tag{1.40}$$

where

$$\beta=\frac{\Omega_0}{\delta_1+\delta_2},\quad \alpha=\frac{B_1+B_2}{\Omega_0\left(\delta_1+\delta_2\right)},\quad \lambda^r=\frac{\delta_1\delta_2-a_1a_2}{\Omega_0\left(\delta_1+\delta_2\right)},$$

$$\gamma^r=\frac{\delta_1\delta_2-a_1a_2}{\Omega_0^2\left(\delta_1+\delta_2\right)}\Delta.$$

Qualitative structures of trajectories of this equation are already known (see Section 1.3), while their interpretation onto system (1.35) is provided in Section 1.4.

Note that, for identical symmetrically coupled rotators, system (1.39) has a unique globally stable integral manifold $x_1=-x_2$. This manifold is decomposed into trajectories by trajectories of the equation of a free pendulum:

$$\ddot{\eta}+\left(\delta+a\right)\dot{\eta}+2B\sin\eta=0. \tag{1.41}$$

During the transformation of system (1.39) to system (1.41), a transformation of time has been made $\mu\tau = \tau_n$. In turn, this equation has equilibrium $O(\eta, \dot{\eta}) = O(0,0)$, which is globally stable, i.e. the dynamics of identical slightly nonlinear rotors in the parameter domain D is quite simple: for any initial condition over the course of time, a synchronization of rotary motions is observed in the coupled system.

3. Rotation characteristics of rotators.

By studying equilibria of system (1.38) we have solved the problem of zero steps of the rotation characteristics of rotators that correspond to the superconducting branches of the current-voltage characteristics of the superconductive junctions in the scheme shown in Fig. 1.38. Zero steps exist and are stable in the interval $0 \le i < i_0$.

Synchronization of rotations of the rotators. Let us turn to system (1.39) and to Eq. (1.40). Eq. (1.40) has two equilibria: $O_1(\eta, \dot{\eta}, \ddot{\eta}) = O_1\left(\arcsin\gamma^r,\ 0,\ 0\right)$ (knot or focus) and $O_2\left(\pi - \arcsin\gamma^r, 0, 0\right)$ (saddle). Equilibrium O_1 is stable in the whole area of existence (see Section 1.3) and corresponds to the limit cycle of system (1.35), i.e. to the regime of stable mutual synchronization of rotators. A holding range (range of existence) of synchronization is defined by a system of inequalities $\left|\gamma^r\right| \le 1$,

$i > i^*$. The first one corresponds to existence of equilibrium of Eq. (1.40), while the second one defines the domain of rotations of rotators. i^* defines the border that separates the domain of rotations from the domain of global stability of equilibrium of system (1.38). The exact value i^* is determined experimentally. Also, the following estimation is valid: $i^* = \max\left(r_1^{-1}\omega_1^{*-},\ r_2^{-1}\omega_2^{*-}\right)$. In the expanded form, the region of existence of synchronization is determined by a double inequality of the form

$$i^* < i < i_*,\quad i_* = \left(\frac{c_0 v_1 v_2}{|r_1 - r_2|\left(c_1 + c_2\right)\left(c_1 c_2 + c_0 c_1 + c_0 c_2\right)}\right)^{\frac{1}{3}}.$$

In the regime of synchronization the mean value of partial frequencies $\Omega_1 = \Omega_1 = \dfrac{\omega_1 + \omega_2}{2} = \dfrac{r_1 + r_2}{2} i,$ which is quite natural.

To obtain the full picture of the rotation characteristic, it is necessary to add branches that correspond to the regimes of beatings of rotators to the synchronization branch.

From the boundedness of derivatives $\dot{\varphi}_{1,2}$ it follows that $\left\langle \ddot{\varphi}_1^* \right\rangle_\tau - \left\langle \ddot{\varphi}_2^* \right\rangle_\tau = \left\langle \ddot{\eta}^* \right\rangle_\tau = 0.$ In this case, by using a change of variables and system (1.39), we obtain:

$$\Omega_{1,2} = \omega_{1,2} + d^{-1}\left(\left(\delta_{2,1} + a_{1,2}\right)\left(\left\langle \dot{\eta}^* \right\rangle_\tau - \mu\Delta\right) + \mu\left(B_1 + B_2\right)\left\langle \sin\eta^* \right\rangle_\tau\right),$$
$$d = \delta_2 - \delta_1 + a_1 - a_2. \tag{1.42}$$

It follows from the properties of Eq. (1.40) that for increased parameter γ^r (increased parameter Δ, and, therefore, increased parameter *i*) $\left\langle \dot{\eta}^* \right\rangle_\tau \to \mu\Delta$, $\left\langle \sin\eta^* \right\rangle_\tau \to 0$. Therefore, $\Omega_{1,2} \to \omega_{1,2}$, i.e. lines $i = r_{1,2}^{-1}\Omega_{1,2}$ represent asymptotes for the branches of beatings. We we assume that $r_1 > r_2$. In this case, $\gamma^r > 0$, $\left\langle \dot{\eta}^* \right\rangle_\tau > 0$, and, therefore, $\Omega_1 - \Omega_2 = \left\langle \dot{\eta}^* \right\rangle_\tau > 0$, $\Omega_1 > \Omega_2$. The branches of the partial frequencies of the rotation characteristics that correspond to the beatings are located on the opposite sides of the synchronization branch. We also note that when the parameter *i* is varied, then parameters $\gamma^r \sim i^3$ and $\lambda^r \sim i$ vary along line $\gamma^r = \alpha\left(\lambda^r\right)^3$, where $\alpha > 0$.

Fig. 1.38 shows one of the bifurcation diagrams in the plane $\left(\lambda^r,\ \gamma^r\right)$ and lines $L_{1,2,3}\left(\gamma^r = \alpha_{1,2,3}\left(\lambda^r\right)^3\right)$, which correspond to qualitatively different cases.

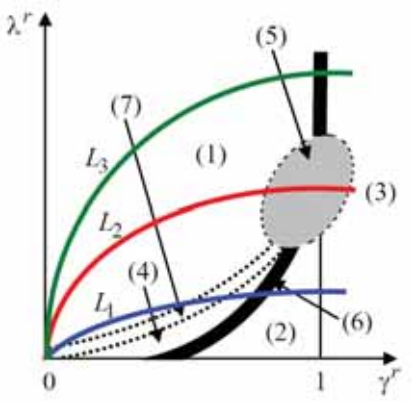

Fig. 1.38. Bifurcation diagram of parameters of Equation (1.40).

Let us remind the reader that for the parameters from region (1) in the phase space of system (1.35), there exists a stable (synchronization) and unstable limit cycles lying on the resonance torus T^2 For the parameter domain (4), resonance limit cycles, as well as stable two-dimensional torus T_1^2 and unstable two-dimensional torus T^2 (beatings), exist in the phase space. For the parameter domain (2), there exist aforementioned limit cycles (lying on the torus; T^2 gets destroyed in the parameter domain (6)), as well as invariant torus T_1^2 (beatings). For the parameter domain (3), there exists torus T_1^2 which is globally stable if parameters are chosen in the parameter domain D_{rr}. It is possible that for certain variations of parameters, subharmonic resonances that correspond to multiple synchronization may originate and disappear on the aforementioned tori [141, 142].

Fig. 1.39 shows qualitative forms of rotation characteristics of both rotators for various parameters of the system.

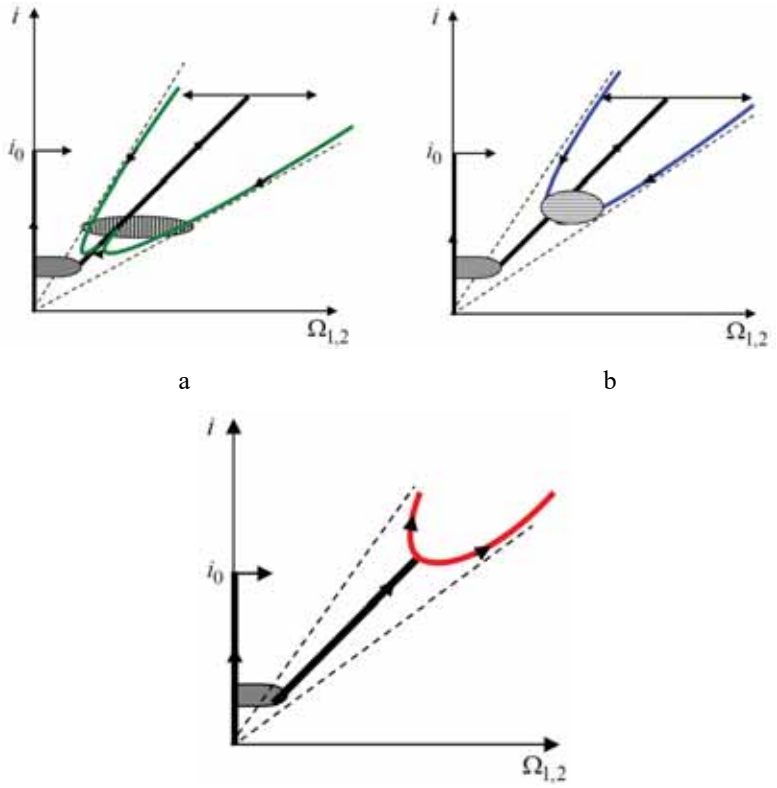

Fig. 1.39. Qualitative forms of rotation characteristics of rotators.

Case 1. Suppose that parameter i is quasi-statically increased from zero, and parameters λ^r, γ^r are varied (increased) along line L_1. In this case, rotators that remain in the equilibrium for $i = 0$, remain

there until equilibrium disappears for $i = i_0 + 0$. This situation defines a zero branch of the rotation characteristic of both rotators. For $i = i_0 + 0$ both rotators suddenly jump into the regime of rotations. Depending on the initial condition, a simple periodic regime of the synchronization or a regime of quasi-periodic beatings can be realized. In the synchronization regime, rotation characteristics have a common branch, shown in Fig. 1.39 by a straight line (within the first approximation by a small parameter). Then the synchronization regime, if it has been realized, is abruptly (the bifurcation of the fusion of stable and unstable resonant limit cycles and their disappearance) replaced by the regime of beatings. The branches of rotation characteristic that correspond to the beatings are located on opposite sides of the synchronization branch. Let us now assume that parameter i is decreased and motions of parameters along line L_1 occur in parameter domain (3). In this case, each rotator remains in the regime of stable beatings until torus T_1^2 disappears due to the merging with unstable torus T_2^2 in domain (7). In the point of disappearance of T_1^2, rotators jump to the regime of synchronization. The upper shaded area corresponds to parameter domain (6). In this area, a destruction of the resonance torus and formation of homoclinic structures related to the homoclinic curve of the saddle resonance limit cycle occur. On the rotation characteristic, this domain is quite narrow, and so is domain (6) ($\sim \mu$), and the chaotic limit set

is not an attractor itself. The lower shaded area is related to an unexplored area of parameters. One can state only one thing: the transition of rotators to equilibrium cannot be related to any limiting sets of trajectories of oscillatory type (regular or chaotic).

Case 2 differs from the previous one: the system returns from the regime of beatings to the regime of synchronization through the chaotization of the rotator's rotations. As it is known from Section 1.3, parameter domain (5) corresponds to chaotic attractors that are associated with the bifurcation of the destruction of the resonant torus T^2 during the transition of parameters from domain (1) to domain (5); with the bifurcation of the destruction of torus T_1^2 during the transition of parameters from domain (3) to domain (5); and with bifurcation of a homoclinic trajectory of saddle resonance limit cycle, as well as with the period doubling (pitchfork) bifurcations of a two-dimensional torus. Chaotic attractors are illustrated by the numerical experiment in Sections 1.3 and 1.4. A scattering of the rotation characteristic of rotators occurs in upper shaded domain.

Case 3 differs from the previous ones by a soft origination of the regime of quasi-periodic beatings at the moment when the system exits the regime of synchronization: the branches of the rotation characteristic that correspond to the regime of beatings adjoin to a straight line that corresponds to the synchronization.

For a system with Josephson junctions, rotation characteristics shown in Fig. 1.38 represent their volt-ampere characteristics.

Note that for parameter values outside of domains D_{00} and D_{rr}, the system of coupled rotators can behave similarly to the rotator-oscillator system, since in these cases such dynamical regimes can be realized, for which motions of one of the rotators remain bounded (one pendulum rotates and the other one oscillates).

CHAPTER 2

CHAOTIC SYNCHRONIZATION OF DYNAMICAL SYSTEMS

The Chapter discusses the synchronization of a pair of coupled oscillators with individual chaotic dynamics – chaotic synchronization. The history of this phenomenon and its properties are presented here. A general definition of the synchronization is provided, which applies both to the case of regular and to the case of chaotic synchronization. Based on this definition, an asymptotic theory of chaotic synchronization of dynamical systems with regular and singular perturbations is constructed, using the theory of perturbations and integral manifolds. Mutual and forced synchronization is considered. Examples of applications of the chaotic synchronization are provided.

2.1. Chaotic synchronization of parametrically excited oscillators. General definition of synchronization

Synchronization of chaotic oscillations (chaotic synchronization) of dissipative-coupled non-identical dynamical systems has been discovered in 1986 [68] when studying the dynamics of coupled para-

metrically excited oscillators (generators) on an analogue machine. Such system is governed by equations of the form:

$$\begin{aligned}
&\dot{x}_1 = y_1, \quad \dot{y}_1 = -k_1 y_1 - \left(1 + q\cos\theta + x_1^2\right)x_1 - \varepsilon\left(y_1 - y_2\right), \\
&\dot{x}_2 = y_2, \quad \dot{y}_2 = -k_2 y_2 - \left(1 + q\cos\theta + x_2^2\right)x_2 + \varepsilon\left(y_1 - y_2\right), \\
&\dot{\theta} = \Omega.
\end{aligned} \tag{2.1}$$

A parametric oscillator of the form

$$\ddot{x} + k\dot{x} + \left(1 + q\cos\Omega t\right)x + x^3 = 0 \tag{2.2}$$

demonstrates chaotic dynamics in a wide range of parameters q, k. Its properties were sufficiently studied by that time [143–145] and reproduced in an analogue experiment. The types of chaotic attractors of the oscillator are shown in Fig. 2.1. Due to the invariance of Eq. (2.2) to replacement $x \to -x$, in the case shown in Fig. 2.1a, there is also a second attractor that is symmetrical to the one shown (a "twin"). The transition to the case shown in Fig. 2.1b during the variations of parameters k or q occurs trough the "crisis of attractors", i.e. through the merging of the of attraction domains of the "twin" attractors.

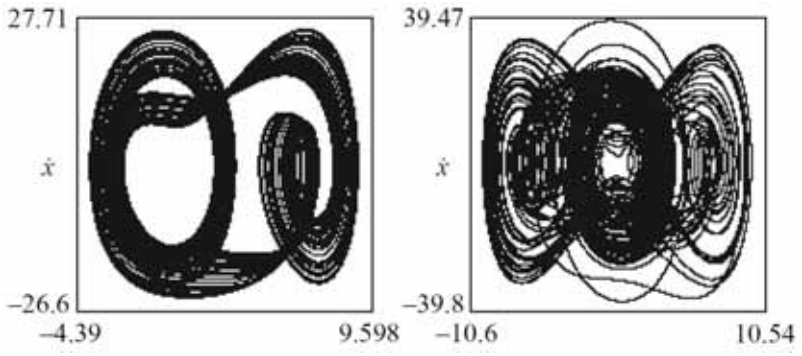

a b

Fig. 2.1. Various types of chaotic attractors of the oscillator (q = 50, Ω = 2): a: k = 0.56; b: k = 0.46.

First, the chaotic synchronization of identical generators was investigated. Unfortunately, at that time, the authors were not aware of the work [67]. Because of that, it was not included in the list of references in [68]. The existence a critical value of the coupling parameter ε^*, was found experimentally such that for all $\varepsilon > \varepsilon^*$, there was a full isochronous synchronization of chaotic oscillations, while for $\varepsilon = \varepsilon^* - \mu$, where $\mu > 0$ and is sufficiently small, only a "partial" synchronization was observed. In this case, the oscillograms of dynamic variables are represented by long synchronized chaotic zugs, alternating with desynchronization and with the restoration of synchronous regime after a short time (see Fig. 2.2).

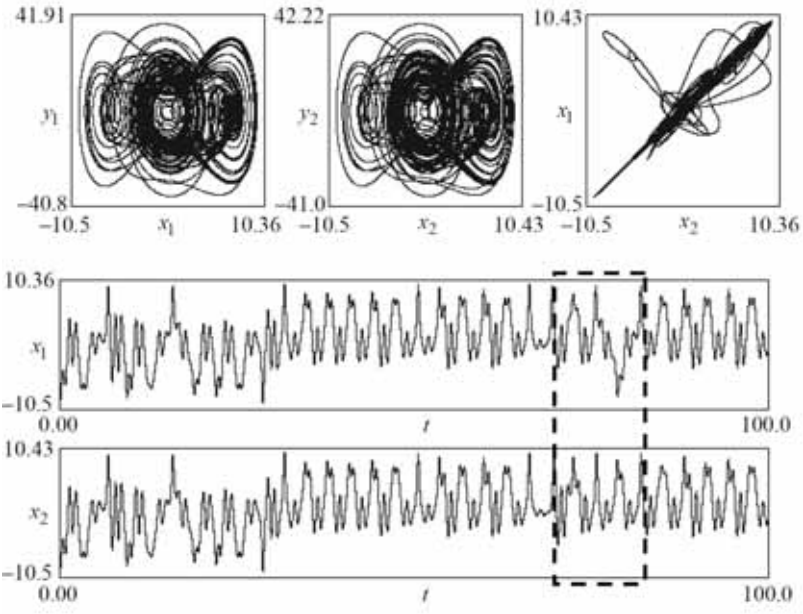

Fig. 2.2. The regime of partial chaotic synchronization of identical oscillators for $q = 50$, $\Omega = 2$, $k = 0.46$, $\varepsilon = 0.33$.

With an increase of the parameter of coupling, the deviation of the projection of the phase trajectory from the diagonals of the planes of the same-titled variables, in particular (x_1, x_2), decreases and diagonals take the form of straight lines covered with “bubbles”. Subsequently, this dynamical regime, which precedes the mutual capture of oscillations, was called the “bubbling synchronization” [146, 147]. Further, the synchronization becomes stable, and the affix does not leave the diagonal. Fig. 2.3 shows projections of the phase trajectory of the coupled system on “partial” phase planes, as

well as the projection onto plane (x_1, x_2) and oscillograms $x_1(t, t_0)$, $x_2(t, t_0)$, illustrating the establishment of mutual capture mode and the synchronization itself. There is a short transient process, after which the motions of the oscillators become synchronized. In the synchronization regime, the "partial" phase portraits of oscillators are identical, and the movement of projections of the affix on the planes of the same-titled variables occurs on diagonals. This can serve as a criterion for whether the synchronization has occurred. "Partial" phase spaces are understood as subspaces $(x_i, \dot{x}_i, t)$ of the phase space of system (2.1). Note that for values of the parameter of coupling $\varepsilon = \varepsilon^* + \alpha$, where $\alpha > 0$ and is sufficiently small, the synchronization is stable for the most part, but not globally. Along with the chaotic attractor corresponding to the synchronization, there exist other attractors. They can be either chaotic or regular (limit cycles) and they correspond to the regimes of chaotic beatings or to classical (periodic) non-isochronous synchronization of oscillators. In dissipative systems, with the increase of the parameter of coupling, these attractors disappear and the regime of chaotic synchronization mode becomes globally stable.

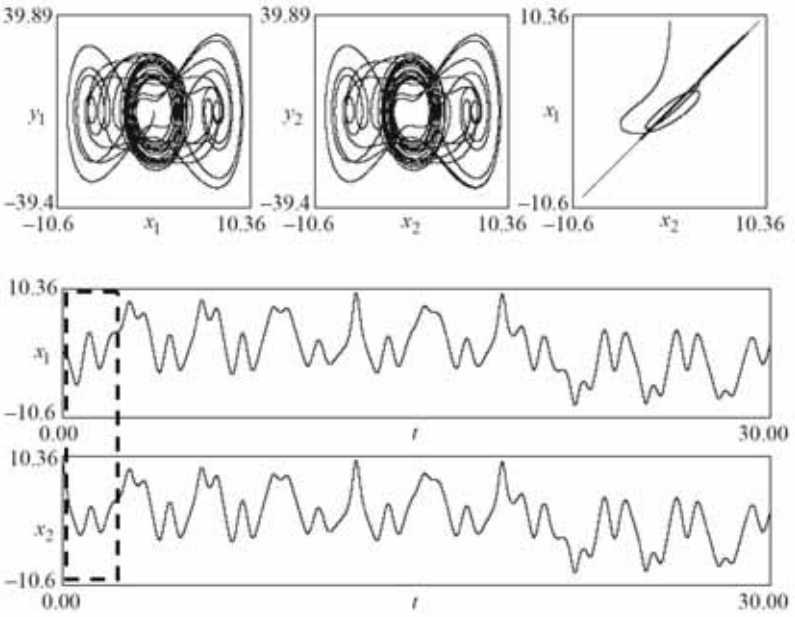

Fig. 2.3. The establishment of the regime of complete chaotic synchronization: $q = 50$, $\Omega = 2$, $k = 0.46$, $\varepsilon = 1.5$.

From a formal point of view, the existence of synchronization of identical systems seems almost obvious, since it follows directly from equations (2.1) that $x_1(t) = x_2(t)$, $y_1(t) = y_2(t)$ is a solution (more precisely, an integral manifold) of the system. This solution corresponds to the synchronization and exists regardless of the value of the coupling parameter. On the manifold, system (2.1) splits into a pair of synchronized oscillators, and if the partial oscillator is chaotic, then both their synchronous movements have a chaotic character. The role of coupling is to ensure the stability of chaotic

synchronization. In other words, for identical systems, there is only one synchronization problem – the problem of its stability.

For non-identical oscillators, the situation is completely different. In this case, the diagonal as an integral manifold does not exist, and in the regime of synchronization (if there is one), the projection of the chaotic trajectory on the plane of the same-titled variables of oscillators occupies the region absorbing the diagonal (Fig. 2.4 shows a small segment of the trajectory). Based on visual observations of the nature of movements in these planes, it is generally impossible to conclude that oscillations are synchronized.

Let us pay attention to the motions of the projection of the affix onto the partial phase portraits and oscillograms of vibrations (see Fig. 2.4). Despite the significant difference in parameters ($k_1 = 0.82$, $k_2 = 0.1$), partial phase portraits in the regime of synchronization are qualitatively the same. This can also be seen from the oscillograms of oscillations below. They contain a certain time shift (in this case, a small one) and can be translated into each another by stretching the coordinates. Phase portraits have the same property: they can be translated into one another by a continuous mapping. This fact is crucial.

We have carried out an experiment for various parameters of system (2.1), as well as for oscillators with chaotic dynamics of the different types [148]. As a result of observations, in [68], a general

definition of synchronization has been proposed, covering both classical synchronization of periodic oscillations and chaotic synchronization.

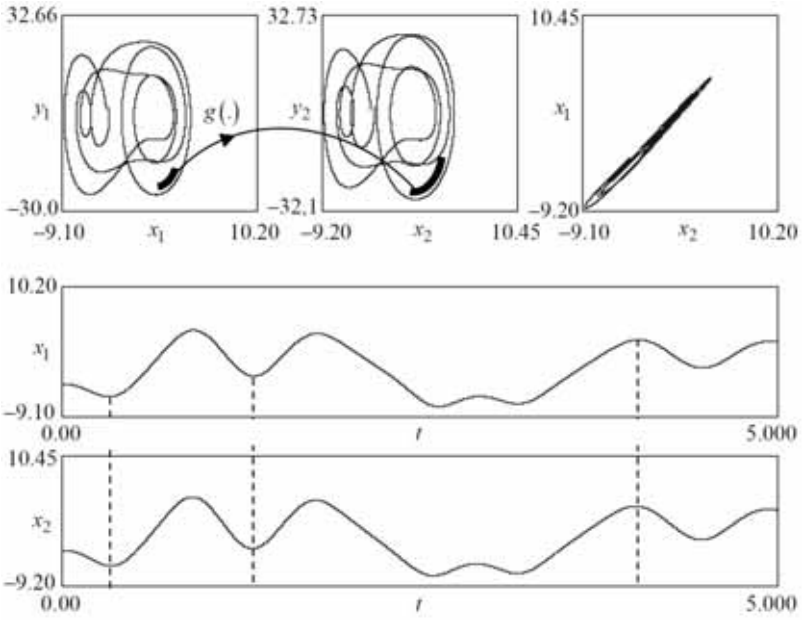

Fig. 2.4. Relationship of partial phase portraits of non-identical oscillators in the regime of synchronization: $q = 50$, $\Omega = 2$, $k_1 = 0.82$, $k_2 = 0.1$, $\varepsilon = 1.5$.

Definition 2.1.1. Consider the following dynamical systems of two oscillators: $\dot{\mathbf{X}}_1 = \mathbf{F}_1(\mathbf{X}_1)$, $\dot{\mathbf{X}}_2 = \mathbf{F}_2(\mathbf{X}_2)$, $\mathbf{X}_1 \in \mathbf{R}^n$, $\mathbf{X}_2 \in \mathbf{R}^m$. Suppose that each of these systems has attractors A_1 and A_2, respectively. Consider a coupled system of the form

$$\dot{\mathbf{X}}_1 = \mathbf{F}_1(\mathbf{X}_1) + \varepsilon \mathbf{f}_1(\mathbf{X}_1, \mathbf{X}_2),$$
$$\dot{\mathbf{X}}_2 = \mathbf{F}_2(\mathbf{X}_2) + \varepsilon \mathbf{f}_2(\mathbf{X}_1, \mathbf{X}_2).$$

We say that a synchronization of oscillators takes place (in particular, chaotic one) for the values of the coupling parameter from the interval $\varepsilon_1 < \varepsilon < \varepsilon_2$, if for these values of ε, there exists attractor A_ε, such that:

1) its images $\pi_1(A_\varepsilon)$ and $\pi_2(A_\varepsilon)$ representing projections on "partial" spaces are translated into each another using a one-to-one, mutually continuous mapping, i.e. they are homomorphic (π_1 and π_2 are the natural projections onto subspaces $\mathbf{X}_1$ and $\mathbf{X}_2$);

2) there exists a homoeomorphic mapping $g : \pi_1(A_\varepsilon) \to \pi_2(A_\varepsilon)$ with the following properties: a) *g*-Lipshitz continuous at $\pi_1(A_\varepsilon)$, b) for any trajectory $\{T^t(X_1, X_2)\} \subset A_\varepsilon$, where T^t is the shift mapping along trajectories of the coupled system $g(\pi_1(T^t(X_1, X_2))) = \pi_2(T^{rt+\alpha(t)}(X_1, X_2))$, such that $\lim_{t\to\infty} \frac{rt + \alpha(t)}{t} = r$ is a rational number.

If $r = 1$, then the synchronization is called *simple* synchronization. In other cases, synchronization is called *multiple* synchronization. Multiple synchronization of chaotic oscillations with the number of

rotation $r = 2$ has been discovered in [149]. Note that the introduced rotation number r is analogous to the Poincaré rotation number on the torus. For example, let us assume that a synchronization of periodic rotations is realized in the "non-autonomous rotator" system (see Section 1.2). In this case, the solution for the rotator's phase has the form

$$\varphi = r\psi + \Phi(\psi), \quad \psi = \omega_0 t + \psi_0,$$

where $\int_0^{2\pi} \Phi(\psi)\, d\psi = 0$. This defines the mapping of circles $S_\varphi = g(S_\psi)$ with all the properties specified in the definition of synchronization. In this case, the following is valid for the number of rotations

$$\lim_{t\to\infty} \frac{\varphi(t)}{\psi(t)} = \lim_{t\to\infty} \frac{r\omega_0 t + \Phi(t)}{\omega_0 t + \psi_0} = r, \quad \alpha(t) = \frac{1}{\omega_0}\Phi(t).$$

Fig. 2.4 illustrates the above definition of synchronization.

The behavior of the dimension and of the power spectra [106] of oscillators (2.1) during the system transition to the synchronization and in the synchronization regime was studied in a numerical experiment in [150].

Fig. 2.5 shows the evolution of a fractal dimension of the attractor of the coupled system as a result of the increase of the coupling pa-

rameter. As the coupling increases, a monotonous drop in dimension occurs and it stabilizes when the system enters a full synchronism. We will explain this graph by, first, recalling the nature of the change in the dimension of the attractor of a coupled system in the case of classical synchronization.

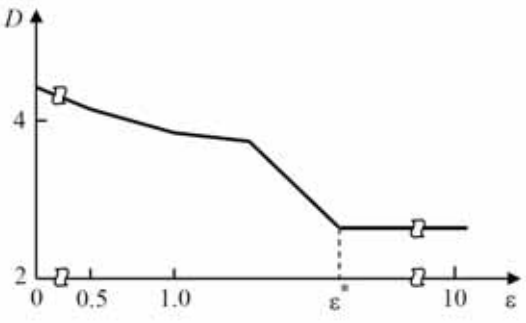

Fig. 2.5. Evolution of the fractal dimension of the chaotic attractor of system (2.1).

Suppose, there is a pair of coupled weakly non-identical (for simplicity) self-oscillating systems with periodic dynamics, for instance, a pair of Van der Pol oscillators. In this case, scenarios of origination of the synchronization are known. For a certain value of the coupling parameter $\varepsilon = \varepsilon^* - 0$, a regime of quasi-periodic beatings occurs, whose image in the phase space of the system is attractor $A_{\varepsilon_1 - 0}$: torus with a quasi-periodic winding. In this case, $\dim A_{\varepsilon_1} = 2.$ As the coupling parameter reaches the value $\varepsilon = \varepsilon^*$, a multiple limit cycle is born on the torus, which then splits into sta-

ble and unstable limit cycles. The attractor of the coupled system becomes a stable limit cycle (synchronization), and the dimension jumps to one, $\dim A_{\varepsilon_1+0}=1$. It remains so throughout the entire interval of the cycle's existence. The jump-like change in the dimension of the attractor of a coupled system that occurs during the bifurcation of a birth of a limit cycle is a property of the classical synchronization. Now let us turn to the system (2.1). Let $\varepsilon=0$; and suppose that A_1 and A_2 are the strange attractors representing combinations of a countable set of saddle limit cycles and a continuum of trajectories stable by Poisson. Suppose, C_i^1 and C_i^2 are the aforementioned limit cycles of attractors numbered according to the ascending order of the periods. In other words, in a formally unified system, there is a countable set of saddle tori of the form $T_{ii}=C_i^1\times C_i^2$. There exist other tori, but we are interested in those ones that can have resonances with a rotation number equal to one. As in the given example, as the coupling parameter increases, saddle limit cycles (local resonance) are born on each of these saddle tori, which builds the “skeleton” of the future chaotic attractor, which represents an image of the synchronization. Due to each of these internal bifurcations, there is a local ordering of motions in the phase space of the system: jumps of the dimension of a small amplitude that is imperceptible in the experiment. In practice, the sequence of these minor jumps appears to be a monotonous drop in

dimension – a “stretched” jump in relation to the coupling parameter – with its further stabilization.

Note that the above definition guarantees equality of partial dimensions equal to the dimension of the attractor itself in the regime of the synchronization:

$$\dim \pi_1 \left(A_\varepsilon \right) = \dim \pi_2 \left(A_\varepsilon \right) = \dim A_\varepsilon .$$

The definition also guarantees qualitatively identical spectra of synchronized chaotic oscillations of oscillators, which can serve as its physical criterion. Fig. 2.6 shows the power spectra of $x_1(t)$ and $x(t) = x_1(t) - x_2(t)$ in the regime of the chaotic synchronization.

Since the 1990s and until the present time, research on chaotic synchronization has been developing intensively, acquiring its own terminology. This includes the aforementioned “bubble synchronization” [146, 147], as well as the “generalized synchronization” [151 – 153], “phase synchronization” [154], “lag synchronization” [155], “riddled basins of attraction” [156 – 159], and “on–off intermittency” [160 – 162]. An extensive bibliography is contained in [80].

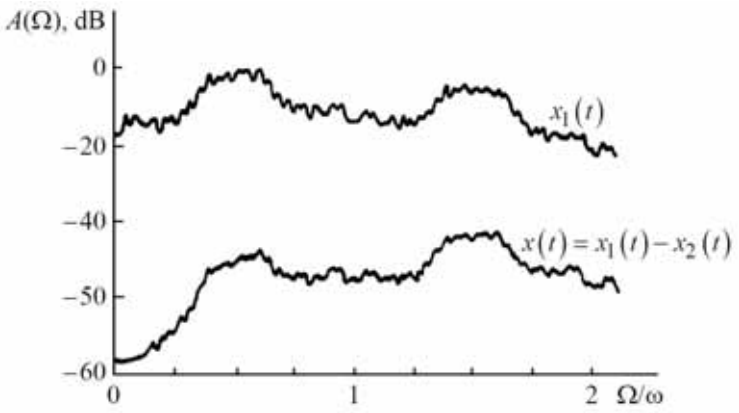

Fig. 2.6. Power spectra of realizations of the variables in the regime of chaotic synchronization of oscillators.

At the end of the section, we will make a note about the definitions of the phase and of the amplitude of oscillations. Let us assume that $\mathbf{X}(t)$ is a certain signal (realization of regular or chaotic process), which we consider the reference signal, i.e. "1" is the reference amplitude, while time "*t*" is the reference phase. Assume, there is a second signal of the form $A\mathbf{X}(rt+\alpha)$. In this case, A is the amplitude, $rt+\alpha$ is the phase of this signal, which are measured in units corresponding to the reference parameters. For instance, for function $A\sin(\omega t+\varphi)$ such reference is $\sin t$. That is, the amplitude, the frequency, and the phase are (just) the conversion parameters of the reference signal. If the reference is not mentioned, then the reference is implicitly implied. Talking about the amplitude and about the phase of a chaotic signal, having implicitly assumed a periodic

motion, is a nonsense. Unfortunately, sometimes this can be found in the literature on chaotic synchronization.

In the case of interacting systems, the reference can be the vector of variables of any of the oscillators, while in the case of forced excitation, it is natural considering the vector of variables of the master oscillator as such.

Due to its generality, the proposed definition allows us to consider the synchronization of chaotic oscillations in the context of the general theory of synchronization of dynamical systems and to use existing and already established terminology, in particular, terminology from the theory of systems of phase synchronization (SPS).

Next we will consider a simple chaotic synchronization and deal with chaotic realizations of the form $A\mathbf{X}\left(t+\alpha\left(t\right)\right)$. In this case, according to definition $\alpha\left(t\right)$ is the phase difference of one of the oscillators relative to another one (reference one). If $\alpha\left(t\right)=\Delta=\text{const},$ then there is a simple chaotic phase synchronization in the coupled system, while for $\left\langle \alpha\left(t,t_0\right)\right\rangle_t=\Delta=\text{const}$ there is a "mean" phase synchronization. In the SPS terminology: the parameter area for all points of which there is a stable synchronization is called the holding area; while the parameter area for all points of which the regime of chaotic synchronization mode is globally stable is called the synchronization capture area [21]. This definition will

form the basis of the asymptotic theory, a special case of which is described in [148] based on the example of chaotic synchronization of Lorentz systems.

2.2. Mutual and forced chaotic synchronization of identical systems

Let us generalize the definition of oscillator and rotator.

Definition 2.2.1. A dynamic system of the form

$$\dot{\mathbf{X}} = \mathbf{F}(\mathbf{X}, t),$$
$$\mathbf{X} = \|x_1 x_2 \ldots x_m\|^T, \quad x_i \in R^1, \quad \mathbf{F}(\mathbf{X}, t): R^{m+1} \to R^m, \tag{2.3}$$

having in the generalized phase space $G(\mathbf{X}, t)$ at least one attractor $A(1)$, different from an equilibrium, is called the generalized oscillator. If one of the scalar variables is cyclic $x = \varphi(\mathrm{mod}\, 2\pi)$, the equation (2.3) is called the general rotator.

We assume that function $\mathbf{F}(\mathbf{X}, t)$ is cyclic in time. Further on we will be assigning additional properties to equations (2.3), such as dissipativity, when it will be necessary. In what follows, the term "generalized" is omitted.

By definition, an oscillator or a rotator can be attached to another subsystem coupled to it and considered as a single object: a generalized oscillator (rotator). For example, a non-autonomous excitation

can be added to an autonomous rotator (see Section 1.1) and system (1.1) can be considered as a generalized rotator. The same applies to the aperiodic link (see Section 1.2) or to the oscillator (see Section 1.4). In what follows, we will use all classical oscillators with chaotic dynamics (see Section 1.1).

We will assume that the dynamical properties of system (2.1) are known. In particular, we assume that the maximum Lyapunov exponent $\lambda(1)$ of attractor $A(1)$ is known. The latter represents the maximum exponent of the equation in variations

$$\dot{\mathbf{U}} = \mathbf{F}'\big(\xi(t)\big)\mathbf{U}, \tag{2.4}$$

where $\boldsymbol{\xi}(t) \in A(1)$, $\mathbf{F}'(\mathbf{X}) = \dfrac{\partial \mathbf{F}(\mathbf{X})}{\partial \mathbf{X}}$ is the Jacobi matrix. Note that for assumptions made, the following is valid $\|\mathbf{U}\| = D\exp\lambda(1)t$, $D = \text{const}$.

Taking into account the assumptions made, we consider a coupled system of the form

$$\begin{aligned} \dot{\mathbf{X}}_1 &= \mathbf{F}(\mathbf{X}_1,\, t) - \varepsilon_1 \mathbf{C}(\mathbf{X}_1 - \mathbf{X}_2), \\ \dot{\mathbf{X}}_2 &= \mathbf{F}(\mathbf{X}_2,\, t) + \varepsilon_2 \mathbf{C}(\mathbf{X}_1 - \mathbf{X}_2). \end{aligned} \tag{2.5}$$

In system (2.5), matrix $\mathbf{C} = (m \times m) = \text{diag}(c_1, c_2, \ldots, c_m)$ defines a set of coupled variables. Elements $c_i \geq 0$; ε_1, ε_2 are the scalar

coupling parameters. If $\varepsilon_1 = 0,$ then we have a case of forced excitation of the first system onto the second one; while for $\varepsilon_1 \neq 0,$ $\varepsilon_2 \neq 0$, we have a case of the interacting systems.

Some properties of chaotic synchronization have already been discussed in the previous section. Here, we establish the relation of synchronization with integral manifolds of the coupled system, for which we formulate the following definition.

Definition 2.2.2 [163]. Set of points *M* of the space $(\mathbf{X},\ t)$ of a certain dynamical system is called the integral manifold if for any point $(\mathbf{X}_0,\ t_0) \in M$, the following is valid: $(\mathbf{X}_0,\ t_0) \in M$ where $\mathbf{X}(t)$ is the solution of this system with initial conditions $\mathbf{X} = \mathbf{X}_0,$ $t = t_0,$ while *t* takes any value from the interval of existence of solution $\mathbf{X}(t)$.

Integral manifold *M* represents a surface (a hyperplane, to be precise) in the phase space of the dynamical system. This surface is filled by phase trajectories, which, if necessary, can be interpreted as trajectories of e certain subsystem, defined on this manifold and having its dimension [17, 18].

In case of system (2.5), hyperplane $M_0 = \{\mathbf{X}_1,\ \mathbf{X}_2 \,|\, \mathbf{X}_1 = \mathbf{X}_2\}$ represents its integral manifold. This is easy to prove by taking the difference in the equations. For the resulting equation,

$\mathbf{U} = \mathbf{X}_1 - \mathbf{X}_2 = 0$ will be the solution. By definition, any phase trajectory that starts on a manifold remains on that manifold. It is easy to see that any solution with initial conditions at M_0 corresponds to the synchronized motions of the oscillators. This follows directly from system (2.5): when the phase point moves on the manifold M_0, the system splits into a pair of equations of synchronized oscillators. We can say that the dynamics of a coupled system on a manifold is equivalent to the dynamics of a single oscillator governed by Eq. (2.1) defined at this manifold, in the sense that the dynamical variables of the interacting oscillators are coupled algebraically to the corresponding variables of the said oscillator.

In this case, the dynamics of the first and second oscillators as subjects of the system (2.5) is shown by synchronous motions of "partial" affixes on the respective partial phase portraits. These affixes are projections of a point moving over a manifold. Hence, partial phase portraits represent projections of the phase portrait of a single oscillator to the partial phase spaces. This is the essence of any synchronization: the collective dynamics is equivalent to the dynamics of one "effective element", and the motions of each of the collective elements are rigidly (functionally) coupled to the motions of this element.

According to Definition 2.1.1, synchronization of identical systems is expressed by relations of the form $\pi_1\left(A(1)\right) \equiv \pi_2\left(A(1)\right)$ and $\alpha(t) \equiv 0.$

Thus, the synchronization stability problem is equivalent to the stability of manifold $M_0,$ more precisely, to the stability of the part of this manifold containing attractor $A(1) \in M_0.$ If this manifold is stable, then any phase trajectory that starts from, at least, a small vicinity of this manifold is attracted by the surface, and hence by attractor $A(1).$ In accordance with the aforesaid, the chaotic synchronization will be observed over time in the coupled system (2.5), the dynamic properties of which will be determined by the properties of the chaotic attractor $A(1)$ of oscillator governed by Eq. (2.1).

We investigate the influence of the structure of oscillator's couplings (form of matrix **C**) on the stability of synchronization. To do so, we study the conditions of globally stable synchronization of certain specific dynamic systems.

1. *Global asymptotic stability of a mutual chaotic synchronization of Lorentz oscillators*.

Consider a symmetrically coupled system of two Lorentz oscillators of the form

$$\begin{aligned}
\dot{x}_1 &= -\sigma\left(x_1 - y_1\right) - \varepsilon c_1\left(x_1 - x_2\right),\\
\dot{y}_1 &= -y_1 + rx_1 - x_1 z_1 - \varepsilon c_2\left(y_1 - y_2\right),\\
\dot{z}_1 &= -z_1 + x_1 y_1 - \varepsilon c_3\left(z_1 - z_2\right),\\
\dot{x}_2 &= -\sigma\left(x_2 - y_2\right) + \varepsilon c_1\left(x_1 - x_2\right),\\
\dot{y}_2 &= -y_2 + rx_2 - x_2 z_2 + \varepsilon c_2\left(y_1 - y_2\right),\\
\dot{z}_2 &= -z_2 + x_2 y_2 + \varepsilon c_3\left(z_1 - z_2\right).
\end{aligned} \tag{2.6}$$

Let us show that system (2.6) is dissipative. Consider the following quadratic form:

$$V = \frac{1}{2}\sum_{k=1}^{2}\left[x_k^2 + y_k^2 + \left(z_k - \sigma - r\right)^2\right].$$

It's derivative, taken along trajectories of system (2.6) has the form

$$\dot{V} = -\sum_{k=1}^{2}\left[\sigma x_k^2 + y_k^2 + z_k^2 - z_k\left(\sigma + r\right)\right] -$$

$$-\varepsilon c_1\left(x_1 - x_2\right)^2 - \varepsilon c_2\left(y_1 - y_2\right)^2 - \varepsilon c_3\left(z_1 - z_2\right)^2.$$

From this expression, one can note that dissipative couplings do not affect the sphere of dissipation of the coupled system. This sphere is the product of the dissipation spheres of two uncoupled Lorentz systems (see Section 1.1).

Thus, all phase trajectories of system (2.6) for $t \to \infty$ are absorbed by the region of the phase space

$$G^* = \left\{ \left| x_{1,2} \right| \le R,\ \left| y_{1,2} \right| \le R,\ \left| z_{1,2} - \sigma - r \right| \le R,\ R = \sqrt{2}\left(\sigma + r\right) \right\}. \quad (2.7)$$

Let us perform the following change of the variables in Eq. (2.6): $x_1 = x_2 + u,\ \ y_1 = y_2 + v,\ \ z_1 = z_2 + w.$ Note that variables u, v, w represent transversals to manifold $M_0 = \left\{ \mathbf{X}_1,\ \mathbf{X}_2 \middle| \mathbf{X}_1 = \mathbf{X}_2 \right\},$ where $\mathbf{X}_1 = \left(x_1,\ y_1,\ z_1 \right)^T.$ With respect to transversals, we obtain a system of the form

$$\begin{aligned} \dot{u} &= -\sigma\left(u - v\right) - 2\varepsilon c_1 u, \\ \dot{v} &= -v + \left(r - z_2\right)u - x_2 w - uw - 2\varepsilon c_2 v, \\ \dot{w} &= -w + y_2 u + x_2 v + uv - 2\varepsilon c_3 w. \end{aligned} \quad (2.8)$$

It is evident that conditions of global stability of solution $u = 0,\ v = 0,\ \ w = 0$ of this system are the conditions of global stability of the manifold and, therefore, conditions of synchronization of Lorenz oscillators is system (2.6).

Consider the Lyapunov function $V = \frac{1}{2}\left(u^2 + v^2 + w^2\right).$ Its derivative taken along the vector field of system (2.8) has the form

$$\begin{aligned} &\dot{V} = -\Phi, \\ &\Phi = \left(2\varepsilon c_1 + \sigma\right)u^2 + \left(2\varepsilon c_2 + 1\right)v^2 + \left(2\varepsilon c_3 + 1\right)w^2 - \\ &-\left(\sigma + r - z_2\right)uv + y_2 uw. \end{aligned} \quad (2.9)$$

The derivative is negative in the whole phase space if the quadratic form Φ with variable coefficient will be positive for any values of u, v, w. Due to already established dissipativity of system (2.6), the values of variables y_2, z_2 can be taken from inequalities (2.7).

Consider results of the visual analysis of quadratic form Φ. First, if the number of coupled variables increases, then conditions of global stability improve, which means the decrease of the scalar coupling parameter ε, which is important for global stability. The best conditions are realized for the coupling matrix $\mathbf{C} = \mathbf{I} = \mathrm{diag}(1, 1, 1)$. Second, if one consider a problem of minimizing the number of couplings determining the regime of synchronization, then it is sufficient to have a coupling by the first variable, i.e. the coupling matrix may have the form $\mathbf{C} = \mathrm{diag}(1, 0, 0)$. In the case of matrices of the form $\mathbf{C} = \mathrm{diag}(0, 1, 0)$ and $\mathbf{C} = \mathrm{diag}(0, 0, 1)$, the conditions of global stability are not reachable for arbitrary values of parameters σ and r. If, for some reason, coupling by variables x_1, x_2 is impossible, then global stability can be provided by matrix $\mathbf{C} = \mathrm{diag}(0, 1, 1)$. These simple conclusions follow from the forms of the coefficients at squared variables and from the form of "cross" terms of the quadratic form.

All coupling matrices **C**, for which a global stability of the synchronization is possible, will be referred to as *acceptable*.

Conditions of global stability of oscillators with coupling matrix $\mathbf{C} = \mathrm{diag}(1, 0, 0)$ are expressed by inequality

$$\varepsilon > \frac{1}{2}\left(\left(\sigma + r - z_2\right)^2 + y_2^2 - \sigma\right).$$

Let us denote

$$\varepsilon^* = \sup_{y_2, z_2 \forall G^*} \frac{1}{2}\left(\left(\sigma + r - z_2\right)^2 + y_2^2 - \sigma\right).$$

From inequality (2.6), it follows that

$$\varepsilon^* = 2\left(\sigma + r\right)^2 - \frac{\sigma}{2}.$$

Thus, when the following inequality is satisfied: $\varepsilon > \varepsilon^*$, an isochronous chaotic synchronization is a globally stable. Not that obtained value ε^* it is greatly overestimated in comparison with the real one, which can be attributed to the "imperfection" of the Lyapunov function. For example, the numerical experiment shows that already at $\varepsilon^* = 10$, chaotic synchronization of Lorentz oscillators is globally stable for $\sigma = 10,\ \ r = 27.$

2. *Global asymptotic stability of the synchronization of Lorenz – Chua oscillators* (see Section 1.1). Consider a coupled system of the form

$$\begin{aligned}
\dot{x}_1 &= -f(x_1) + \alpha y_1 - \varepsilon c_1 (x_1 - x_2), \\
\dot{y}_1 &= -x_1 - y_1 - z_1 - \varepsilon c_2 (y_1 - y_2), \\
\dot{z}_1 &= \beta y_1 - \gamma z_1 - \varepsilon c_3 (z_1 - z_2), \\
\dot{x}_2 &= -f(x_2) + \alpha y_2 + \varepsilon c_1 (x_1 - x_2), \\
\dot{y}_2 &= -x_2 - y_2 - z_2 + \varepsilon c_2 (y_1 - y_2), \\
\dot{z}_2 &= \beta y_2 - \gamma z_2 + \varepsilon c_3 (z_1 - z_2).
\end{aligned} \tag{2.10}$$

We will assume that $f(x)$ is a differentiable function with conditions discussed in Section 1.1. We investigate the effect of couplings on the dissipation sphere of the system.

Consider the quadratic form $V = \frac{1}{2}\sum_{k=1}^{2}\left(x_k^2 + \alpha y_k^2 + \frac{\alpha}{\beta} z_k^2 \right)$. Its derivative taken along the vector field of system (2.10) has the form

$$\dot{V} = -\alpha \sum_{k=1}^{2}\left(x_k f(x_k) + \alpha y_k^2 + \frac{\alpha\gamma}{\beta} z_k^2 \right) -$$

$$-\varepsilon c_1 (x_1 - x_2)^2 - \varepsilon c_2 (y_1 - y_2)^2 - \varepsilon c_3 (z_1 - z_2)^2 .$$

Analysing the derivative, we conclude that, first, the expression under the sum sign is a derivative in the direction of the field of a single oscillator (see Section 1.1), and secondly, that dissipative connections do not affect the sphere of dissipation of the coupled system. Just as in the previous case, this sphere represents the product of the spheres of two uncoupled oscillators.

Let us study global stability of isochronous synchronization. We applying to system (2.10) a change of the variables of the form $x_1 = x_2 + u$, $y_1 = y_2 + v$, $z_1 = z_2 + w$. As a result, we obtain the following system:

$$\begin{aligned} \dot{u} &= -f'(\xi)u + \alpha v - 2\varepsilon c_1 u, \\ \dot{v} &= -v - u - w - 2\varepsilon c_2 v, \\ \dot{w} &= \beta v - \gamma w - 2\varepsilon c_3 w. \end{aligned} \tag{2.11}$$

In the transition from system (2.10) to system (2.11), the Lagrange theorem was applied, $\xi \in [x_1, x_2]$ is a certain point from the interval. Because of the arbitrariness of x_1, x_2, ξ is also arbitrary.

Consider the Lyapunov function

$$V = \frac{1}{2}\left(u^2 + \alpha v^2 + \frac{\alpha}{\beta} w^2\right).$$

Its derivative taken along the vector field of system (2.11) has the form

$$\dot{V} = -\left(f'(\xi) + 2\varepsilon c_1\right)u^2 - \left(\alpha + 2\varepsilon c_2\right)v^2 - \left(\frac{\alpha\gamma}{\beta} + 2\varepsilon c_3\right)w^2. \tag{2.12}$$

It follows from expression (2.12) that elements c_2, c_3 of the coupling matrix do not affect conditions of global stability. In other words, conditions of global stability of synchronization of oscilla-

tors with coupling matrix $\mathbf{C} = \mathrm{diag}(1, 0, 0)$ are the same as for any other one that has $c_1 = 1$.

We find conditions of global stability by assessing the derivative of the Lyapunov function

$$\dot{V} = -\left(h'(\xi) + 2\varepsilon\right)u^2 - \alpha v^2 - \frac{\alpha\gamma}{\beta}w^2 \le -\left(-|m_0| + 2\varepsilon\right)u^2 - \alpha v^2 - \frac{\alpha\gamma}{\beta}w^2,$$

where $\inf_{\forall x} f'(x) = m_0 < 0$. From here, we obtain that the derivative is negative in the whole phase space if $\varepsilon > \frac{|m_0|}{2}$. This is the condition of global stability of isochronous chaotic synchronization of oscillators.

Note that study of the global stability of forced synchronization can be performed with a complete analogy with mutual synchronization.

From the results of the study of global stability of the synchronization of oscillators with different types of nonlinearity, we make an important conclusion: there always exists a coupling matrix **C** and an interval of values of the scalar parameter ε, at which the chaotic synchronization of oscillators is stable.

Let us turn to the study of conditions of local stability of the chaotic synchronization.

We introduce variable $\mathbf{U} = \mathbf{X}_1 - \mathbf{X}_2$ in system (2.5) – transversal of a manifold – and consider the following equation:

$$\dot{\mathbf{U}} = \left(\mathbf{F}'\left(\xi(t)\right) - \left(\varepsilon_1 + \varepsilon_2\right)\mathbf{C}\right)\mathbf{U}, \tag{2.13}$$

here $\xi(t) = \mathbf{X}_1 = \mathbf{X}_2$ is the solution of Eq. (2.3) that corresponds to a trajectory of the chaotic attractor $A(1)$. That is, Eq. (2.13) is linearized equation with respect to the manifold.

Note that for $\varepsilon_1 = \varepsilon_2 = 0,$ this equation coincides with equation in variations (2.4). The maximum Lyapunov exponent of solutions for this equation is $\lambda(1)$. The following theorem [164] is valid for the conditions of local stability of synchronization as conditions of stability of solution $\mathbf{U} = 0$ of equation (2.13).

Theorem 2.2.1. 1. If the coupling matrix $\mathbf{C = I},$ then a mutual chaotic synchronization is stable for $\varepsilon_1 + \varepsilon_2 > \lambda(1)$. the opposite inequality, the synchronization is unstable. 2. For all other possible coupling matrices, the synchronization is stable for $\varepsilon_1 + \varepsilon_2 > \varepsilon^*\left(\lambda(1)\right)$. For the opposite inequality, the synchronization is unstable. The threshold value $\varepsilon^*\left(\lambda(1)\right)$ is determined by the structure of couplings of oscillators. 3. Conditions of stability of forced synchronization are governed by the same inequalities, for which $\varepsilon_1 = 0.$

Proof.

1. Suppose that $\mathbf{C} = \mathbf{I}$. We perform a change of the variable $\mathbf{U} = e^{-(\varepsilon_1+\varepsilon_2)t}\mathbf{V}$, so that equation (2.13) is reduced to the form

$$\dot{\mathbf{V}} = \mathbf{F}'\left(\xi(t)\right)\mathbf{V}.$$

This equation, accurate within notations, coincides with system (2.4), i.e. $\|\mathbf{V}\| = D\exp\lambda(1)t$. As a result of this change, we obtain $\|\mathbf{U}\| = e^{-(\varepsilon_1+\varepsilon_2)t}\|\mathbf{V}\| = De^{\left(-(\varepsilon_1+\varepsilon_2)+\lambda(1)\right)t}$. From here it follows that if $\varepsilon_1 + \varepsilon_2 > \lambda(1)$, then $\|\mathbf{U}\| \to 0$ for $t \to \infty$ and the synchronization is stable, while if $\varepsilon_1 + \varepsilon_2 < \lambda(1)$, then $\|\mathbf{U}\| \to 0$ for $t \to \infty$, which means tha the synchronization is unstable.

2. Assume that matrix **C** belongs to the number of allowed matrices. Since global stability of the synchronization is possible with such a matrix, then its local stability is also possible. In other words there is a threshold value $\varepsilon^*\left(\lambda(1)\right)$, which depends on matrix **C**, such that for $\varepsilon_1 + \varepsilon_2 > \varepsilon^*\left(\lambda(1)\right)$, the synchronization is stable, while for the opposite inequality it is unstable.

3. The condition $\varepsilon_1 = 0$ (forced synchronization) does not change the reasoning. Note that if attractor $A(1)$ is regular (e.g. represents a limit cycle), then $\lambda(1) \le 0$ and the synchronization is stable for an

arbitrary small coupling of the oscillators, which is a well-known fact [26]. The existence of threshold values of the coupling parameters that determine the holding range of chaotic synchronization is one of its distinctive and defining properties. In the case of a symmetrical mutual connection, the threshold equals to $\lambda(1)/2$ or to $\varepsilon^*(\lambda(1))/2$, while in the case of a forced synchronization it equals to $\lambda(1)$ or to $\varepsilon^*(\lambda(1))$, depending on the form of matrix **C**.

In addition, this theorem justifies a fast, simple and, as practice shows, fairly accurate method for measuring the maximum Lyapunov exponents of chaotic attractors when visually observing synchronization on a monitor or on an oscilloscope screen (in a field experiment). It is more convenient to use a forced synchronization. The order of the measurement is as follows. First, the forced synchronization scheme is modelled according to equations (2.5). Second, a regime of a chaotic attractor, the maximum value of which should be measured is set in the master oscillator. Third, a fairly large value of the coupling parameter ε is set, for which the slave oscillator is synchronized and the motion of the affix occurs on the diagonal of the same-titled variables, as Fig. 2.3 shows. Further, is decreased to the value ε^*, for which the affix begins to leave the diagonal (the boundary of stability of the synchronization). This value of the parameter equals to the Lyapunov exponent, which is being measured: $\varepsilon^* = \lambda(1)$.

The theorem is tested on the Lorentz system with parameters $\{\sigma, r, b\} = \{10, 26, 8/3\}$. Measurements according to theorem 2.2.1 result in $\lambda(1) = 0.89$ [164]. For the same parameters, in the framework of standard algorithms $\lambda(1) = 0.9$ [165]. Fig. 2.7 shows results of the measurement of the Lyapunov exponents for the Lorentz and Chua attractors. Parameters of the Lorenz oscillator are: $\{\sigma, b, r\} = \{10, 8/3, r\}$. Parameters of the Chua oscillator are: $(\alpha, \beta, \gamma, m_0, m_1) = (\alpha, 14, 0.1, -1/7, 2/7)$.

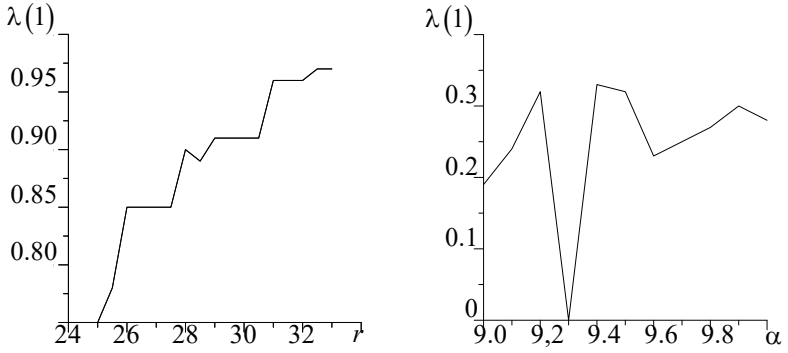

a b

Fig. 2.7. Lyapunov exponents. a: Lorenz oscillator, b: Chua's oscillator.

2.3. Asymptotic theory of mutual chaotic synchronization of slightly non-identical systems

According to Definition 2.1.1, the structure of the synchronization theory provides solutions for the following problems [166, 167]:

1) Existence and stability of synchronization;

2) Determination of the mapping of partial phase portraits of oscillators in the regime of synchronization;

3) Determination of an effective dynamic system with attractor $A_{\varepsilon,\mu}$ that represents an image of the synchronization.

The proposed theory is a generalization of various special cases [148, 168, 169].

We consider a cross-coupled system of non-identical chaotic oscillators of the form

$$\begin{aligned} \dot{\mathbf{X}}_1 &= \mathbf{F}_1\left(\mathbf{X}_1\right) - \varepsilon\mathbf{C}\left(\mathbf{X}_1 - \mathbf{X}_2\right), \\ \dot{\mathbf{X}}_2 &= \mathbf{F}_2\left(\mathbf{X}_2\right) + \varepsilon\mathbf{C}\left(\mathbf{X}_1 - \mathbf{X}_2\right). \end{aligned} \tag{2.14}$$

Here $\mathbf{X}_{1,2} \in R^m$, $\mathbf{F}_{1,2} : R^m \to R^m$, $\mathbf{C} = \operatorname{diag}\left(c_1, c_2, ..., c_m\right)$, $c_i \geq 0$, $\varepsilon \geq 0$.

We will assume that the dynamical systems of individual oscillators, as well as the coupled system (2.14) are dissipative, i.e. there is a sphere of dissipation in the phase space (2.14), and all its solu-

tions are bounded for $t \to \infty$. We will also assume that functions $\mathbf{F}_{1,2}(\mathbf{X})$ are analytic.

Let us represent nonlinear functions in the form $\mathbf{F}_1(\mathbf{X}_1) = = \mathbf{F}(\mathbf{X}_1) + \mu\mathbf{F}_1^*(\mathbf{X}_1)$, $\mathbf{F}_2(\mathbf{X}_2) = \mathbf{F}(\mathbf{X}_2) + \mu\mathbf{F}_2^*(\mathbf{X}_2)$, where μ is a certain small parameter, associated with parameters of non-identity of the oscillators. In this case, system (2.14) takes the form

$$\begin{aligned} \dot{\mathbf{X}}_1 &= \mathbf{F}(\mathbf{X}_1) - \varepsilon\mathbf{C}(\mathbf{X}_1 - \mathbf{X}_2) + \mu\mathbf{F}_1^*(\mathbf{X}_1, \mu), \\ \dot{\mathbf{X}}_2 &= \mathbf{F}(\mathbf{X}_2) + \varepsilon\mathbf{C}(\mathbf{X}_1 - \mathbf{X}_2) + \mu\mathbf{F}_2^*(\mathbf{X}_2, \mu). \end{aligned} \tag{2.15}$$

For $\mu = 0$, (2.15) represents a couple system of identical oscillators, which we call the *generating system*, and its integral manifold $M_0 = \{\mathbf{X}_1, \mathbf{X}_2 \,|\, \mathbf{X}_1 = \mathbf{X}_2\}$ is called the *generating integral manifold*. Let's introduce a new variable $\mathbf{U} = \mathbf{X}_1 - \mathbf{X}_2$ in the system (2.15) and consider an equation of the form

$$\dot{\mathbf{U}} = \left(\mathbf{F}'(\xi(t)) - 2\varepsilon\mathbf{C}\right)\mathbf{U} + \mu\mathbf{F}^*(\mathbf{X}_2(t), \mathbf{U}, \mu). \tag{2.16}$$

Here $\mathbf{F}'(.)$ is the Jacobi matrix for function $\mathbf{F}(\mathbf{X})$, $\mathbf{F}^* = \mathbf{F}_1^* - \mathbf{F}_2^*$.

As before, the Lagrange theorem was applied during the transition from system (2.15) to equation (2.16), $\xi(t) \in [\mathbf{X}_1, \mathbf{X}_2]$. Generating manifold $(\mu = 0)$ corresponds to solution $\mathbf{U} = 0$ of this equation.

Next, we will use the theory of integral manifolds of quasilinear systems developed in [17–19]. If $\xi(t) \in M_0$, then Eq. (2.16) for $\mu = 0$ is an equation in variations with respect to the generating manifold M_0, while for $\mu = 0,\ \varepsilon = 0,\ \xi(t) \in A(1) \in M_0$ it represents an equation in variations (2.4) for the equation of a single oscillator (2.3). We assume that the maximum Lyapunov exponent of its attractor is known and equals to $\lambda(1)$.

Let's assume that matrix **C** is selected from the number of valid matrices. In this case, according to Theorem 2.2.1, the trivial solution $\mathbf{U} = 0$ is stable for $\varepsilon > \varepsilon^*(\lambda(1))$, i.e. all characteristic exponents of solutions of the generating equation (2.16) are strictly negative. Under these conditions, equation (2.16) for small μ is a quasi-linear equation with limited perturbations (non-critical case). Such an equation in the interval $\mu \in [0, \mu^*)$ has a stable, smooth, and unique integral manifold of the form $\mathbf{U} = \mu \mathbf{U}^*(\mathbf{X}_2(t), \mathbf{U}, \mu)$ [17 – 19]. Reformulating the above for system (2.15), we obtain that it has a unique and stable manifold of the form $M_\mu = \left\{ \mathbf{X}_1, \mathbf{X}_2 \middle| \mathbf{X}_1 = \mathbf{X}_2 + \mu \mathbf{X}^*(\mathbf{X}_2, \mu) \right\}$, coinciding with the generating manifold for $\mu = 0$. In this case, the nature of the stability of manifold M_μ is the same as of M_0. Its stability conditions exactly

match the stability conditions given in Theorem 2.2.1 within the accuracy of μ.

Thus, under the conditions of Theorem 2.2.1, a stable hypersurface M_μ exists in the phase space of system (2.15), the dimension of which is equal to the dimension of a single oscillator. The phase trajectories of this manifold are the trajectories of some "effective" oscillator with attractor A_μ. Projections of the phase trajectories of this attractor on the partial phase spaces of the oscillators determine the partial phase portraits. These phase portraits are functionally related, and in this case, by definition, the motions of the oscillators are synchronized. In other words, the existence of manifold M_μ is equivalent to the existence of synchronization in the oscillator system. We will consider the first problem solved, and the chaotic synchronization implemented.

Let's turn to the solution of the second and third problems, which consist in determining the mapping of partial phase portraits and a dynamical system on manifold M_μ with attractor A_μ, representing an image of the synchronization.

Let us rewrite the coupling of oscillator's variables in the regime of synchronization in parametric form: in the form of power series by a small parameter:

$$\mathbf{X}_1 = \mathbf{X} + \mu\mathbf{X}_{11}(\mathbf{X}) + \mu^2\mathbf{X}_{12}(\mathbf{X}) + \dots,$$
$$\mathbf{X}_2 = \mathbf{X} + \mu\mathbf{X}_{21}(\mathbf{X}) + \mu^2\mathbf{X}_{22}(\mathbf{X}) + \dots. \tag{2.17}$$

Note that equations (2.17) are a parametric notation of manifold M_μ with parameter **X**.

Suppose that manifold M_μ is divided into trajectories by the phase trajectories of a dynamic system of the form

$$\dot{\mathbf{X}} = \mathbf{F}(\mathbf{X}) + \mu\mathbf{F}_*(\mathbf{X}) + \mu^2\mathbf{F}_{**}(\mathbf{X}) + \dots. \tag{2.18}$$

If we find functions $\mathbf{F}_*(\mathbf{X})$, $\mathbf{F}_{**}(\mathbf{X}), \dots$, $\mathbf{X}_{11}(\mathbf{X})$, $\mathbf{X}_{21}(\mathbf{X}), \dots$ in a certain way, then equations (2.17) determine (parametrically) the desired mapping of partial phase portraits of oscillators along the trajectories of attractor A_μ of dynamical system (2.18). We will choose functions from the right-hand side of equation (2.18), so that equations defining functions (2.17) have a bounded solution with a stability condition that coincides with the stability condition of the generating manifold.

We use the technique of a small parameter. We perform the decomposition of functions $\mathbf{F}(\mathbf{X}_i)$ and $\mathbf{F}_i^*(\mathbf{X}_i)$, $i = 1, 2,$ into power series by a small parameter:

$$\mathbf{F}(\mathbf{X} + \mu\mathbf{X}_{i1}(\mathbf{X}) + \dots) = \mathbf{F}(\mathbf{X}) + \mu\mathbf{F}'\mathbf{X}_{i1} + \dots,$$

$$\mathbf{F}_i^*\left(\mathbf{X}+\mu\mathbf{X}_{i1}\left(\mathbf{X}\right)+...\right)=\mathbf{F}_i^*\left(\mathbf{X}\right)+...$$

and substitute equations (2.17) into system (2.15). Given the form of the equation (2.18) and equating the terms of the same orders by a small parameter, we obtain a system of equations that define the desired functions. In particular, in the first approximation, the equations for the functions have the form

$$\mathbf{F}_*+\dot{\mathbf{X}}_{11}=\mathbf{F}'\mathbf{X}_{11}-\varepsilon\mathbf{C}\left(\mathbf{X}_{11}-\mathbf{X}_{21}\right)+\mathbf{F}_1^*,$$
$$\mathbf{F}_*+\dot{\mathbf{X}}_{21}=\mathbf{F}'\mathbf{X}_{21}+\varepsilon\mathbf{C}\left(\mathbf{X}_{11}-\mathbf{X}_{21}\right)+\mathbf{F}_2^*.$$

Hereinafter, expression $\mathbf{F}'\left(\mathbf{X}\right)\equiv\dfrac{\partial\mathbf{F}}{\partial\mathbf{X}}$ is a Jacobi matrix for function $\mathbf{F}\left(\mathbf{X}\right)$. The next step is to select functions $\mathbf{F}_*$, $\mathbf{X}_{11}$, $\mathbf{X}_{21}$.

Note that with respect to variable $\mathbf{U}=\mathbf{X}_{11}+\mathbf{X}_{21}$, an equation of the following form is valid:

$$2\mathbf{F}_*+\dot{\mathbf{U}}=\mathbf{F}'\mathbf{U}+\mathbf{F}_1^*+\mathbf{F}_2^*. \tag{2.19}$$

We select function $\mathbf{F}_*$ in the following way: $\mathbf{F}_*=\left(\mathbf{F}_1^*+\mathbf{F}_2^*\right)\big/2+$ $+\varepsilon\mathbf{C}\mathbf{U}$. In this case, Eq. (2.19) takes the form

$$\dot{\mathbf{U}}=\mathbf{F}'\mathbf{U}-2\varepsilon\mathbf{C}\mathbf{U}.$$

This equation coincides with the generating equation (2.16) and has the same meaning. When the following inequality is satisfied:

$\varepsilon > \varepsilon^*(\lambda_{\max})$, solution $\mathbf{U} = 0$ of this equation is stable and equations for functions $\mathbf{X}_{11}$ and $\mathbf{X}_{21}$ have the form

$$\begin{aligned} &\mathbf{X}_{21} = -\mathbf{X}_{11}, \\ &\dot{\mathbf{X}}_{11} = \mathbf{F}'\,\mathbf{X}_{11} - 2\varepsilon\mathbf{C}\mathbf{X}_{11} + \left(\mathbf{F}_1^* - \mathbf{F}_2^*\right)\Big/2. \end{aligned} \tag{2.20}$$

Note that due to the stability of the homogeneous equation and the boundedness of $\mathbf{F}^* = \left(\mathbf{F}_1^* - \mathbf{F}_2^*\right)\Big/2$, any solution of (2.20) is bounded.

The following partial differential equation corresponds to the second equation of the system (2.20):

$$\frac{\partial \mathbf{X}_{11}}{\partial \mathbf{X}}\mathbf{F} - \frac{\partial \mathbf{F}}{\partial \mathbf{X}}\mathbf{X}_{11} + 2\varepsilon\mathbf{C}\mathbf{X}_{11} = \left(\mathbf{F}_1^* - \mathbf{F}_2^*\right)\Big/2. \tag{2.21}$$

Suppose $\mathbf{X}_{11} = \mathbf{X}_{11}(\mathbf{X})$ is a solution of Eq. (2.21). In this case, formulae $\mathbf{X}_1 = \mathbf{X} + \mu\mathbf{X}_{11}(\mathbf{X})$, $\mathbf{X}_2 = \mathbf{X} - \mu\mathbf{X}_{11}(\mathbf{X})$ (within the accuracy of μ^2) determine the parametric coupling of variables in regime of the synchronization. In this case, the properties and parameters of the synchronous chaotic regime (spectrum, dimension, etc.) are determined (within the accuracy of μ^2) by the properties of attractor A_μ of an "arithmetic mean" oscillator of the form

$$\dot{\mathbf{X}} = \frac{1}{2}\left(\mathbf{F}_1(\mathbf{X}) + \mathbf{F}_2(\mathbf{X})\right).$$

Thus, the problem of the form of the mapping of partial phase portraits is reduced to the solution of the quasilinear equation (2.21). In a general case, this task is quite time-consuming. Solving this equation makes sense for specific systems and specific types of perturbations. We will indicate one of such solutions related to actual applications. Let vector $\mathbf{F}^* = \left(\mathbf{F}_1^* - \mathbf{F}_2^*\right)/2$ be collinear to the vector $\mathbf{F}$, $\mathbf{F}^* = \nu\mathbf{F}$, where ν is a number. We assume that (for simplicity) $\mathbf{C} = \mathbf{I}$. In this case, function $\mathbf{X}_{11} = \Delta \cdot \mathbf{F}(\mathbf{X})$, $\Delta = \nu/2\varepsilon$ is the solution of equation (2.21). This can be confirmed by a direct substitution. We show that this solution is stable. In Eq. (20) we will make a change of a variables of the form $\mathbf{X}_{11} = \Delta\dot{\mathbf{X}} + \boldsymbol{\eta}$. We obtain equation of the form

$$\Delta\ddot{\mathbf{X}} + \dot{\boldsymbol{\eta}} = \mathbf{F}'\Delta\dot{\mathbf{X}} + \mathbf{F}'\boldsymbol{\eta} - 2\varepsilon\Delta\dot{\mathbf{X}} - 2\varepsilon\boldsymbol{\eta} + 2\varepsilon\Delta\mathbf{F}.$$

Taking into account that $\ddot{\mathbf{X}} \equiv \mathbf{F}'\dot{\mathbf{X}}$, we obtain the following equation with respect to $\boldsymbol{\eta}$: $\dot{\boldsymbol{\eta}} = \mathbf{F}'\boldsymbol{\eta} - 2\varepsilon\boldsymbol{\eta}$. A trivial solution $\boldsymbol{\eta} = 0$ of this equation is stable for $\varepsilon > \lambda_{\max}/2$.

The coupling of variables of the oscillators in the regime of synchronization is written as follows: $\mathbf{X}_1 = \mathbf{X} + \mu\Delta\dot{\mathbf{X}}$,

$\mathbf{X}_2 = \mathbf{X} - \mu\Delta\dot{\mathbf{X}}$. Or, within the accuracy of μ^2, $\mathbf{X}_1(t) = \mathbf{X}_2(t + 2\mu\Delta)$.

Thus, in the case of perturbations of equations of the oscillators of the specified type, the phase synchronization of oscillators takes place in the system. The mapping of phase portraits of oscillators is identical, acting at a constant phase shift $\alpha(t) = 2\mu\Delta = \text{const}$. That is, if one observes the motions of the affixes in "partial" phase spaces, one would find out that they move along the same trajectories, but with a constant time shift – with the phase difference, which is equal to $\alpha(t) = 2\mu\Delta = \text{const}$. By "partial" affixes we mean projections of the affix in the phase space of the coupled system moving on attractor A_μ. Note, if $\mathbf{F}^* = \nu\mathbf{CF}$, then then the aforementioned solution of equation (2.21) also exists.

We solve the inverse problem that has an applied interest. The problem is formulated as follows: to determine the type of perturbations of equations of the oscillators, as well as the matrix **C**, if the coupling of the variables of oscillators in the regime of synchronization is set.

We will demonstrate the solution to this problem using the example of cross-coupled Lorentz systems. We consider a system of the form (2.15), with

$$\mathbf{X}_{1,2} = \left(x_{1,2}, y_{1,2}, z_{1,2}\right)^T,$$

$$\mathbf{F}\left(\mathbf{X}\right) = \left(-\sigma\left(x-y\right), -y + rx - xz, -bz + xy\right)^T.$$

Let us assume that the coupling of the variables in the regime of synchronization (mapping of the phase portraits) has the form

$$\mathbf{X}_1 = \mathbf{X} + \mu\,\mathbf{X}_{11}, \quad \mathbf{X}_2 = \mathbf{X} - \mu\,\mathbf{X}_{11},$$

where $\mathbf{X}_{11} = \alpha\,\mathbf{X} + \Delta\dot{\mathbf{X}}$, α and Δ are certain set numbers. We need to find the perturbation vector $\mu\mathbf{F}^*\left(\mathbf{X}\right)$ and matrix $\mathbf{C}$, corresponding to a given coupling of the variables of the Lorentz oscillator. In addition, we require a minimum number of coupled variables of the oscillators. The vectors and matrices necessary for solving the problem have the form

$$\mathbf{F} = \begin{pmatrix} -\sigma\left(x-y\right) \\ -y + rx - xz \\ -bz + xy \end{pmatrix}, \quad \mathbf{X}_{11} = \begin{pmatrix} \alpha x + \Delta\dot{x} \\ \alpha y + \Delta\dot{y} \\ \alpha z + \Delta\dot{z} \end{pmatrix}, \quad \frac{\partial\mathbf{F}}{\partial\mathbf{X}} = \begin{pmatrix} -\sigma & \sigma & 0 \\ r-z & -1 & -x \\ y & x & -b \end{pmatrix},$$

$$\frac{\partial\mathbf{X}_{11}}{\partial\mathbf{X}} = \begin{pmatrix} \alpha - \Delta\sigma & \Delta\sigma & 0 \\ \Delta\left(r-z\right) & \alpha - \Delta & -\Delta x \\ \Delta y & \Delta x & \alpha - \Delta b \end{pmatrix}.$$

Substituting these expressions in equation (2.21) and performing transformations, we obtain the equation for the perturbation vector $\mathbf{F}^*$:

$$\alpha\begin{pmatrix}0\\ -xz\\ xy\end{pmatrix}+2\varepsilon\alpha\begin{pmatrix}c_1x\\ c_2y\\ c_3z\end{pmatrix}+2\varepsilon\Delta\begin{pmatrix}-c_1\sigma(x-y)\\ c_2(-y+rx-xz)\\ c_3(-bz+xy)\end{pmatrix}=\mathbf{F}^*.$$

From the condition of the minimum number of couplings, we assume that $c_1=0$. Secondly, if (additionally) we require a linearity of the perturbations, we obtain the following conditions for the parameters: $\alpha+2\varepsilon\Delta c_2=0$, $\alpha+2\varepsilon\Delta c_3=0$. As a result, the desired perturbation vector is of the form $\mathbf{F}^*=(0,\ \lambda_1x+\lambda_2y,\ \lambda_3z)^T$, $\lambda_1=-\alpha$, $\lambda_2=-\alpha r$, $\lambda_3=(\Delta b-\alpha)\alpha/\Delta$. Thus, for linear perturbations of the second and third equations of Lorentz systems (sufficient to take place in one of the systems), in the regime of synchronization within the accuracy of μ^2, variables of the oscillators are coupled by the following equations:

$$x_1=x+\mu(\alpha x+\Delta\dot{x}),\ x_2=x-\mu(\alpha x+\Delta\dot{x}),$$

$$y_1=y+\mu(\alpha y+\Delta\dot{y}),\ y_2=y-\mu(\alpha y+\Delta\dot{y}),$$

$$z_1=z+\mu(\alpha z+\Delta\dot{z}),\ z_2=z-\mu(\alpha z+\Delta\dot{z}).$$

By excluding *x*, *y*, *z* from these equations, we obtain explicit coupling of variables of the oscillators in the regime of synchronization (within the accuracy of μ^2):

$$x_1(t) = (1 + 2\mu\alpha)x_2(t + 2\mu\Delta), \quad y_1(t) = (1 + 2\mu\alpha)y_2(t + 2\mu\Delta),$$
$$z_1(t) = (1 + 2\mu\alpha)z_2(t + 2\mu\Delta).$$

Thus, under perturbations of the Lorentz equations of the indicated type, the mapping of phase portraits of oscillators in the regime of synchronization represents a uniform compression (tension) acting at a constant phase shift $\alpha(t) = 2\mu\Delta$. Moreover, the nature of the synchronous motions is determined by the Lorentz system, which has parameter values equal to the arithmetic mean values of parameters of the interacting oscillators. One can say that this type of perturbation of parameters of the oscillators leads to a perturbation of the amplitude and phase of chaotic oscillations of one oscillator with respect to another, which is taken as a standard (reference oscillator).

Note. The proposed theory is considered as a qualitative one, rather than a theory of engineering calculations. Our interest is related precisely with the qualitative changes (it does not matter that they are small) in the synchronization regimes when varying the parameters of the systems, and not with their quantitative characteristics. For this reason, it is sufficient to consider only the first approximations by a small parameter since they contain practical information about the significant properties of synchronization.

2.4. Mutual synchronization of strongly non-identical systems

Systems of oscillators with nonidentity of all or of a part of their parameters $\sim \mu^0$, where μ is a small parameter are called strongly nonidentical systems. A simple analysis of system (2.14) shows that synchronization of such oscillators is possible if the scalar coupling parameter for strongly non-identical scalar equations of the oscillators is sufficiently large, $\varepsilon \sim \mu^{-1}$ (strong coupling). For equations with weakly non-identical parameters, the strong coupling condition is not required. Here, we take $\mu = \varepsilon^{-1}$ as a small parameter [166, 167].

Suppose that parameters of k equations of coupled system (2.14) are strongly non-identical and contain strong coupling, while parameters of $m-k$ equations are weakly non-identical and the corresponding equations do not contain strong couplings. By separating both types of equations into groups, we consider a coupled system of the form

$$\begin{aligned}
\dot{\mathbf{X}}_1 &= \mathbf{F}_1(\mathbf{X}_1, \mathbf{Y}_1) - \mu^{-1}\mathbf{C}(\mathbf{X}_1 - \mathbf{X}_2),\\
\dot{\mathbf{Y}}_1 &= \mathbf{\Phi}(\mathbf{X}_1, \mathbf{Y}_1) - \mathbf{D}(\mathbf{Y}_1 - \mathbf{Y}_2) + \mu\mathbf{\Phi}_1^*(\mathbf{X}_1, \mathbf{Y}_1),\\
\dot{\mathbf{X}}_2 &= \mathbf{F}_2(\mathbf{X}_2, \mathbf{Y}_2) + \mu^{-1}\mathbf{C}(\mathbf{X}_1 - \mathbf{X}_2),\\
\dot{\mathbf{Y}}_2 &= \mathbf{\Phi}(\mathbf{X}_2, \mathbf{Y}_2) + \mathbf{D}(\mathbf{Y}_1 - \mathbf{Y}_2) + \mu\mathbf{\Phi}_2^*(\mathbf{X}_2, \mathbf{Y}_2).
\end{aligned} \tag{2.22}$$

Here $\mathbf{X}_{1,2} \in R^k$, $\mathbf{Y}_{1,2} \in R^{m-k}$, $\mathbf{C} = \mathrm{diag}(c_1, c_2, ..., c_k)$, $\mathbf{D} = \mathrm{diag}(d_1, d_2, ..., d_{m-k})$, $c_i > 0$, $d_j \geq 0$, $\varepsilon^{-1} = \mu$ is a small parameter.

System (2.22) is a system with singularly-regular perturbations (multiplying the first and third equations by μ, we obtain a small parameter in front of the derivatives). It is easy to see that the generating manifold of this system is $M_0 = \{\mathbf{X}_1 = \mathbf{X}_2,\ \mathbf{Y}_1 = \mathbf{Y}_2\}$. It is also easy to reduce this system to a special form [18] and thereby to show that it has a unique and stable integral manifold M_μ, asymptotically close to manifold M_0. That is, we consider that the problem of existence and stability of synchronization is resolved. As in the previous case, we are searching for a parametric representation of manifold M_μ in the form of power series by a small parameter of the form

$$\begin{aligned}
\mathbf{X}_1 &= \mathbf{X} + \mu\mathbf{X}_{11}(\mathbf{X}, \mathbf{Y}) + \mu^2\mathbf{X}_{12}(\mathbf{X}, \mathbf{Y}) + \dots, \\
\mathbf{Y}_1 &= \mathbf{Y} + \mu\mathbf{Y}_{11}(\mathbf{X}, \mathbf{Y}) + \mu^2\mathbf{Y}_{12}(\mathbf{X}, \mathbf{Y}) + \dots, \\
\mathbf{X}_2 &= \mathbf{X} + \mu\mathbf{X}_{21}(\mathbf{X}, \mathbf{Y}) + \mu^2\mathbf{X}_{22}(\mathbf{X}, \mathbf{Y}) + \dots, \\
\mathbf{Y}_2 &= \mathbf{Y} + \mu\mathbf{Y}_{21}(\mathbf{X}, \mathbf{Y}) + \mu^2\mathbf{Y}_{22}(\mathbf{X}, \mathbf{Y}) + \dots.
\end{aligned} \tag{2.23}$$

We assume that the dynamical system at the manifold has the form

$$\dot{\mathbf{X}} = \mathbf{F}(\mathbf{X}, \mathbf{Y}) + \mu \mathbf{F}_*(\mathbf{X}, \mathbf{Y}) + \mu^2 \mathbf{F}_{**}(\mathbf{X}, \mathbf{Y}) + \dots,$$
$$\dot{\mathbf{Y}} = \mathbf{\Phi}(\mathbf{X}, \mathbf{Y}) + \mu \mathbf{\Phi}_*(\mathbf{X}, \mathbf{Y}) + \mu^2 \mathbf{\Phi}_{**}(\mathbf{X}, \mathbf{Y}) + \dots. \tag{2.24}$$

Substituting (2.23) into system (2.22), expanding the functions into power series and equating terms of the same orders, we obtain equations that determine the functions of the right-hand sides of system (2.24) and functions (2.23). In particular, equations of the first approximation have the form

$$\mathbf{F} + \mu \mathbf{F}_* + \mu \dot{\mathbf{X}}_{11} = \mathbf{F}_1 + \mu \left(\frac{\partial \mathbf{F}_1}{\partial \mathbf{X}} \mathbf{X}_{11} + \frac{\partial \mathbf{F}_1}{\partial \mathbf{Y}} \mathbf{Y}_{11} \right) - \mathbf{C}(\mathbf{X}_{11} - \mathbf{X}_{21}),$$
$$\mathbf{F} + \mu \mathbf{F}_* + \mu \dot{\mathbf{X}}_{21} = \mathbf{F}_2 + \mu \left(\frac{\partial \mathbf{F}_2}{\partial \mathbf{X}} \mathbf{X}_{21} + \frac{\partial \mathbf{F}_2}{\partial \mathbf{Y}} \mathbf{Y}_{21} \right) + \mathbf{C}(\mathbf{X}_{11} - \mathbf{X}_{21}). \tag{2.25}$$

$$\mathbf{\Phi}_* + \dot{\mathbf{Y}}_{11} = \frac{\partial \mathbf{\Phi}}{\partial \mathbf{X}} \mathbf{X}_{11} + \frac{\partial \mathbf{\Phi}}{\partial \mathbf{Y}} \mathbf{Y}_{11} - \mathbf{D}(\mathbf{Y}_{11} - \mathbf{Y}_{21}) + \mathbf{\Phi}_1^*,$$
$$\mathbf{\Phi}_* + \dot{\mathbf{Y}}_{21} = \frac{\partial \mathbf{\Phi}}{\partial \mathbf{X}} \mathbf{X}_{21} + \frac{\partial \mathbf{\Phi}}{\partial \mathbf{Y}} \mathbf{Y}_{21} + \mathbf{D}(\mathbf{Y}_{11} - \mathbf{Y}_{21}) + \mathbf{\Phi}_2^*. \tag{2.26}$$

Adding the equations of system (2.25) and choosing the functions $\mathbf{F}$ and $\mathbf{F}_*$ as follows:

$$\mathbf{F} = (\mathbf{F}_1 + \mathbf{F}_2)/2 + \mathbf{C}(\mathbf{X}_{11} + \mathbf{X}_{21}),$$
$$\mathbf{F}_* = \frac{1}{2} \left(\frac{\partial \mathbf{F}_1}{\partial \mathbf{X}} \mathbf{X}_{11} + \frac{\partial \mathbf{F}_2}{\partial \mathbf{X}} \mathbf{X}_{21} + \frac{\partial \mathbf{F}_1}{\partial \mathbf{Y}} \mathbf{Y}_{11} + \frac{\partial \mathbf{F}_2}{\partial \mathbf{Y}} \mathbf{Y}_{21} \right),$$

We obtain equation

$$\mu\left(\mathbf{X}_{11}+\mathbf{X}_{21}\right)^{\cdot}=-2\mathbf{C}\left(\mathbf{X}_{11}+\mathbf{X}_{21}\right).$$

Due to the nondegeneracy of matrix **C**, solution $\mathbf{X}_{11}+\mathbf{X}_{21}=0$ of this equation is stable. Taking this into account, after adding equations (2.26), we choose the function $\mathbf{\Phi}_{*}$ as follows:

$$\mathbf{\Phi}_{*}=\left(\mathbf{\Phi}_{1}^{*}+\mathbf{\Phi}_{2}^{*}\right)\Big/2+\mathbf{D}\left(\mathbf{Y}_{11}+\mathbf{Y}_{21}\right).$$

As a result, we obtain equation

$$\left(\mathbf{Y}_{11}+\mathbf{Y}_{21}\right)^{\cdot}=\frac{\partial\mathbf{\Phi}}{\partial\mathbf{Y}}\left(\mathbf{Y}_{11}+\mathbf{Y}_{21}\right)-2\mathbf{D}\left(\mathbf{Y}_{11}+\mathbf{Y}_{21}\right).$$

We are interested in the stability of solution $\mathbf{Y}_{11}+\mathbf{Y}_{21}=0$ of this equation. There are two possibilities for this:

a) a trivial solution $\mathbf{Y}_{11}+\mathbf{Y}_{21}=0$ is stable for $\mathbf{D}=0.$ In this case, it is stable for any of the possible matrices **D**. In other words, dissipative couplings with respect to the corresponding variables are not decisive to ensure the synchronization of such oscillators;

b) a trivial solution of this equation with matrix $\mathbf{D}=0$ is unstable. In this case, there is always such a matrix **D** (structure of couplings), in which the aforementioned solution will be stable.

Thus, the required stability condition is always achievable. We will assume that it is fulfilled. Given that $\mathbf{X}_{11}+\mathbf{X}_{21}=0,\ \mathbf{Y}_{11}+\mathbf{Y}_{21}=0$, equations for the sought functions have the form:

$$\mu\dot{\mathbf{X}}_{11}=\frac{1}{2}\left(\mathbf{F}_1-\mathbf{F}_2\right)-2\mathbf{C}\mathbf{X}_{11}+\mu\left(\frac{\partial\left(\mathbf{F}_1-\mathbf{F}_2\right)}{\partial\mathbf{X}}\mathbf{X}_{11}+\frac{\partial\left(\mathbf{F}_1-\mathbf{F}_2\right)}{\partial\mathbf{Y}}\mathbf{Y}_{11}\right),$$
$$\dot{\mathbf{Y}}_{11}=\frac{\partial\mathbf{\Phi}}{\partial\mathbf{Y}}\mathbf{Y}_{11}-2\mathbf{D}\,\mathbf{Y}_{11}+\frac{\partial\mathbf{\Phi}}{\partial\mathbf{X}}\mathbf{X}_{11}+\frac{1}{2}\left(\mathbf{\Phi}_1^*-\mathbf{\Phi}_2^*\right).$$

(2.27)

As singularly perturbed, the first equation of system (2.27) has a stable integral surface of slow motions, which, in the zero approximation, is defined as follows: $\mathbf{X}_{11}=\mathbf{C}^{-1}\left(\mathbf{F}_1-\mathbf{F}_2\right)/4$. Given this solution, to find the function $\mathbf{Y}_{11}$, we solve the second equation of the system or a corresponding to it partial differential equation of the form

$$\frac{\partial\mathbf{Y}_{11}}{\partial\mathbf{X}}\mathbf{F}+\frac{\partial\mathbf{Y}_{11}}{\partial\mathbf{Y}}\mathbf{\Phi}-\frac{\partial\mathbf{\Phi}}{\partial\mathbf{Y}}\mathbf{Y}_{11}+2\mathbf{D}\mathbf{Y}_{11}=\frac{\partial\mathbf{\Phi}}{\partial\mathbf{X}}\mathbf{X}_{11}+\left(\mathbf{\Phi}_1^*-\mathbf{\Phi}_2^*\right)/2.$$

Thus, in the stable regime of synchronization, the phase variables of the oscillators are coupled (accuracy by μ^2) by parametric equations of the form

$$\mathbf{X}_1=\mathbf{X}+\mu\mathbf{C}^{-1}\left(\mathbf{F}_1\left(\mathbf{X},\mathbf{Y}\right)-\mathbf{F}_2\left(\mathbf{X},\mathbf{Y}\right)\right)/4,\quad \mathbf{Y}_1=\mathbf{Y}+\mu\mathbf{Y}_{11},$$
$$\mathbf{X}_2=\mathbf{X}-\mu\mathbf{C}^{-1}\left(\mathbf{F}_1\left(\mathbf{X},\mathbf{Y}\right)-\mathbf{F}_2\left(\mathbf{X},\mathbf{Y}\right)\right)/4,\quad \mathbf{Y}_2=\mathbf{Y}-\mu\mathbf{Y}_{11}.$$

In this case, the properties of the synchronous regime within the accuracy of μ^2 are determined by the properties of chaotic attractor A_μ of dynamical system of the form

$$\dot{\mathbf{X}} = \left(\mathbf{F}_1(\mathbf{X},\mathbf{Y}) + \mathbf{F}_2(\mathbf{X},\mathbf{Y})\right)/2 + \mu\mathbf{F}_*,$$
$$\dot{\mathbf{Y}} = \left(\mathbf{\Phi}_1 + \mathbf{\Phi}_2\right)/2.$$

Note that if $\mathbf{F}_1 \equiv \mathbf{F}_2 = \mathbf{F}$, $\mathbf{\Phi}_1 \equiv \mathbf{\Phi}_2 = \mathbf{\Phi}$, then $\mathbf{F}_* = 0$ and solutions $\mathbf{X}_{11} = \mathbf{X}_{21} = 0$, $\mathbf{Y}_{11} = \mathbf{Y}_{21} = 0$ are stable, that is, there is a transition to the identical synchronization regime.

Example 1. Consider synchronization in a coupled system of Lurie oscillators

$$\begin{aligned}
\dot{x}_1 &= \alpha_1\left(-f(x_1) + \mathbf{a}^T\mathbf{y}_1\right) + \varepsilon(x_2 - x_1),\\
\dot{\mathbf{y}}_1 &= \mathbf{B}\mathbf{y}_1 + \mathbf{b}x_1,\\
\dot{x}_2 &= \alpha_2\left(-f(x_2) + \mathbf{a}^T\mathbf{y}_2\right) - \varepsilon(x_2 - x_1),\\
\dot{\mathbf{y}}_2 &= \mathbf{B}\mathbf{y}_2 + \mathbf{b}x_2.
\end{aligned} \tag{2.28}$$

Suppose that parameters α_1 and α_2 differ significantly. In this case, the value of the coupling parameter ε shall be large enough and suppose that $\varepsilon^{-1} = \mu$ is a small parameter. The case that has been already discussed above takes place. A dynamic system whose attractor A_μ defines the properties of the synchronous regime, has the form

$$\begin{aligned}
\dot{x} &= F(x, \boldsymbol{y}) + \mu F_*,\\
\dot{\mathbf{y}} &= \mathbf{B}\mathbf{y} + \mathbf{b}x,
\end{aligned} \tag{2.29}$$

where $F(x,\mathbf{y})=\frac{1}{2}(\alpha_1+\alpha_2)\left(-f(x)+\mathbf{a}^T\mathbf{y}\right)$. Accordingly, for function X_{11} we have expression $X_{11}=\frac{1}{4}(F_1-F_2)=$

$=\frac{\alpha_1-\alpha_2}{2(\alpha_1+\alpha_2)}F=\Delta F=\Delta\dot{x}$, where $\Delta=\frac{\alpha_1-\alpha_2}{2(\alpha_1+\alpha_2)}$ (term μF_* belongs to the next approximation).

Let us show that function $\mathbf{Y}_{11}$, has the same form, i.e. $\mathbf{Y}_{11}=\Delta\dot{\mathbf{y}}$. Indeed, taking into account that $\mathbf{\Phi}=\mathbf{B}\mathbf{y}+\mathbf{b}x$, $\frac{\partial\mathbf{\Phi}}{\partial\mathbf{y}}=\mathbf{B}$, $\frac{\partial\mathbf{\Phi}}{\partial x}=\mathbf{b}$, $\mathbf{\Phi}_1^*=\mathbf{\Phi}_2^*=0$, and substituting expression $\mathbf{Y}_{11}=\Delta\dot{\mathbf{y}}$ into the second equation of system (2.27), we obtain an equation of the form $\Delta\ddot{\mathbf{y}}=\Delta\mathbf{B}\dot{\mathbf{y}}+\Delta\mathbf{b}\dot{x}$ or $\dot{\mathbf{y}}=\mathbf{B}\mathbf{y}+\mathbf{b}x$, i.e. the second equation of system (2.29).

Thus, in this case, there is phase synchronization of chaotic oscillations of oscillators with a phase shift $\phi_0=2\Delta=\frac{\alpha_1-\alpha_2}{\varepsilon(\alpha_1+\alpha_2)}$.

Example 2. Synchronization of chaotic self-oscillations of two Chua oscillators: numerical experiment. Consider a coupled dynamical system of the form

$$\begin{aligned}
\dot{x}_1 &= \alpha_1\left(y_1 - h\left(x_1\right)\right) - \varepsilon\left(x_1 - x_2\right),\\
\dot{y}_1 &= x_1 - y_1 + z_1,\\
\dot{z}_1 &= -\beta y_1 - \gamma z_1,\\
\dot{x}_2 &= \alpha_2\left(y_2 - h\left(x_2\right)\right) + \varepsilon\left(x_1 - x_2\right),\\
\dot{y}_2 &= x_2 - y_2 + z_2,\\
\dot{z}_2 &= -\beta y_2 - \gamma z_2,
\end{aligned}$$

$$h\left(x\right) = m_1 x + \frac{1}{2}\left(m_2 - m_1\right)\left(\left|x+1\right| - \left|x-1\right|\right).$$

The values of parameters are: $\left\{\alpha_1, \alpha_2, \beta, \gamma, m_2, m_1, \varepsilon\right\} = \left\{14, 4, 14, 0.1, -1/2, 2/7, 2\right\}$. Projections of attractor A_μ onto the coordinate planes of the oscillators and the time histories of the corresponding variables, illustrating the phase shift, are shown in Fig. 2.8.

Note that in the experiment, the parameter $\mu = \varepsilon^{-1} = 1/2$ is far from small. However, the result shows that the obtained conclusion about the properties of the synchronization remains valid (the well-known "miracle of a small parameter"). It also remains in force that the attractor A_μ of a coupled system has properties close to the attractor of a single oscillator with parameter $\alpha = \left(\alpha_1 + \alpha_2\right)/2 = 9$. This is already revealed at the visual level, from observing the trajectories of the attractor of a coupled system and the attractor of a single oscillator with parameter $\alpha = 9$. We also note that this system is not smooth, but results of the theory remain valid.

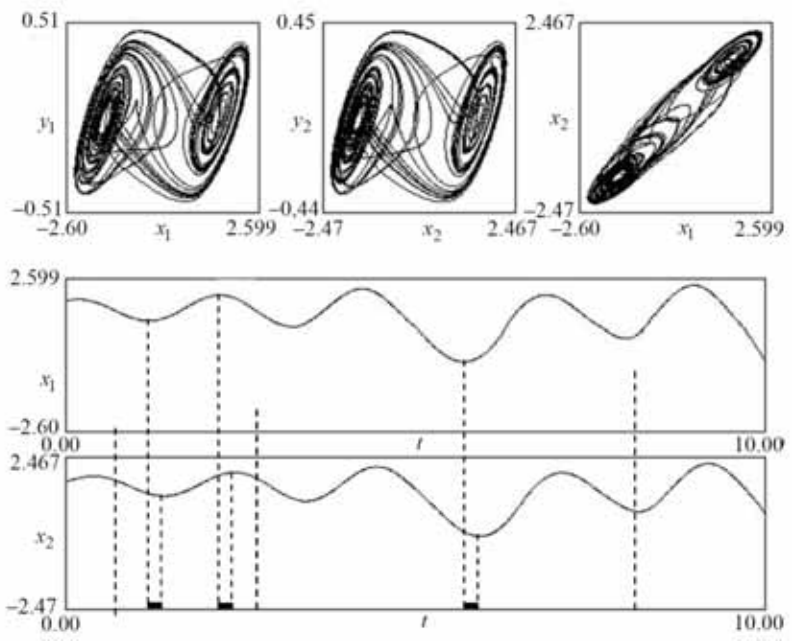

Fig. 2.8. Projections of attractor A_μ onto the coordinate planes of the oscillators and segments of the same-named time-histories illustrating the phase shift $\phi_0 = (\alpha_1 - \alpha_2)/\varepsilon(\alpha_1 + \alpha_2)$.

2.5. Forced synchronization of chaotic oscillations

All theorems on the existence and stability of integral manifolds, which justify the mutual synchronization, are also valid the case of systems with nonreciprocal couplings. In addition, for the asymptotic study, a forced synchronization is technically simpler, since in this case the dynamical system at the integral manifold is prescribed, and represents a system of the master oscillator. That is, if

the conditions for the existence and stability of synchronization are considered fulfilled, then the task is reduced to determining the mapping of the phase portraits of the master and slave oscillators, which, in turn, will determine the properties of their synchronization. In this case, this mapping will be presented explicitly.

Similarly to the case of the mutual synchronization, we will consider the cases of weakly and strongly non-identical systems [166, 167].

Weakly non-identical systems. Consider a coupled system of the form

$$\begin{aligned} \dot{\mathbf{X}} &= \mathbf{F}(\mathbf{X}), \\ \dot{\mathbf{X}}_1 &= \mathbf{F}(\mathbf{X}_1) - \varepsilon \mathbf{C}(\mathbf{X}_1 - \mathbf{X}) + \mu \mathbf{F}_1^*(\mathbf{X}_1). \end{aligned} \tag{2.30}$$

Here μ is some small parameter associated with the weak non-identity of the parameters of the systems. The first equation defines the master oscillator, while the second defines the slave one.

It follows from equations (2.30) that for $\mu = 0$ this generating system has integral manifold $M_0 = \{\mathbf{X} = \mathbf{Y}\}$. Under the condition that will be indicated below, theorems on integral manifolds [17–19] for sufficiently small $\mu \neq 0$ guarantee the existence of manifold M_μ in (2.30), transforming to M_0 for $\mu = 0$. As already noted, for coupled

systems, this is equivalent to the fact that their synchronization exists.

Similarly to the case of mutual synchronization, we define integral manifold M_μ of system (2.30) as a power series by a small parameter:

$$\mathbf{X}_1 = \mathbf{X} + \mu \mathbf{X}_{11}(\mathbf{X}) + \mu^2 \mathbf{X}_{12}(\mathbf{X}) + \ldots .$$

Substituting this series into (2.30) and performing the same transformations as before, we obtain the equations defining functions $\mathbf{X}_{1j}$. In particular, for the function of the first approximation, we obtain an equation of the form

$$\dot{\mathbf{X}}_{11} = \frac{\partial \mathbf{F}}{\partial \mathbf{X}} \mathbf{X}_{11} - \varepsilon \mathbf{C} \mathbf{X}_{11} + \mathbf{F}_1^*(\mathbf{X}). \tag{2.31}$$

The respective partial differential equation has the form

$$\frac{\partial \mathbf{X}_{11}}{\partial \mathbf{X}} \mathbf{F} - \frac{\partial \mathbf{F}}{\partial \mathbf{X}} \mathbf{X}_{11} + \varepsilon \mathbf{C} \mathbf{X}_{11} = \mathbf{F}_1^*(\mathbf{X}). \tag{2.32}$$

Note that for $\varepsilon = 0$ and $\mathbf{F}_1^*(\mathbf{X}) = 0$ equation (2.31) coincides with the equation in variations for the solution corresponding to the trajectory of the chaotic attractor of the master oscillator. Suppose $\lambda_{\max} > 0$ is the maximum Lyapunov exponent of solutions of this equation. In this case, among the number of admissible matrices,

there is a nonzero matrix **C**, for which homogeneous equation $\left(\mathbf{F}_1^*(\mathbf{X}) = 0\right)$ corresponding to (2.31) will be stable. By Theorem 2.1.1, the stability condition is defined by inequality $\varepsilon > \varepsilon^*(\lambda_{\max})$. Due to the boundedness of perturbation $\mathbf{F}_1^*(\mathbf{X})$ any solution of equation (2.31) is bounded for the given **C** and ε, that is, the conditions for the convergence of the power series are satisfied. This condition is the condition for the existence of a (stable) manifold M_μ, i.e. the condition of systems synchronization.

Thus, similarly to the case of mutual synchronization, the problem of the required mapping of the phase portraits of the oscillators has been reduced to solving the quasilinear partial differential equation (2.32) for a given perturbation vector $\mathbf{F}_1^*(\mathbf{X})$. Solving this equation is a technically challenging task. However, the inverse problem, which is more interesting for applications, consists in determining the type of perturbation $\mathbf{F}_1^*(\mathbf{X})$ for a given type of function $\mathbf{X}_{11}$, solved without much difficulty. Recall that the form of this function determines the properties of synchronization. If these properties are determined in advance, then the corresponding perturbation vector is determined from (2.32).

We only note one of the solutions of equation (2.32). Let us assume that the perturbation in (2.30) has the form $\mathbf{F}_1^*(\mathbf{X}) = \nu\mathbf{C}\mathbf{F}$, where ν

is a number. In this case $\mathbf{X}_{11} = \frac{\nu}{\varepsilon}\mathbf{F}(\mathbf{X})$ is the solution to this equation.

This can be confirmed by a direct substitution.

Example 1. Consider a forced synchronization in a coupled system of non-identical Lurie oscillators:

$$\begin{aligned}
&\dot{x} = \alpha\left(-f(x) + \mathbf{a}^T\mathbf{y}\right),\\
&\dot{\mathbf{y}} = \mathbf{B}\mathbf{y} + \mathbf{b}x,\\
&\dot{x}_1 = \alpha_1\left(-f(x_1) + \mathbf{a}^T\mathbf{y}_1\right) + \varepsilon(x - x_1),\\
&\dot{\mathbf{y}}_1 = \mathbf{B}\mathbf{y}_1 + \mathbf{b}x_1.
\end{aligned}$$

To write this system in the form (2.30), the necessary vectors and the coupling matrix are as follows:

$$\boldsymbol{X} = (x,\ \mathbf{y})^T,\ \ \mathbf{X}_1 = (x_1,\ \mathbf{y}_1)^T,\ \ \mathbf{C} = \operatorname{diag}(1,\ 0,\ ...,\ 0),$$

$$\mathbf{F}(\mathbf{X}) = \left(\alpha\left(-f(x) + \mathbf{a}^T\mathbf{y}\right),\ \mathbf{B}\mathbf{y} + \mathbf{b}x\right)^T,$$

$$\mathbf{F}_1(\mathbf{X}_1) = \left(\alpha_1\left(-f(x_1) + \mathbf{a}^T\mathbf{y}_1\right),\ \mathbf{B}\mathbf{y}_1 + \mathbf{b}x_1\right).$$

We write vector $\mathbf{F}_1(\mathbf{X}_1)$ in the following way:

$$\mathbf{F}_1(\mathbf{X}_1) = \mathbf{F}(\mathbf{X}_1) + \mu\mathbf{C}\mathbf{F}^*(\mathbf{X}_1),$$

where $\mathbf{F}^*(\mathbf{X}_1) = \left(\frac{(\alpha_1 - \alpha)}{\mu} \left(-f(x_1) + \mathbf{a}^T \mathbf{y}_1 \right),\ \mathbf{B}\mathbf{y}_1 + \mathbf{b}x_1 \right)^T$. Comparing this expression with the right-hand side of the second equation of system (2.30), we obtain

$$\mathbf{F}_1^*(\mathbf{X}) = \mu\nu\mathbf{C}\mathbf{F}(\mathbf{X}),$$

where $\nu = \alpha^* / \alpha,\ \alpha^* = (\alpha_1 - \alpha)/\mu.$

One can see that this example fits the above-described type of perturbation of the equations of the slave oscillator. From here we obtain $\mathbf{X}_{11} = \frac{\nu}{\varepsilon}\mathbf{F}(\mathbf{X}) = \frac{\nu}{\varepsilon}(\dot{x},\ \dot{\mathbf{y}})^T$. This means that in the regime of synchronization, the variables of the oscillators are linked by the relations

$$x_1 = x + \mu\frac{\nu}{\varepsilon}\dot{x} + O(\mu^2),$$
$$\mathbf{y}_1 = \mathbf{y} + \mu\frac{\nu}{\varepsilon}\dot{\mathbf{y}} + O(\mu^2).$$

or (within the accuracy of μ^2) by relations of the form

$$x_1(t) = x(t + \varphi),$$
$$\mathbf{y}_1(t) = \mathbf{y}(t + \varphi),$$

where $\varphi = \frac{\alpha_1 - \alpha}{\varepsilon\alpha}.$

Strongly non-identical systems with strong couplings. Here, as in the case of the mutual synchronization, we divide the equations of the slave oscillator into groups with strong and weak non-identity of the respective parameters.

Suppose that the parameters of k equations of the slave oscillator are differ significantly from the corresponding parameters of the master oscillator. As already known, in this case, in order to achieve the synchronism between the systems, the equations must have a strong coupling. We take the value of the connection as a "large" parameter. Let us assume that the parameters of the remaining $m-k$ equations are weakly non-identical, and the equations themselves contain either a "moderate" coupling or do not contain it at all. Combining the corresponding equations into groups, we consider a coupled system of the form

$$\begin{aligned}
&\dot{\mathbf{X}} = \mathbf{F}\left(\mathbf{X}, \mathbf{Y}\right),\\
&\dot{\mathbf{Y}} = \mathbf{\Phi}\left(\mathbf{X}, \mathbf{Y}\right),\\
&\dot{\mathbf{X}}_1 = \mathbf{F}_1\left(\mathbf{X}_1, \mathbf{Y}_1\right) - \varepsilon\mathbf{C}\left(\mathbf{X}_1 - \mathbf{X}\right),\\
&\dot{\mathbf{Y}}_1 = \mathbf{\Phi}\left(\mathbf{X}_1, \mathbf{Y}_1\right) - \mathbf{D}\left(\mathbf{Y}_1 - \mathbf{Y}\right) + \mu\mathbf{\Phi}_1^*\left(\mathbf{X}_1, \mathbf{Y}_1\right).
\end{aligned} \tag{2.33}$$

Here $\mathbf{X}_{1,2} \in R^k$, $\mathbf{Y}_{1,2} \in R^{m-k}$, $\mathbf{C} = \mathrm{diag}\left(c_1, c_2, ..., c_k\right)$, $\mathbf{D} = \mathrm{diag}\left(d_1, d_2, ..., d_{m-k}\right)$, $c_i > 0$, $d_j \geq 0$, $\varepsilon^{-1} = \mu$ is a small parameter.

As in the previous case, we define an integral manifold of the system M_μ in the form of power series by a small parameter of the form

$$\mathbf{X}_1 = \mathbf{X} + \mu \mathbf{X}_{11}(\mathbf{X}, \mathbf{Y}) + \mu^2 \mathbf{X}_{12}(\mathbf{X}, \mathbf{Y}) + ...,$$
$$\mathbf{Y}_1 = \mathbf{Y} + \mu \mathbf{Y}_{11}(\mathbf{X}, \mathbf{Y}) + \mu^2 \mathbf{Y}_{12}(\mathbf{X}, \mathbf{Y}) + ...$$

Performing the already known transformations with power series, we obtain the following equations for the functions of the first approximation:

$$\mu \dot{\mathbf{X}}_{11} = \mathbf{F}_1 - \mathbf{F} - \mathbf{C}\mathbf{X}_{11} + \mu\left(\frac{\partial \mathbf{F}_1}{\partial \mathbf{X}}\mathbf{X}_{11} + \frac{\partial \mathbf{F}_1}{\partial \mathbf{Y}}\mathbf{Y}_{11}\right),$$
$$\dot{\mathbf{Y}}_{11} = \frac{\partial \mathbf{\Phi}}{\partial \mathbf{Y}}\mathbf{Y}_{11} - \mathbf{D}\,\mathbf{Y}_{11} + \frac{\partial \mathbf{\Phi}}{\partial \mathbf{X}}\mathbf{X}_{11} + \mathbf{\Phi}_1^*. \tag{2.34}$$

As a singularly perturbed, the first equation of system (2.34) has a stable integral surface of slow motions, which in the zero approximation is defined as follows: $\mathbf{X}_{11} = \mathbf{C}^{-1}(\mathbf{F}_1 - \mathbf{F})$. Since $\mathbf{X}_{11}$ is found, the function $\mathbf{Y}_{11}$ is found by solving either the second equation of the system or the corresponding partial differential equation of the form

$$\frac{\partial \mathbf{Y}_{11}}{\partial \mathbf{X}}\mathbf{F} + \frac{\partial \mathbf{Y}_{11}}{\partial \mathbf{Y}}\mathbf{\Phi} - \frac{\partial \mathbf{\Phi}}{\partial \mathbf{Y}}\mathbf{Y}_{11} + \mathbf{D}\mathbf{Y}_{11} = \frac{\partial \mathbf{\Phi}}{\partial \mathbf{X}}\mathbf{X}_{11} + \mathbf{\Phi}_1^*. \tag{2.35}$$

Assume that we have found a solution to this equation. In this case, the coupling of the variables of oscillators in the forced synchronization regime is determined by equations of the form

$$\mathbf{X}_1 = \mathbf{X} + \mu \mathbf{C}^{-1}\left(\mathbf{F}_1\left(\mathbf{X}, \mathbf{Y}\right) - \mathbf{F}\left(\mathbf{X}, \mathbf{Y}\right)\right), \quad \mathbf{Y}_1 = \mathbf{Y} + \mu \mathbf{Y}_{11},$$

where $\mathbf{X} = \mathbf{X}(t)$, $\mathbf{Y} = \mathbf{Y}(t)$ is the solution corresponding to a certain trajectory of the chaotic attractor of the master oscillator. The accuracy of the found equations is μ^2.

Example 2. Let us consider the same system of Lurie oscillators, now assuming a significant difference in the parameters $(\alpha_1 - \alpha)/\alpha \sim \mu^0$ and considering the inversed value of the coupling parameter as a small parameter. In this case $\mathbf{C} = 1$ (scalar), $\mathbf{D} = 0, \quad \mathbf{\Phi}_1^* = 0, \quad F_1(x, \mathbf{y}) - F(x, \mathbf{y}) = \alpha_1\left(-f(x) + \mathbf{a}^T\mathbf{y}\right) -$ $- \alpha\left(-f(x) + \mathbf{a}^T\mathbf{y}\right) = \dfrac{\alpha_1 - \alpha}{\alpha} F(x, \mathbf{y}) = \dfrac{\alpha_1 - \alpha}{\alpha}\dot{x}.$ By direct substitution in (2.35), we find that $\mathbf{Y}_{11} = \dfrac{\alpha_1 - \alpha}{\alpha}\mathbf{\Phi} = \dfrac{\alpha_1 - \alpha}{\alpha}\dot{\mathbf{y}}$ is his decision. Thus, within the accuracy of μ^2 the regime of synchronization defines the coupling of the variables of oscillators in the same form as in Example 1: $x_1 = x + \dfrac{\alpha_1 - \alpha}{\varepsilon\alpha}\dot{x}, \quad \mathbf{y}_1 = \mathbf{y} + \dfrac{\alpha_1 - \alpha}{\varepsilon\alpha}\dot{\mathbf{y}}$ or

$x_1(t) = x(t+\varphi)$, $\mathbf{y}_1(t) = \mathbf{y}(t+\varphi)$ with the same expression for the phase shift $\varphi = \dfrac{\alpha_1 - \alpha}{\varepsilon\alpha}$.

Numerical experiment. Fig. 2.9 shows the phase portraits of the chaotic attractors of the master Chua oscillator and the slave oscillator synchronized by it for the following parameter set:

$$\{\alpha, \alpha_1, \beta, \gamma, m_2, m_1, \varepsilon\} = \left\{9.1, 4.0, 14, 0.1, -\frac{1}{7}, \frac{2}{7}, 3.0\right\}.$$

As one can see, the value of the coupling parameter is not so large, and its inverse value (1/3) is of the same order as the relative mistuning of the parameters. Nevertheless, the fact of synchronization of oscillators is obvious even at the "visual" level.

Fig. 2.10 shows the segments of time histories of synchronized chaotic oscillations of the oscillators, illustrating the phase shift. In this case, the phase shift is negligible. This effect will manifest itself more clearly in the stream chain of oscillators, the study of which will be discussed in Section 3.6.

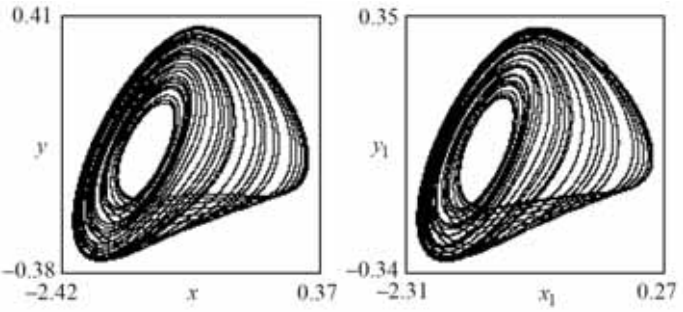

Fig. 2.9. Chaotic attractors of synchronized Chua oscillators.

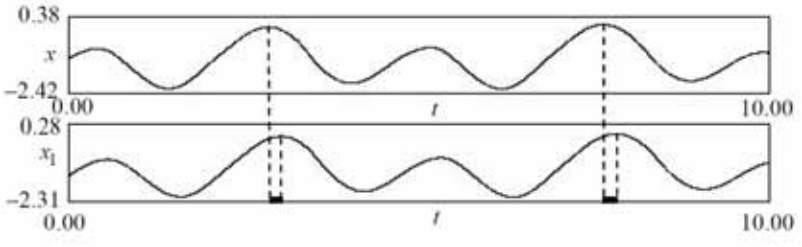

Fig. 2.10. Segments of chaotic time-histories of synchronized oscillations.

A note on systems with slowly varying parameters. Suppose that $\mathbf{X}_{11} = \mathbf{X}_{11}\left(\mathbf{X}(t), \mathbf{a}\right)$ is some solution of the respective equation for the function of the first approximation, where **a** is a constant vector of parameters. Suppose $\mathbf{a} = \mathbf{a}(\eta)$ is a smooth or piecewise-smooth function with a bounded derivative, and $\dot{\eta} = \mu$, where μ is a small parameter, i.e. $\mathbf{a} = \mathbf{a}(\mu t)$ is a slowly varying parameter. In this case, the expression for the derivative of the solution has the form $\dot{\mathbf{X}}_{11} = \dfrac{\partial \mathbf{X}_{11}}{\partial \mathbf{X}}\dot{\mathbf{X}} + \dfrac{\partial \mathbf{X}_{11}}{\partial \mathbf{a}}\dfrac{\partial \mathbf{a}}{\partial \eta}\mu$. It follows from these conditions that

$\left\| \mu \frac{\partial \mathbf{X}_{11}}{\partial \mathbf{a}} \frac{\partial \mathbf{a}}{\partial \eta} \right\| < \mu K$ (by virtue of the natural assumption about the smoothness of the right-hand sides of equations of the oscillators with respect to parameters, the partial derivatives of solutions of the equations for functions $\mathbf{X}_{ij}$, $\mathbf{Y}_{ij}$ are bounded by the respective parameters [128]). This means that expression $\mu \frac{\partial \mathbf{X}_{11}}{\partial \mathbf{a}} \frac{\partial \mathbf{a}}{\partial \eta}$ will determine the function of the asymptotic series $\mathbf{X}_{12}$ (approximation μ^2). In other words, in the case of slowly varying parameters, equations for the functions if the first approximation that determine the mapping of the phase portraits of the oscillators will be the same as in the case of constant parameters. This means that conclusions of the theory of synchronization of systems with constant parameters are also valid for the case of systems with slowly varying parameters with an appropriate interpretation of the results. This topic is of a great practical importance and deserves an independent discussion.

2.6. Formation of signals with a given modulation law of a chaotic carrier and information transfer

Consider an oscillator (self-oscillator) with chaotic dynamics. What parameters of the oscillator should be modulated such that the chaotic oscillations of this oscillator would have a given modulation law with respect to the chaotic oscillations of the unperturbed oscillator (standard) [166, 167]. Let's formulate this problem using the language of synchronization: consider a coupled system of the form

$$\begin{aligned}\dot{\mathbf{X}} &= \mathbf{F}(\boldsymbol{X}) + \mu\mathbf{f}(\mathbf{X}, \eta),\\ \dot{\mathbf{X}}_1 &= \mathbf{F}(\mathbf{X}_1) - \varepsilon\mathbf{C}(\mathbf{X}_1 - \mathbf{X}),\\ \dot{\eta} &= \mu.\end{aligned} \tag{2.36}$$

Here μ is a small parameter, $\mathbf{f}(\mathbf{X}, \eta)$ is a function with slowly varying parameters, which we will call a modulator. It is necessary to find a modulator $\mathbf{f}(\mathbf{X}, \eta)$ and matrix $\mathbf{C}$ such that in the regime of forced synchronization, the specified coupling of the variables of the master and slave oscillators is ensured.

We search for the solution to this problem using the technique discussed above.

1. We define the coupling of variables $\mathbf{X}_1$ and $\mathbf{X}$ in the form of power series

$$\mathbf{X}_1 = \mathbf{X} + \mu\mathbf{X}_{11}(\mathbf{X}, \eta) + \mu^2\mathbf{X}_{12}(\mathbf{X}, \eta) + \ldots . \tag{2.37}$$

2. We substitute this series into the second equation of system (2.36). Carrying out the necessary expansions of functions and taking into account the form of the first equation of the system, we obtain the following equation for the function of the first approximation:

$$\frac{\partial \mathbf{X}_{11}}{\partial \mathbf{X}}\mathbf{F} - \frac{\partial \mathbf{F}}{\partial \mathbf{X}}\mathbf{X}_{11} + \varepsilon \mathbf{C}\mathbf{X}_{11} = -\mathbf{f}\left(\mathbf{X}, \eta\right). \tag{2.38}$$

Since function $\mathbf{X}_{11}$ is given, then equation (2.38) determines the sought modulator.

For example, let the vector function $\mathbf{X}_{11}$ have the form $\mathbf{X}_{11} = \alpha\mathbf{X} + \Delta\dot{\mathbf{X}}$, where $\alpha\left(\mu t\right)$ is a diagonal matrix, $\Delta\left(\mu t\right)$ is a scalar function. In this case, from equation (2.37), we obtain that $\mathbf{X}_1 = \left(\mathbf{I} + \mu\alpha\left(\mu t\right)\right)\mathbf{X}\left(t + \mu\Delta\left(\mu t\right)\right)$ (within the accuracy of μ^2). That is, this form of function $\mathbf{X}_{11}$ corresponds to the amplitude-phase modulation of the chaotic carrier of the master oscillator. If $\Delta\left(\mu t\right) = 0$, then a pure amplitude modulation takes place, and if $\alpha\left(\mu t\right) = 0$ then a phase one takes place.

Example. Let us find a modulator that sets the phase modulation of chaotic oscillations of the Lorentz oscillator.

Substituting expression $\mathbf{X}_{11} = \Delta\dot{\mathbf{X}} = \Delta\mathbf{F}$ into equation (2.38), we obtain the equation defining the modulator:

$$\varepsilon\Delta\begin{pmatrix} -c_1\sigma(x-y) \\ c_2(-y+rx-xz) \\ c_3(-bz+xy) \end{pmatrix} = \mathbf{f}(\mathbf{X},\eta).$$

From the condition of simplicity of the modulator as the minimum number of modulated parameters, we determine the elements of the matrix $\mathbf{C}$: $c_1 = 1,\ c_2 = 0,\ c_3 = 0$ (admissible matrix). As a result, we obtain vector $\mathbf{f}(\mathbf{X},\mu t) = \left(-\varepsilon\Delta(\mu t)\sigma(x-y), 0, 0\right)^T$. The equations of the Lorentz oscillator with a phase modulation of a chaotic carrier have the form

$$\begin{aligned} \dot{x} &= -\left(1+\mu\varepsilon\Delta(\mu t)\right)\sigma(x-y), \\ \dot{y} &= -y + rx - xz, \\ \dot{z} &= -bz + xy. \end{aligned} \tag{2.39}$$

The information signal $\Delta(\mu t)$ can be any bounded function, smooth function, or piecewise-smooth function bounded derivative. It is possible that this signal itself can be an implementation of a random process. Fig. 2.11 shows a simple block-diagram of the information transfer with a direct synchronization of oscillators and phase detection of the sought signal. Figs. 2.12, 2.13 show the results of a numerical experiment carried out according to the diagram shown in Fig. 2.11. The master self-oscillator is the Lorentz oscillator (2.39) with a modulation signal $\Delta(\mu t) = A\sin\mu\omega t$. Parameters of the Lorenz system are: $\sigma = 10,\ r = 27,\ b = 8/3$. An

unperturbed Lorentz oscillator with the same parameters represents a tunable oscillator. The coupling of the oscillators is made according to equations (2.39) with the matrix $\mathbf{C} = \mathrm{diag}(1, 0, 0)$. The filter is resonant.

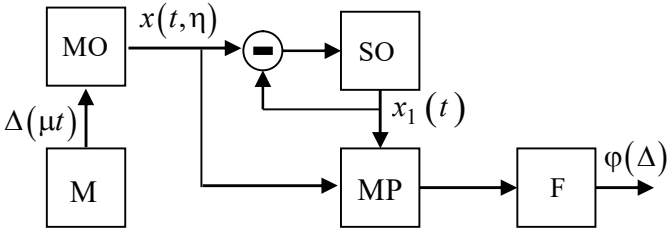

Fig. 2.11. Block diagram of information transmission: MO is the master oscillator, SO is the tunable oscillator, M is the modulator, MP is the multiplier, F is the filter.

Fig. 2.12 illustrates the regime of beatings of oscillators: the coupling parameter $\varepsilon = 0.5$ is small, therefore, the tuned oscillator is out of the synchronization holding range. On surface $(\Delta,\ \varphi(\Delta))$, a chaotic movement is observed.

Fig. 2.13 illustrates the regime of locking the synchronization of chaotic oscillations of oscillators $(\varepsilon = 10)$. The narrow strip on the plane (x_1, x), the width of which $\sim \mu$, is the projection of manifold M_μ onto this plane. On the plane $(\Delta,\ \varphi(\Delta))$, a periodic movement with a period of the modulation signal is observed.

The use of chaotic signals generated by dynamical systems as carriers of useful information is only one of the applications of chaotic synchronization, which, one might say, lies on the surface. The diagram shown in Fig. 2.11 is technically incomplete for a real application and serves only as an illustration of the proposed theory and the of a fundamental possibility of transmitting information with a chaotic carrier. In reality, however, technical problems arise associated, for example, with the effective detection of a useful signal and its filtering.

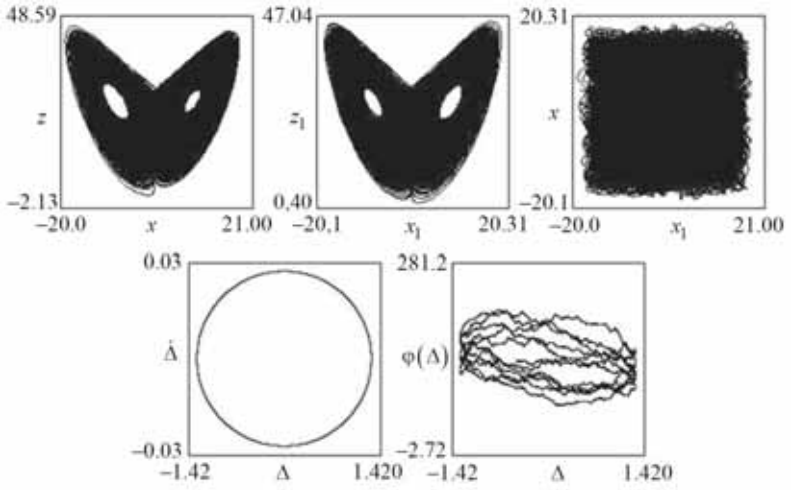

Fig. 2.12. System dynamics out of the synchronization holding range.

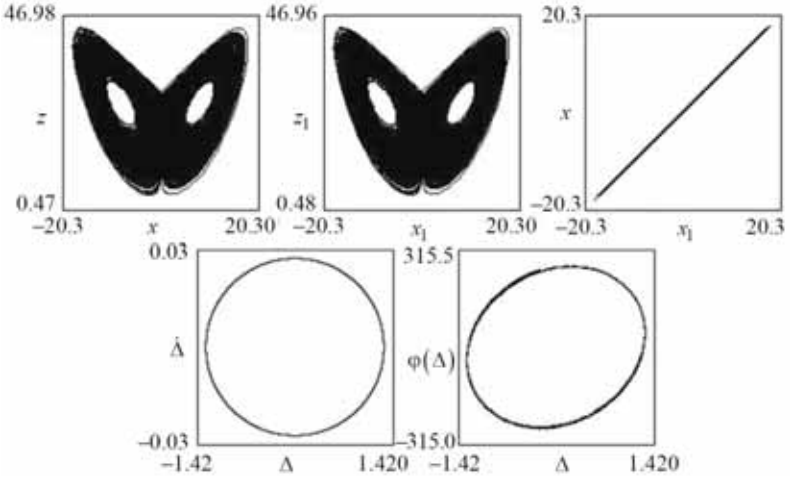

Fig. 2.13. System dynamics in the synchronization locking regime.

CHAPTER 3

SYNCHRONIZATION IN HOMOGENEOUS AND INHOMOGENEOUS LATTICES

Many objects of animate and inanimate nature have a lattice, network structure. In particular, these are antenna arrays and networks of phase synchronization systems [65], neural ensembles [75, 76], and neuron-like networks for information processing [74–76]. In addition, lattice structures can arise in active continuous media, which makes it possible to adequately model the respective processes with discrete oscillator lattices [79, 80]. In particular, this can be done to study the mechanisms of turbulence development. As an example, Fig. 3.1a shows a diagram of convective rolls arising in a layer of liquid heated from below. Visualization of the process shows [170] that in a steady state regime, the flow represents a system of convective cells with identical, synchronized fluid motion in each of them. In general, the flow is such that, in fact, the liquid layer can be divided into cells by ideal walls without disturbing its structure (Fig. 3.1b).

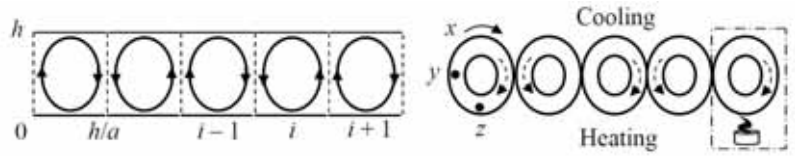

a b

Fig. 3.1. Diagram of convective rolls (a)
and a system of convective tubes (b).

According to results of experiments, the perturbed structure in the course of time comes to its initial state with the same set of elements (the structure is stable). In this case, the thermodynamic parameters of an individual convective roll, its geometrical dimensions and shape are reproduced. The number of convective cells in the gutter is constant for the fixed parameters of the experiment. This means that a single cell can be referred to as a basic structure element. Without pretending for a complete adequacy of the model, the system of rolls can be represented as a chain of interacting "convective tubes" [106, 171]: toroidal tubes with liquid (see Fig. 3.1b). It is known that the flow in such a tube is governed by the Lorentz system

$$\begin{cases} \dot{x} = \sigma x + \sigma y, \\ \dot{y} = -xz + rx - y, \\ \dot{z} = xy - bz, \end{cases}$$

where x is the flowrate, y, z is the liquid temperature at the middle and at the lower points of the tube, respectively; the dot denotes the

derivative over the dimensionless time. Parameter b is determined by the shape of the tube (for a circular tube, $b = 1$).

Let us consider the physical meaning of the coefficients of this system in more detail:

1. $\sigma = \frac{\nu}{\chi}$ is the Prandtl number, depending on the properties of the liquid, such as viscosity and thermal diffusivity: the higher the thermal diffusivity, the lower the Prandtl number.

2. $b = \frac{4}{(1+a)^2}$, where a is the ratio of geometric dimensions.

3. $r = \frac{R}{R_c}$ is the external control parameter, where $R = \frac{g\beta\theta L^2}{\nu\chi}$ is the Rayleigh number (proportional to Archimedean force and inversely proportional to viscosity and thermal diffusivity), $R_c = \frac{\pi^4 \left(a^2 + n^2\right)^2}{a^2}$ is the critical value of the Rayleigh number.

Thus, within certain limits, such dynamical regime of convection in a liquid layer can be considered as a synchronization regime in a chain of discrete Lorentz oscillators.

This chapter is devoted to the study of the stability of synchronization in homogeneous lattices of dynamical systems, which determines the spatially homogeneous dynamic state of the lattices or a

quasi-homogeneous state in the inhomogeneous lattices. Lattices of various geometric dimensions with diffusive couplings are considered.

3.1. General information about synchronization in lattices of dynamical systems

Consider a homogeneous lattice of diffusive-coupled dynamical systems of the form

$$\begin{aligned} &\dot{\mathbf{X}}_i = \mathbf{F}\left(\mathbf{X}_i,\ t\right) + \varepsilon \mathbf{C}\left(\mathbf{X}_{i-1} - 2\mathbf{X}_i + \mathbf{X}_{i+1}\right), \\ &i = \overline{1, N}. \end{aligned} \tag{3.1}$$

An individual system in (3.1) is governed by equation

$$\begin{aligned} &\dot{\mathbf{X}} = \mathbf{F}\left(\mathbf{X},\ t\right), \\ &\mathbf{X} = \left(x_1, x_2, ..., x_m\right)^T,\ x \in R^1,\ \mathbf{F}\left(\mathbf{X}\right): R^m \to R^m. \end{aligned} \tag{3.2}$$

In principle, any model of physical systems discussed in the previous sections can act here as an individual dynamical system.

We will assume that the dynamical properties of system (3.2) are known. In particular, we assume that in the extended phase space $G\left(\mathbf{X},\ t\right)$ there exists attractor $A\left(1\right)$ with maximum Lyapunov exponent $\lambda\left(1\right)$. The latter represents the maximum exponent of the equation in variations

$$\dot{\mathbf{U}} = \mathbf{F}'\left(\xi(t)\right)\mathbf{U},$$

where $\xi(t) \in A(1)$, $\mathbf{F}'(\mathbf{X}) = \dfrac{\partial \mathbf{F}(\mathbf{X})}{\partial \mathbf{X}}$ is the Jacobi matrix. Note that for assumptions made the following is valid: $\|\mathbf{U}\| = D\exp\lambda(1)t$, $D = \text{const}$.

Matrix **C** in Eqs. (5.1) defines a structure of couplings of partial systems, while ε represents a scalar parameter.

Coming back to modeling convection in a liquid layer, we recall that system (3.2) for a convective cell can be obtained from the equations of hydrodynamics by the Bubnov – Galerkin method. Within the framework of this method, the three-mode approximation of the Navier – Stokes equations (under the Boussinesq conditions) gives the well-known Lorentz system [102, 104]. In this case $\mathbf{X} = (x,\ y,\ z)^T$, $\mathbf{F}(\mathbf{X}) = \left(-\sigma(x-y),\ -y + rx - xz,\ -bz + xy\right)^T$, $x,\ y,\ z$ are the dimensionless amplitudes of modes, $\sigma = \nu/\kappa$ is the Prandtl number, ν, κ are the coefficients of kinematic viscosity and thermal conductivity, $r = R/R_c$ is the Rayleigh number normalized to the critical one: $R = g\gamma h^3 \Delta T/\nu\kappa$, $R_c = \pi^4 a^{-2}\left(1 + a^2\right)^3$, a is the ratio of the vertical and horizontal dimensions of the convective cell, g is the gravity acceleration, γ is the coefficient of thermal expansion of the liquid, h s the thickness of the layer, ΔT is the tem-

perature difference between its surfaces, b is the coefficient associated with the geometry of the convective cell.

To determine the coupling of the oscillators, we proceed from the following natural assumptions: a) in the steady state, all the respective dynamic parameters of the oscillators are the same: $\mathbf{X}_i = \mathbf{X}_{i+1},\ i = 1,\ 2,\ ...,\ N-1$; b) in the steady state, dynamic couplings turn to zero (vanish); c) the nature of the interaction of any oscillator with its neighbors (left, right) is physically the same. Within the framework of these assumptions, we come to the conclusion that the sought-for coupling of the oscillators has the form $-\left(\mathbf{f}\left(-\mathbf{X}_{i-1}+\mathbf{X}_i\right)+\mathbf{f}\left(\mathbf{X}_i-\mathbf{X}_{i+1}\right)\right)$, and $\mathbf{f}(0)=0$.

If the coupling is linear or the perturbations of the stationary structure are small, then it takes the form $-\varepsilon\mathbf{C}\left(-\mathbf{X}_{i-1}+2\mathbf{X}_i-\mathbf{X}_{i+1}\right)$, where $\mathbf{C}$ is a constant matrix, ε is a scalar parameter. To determine the matrix and the parameter, additional assumptions shall be made or experimental data must be used. In particular, for the case of a chain of interacting convective tubes $\mathbf{C}=\operatorname{diag}(0,\ 1,\ 0)$, ε is the coefficient of thermal conductivity.

If one of the scalar variables (3.2) is cyclic $x = \varphi(\mathrm{mod}\,2\pi)$, then the system can be interpreted as a generalized rotator. The name is justified by the fact that all the mathematical models considered above can be reduced to the form (3.2), if the rotator itself is considered as

a system with one degree-of-freedom in conjunction with external disturbances and loads. We assume that function $\mathbf{F}(\mathbf{X},t)$ is cyclic in time.

For the boundary conditions of the form $\mathbf{X}_0 \equiv \mathbf{X}_1,\ \ \mathbf{X}_N \equiv \mathbf{X}_{N+1}$ system (3.1) represents a chain, while for $\mathbf{X}_0 \equiv \mathbf{X}_N,\ \mathbf{X}_1 \equiv \mathbf{X}_{N+1}$, it represents a ring.

It will be seen from further discussion that the synchronization, which represents our main interest, is closely related to the existence of so-called integral manifolds representing singular surfaces in the phase space of coupled systems filled with trajectories. This mathematical object is such that if the initial conditions of the system are specified on the integral surface, then the affix that moves along the corresponding phase trajectory never leaves this surface.

It follows directly from system (3.1) that hyperplane $M_0 = \{\mathbf{X}_1 = \mathbf{X}_2 = ... = \mathbf{X}_{N-1} = \mathbf{X}_N\}$ represents its integral manifold. We can draw this conclusion by solving equation $\mathbf{X}_{i-1} - 2\mathbf{X}_i + \mathbf{X}_{i+1} = 0.$ The traces of this hyperplane on coordinate planes of the corresponding variables of different partial systems are the bisectors of the first and third coordinate angles. We also note that the geometric dimension of the hyperplane coincides with the dimension of the phase space of the individual system.

Our special interest in this manifold will become clear from the following considerations. Let us imagine that the initial conditions for system (3.1) are given at M_0. In this case, as it directly follows from (5.1), the coupled system falls into N separate systems of the form (3.2). Apart from that, the motions of these independent systems will be synchronized, since, in principle, these are the motions of identical systems with identical initial conditions. In other words, the synchronization of interest corresponds to the motion of a phase point along trajectories located on the integral manifold of system (3.1). The question that remains is: what is the nature of these trajectories? The answer is quite simple: since projections of these trajectories onto the phase spaces of individual systems (partial phase portraits) are the trajectories of partial systems, then trajectories on the hyperplane M_0 are induced by the same system of the form (3.2).

Of course, setting up exact initial conditions (on an integral manifold) lays behind the scope of a real experiment. To solve the problem of synchronization, the problem of stability of an integral manifold must be solved.

Assume that the integral manifold is stable. In this case, the process of synchronization can be described as follows. For any initial condition from the neighborhood of the manifold (at least from a small neighborhood of it), the affix runs to the surface of M_0 and, after some time, starts moving almost along the trajectory of attractor

$A(1)$ of system (3.2) defined on this manifold. In this case, all of the partial phase points in the spaces of individual systems (projections of the phase point of system (3.1)) move in mutual synchronism along the corresponding trajectories of their partial phase portraits, i.e. along identical trajectories of identical attractors $A(1)$. In other words, there is a stable regime of mutual synchronization of interacting subjects in the lattice (3.1).*Synchronization in a chain.* Consider the local stability of synchronization as a local stability of a "part" of the manifold that contains attractor $A(1)$. It can be established that, with respect to transversals $\mathbf{U} = (\mathbf{U}_1, \mathbf{U}_2, ..., \boldsymbol{U}_p)$ of manifold M_0, where $\mathbf{U}_k = \mathbf{X}_k - \mathbf{X}_{k+1}$, $k = \overline{1, p}$, $p = N - 1$, linearized system (3.1) can be reduced to one equation of the form

$$\dot{\mathbf{U}} = (\mathbf{I}_p \otimes \mathbf{J}_m(t) - \varepsilon \mathbf{D}_p \otimes \mathbf{C})\mathbf{U}. \tag{3.3}$$

Here $J_m(\xi(t))$ is the Jacobi matrix of an elementary oscillator, $\xi(t) \in A(1)$, $\otimes$ is the symbol of the direct (Kronecker) product of matrices, $\mathbf{I}_p$ is the unit matrix of the corresponding order, $\mathbf{D}_p$ is the symmetric matrix of the form

$$\mathbf{D}_p = \begin{pmatrix} 2 & -1 & 0 & 0 & & & & \\ -1 & 2 & -1 & 0 & & & & \\ 0 & -1 & 2 & -1 & & \mathbf{0} & & \\ 0 & 0 & -1 & 2 & & & & \\ & & & & \ddots & & & \\ & & & & & 2 & -1 & 0 & 0 \\ & & \mathbf{0} & & & -1 & 2 & -1 & 0 \\ & & & & & 0 & -1 & 2 & -1 \\ & & & & & 0 & 0 & -1 & 2 \end{pmatrix}.$$

Stable isochronous synchronization corresponds to the stable solution $\mathbf{U} = 0$ of Eq. (3.3). This equation has one property that radically simplifies solution of the problem that we formulate in the form of a lemma (see also [172].

Lemma 3.1.1. Suppose $\lambda_{\min} = \lambda_1 < \lambda_2 < \lambda_3 < ... < \lambda_{p-1} < \lambda_p = \lambda_{\max}$ is the spectrum of eigenvalues of constant matrix $\mathbf{D}_p$. In this case, Eq. (3.3), as a result of a nondegenerate transformation $\mathbf{U} = \mathbf{SV}$, is reduced to the form

$$\begin{aligned} &\dot{\mathbf{V}}_j = \left(\mathbf{J}_m(t) - \varepsilon\lambda_j \mathbf{C}\right)\mathbf{V}_j, \\ &j = \overline{1, p}. \end{aligned} \tag{3.4}$$

Proof. Suppose $\mathbf{S}_0$ is the transform matrix of matrix $\mathbf{D}_p$, while $\mathbf{S}$ is the transform matrix of matrix $\mathbf{D}_p \otimes \mathbf{C}$, i.e. $\mathbf{S}_0^{-1}\mathbf{D}_p\mathbf{S}_0 = \mathbf{D}_0 = \operatorname{diag}\left(\lambda_1, \lambda_2, ..., \lambda_p\right)$. It is known that the roots of

matrix $\mathbf{D}_p \otimes \mathbf{C}$ are all possible products of the roots of matrix-factors: $\lambda_1 c_1, \lambda_1 c_2, ..., \lambda_1 c_m$; $\lambda_2 c_1, \lambda_2 c_2, ..., \lambda_2 c_m$; ...; $\lambda_p c_1, \lambda_p c_2, ..., \lambda_p c_m$, i.e. $\mathbf{S}^{-1}\left(\mathbf{D}_p \otimes \mathbf{C}\right)\mathbf{S} = \mathbf{D}_0 \otimes \mathbf{C}$. Let us show that $\mathbf{S} = \mathbf{S}_0 \otimes \mathbf{I}_m$. Applying the properties of direct product of matrices [173, 174], we obtain

$$\mathbf{S}^{-1}\left(\mathbf{D}_p \otimes \mathbf{C}\right)\mathbf{S} = \mathbf{S}^{-1}\left(\mathbf{S}_0\mathbf{D}_0\mathbf{S}_0^{-1} \otimes \mathbf{I}_m\mathbf{C}\mathbf{I}_m^{-1}\right)\mathbf{S} =$$

$$= \mathbf{S}^{-1}\left(\mathbf{S}_0 \otimes \mathbf{I}_m\right)\left(\mathbf{D}_0 \otimes \mathbf{C}\right)\left(\mathbf{S}_0^{-1} \otimes \mathbf{I}_m\right)\mathbf{S} = \mathbf{D}_0 \otimes \mathbf{C}.$$

From here it follows that $\mathbf{S}^{-1}\left(\mathbf{S}_0 \otimes \mathbf{I}_m\right) = \mathbf{I}_{mp}$ and $\mathbf{S} = \mathbf{S}_0 \otimes \mathbf{I}_m$.

Let us perform the transformation $\mathbf{U} = \mathbf{S}\mathbf{V}$ in Eq. (3.3). As a result, we obtain an equation of the form

$$\dot{\mathbf{V}} = \mathbf{S}^{-1}\left(\mathbf{I}_p \otimes \mathbf{J}_m\right)\mathbf{S}\mathbf{V} - \varepsilon\mathbf{S}^{-1}\left(\mathbf{D}_p \otimes \mathbf{C}\right)\mathbf{S}\mathbf{V}.$$

Let us show that matrix $\mathbf{S}^{-1}\left(\mathbf{I}_p \otimes \mathbf{J}_m\right)\mathbf{S}$ is cell-diagonal. Using the properties of the direct product of matrices, we obtain:

$$\mathbf{S}^{-1}\left(\mathbf{I}_p \otimes \mathbf{J}_m\right)\mathbf{S} = \left(\mathbf{S}_0^{-1} \otimes \mathbf{I}_m\right)\left(\mathbf{I}_p \otimes \mathbf{J}_m\right)\left(\mathbf{S}_0 \otimes \mathbf{I}_m\right) =$$

$$= \left(\mathbf{S}_0^{-1}\mathbf{I}_p\mathbf{S}_0\right) \otimes \left(\mathbf{I}_m\mathbf{J}_m\mathbf{I}_m\right) = \mathbf{I}_p \otimes \mathbf{J}_m = \mathrm{diag}\left(\mathbf{J}_m, \mathbf{J}_m, ..., \mathbf{J}_m\right).$$

Taking into account all transformations with respect to the coordinates of vector **V** we obtain system of Eqs. (3.4), equivalent to Eq. (3.3).

We note that the transformation of Eq. (3.3) to Eq. (3.4) is analogous by sense to the reduction of a system of linear and linearly coupled oscillators to normal vibrations (normal form).

On the basis of this lemma, we formulate the following theorem on the local stability of synchronization.

Theorem 3.1.1. Suppose $\lambda(1)$ is the maximal exponent of attractor $A(1)$ of a partial oscillator, while $\lambda_{\min}$, $\lambda_{\max}$ are, respectively, the minimum and maximum eigenvalues of matrix $\mathbf{D}_p$. If matrix then synchronization in a coupled system of oscillators is stable for $\varepsilon > \lambda(1)/\lambda_{\min}$. For $\varepsilon < \lambda(1)/\lambda_{\max}$ it is unstable in all directions transverse to manifold M_0. For intermediate values of the parameter of coupling, the synchronization is multistable. For the other matrix **C** (among the admissible matrices) the same inequalities are valid, but for a change $\lambda(1) \to \varepsilon^*(\lambda(1))$, where the value of ε^* depends on this matrix.

Proof. Suppose that $\mathbf{C} = \mathbf{I}$. Let us perform a change of the variables in Eq. (3.4) $\mathbf{V}_j = e^{-\varepsilon\lambda_j t}\mathbf{W}_j$. which results in a system of identical equations of the form

$$\dot{\mathbf{W}}_j = \mathbf{J}_m(t)\mathbf{W}_j.$$

By their form, each of these equations is an equation in variation with respect to the solution corresponding to a trajectory of the attractor of a single oscillator, i.e. $\|\mathbf{W}_j\| = Ce^{\lambda(1)t}$, where C is a certain constant. As a result of the change of the variables, we obtain $\|\mathbf{V}_j\| = Ce^{(\lambda(1)-\varepsilon\lambda_j)t}$. From here, it follows that if $\varepsilon > \lambda(1)/\lambda_j$, then $\|\mathbf{V}_j\| \to 0$ for $t \to \infty$, as well as $\|\mathbf{V}_j\| \to \infty$ for $t \to \infty$, if $\varepsilon < \lambda(1)/\lambda_j$. It means that if $\varepsilon > \lambda(1)/\lambda_{\min}$, then all Eqs. (3.4) are stable, and if $\varepsilon < \lambda(1)/\lambda_{\max}$, then all equations of (3.4) are unstable. According to the lemma, the conditions of stability and instability are also transferred to Eq. (3.3). For intermediate values of parameter ε a number of equations is stable and the rest are unstable: solution $\mathbf{V} = 0$, and, therefore, also $\mathbf{U} = 0$ have a saddle type, which corresponds to multistable, or, in other words, to partial synchronization.

The property of function $\varepsilon^*(\lambda(1))$: equals to zero for $\lambda(1) \le 0$ and grows for $\lambda(1) > 0$. Apart from that, it depends on the structure of coupling of the oscillators representing elements c_i of matrix $\mathbf{C}$. In particular, if $\mathbf{C} = \mathbf{I}$, then $\varepsilon^*(\lambda(1)) = \lambda(1)$.

Let us analyze conditions of stability of synchronization. Determination of the eigenvalues of matrix $\mathbf{D}_p$ [173, 175] for the minimum root results in: $\lambda_{\min} = 4\sin^2 \frac{\pi}{2N}$. After this, the condition of stability of synchronization takes the form

$$\varepsilon > \varepsilon^* \left(\lambda(1)\right) \Big/ \left(4\sin^2 \frac{\pi}{2N} \right). \tag{3.5}$$

Let us assume that the attractor of an individual system is regular (such as with a stable limit cycle or torus), i.e. $\lambda(1) < 0$, $\varepsilon^* \left(\lambda(1)\right) = 0$. As one can see from (3.5), in this case, synchronization in the chain is stable for any value of the parameter of coupling, including arbitrary, small values. And this is the case for chains with any number of elements.

A completely different situation arises in the case when the attractor of an individual system is chaotic. In this case, $\lambda(1) > 0$, $\varepsilon^* \left(\lambda(1)\right) > 0$, and, therefore, the right-hand side of (3.5) establishes a threshold value of the parameter of coupling that depends on the degree of randomness of the attractor, the measure of which is $\lambda(1)$, as well as on the number of dynamical systems N in the chain. For a fixed value of ε, the number of systems in the chain for which a chaotic synchronization can take place is defined by an inequality of the form

$$N \le N_0 = \left[\frac{\pi}{\arccos \nu} \right], \quad \nu = 1 - \frac{\varepsilon^* \left(\lambda(1) \right)}{2\varepsilon}.$$

In particular, if $N_0 >> 1,$ then the following asymptotic formulae are valid: $\varepsilon > \pi^{-2} N^2 \varepsilon^* \left(\lambda(1) \right), \quad N \le N_0 = \left[\pi \sqrt{\varepsilon / \varepsilon^*} \right].$

Synchronization in a ring. Consider the stability of the synchronization in the ring. Taking into account boundary conditions $\mathbf{X}_0 \equiv \mathbf{X}_N, \quad \mathbf{X}_1 \equiv \mathbf{X}_{N+1}$ with respect to variables $\mathbf{U}_k = \mathbf{X}_k - \mathbf{X}_{k+1},$ $k = \overline{1, N-1}$ representing transversals to the "part" of the manifold that contains the chaotic attractor, we obtain an equation of the same form as (3.3), with matrix $\mathbf{D}_p, \; p = N-1,$ of the form

$$\mathbf{D}_p = \begin{pmatrix} 3 & 0 & 1 & 1 & \dots & 1 & 1 & 1 & 1 \\ -1 & 2 & -1 & 0 & \dots & 0 & 0 & 0 & 0 \\ 0 & -1 & 2 & -1 & \dots & 0 & 0 & 0 & 0 \\ 0 & 0 & -1 & 2 & \dots & 0 & 0 & 0 & 0 \\ \vdots & \vdots & \vdots & \vdots & \ddots & \vdots & \vdots & \vdots & \vdots \\ 0 & 0 & 0 & 0 & \dots & 2 & -1 & 0 & 0 \\ 0 & 0 & 0 & 0 & \dots & -1 & 2 & -1 & 0 \\ 0 & 0 & 0 & 0 & \dots & 0 & -1 & 2 & -1 \\ 1 & 1 & 1 & 1 & \dots & 1 & 1 & 0 & 3 \end{pmatrix}.$$

Eigenvalues of matrix $\mathbf{D}_p$ are expressed by formula $\lambda_j = 4 \sin^2 \pi j / N, \quad j = \overline{1, N-1},$ from which it follows that

$\lambda_{\min} = 4\sin^2\dfrac{\pi}{N}$, and $\lambda_{\max} = 4\sin^2\dfrac{\pi j^*}{N}$, where $j^* = \dfrac{N}{2}$, if N is an even number, and $j^* = \dfrac{N+1}{2}$, if N is an odd one.

Thus, isochronous synchronization in a ring of dynamical systems is stable if $\varepsilon > \varepsilon^* \Big/ 4\sin^2\dfrac{\pi}{N}$, and it is unstable if $\varepsilon < \varepsilon^* \Big/ 4\sin^2\dfrac{\pi j^*}{N}$.

Synchronization in a two-dimensional lattice. Consider the stability of the synchronization of dynamical systems in a two-dimensional rectangular lattice modeled by differential equations of the form

$$\dot{\mathbf{X}}_{ij} = \mathbf{F}\left(\boldsymbol{X}_{ij}\right) - \varepsilon\mathbf{C}\left(4\mathbf{X}_{ij} - \mathbf{X}_{i-1\,j} - \mathbf{X}_{i+1\,j} - \mathbf{X}_{ij-1} - \mathbf{X}_{ij+1}\right),$$
$$i = 1, 2, ..., N_1, \quad j = 1, 2, ..., N_2, \tag{3.6}$$

with boundary conditions $\mathbf{X}_{0\,j} = \mathbf{X}_{1j}$, $\mathbf{X}_{N_1+1\,j} = \mathbf{X}_{N_1 j}$, $\mathbf{X}_{i0} = \mathbf{X}_{i1}$, $\mathbf{X}_{iN_2+1} = \mathbf{X}_{iN_2}$.

Using the chain as an example, we have seen that the study of the stability of synchronization is ultimately reduced to the study of the eigenvalues of matrix $\mathbf{D}_p$, which is responsible for couplings of individual systems. Obviously, the same should take place in the case of Eqs. (3.6). The problem of finding the corresponding matrix can be solved by a fusion of a two-dimensional lattice from the corresponding chains, using them as “elements” of the lattice.

Consider a rectangular lattice as a “parallel” coupling of chains. To do so, we equip the vectors of the elementary oscillator in (5.1) with a second subscript: we introduce vectors $\mathbf{Y}_j =$ $= \mathrm{col}\left(\mathbf{X}_{1j}, \mathbf{X}_{2j}, ..., \mathbf{X}_{N_1 j}\right)$, $\Phi\left(\mathbf{Y}_j\right) = \mathrm{col}\left(\mathbf{F}\left(\mathbf{X}_{1j}\right), \mathbf{F}\left(\mathbf{X}_{2j}\right), ..., \mathbf{F}\left(\mathbf{X}_{N_1 j}\right)\right)$ and rewrite an arbitrary chain (system (3.1)) with one equation:

$$\dot{\mathbf{Y}}_j = \Phi\left(\mathbf{Y}_j\right) - \varepsilon\left(\mathbf{B}_{N_1} \otimes \mathbf{C}\right)\mathbf{Y}_j, \tag{3.7}$$

where $\mathbf{B}_{N_1}$ is a diffusion matrix of the form

$$\mathbf{B}_{N_1} = \begin{Vmatrix} 1 & -1 & 0 & \cdots & \cdots & 0 & 0 \\ -1 & 2 & -1 & \ddots & \cdots & 0 & 0 \\ 0 & -1 & 2 & \ddots & \ddots & 0 & 0 \\ \vdots & \ddots & \ddots & \ddots & \ddots & \ddots & \vdots \\ \vdots & \vdots & \ddots & \ddots & 2 & -1 & 0 \\ 0 & 0 & 0 & \ddots & -1 & 2 & -1 \\ 0 & 0 & 0 & \cdots & 0 & -1 & 1 \end{Vmatrix}.$$

Since, for a parallel coupling of the chains, all elements of vector $\mathbf{Y}_j$ are coupled to the corresponding elements of the neighboring vectors $\mathbf{Y}_{j-1}$ and $\mathbf{Y}_{j+1}$, the matrix of the fusion of the lattice from the elements of (3.7) represents a unit matrix $\mathbf{I}_{N_1}$. Taking the aforesaid parts, as well as Eqs. (5.7), the equations of the lattice take the form

$$\dot{\mathbf{Y}}_j = \Phi\left(\mathbf{Y}_j\right) - \varepsilon\left(\mathbf{B}_{N_1} \otimes \mathbf{C}\right)\mathbf{Y}_j - \varepsilon\left(\mathbf{I}_{N_1} \otimes \mathbf{C}\right)\left(-\mathbf{Y}_{j-1} + 2\mathbf{Y}_j - \mathbf{Y}_{j+1}\right),$$
$$j = 1, 2, ..., N_2. \tag{3.8}$$

The boundary conditions in system (3.8) have the form $\mathbf{Y}_0 = \mathbf{Y}_1$, $\mathbf{Y}_{N_2} = \mathbf{Y}_{N_2+1}$.

Performing matrix operations and writing this system with respect to elementary oscillators, one can verify the equivalence of systems (3.8) and (3.6). Let us pay attention to the similarity of the forms of Eqs. (3.8) and (3.1).

In contrast to the previous section, where the linearization was carried out for variables $\mathbf{U}_i = \mathbf{X}_i - \mathbf{X}_{i+1}$ (transversals of the manifold), here we will linearize Eqs. (3.8) in a standard way, for variables $\mathbf{U}_{ij} = \mathbf{X}_{ij} - \xi(t)$ in the vicinity of solution $\mathbf{X}_{ij} = \xi(t) \in A(1)$.

After convolving the linearized system into one equation, we obtain

$$\dot{\mathbf{U}} = \mathbf{I}_{N_1 N_2} \otimes \mathbf{J}_m\left(\xi\right)\mathbf{U} - \varepsilon\left(\mathbf{I}_{N_2} \otimes \mathbf{B}_{N_1} + \mathbf{B}_{N_2} \otimes \mathbf{I}_{N_1}\right) \otimes \mathbf{C}\mathbf{U}. \tag{3.9}$$

We note that the method of linearization does not fundamentally change the essence of the matter. The formal difference is that, in this case, the dimension of matrix $\mathbf{D}_p = \mathbf{I}_{N_2} \otimes \mathbf{B}_{N_1} + \mathbf{B}_{N_2} \otimes \mathbf{I}_{N_1}$ is one unit higher than the one that would be obtained from the first case, and in its spectrum there is one zero root. All other eigenval-

ues are positive and coincide with the eigenvalues of the matrix obtained in the first case (the matrices are related by equivalent transformations). Without going into much detail, in what follows, we will not take the zero root into account.

As one can see, Eq. (3.9) falls under the above formulated lemma. Consequently, the stability of the synchronization is determined by the roots of matrix $\mathbf{D}_p = \mathbf{I}_{N_2} \otimes \mathbf{B}_{N_1} + \mathbf{B}_{N_2} \otimes \mathbf{I}_{N_1}$.

A study of this matrix shows that its minimal eigenvalue is expressed by the formula, which is already familiar to us from the previous section: $\lambda_{\min} = 4\sin^2 \frac{\pi}{2N}$, where $N = \max\{N_1, N_2\}$. We obtain an interesting and unexpected result: the condition of the stability of synchronization is defined by inequality $\varepsilon > \frac{\varepsilon^*(\lambda(1))}{4\sin^2 \frac{\pi}{2N}}$, coinciding with the condition of stability of synchronization in a chain whose "length" is equal to the greatest "side" of a rectangular lattice of oscillators.

Synchronization in a three-dimensional lattice. We consider the stability of a spatially homogeneous structure in a three-dimensional lattice of dynamical systems governed by equations of the form

$$\dot{\mathbf{X}}_{ijk} = \mathbf{F}\left(\mathbf{X}_{ijk}\right) -$$
$$- \varepsilon\mathbf{C}\left(6\mathbf{X}_{ijk} - \mathbf{X}_{i-1jk} - \mathbf{X}_{i+1jk} - \mathbf{X}_{ij-1k} - \mathbf{X}_{ij+1k} - \mathbf{X}_{ijk-1} - \mathbf{X}_{ijk+1}\right),$$
$$i = 1, 2, ..., N_1, \quad j = 1, 2, ..., N_2, \quad k = 1, 2, ..., N_3. \tag{3.10}$$

To find the desired matrix, we proceed analogously to the two-dimensional case, by considering a three-dimensional lattice in the form of a "parallel" coupling of layers – two-dimensional lattices of the form (3.6). We equip each elementary oscillator in (3.8) by the third index and write the equation of an arbitrary layer (system (3.8)) in the form of a single equation:

$$\dot{\mathbf{Z}}_k = \mathrm{H}\left(\mathbf{Z}_k\right) - \varepsilon\left(\mathbf{I}_{N_2} \otimes \mathbf{B}_{N_1} + \mathbf{B}_{N_2} \otimes \mathbf{I}_{N_1}\right) \otimes \mathbf{C}\mathbf{Z}_k.$$

Now, by considering the three-dimensional lattice as a "parallel coupling of layers", we rewrite it in the following form:

$$\dot{\mathbf{Z}}_k = \mathrm{H}\left(\mathbf{Z}_k\right) - \varepsilon\left(\mathbf{I}_{N_2} \otimes \mathbf{B}_{N_1} + \mathbf{B}_{N_2} \otimes \mathbf{I}_{N_1}\right) \otimes \mathbf{C}\mathbf{Z}_k -$$
$$- \varepsilon\left(\mathbf{I}_{N_1N_2} \otimes \mathbf{C}\right)\left(-\mathbf{Z}_{k-1} + 2\mathbf{Z}_k - \mathbf{Z}_{k+1}\right),$$
$$k = 1, 2, ..., N_3$$

with boundary conditions $\mathbf{Z}_0 = \mathbf{Z}_1, \ \mathbf{Z}_{N_3} = \mathbf{Z}_{N_3+1}$.

Obtained system is equivalent to (3.10). It's linearization in the vicinity of solution $\mathbf{X}_{ijk} = \xi(t) \in A(1)$ and its subsequent reduction to one equation gives the following result:

$$\dot{\mathbf{U}} = \mathbf{I}_{N_1N_2N_3} \otimes \mathbf{J}_m(\xi)\mathbf{U} -$$
$$- \varepsilon\left(\mathbf{I}_{N_3} \otimes \mathbf{I}_{N_2} \otimes \mathbf{B}_{N_1} + \mathbf{I}_{N_3} \otimes \mathbf{B}_{N_2} \otimes \mathbf{I}_{N_1} + \mathbf{B}_{N_3} \otimes \mathbf{I}_{N_1N_2}\right) \otimes \mathbf{C}\mathbf{U}.$$

As one can see, this equation has the required form of the equation of the lemma. Consequently, the problem of stability of the synchronization is reduced to determining the eigenvalues of matrix $\mathbf{D}_p = \mathbf{I}_{N_3} \otimes \mathbf{I}_{N_2} \otimes \mathbf{B}_{N_1} + \mathbf{I}_{N_3} \otimes \mathbf{B}_{N_2} \otimes \mathbf{I}_{N_1} + \mathbf{B}_{N_3} \otimes \mathbf{I}_{N_1N_2}$.

During the study of this matrix, we establish the aforementioned fact: the minimum root of matrix $\mathbf{D}_p$ equals to $4\sin^2\dfrac{\pi}{2N}$, where $N = \max\{N_1,\ N_2,\ N_3\}$. Hence, we obtain the synchronization stability condition, which is already known to us: $\varepsilon > \varepsilon^*(\lambda(1))\Big/\left(4\sin^2\dfrac{\pi}{2N}\right)$, where $N = \max\{N_1,\ N_2,\ N_3\}$. The conclusions regarding the influence of parameters of the attractors of an individual dynamical system and the parameters of the lattice on the stability of the synchronization will be the same as in the case of a chain.

3.2. Spatially homogeneous autowave processes – global synchronization in systems with transport and diffusion

Autowave processes for a wide class of physical, biological, chemical, and other systems [176] are modeled by differential equations of the form [177]

$$\frac{\partial x}{\partial t} = -f(x) + \mathbf{a}^T \mathbf{y} + g(t) + k\frac{\partial x}{\partial s} + d\frac{\partial^2 x}{\partial s^2},$$
$$\frac{\partial \mathbf{y}}{\partial t} = \mathbf{B}\mathbf{y} + \mathbf{b}x + \mathbf{q}(t). \tag{3.11}$$

Here x is a scalar, $\mathbf{y} = (y_1, y_2, ..., y_n)^T$, $\mathbf{B}$ is a constant Hurwitz (stable) matrix, $\mathbf{a}$, $\mathbf{b}$ are $(n \times 1)$ constant vectors, k, d are the coefficients of transfer (flow) and diffusion, $g(t)$ is a scalar and $\mathbf{q}(t)$ is $(n \times 1)$ vector bounded functions: $\|g(t)\| < D_1$, $\|\mathbf{q}(t)\| < D_2$, s is a spatial coordinate, $s \in [0, L]$. It is assumed that functions $g(t)$ and $\mathbf{q}(t)$ can be any functions, including that they can be time-histories of a random process.

Examples of systems modeled by equations (3.11) are nonlinear long lines, nerve fibers, and distributed chemical systems with autocatalysis [176]. Equations (3.11) can be considered a generalization of known basic models: if $\mathbf{a} = 0$, $k = 0$, $g(t) \equiv 0$, then Eqs. (3.11) are the equations of Kolmogorov – Petrovsky – Piskunov (KPP); if $n = 1$, $k = 0$, $\mathbf{q}(t) \equiv 0$, $g(t) \equiv 0$, then (3.11) are the Fitz-Hugh – Nagumo equations [78, 79, 178]; if $k = d = 0$, $\mathbf{q}(t) \equiv 0$, $g(t) \equiv 0$, $n = 2$, then (3.11) are the equations of various Chua oscillators, etc. The physical meaning of variables and parameters will be deciphered below using the example of a physical system.

Spatially homogeneous states are the most accessible class of dynamic processes for research. In this case $\frac{\partial x}{\partial s} \equiv 0, \quad \frac{\partial \mathbf{y}}{\partial s} \equiv 0,$ $\frac{\partial x}{\partial t} \equiv \frac{dx}{dt}, \quad \frac{\partial \mathbf{y}}{\partial t} \equiv \frac{d\mathbf{y}}{dt}$ and $x(s, t) = x(t), \quad \mathbf{y}(s, t) = \mathbf{y}(t)$ is the solution of the respective system of ordinary differential equations. If we assume that the dynamical properties of this system are known, then only the question of stability of the indicated solutions in the phase space of system (3.11) remains open. This problem is very difficult, so we will replace it with the problem of studying stability in the finite-difference model of system (3.11).

Following the method of finite differences (writing the spatial derivatives by finite differences [179]) and taking into account the homogeneous boundary conditions $\left.\frac{\partial x}{\partial s}\right|_{s=0} \equiv 0, \quad \left.\frac{\partial x}{\partial s}\right|_{s=L} \equiv 0,$ we obtain a finite-difference model of equations (3.11) [177, 180]:

$$\begin{aligned} \dot{x}_k &= -f(x_k) + \mathbf{a}^T \mathbf{y}_k + \varepsilon_1 (x_{k-1} - x_k) - \varepsilon_2 (x_k - x_{k+1}) + g(t), \\ \dot{\mathbf{y}}_k &= \mathbf{B}\mathbf{y}_k + \mathbf{b}x_k + \mathbf{q}(t), \quad k = \overline{1, N}, \end{aligned} \tag{3.12}$$

with boundary conditions $x_0 \equiv x_1, \quad x_N \equiv x_{N+1}.$ Here $\varepsilon_1 = \frac{k}{h} + \frac{d}{h^2},$ $\varepsilon_2 = \frac{d}{h^2},$ h is the discretization step.

Thus, system (3.11) is modeled by a chain of non-autonomous Lurie oscillators

$$\begin{aligned} \dot{x} &= -f(x) + \mathbf{a}^T \mathbf{y} + g(t), \\ \dot{\mathbf{y}} &= \mathbf{B}\mathbf{y} + \mathbf{b}x + \mathbf{q}(t). \end{aligned} \tag{3.13}$$

The spatially homogeneous autowave motions of the system (3.11) correspond to isochronous synchronization of the oscillators of the chain (3.12).

Let us provide an example of a physical system modeled by these equations. Fig. 3.2 shows the electric circuit diagram of a chain of dissipativity coupled Chua oscillators (see Section 1.1).

In physical variables and parameters, the meaning of which is reflected in Fig. 3.2, the dynamics of the chain is governed by equations of the form

$$\begin{aligned} C\dot{V}_k &= I_k - I(V_k) + \frac{V_{k-1} - V_k}{R_0} - \frac{V_k - V_{k+1}}{R_0}, \\ L\dot{I}_k &= -RI_k + V_k^* - V_k, \\ C^*\dot{V}_k^* &= -I_k - GV_k^*, \quad k = \overline{1,N}, \end{aligned}$$

where $I(V)$ is the current-voltage characteristic of a nonlinear element with nonlinear conductivity G^*.

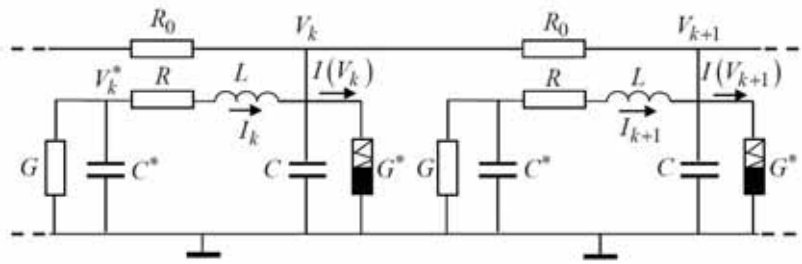

Fig. 3.2. The chain of Chua's oscillators.

By introducing dimensionless variables and parameters:

$$V_k = V_0 x_k, \quad I_k = I_0 y_k, \quad V_k^* = V_0^* z_k,$$
$$\frac{R}{L} t = \tau, \quad \frac{L}{CR^2} = \alpha, \quad \frac{L}{C^* R^2} = \beta, \quad \frac{GL}{C^* R} = \gamma,$$
$$\frac{L}{CRR_0} = \varepsilon, \quad \frac{\alpha I(V_0 x_k)}{I_0} = f(x_k)$$

We obtain dynamical system of the form

$$\begin{aligned} \dot{x}_k &= -f(x_k) + \alpha y_k + \varepsilon(x_{k-1} - 2x_k + x_{k+1}), \\ \dot{y}_k &= -y_k + z_k - x_k, \\ \dot{z}_k &= -\beta y_k - \gamma z_k, \quad k = \overline{1, N}, \end{aligned} \tag{3.14}$$

with boundary conditions $x_0 \equiv x_1$, $x_N \equiv x_{N+1}$.

Based on what has been said in Section 1.1, we assume that for the autonomous system (system (1.2)) corresponding to system (3.13), conditions (1.3) are satisfied, and the properties of the auxiliary system (1.4) are also satisfied.

The indicated conditions for the partial system are sufficient to formulate the conditions for the global stability of isochronous synchronization in the chain (3.12) for various cases of couplings.

We consider equations (3.13) for $\varepsilon_1 \neq 0,\ \varepsilon_2 \neq 0$. The conditions of the global asymptotic stability of synchronization of oscillators (of a spatially homogeneous state) are formulated in the form of the following theorem.

Theorem 3.2.1. Suppose $\lambda_0 = \inf\limits_{\forall x \in R} f'(x),\ \ xf(x) \geq mx^2 - l,\ \ x \in R$ and conditions (1.8) are satisfied for the autonomous system corresponding to system (3.13). Then, under the conditions

1) $\varepsilon_2 \neq 0,\ \ 0 < \nu < 1,\ \ N \leq N_0 = \left[\dfrac{\pi}{\arccos \nu}\right],\ \ \nu = \dfrac{\lambda_0 + \varepsilon_1 + \varepsilon_2 - m}{\varepsilon_1 + \varepsilon_2},$

2) $\varepsilon_2 \neq 0,\ \ \nu > 1$ and arbitrary large N

the isochronous synchronization in system (3.12) is globally stable.

Proof. We transform system (3.12) to variables $U_k = x_k - x_{k+1}$, $\mathbf{W}_k = \mathbf{y}_k - \mathbf{y}_{k+1}$:

$$\begin{aligned} &\dot{U}_k = -\lambda_k(\xi_k)U_k + \mathbf{a}^T\mathbf{W}_k + \varepsilon_1(U_{k-1} - U_k) - \varepsilon_2(U_k - U_{k+1}), \\ &\dot{\mathbf{W}}_k = \mathbf{B}\mathbf{W}_k + \mathbf{b}U_k, \\ &k = \overline{1, N-1}. \end{aligned} \tag{3.15}$$

Here $\lambda_k = f'(\xi_k), \quad \xi_k \in [x_k,\ x_{k+1}]$ (Lagrange's theorem) and boundary conditions $U_0 = 0,\ U_N = 0.$

Note that in this case $x_k,\ x_{k+1}$ are the coordinates of an arbitrary point of the phase space of system (3.12). Consider the Lyapunov function $V = \frac{1}{2}\sum_{k=1}^{N-1}\left(U_k^2 + \mathbf{W}^T\mathbf{H}\mathbf{W}\right).$ It is easy to proof that its derivative calculated along the trajectories of system (3.15) satisfies the inequality $\dot{V} \le -\sum_{k=1}^{N-1} Q_k\left(U_k,\ \mathbf{W}_k\right) - \frac{\varepsilon_1 + \varepsilon_2}{2}\sum_{k=1}^{N-1}\left(2\nu U_k^2 - 2U_k U_{k+1}\right),$

where $\nu = \frac{\varepsilon_1 + \varepsilon_2 + \lambda_0 - m}{\varepsilon_1 + \varepsilon_2}.$ In turn, this derivative is negative in the entire phase space if the quadratic form $P = \sum_{k=1}^{N-1}\left(2\nu U_k^2 - 2U_k U_{k+1}\right)$ is positive.

It can be proven that the values of the major minors Δ_k of a matrix of the quadratic form P

$$\begin{pmatrix} 2\nu & -1 & 0 & 0 & & & & \\ -1 & 2\nu & -1 & 0 & 0 & & \mathbf{0} & \\ 0 & -1 & 2\nu & -1 & & & & \\ 0 & 0 & -1 & 2\nu & & & & \\ & 0 & & & \ddots & & 0 & \\ & & & & & 2\nu & -1 & 0 & 0 \\ & & & & & -1 & 2\nu & -1 & 0 \\ & \mathbf{0} & & & 0 & 0 & -1 & 2\nu & -1 \\ & & & & & 0 & 0 & -1 & 2\nu \end{pmatrix}$$

are solutions of a recurrent equation of the form

$$\Delta_k = 2\nu\Delta_{k-1} - \Delta_{k-2},\ \ \Delta_{-1} = 0,\ \ \Delta_0 = 1,\ \ k = \overline{1, N-1}. \tag{3.16}$$

1) If $0 < \nu < 1,$ then solution (3.16) has the form

$$\Delta_k = \frac{\sin(k+1)\theta}{\sin\theta},$$

where $\theta = \arccos\nu.$ From this we obtain that for all $N \le N_0 = \left[\frac{\pi}{\arccos\nu}\right]$, the values $\Delta_k > 0,\ k = \overline{1, N-1}.$ That is, quadratic form P is positive in the whole phase space and hence the trivial solution (3.15) corresponding to isochronous synchronization is a globally stable.

2) If $\nu > 1,$ then the solution of recurrent equation (3.16) has the form

$$\Delta_k = \frac{\left(\nu + \sqrt{\nu^2 - 1}\right)^{k+1} - \left(\nu - \sqrt{\nu^2 - 1}\right)^{k+1}}{2\sqrt{\nu^2 - 1}}, \quad k = \overline{1, N-1}.$$

Hence, we obtain that all minors of the quadratic form P are positive for arbitrarily large value of N, which proves the second part of the theorem.

Let us draw conclusions from this theorem. First, since parameter m can be arbitrarily small (a chain of Chua oscillators), the parameter $\nu = \frac{\varepsilon_1 + \varepsilon_2 + \lambda_0 - m}{\varepsilon_1 + \varepsilon_2} = 1 + \frac{\lambda_0}{\varepsilon_1 + \varepsilon_2}$. From this we obtain that if $\lambda_0 = \inf_{\forall x \in R} f'(x) > 0$, then synchronization of oscillators is globally stable for a chain of an arbitrarily long length. Under this condition, the function $f(x)$ (current-voltage characteristic of a nonlinear element of the respective oscillator) increases everywhere and equilibrium $O(0, 0, 0)$ of a single oscillator is globally stable (underexcited self-oscillator). This is easy to prove using the same Lyapunov function $V = \frac{1}{2}x^2 + \frac{\alpha}{2}y^2 + \frac{\alpha}{2\beta}z^2$, applied to the autonomous oscillator system from system (3.15). Under these conditions, the oscillator has no oscillatory properties and its dynamics is similar to a linear stable system. Physically, this case is mot of a major interest.

Apart from that, one cannot but pay attention to the fact that the conditions of local and global stability of synchronization coincide in their form: under the conditions of global stability, inequality $N < \dfrac{\pi}{\arccos \nu}$ is equivalent to inequality $\varepsilon > |\lambda_0 - m| \Big/ 4\sin^2 \dfrac{\pi}{2N}$ $(\varepsilon_1 = \varepsilon_2 = \varepsilon)$, and the condition of local stability is defined by an inequality of the form $\varepsilon > \varepsilon^* \Big/ 4\sin^2 \dfrac{\pi}{2N}$. Hence, it can be assumed that the condition for the stability of synchronization will mostly have the same form.

Finally, the conditions of both local and global stability of synchronization are related to the finite value of the number of oscillators *N*. One can say that a "moderate" diffusive coupling is capable of providing synchronization of only a limited (and, moreover, a relatively small) number of oscillators with chaotic dynamics. In other words, if one imagines the formation of chains as auto-synthesis in a homogeneous "brine of oscillators", then chains of limited length, determined by the stability conditions, will be synthesized.

Fig. 3.3 shows a sequence of phase portraits corresponding to a globally stable isochronous chaotic synchronization in a diffusive chain of $N = 6$ identical Chua oscillators. Oscillator coupling matrix $\mathbf{C} = \mathrm{diag}(1, 0, 0)$. other parameters of the experiment: $(\alpha, \beta, \gamma, m_0, m_1, \varepsilon) = (9.5, 14, 0.1, -1/7, 2/7, 5.0)$.

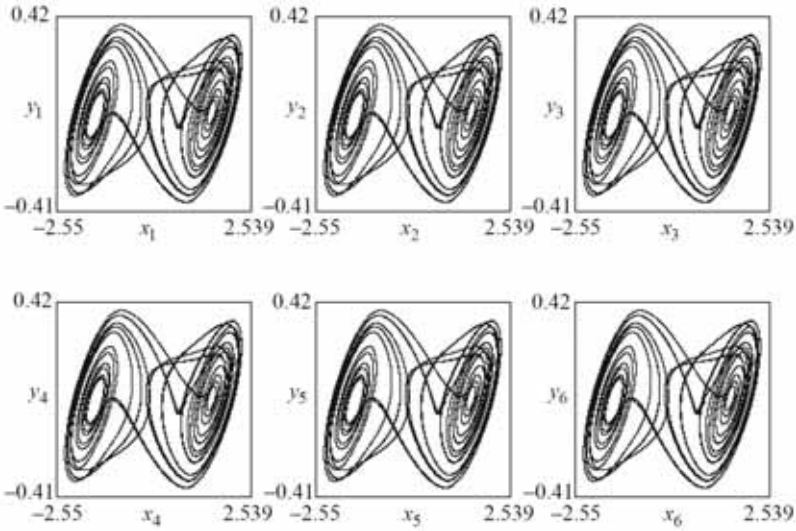

Fig. 3.3. Stable isochronous chaotic synchronization in the diffusive chain of Chua's oscillators.

3.3. Synchronization of rotations in a chain and in a ring of diffusive-coupled autonomous and non-autonomous rotators

Let us study the processes of synchronization in a system of coupled rotators of the form

$$\begin{aligned} &I\ddot{\varphi}_i + \dot{\varphi}_i + \sin\varphi_i = \gamma + \varepsilon\left(\dot{\varphi}_{i-1} - 2\dot{\varphi}_i + \dot{\varphi}_{i+1}\right) + A\sin\psi, \\ &\dot{\psi} = \omega_0, \\ &i = \overline{1,N}, \end{aligned} \tag{3.17}$$

with boundary conditions of two types: a) $\varphi_0 \equiv \varphi_1$, $\varphi_N \equiv \varphi_{N+1}$, corresponding to a chain, and b) $\varphi_0 \equiv \varphi_N$, $\varphi_{N+1} \equiv \varphi_1$, corresponding to a ring.

Variables and parameters in system (3.17) are dimensionless, and this system is defined in the toroidal phase space $G\left(\varphi_1, ..., \varphi_N, \psi, \dot{\varphi}_1, ..., \dot{\varphi}_N\right) = T^{N+1} \times R^N$. Parameters $I > 0$, $\gamma > 0$ have a sense of the moment of inertia and constant torque of rotator, respectively; A, ω_0 are the amplitude and frequency of external force (see Section 1.2), respectively; and ε the parameter of coupling of the rotators.

Let us provide examples of physical systems, whose dynamics is modeled by Eqs. (3.17).

Example 1. Fig. 3.4 shows a chain of Froude pendulums [181]. Sleeves of identical pendulums are mounted on the shaft, which is driven into rotational motion with a constant speed of rotation $\Omega = \omega$ or into rotational-oscillatory motion with frequency $\Omega = \omega + B \sin \Omega_0 t$. There is viscous friction between all sleeves and the shaft as well as between all contacting couplings.

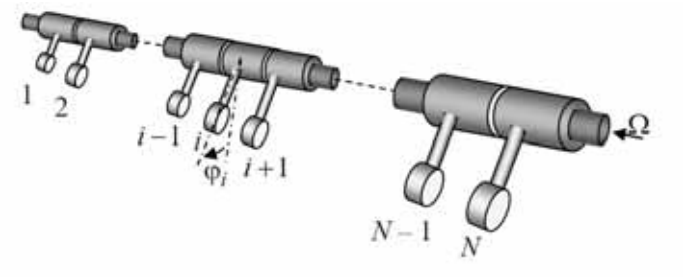

Fig. 3.4. A chain of Froude pendulums.

In physical variables and parameters, the equations of motion of the chain have the form

$$
\begin{aligned}
& ml^2\ddot{\varphi}_i + d\dot{\varphi}_i + mgl\sin\varphi_i = R\left(\omega + B\sin\psi - \dot{\varphi}_i\right) + \\
& + \lambda\left(\dot{\varphi}_{i-1} - \dot{\varphi}_i\right) + \lambda\left(\dot{\varphi}_{i+1} - \dot{\varphi}_i\right), \\
& \dot{\psi} = \Omega_0, \\
& i = \overline{1, N},
\end{aligned}
$$

where m, l are the reduced mass and length of the pendulum, respectively; d is the constant coefficient of viscous damping of the medium; $R\left(\omega + B\sin\psi - \dot{\varphi}_i\right)$ is the moment of force of viscous friction acting from the shaft side; $\lambda\left(\dot{\varphi}_{i-1} - \dot{\varphi}_i\right)$, $\lambda\left(\dot{\varphi}_{i+1} - \dot{\varphi}_i\right)$ are the moments of the friction forces from the neighboring pendulums; and R, λ are the constant coefficients.

Dividing the equations by mgl and introducing dimensionless time $\frac{mgl}{d+R}t=\tau$, we obtain Eqs. (3.17). The relation between dimensional and dimensionless parameters is defined by formulae

$$I=\frac{l}{g}\left(\frac{mgl}{d+R}\right)^2,\ \gamma=\frac{R\omega}{mgl},\ \varepsilon=\frac{\lambda}{d+R},\ \omega_0=\Omega_0\frac{d+R}{mgl},\ A=\frac{RB}{mgl}.$$

Example 2. As stated in Section 1.2, a dynamical state of a superconductive junction is governed by two variables: φ, representing the difference of phases of quantum-mechanical functions of order, and $\dot{\varphi}=V$ the potential difference of superconductors (the Josephson ratio in dimensionless time). In a resistive model written in dimensionless variables and parameters, a separate non-autonomous superconductive junction is described by a pendulum equation.

Fig. 3.5 shows a chain of dissipative-coupled superconductive junctions with uniform injection of a constant current in an external microwave field. Superconductive junctions are indicated by crosses.

Equations for electric currents (we consider nodes A_i) define the dynamical system of the chain

$$\begin{aligned}
&c\ddot{\varphi}_i+\dot{\varphi}_i+\sin\varphi_i=\gamma+\frac{1}{r}\left(\dot{\varphi}_{i-1}-\dot{\varphi}_i\right)+\frac{1}{r}\left(\dot{\varphi}_{i+1}-\dot{\varphi}_i\right)+A\sin\psi,\\
&\dot{\psi}=\omega_0,\\
&i=\overline{1,N},
\end{aligned}$$

with boundary conditions $\varphi_0 \equiv \varphi_1$, $\varphi_N \equiv \varphi_{N+1}$. Here, the dimensionless parameters are: c is the capacitance of the junction; γ is the constant electric current of the external power supply; A, ω_0 are the amplitude and frequency of external microwave field, respectively; and r is the resistance of the coupling. Assuming $1/r = \varepsilon$ (dimensionless conductivity), we obtain Eqs. (3.17). Condition $\langle \dot{\varphi}_i \rangle_t = 0$ (equilibriums and oscillatory motions of the i-th pendulum, see. Fig. 3.4) corresponds to the superconducting state of the respective junction, and rotational motion of the pendulum corresponds to its resistive state (generation mode).

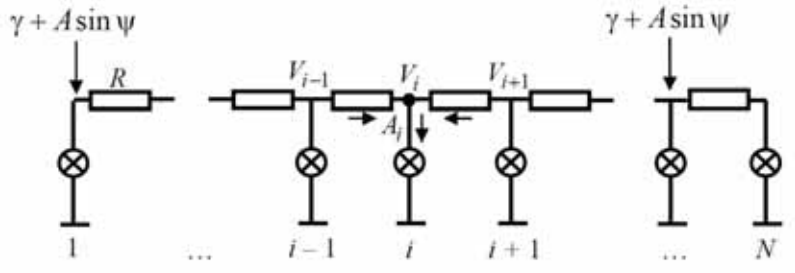

Fig. 3.5. A chain of superconductive junctions.

Example 3. Fig. 3.6 shows a block-scheme of a ring of dissipative-coupled superconductive junctions. By writing the physical equations for each of them, we obtain dynamical system (3.18) with periodic conditions $\varphi_0 \equiv \varphi_N$, $\varphi_{N+1} \equiv \varphi_1$. The count of the sequential number of junctions starts from an arbitrary element.

From a comparison of equations of physical systems outlined in Examples 1 and 2, we obtain the following electromechanical analogy of the variables: V (voltage) $\sim \dot{\varphi} = \omega$ (frequency of rotation), $1/R$ (conductivity of the coupling) $\sim \varepsilon$ (coefficient of viscous damping), J (current); and $\sim M$ (moment). The expression for the electric current of the coupling (Ohm's law) $\left(V_{i+1} - V_i\right)/R = J_{i+1}$ н, that flows from junction $(i+1)$ to junction i, is equivalent to the expression for the moment of force of viscous friction acting from pendulum $(i+1)$ on pendulum i.

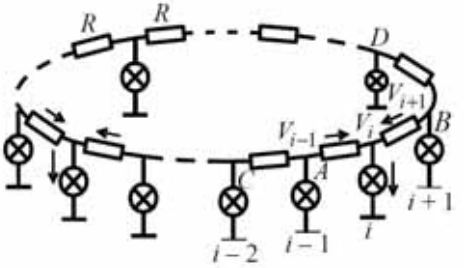

Fig. 3.6. A ring of dissipative-coupled Josephson junctions.

An autonomous chain and a ring.

Assuming $A = 0$ in (3.17) and transforming time $\sqrt{I^{-1}}\tau = \tau_n$, we obtain a system of the form

$$\ddot{\varphi}_i + \lambda\dot{\varphi}_i + \sin\varphi_i = \gamma + \sigma\left(\dot{\varphi}_{i-1} - 2\dot{\varphi}_i + \dot{\varphi}_{i+1}\right),$$
$$i = \overline{1, N}, \tag{3.18}$$

where $\lambda = \sqrt{I^{-1}}$, $\sigma = \varepsilon\sqrt{I^{-1}}$. The boundary conditions have the form $\varphi_0 = \varphi_1$, $\varphi_N = \varphi_{N+1}$ or $\varphi_0 = \varphi_N$, $\varphi_{N+1} = \varphi_1$.

Let us list some general properties of system (3.18).

1) In the phase space of the system $G\left(\varphi, \dot{\varphi}\right) = T^N \times R^N$ there are no closed trajectories of vibrational type (O-trajectories). This property is established by means of the periodic Lyapunov function: we consider the function (quadratic form plus integral of the nonlinearity) of the form $V = \sum_{i=1}^{N}\left(\frac{1}{2}\dot{\varphi}_i^2 + \int_{\varphi_{0i}}^{\varphi_i}\left(\sin\varphi_i - \gamma\right)d\varphi_i\right)$. Whose derivative taken along trajectories of Eqs. (3.18), $V = \sum_{i=1}^{N}\left(\frac{1}{2}\dot{\varphi}_i^2 + \int_{\varphi_{0i}}^{\varphi_i}\left(\sin\varphi_i - \gamma\right)d\varphi_i\right)$. The negative sign of the derivative in the whole phase space $G\left(\varphi, \dot{\varphi}\right)$ proves the property.

Thus, the possible attractors of system (3.18) can be: equilibrium states, rotational-oscillatory and rotational limit cycles, tori, and, perhaps, chaotic attractors with a rotating phase.

2) In the phase space of the system, there exists the "main" integral manifold $M_0 = \{\varphi_1 = \varphi_2 = ... = \varphi_N,\ \dot{\varphi}_1 = \dot{\varphi}_2 = ... = \dot{\varphi}_N\}$ representing cylinder $(\varphi, \dot{\varphi})$, filled by phase trajectories of the equation of a single rotator, i.e. a pendulum equation:

$$\ddot{\varphi} + \lambda\dot{\varphi} + \sin\varphi = \gamma.$$

This property is obvious. Properties of the pendulum equation are described in detail in Section 1.2.

Let us study stationary, spatially homogeneous dynamical regimes of the chain (synchronization) that correspond to stable limit sets of phase trajectories lying on the main manifold M_0. Stable equilibrium $O_1(\arcsin\gamma, 0)$ corresponds to the resting Froude's pendula, located at the same angle with respect to the vertical. The limit cycle corresponds to the in-phase rotation of all of the pendula of the chain. Using the example of this system, let us repeat the proof that these limit sets are stable along directions that are transverse to M_0.

Using a change of the variables $u_i = \varphi_i - \varphi_{i+1},\ \ \dot{u}_i = v_i$ we reduce Eqs. (3.18) to manifold M_0, we obtain

$$\begin{aligned} &\dot{u}_i = v_i, \\ &\dot{v}_i = -\lambda v_i - (\cos\xi_i)u_i + \sigma(v_{i-1} - 2v_i + v_{i+1}), \\ &i = \overline{1, N-1}. \end{aligned} \tag{3.19}$$

The boundary conditions in (3.19): $v_0 \equiv 0, \quad v_N \equiv 0.$ During the transition to system (3.19) the Lagrange theorem is used: $\xi_i \in (\varphi_i, \varphi_{i+1}).$

We remind that if $\xi_1 = \varphi_1 = \varphi_2 = \xi_2 = ... = \varphi_N = \varphi,$ where $\varphi(t)$ is an arbitrary solution and $(\varphi, \dot{\varphi}) \in M_0,$ then system (3.19) is a system in variation with respect to the whole manifold. If solution $\varphi(t) = \varphi^*(t)(\varphi, \dot{\varphi}) \in M_0,$ corresponds to a certain limit set of trajectories of the pendulum equation (equilibrium, limit cycle), then system (3.19) is a system in variations with respect to the "piece" $M_0,$ containing this limit set and its domain of attraction. If a trivial solution to system (3.19), written with respect to $\xi(t) = \varphi^*(t),$ is stable, then the respective spatially homogeneous dynamical regime of the chain is also stable.

We investigate the stability of manifold $M_0.$

We rewrite system (3.19) as a single equation of the form

$$\dot{\mathbf{U}} = (\mathbf{I}_{N-1} \otimes \mathbf{J}_0(\xi) - \sigma \mathbf{D}_{N-1} \otimes \mathbf{C})\mathbf{U}, \tag{3.20}$$

where $\mathbf{U} = (u_1, v_1, u_2, v_2, ..., u_{N-1}, v_{N-1})^T,$ $\mathbf{J}_0 = \begin{pmatrix} 0 & 1 \\ -\cos\xi & -\lambda \end{pmatrix},$

$\mathbf{C} = \begin{pmatrix} 0 & 0 \\ 0 & 1 \end{pmatrix},$

$$\mathbf{D}_{N-1} = \begin{pmatrix} 2 & -1 & 0 & 0 & & & & \\ -1 & 2 & -1 & 0 & & & & \\ 0 & -1 & 2 & -1 & & \mathbf{0} & & \\ 0 & 0 & -1 & 2 & & & & \\ & & & & \ddots & & & \\ & & & & & 2 & -1 & 0 & 0 \\ & & \mathbf{0} & & & -1 & 2 & -1 & 0 \\ & & & & & 0 & -1 & 2 & -1 \\ & & & & & 0 & 0 & -1 & 2 \end{pmatrix}.$$

According to Lemma 3.1.1 equation (3.20) is decomposed into $N-1$ two-dimensional systems with respect to $\left(x_i, y_i\right)^T = \mathbf{V}_i$ of the form

$$\begin{aligned} &\dot{x}_i = y_i, \\ &\dot{y}_i = -\lambda y_i - \left(\cos \xi_i\right) x_i - \sigma \lambda_i y_i, \\ &i = \overline{1, N-1}, \end{aligned} \tag{3.21}$$

where $\lambda_j = 4\sin^2 \pi j / 2N$, $j = \overline{1, N-1}$ are the eigenvalues of matrix $\mathbf{D}_{N-1}$.

If $\sigma = 0$, then each of these systems is a stable system in variation (unperturbed system) with respect to the solution that corresponds to one of the stable limit trajectories of the pendulum equation (stable equilibrium, stable limit cycle). On the other hand, if $\sigma \neq 0$, then for any fixed $t = t_0$ there is a right rotation of the vector field

of each of systems (3.21) on the trajectories of the unperturbed system. In other words, since all trajectories of the unperturbed system (in the extended phase space) enter inside some cylinder $Z\left\{t > t_0,\ x^2 + y^2 \le R^2\left(t_0\right)\right\}$, $\lim\limits_{t_0 \to \infty} R\left(t_0\right) = 0,$ and stay there, then the same holds for trajectories of the perturbed system. Thus, the stability of each system from (3.21) follows from the stability of the unperturbed system. Consequently, the solution $\mathbf{V} = 0,$ and, therefore, $\mathbf{U} = 0$ is also stable. Physically, this fact is quite understandable: an additional dissipation is introduced into the stable system, which, naturally, only improves its stability.

Thus, the spatially uniform dynamical regime of the chain (synchronization) is stable for any value of diffusive coupling, including arbitrarily small ones.

Let us turn to the bifurcation diagram shown in Fig. 1.7. For the parameters from domain (1), and for the initial conditions given in the general case in a small neighborhood of manifold $M\left(1\right)$ the spatially uniform state of the chain is the equilibrium state: all of the pendula of the chain in the course of time come to equilibrium; that is, they hang under one angle. In parameter domain (2), depending on the initial conditions on manifold $M\left(1\right)$, equilibrium for a spatially homogeneous regime of synchronous rotations of pendula of the chain can be realized. Finally, in parameter domain (3), for any initial conditions given in a neighborhood of manifold

$M(1)$, a spatially homogeneous regime of in-phase rotations is realized.

For an autonomous ring, we obtain an equation of the form (3.20) with matrix $\mathbf{D}_{N-1}$ from Section 3.1. Therefore, for the ring we obtain the same conclusions as for the chain of rotators.

Non-autonomous chain and a ring.

Let us study dynamical properties of non-autonomous system (3.17) using a method of the averaging in the zone of main resonance. Following the algorithms for transformation of systems of coupled rotators, using a change of the variables of the form

$$\dot{\varphi}_i = \omega_0 + \mu F_i(\varphi_i, \psi, \xi), \quad F_i = \frac{\cos\varphi_i}{\omega_0} - \frac{A\cos\psi}{\omega_0} + \xi_i, \quad \eta_i = \varphi_i - \psi$$

we obtain a system equivalent to (3.17) in a standard form

$$\begin{aligned} \dot{\xi}_i &= \mu\left(-F_i\frac{\partial F_i}{\partial\varphi_i} - F_i + \sigma\left(F_{i-1} - 2F_i + F_{i+1}\right) + \Delta\right), \\ \dot{\eta}_i &= \mu F_i, \\ \dot{\psi} &= \omega_0, \end{aligned} \tag{3.22}$$

where $\mu = I^{-1}$, $\gamma - \omega_0 = \mu\Delta$ is the frequency mistuning (zone of the main resonance), and, $\eta_i = \varphi_i - \psi$ are the phase mistunings.

Further we assume that the parameters of an individual rotator are selected from region (2) or (3) shown in Fig. 1.17, for which, in the phase space, there is a rotational limit cycle. We assume that $\mu \ll 1$.

Having averaged system (3.22) over a fast-spinning phase and transforming time $\mu\tau = \tau_n$, we obtained a system of the form

$$\begin{aligned} &\dot{\eta}_i = \xi_i, \\ &\dot{\xi}_i = -\xi_i - \frac{A}{2\omega_0^2}\sin\eta_i + \Delta + \sigma\left(\xi_{i-1} - 2\xi_i + \xi_{i+1}\right) \end{aligned} \tag{3.23}$$

with boundary conditions $\xi_0 = \xi_1$, $\xi_N = \xi_{N+1}$. Then, by using a change of time of the form $\sqrt{\frac{A}{2\omega_0^2}}\tau_n = \tau_{nn}$ system (3.23) is reduced to equations

$$\begin{aligned} &\ddot{\eta}_i + \lambda_1^r\dot{\eta}_i + \sin\eta_i = \gamma_1^r + \sigma_0\left(\dot{\eta}_{i-1} - 2\dot{\eta}_i + \dot{\eta}_{i+1}\right), \\ &i = \overline{1,N}, \end{aligned} \tag{3.24}$$

with boundary conditions $\eta_0 \equiv \eta_1$, $\eta_N \equiv \eta_{N+1}$, where $\lambda_1^r = \sqrt{\frac{2\omega_0^2}{A}}$, $\gamma_1^r = \frac{2\omega_0^2\Delta}{A}$, $\sigma_0 = \sqrt{\frac{2\omega_0^2}{A}}\,\sigma$.

As one can see, the averaged system (3.24) has the same form as the system of equations of the autonomous chain. This means that

the character of the spatially homogeneous dynamic regime of the chain is determined by the dynamics of the "averaged" rotator:

$$\ddot{\eta} + \lambda_1^r \dot{\eta} + \sin\eta = \gamma_1^r.$$

The bifurcation diagram of this equation on the parameter plane $\left(\gamma_1^r, \lambda_1^r\right)$ is shown in Fig. 1.10. What remains is to interpret the result obtained. Let us recall that from the principle of the averaging it follows that if L is some limit set of trajectories of the averaged autonomous system, then $L \times S^1$ is a corresponding limit set of the non-autonomous system including conditions of stability of L. Based on this, domain (1) on the parameter plane $\left(\gamma_1^r, \lambda_1^r\right)$ is a domain of global asymptotic stability of the limit cycle of a non-autonomous rotator (synchronization region); (3) is the area of existence of a single and stable two-dimensional torus T^2; (2) is the domain of existence of both limit sets, which are realized depending on the initial conditions; (4) is the domain of existence of chaotic attractors associated with bifurcations of destruction of a two-dimensional torus.

Interpreting this for a chain, we find that for the parameters from domain (1), there is a spatially homogeneous regime of synchronous rotations in the chain of non-autonomous rotators (3.17); for domain (3) there is a regime of quasiperiodic rotations; for domain (2) there can be either one or the other regime is implemented de-

pending on the initial conditions. According to the property of the autonomous system proven above, the listed dynamical regimes are stable for an arbitrarily small value of the coupling parameter σ_0. According to the results presented in Section 1.2, the parameter domain (4) corresponds to complex limit sets of trajectories and their bifurcations, including stable ones. The corresponding chaotic attractors also lie on the integral manifold M_0 (the equation of a non-autonomous rotator is defined on the manifold). These attractors correspond to the inphase synchronization of chaotic rotations. In contrast to the previous cases, the stability of this dynamic regime is realized when the coupling values are not smaller than the threshold one, which depends both on the Lyapunov exponents of the attractors and on the number of rotators in the chain (or ring) (see Section 3.1).

In conclusion of this section, we make a remark about one of the possible applications of chains of superconductive junctions. Section 1.2 has already discussed the use of the Josephson effect in the design of the volt standard. In the case of a single element, the stabilized voltage is a few millivolts, which is an inconveniently small value. In this regard, the use of synchronized chains, such as one shown in Fig. 3.7 presents a simple way to improve the performance of a standard. In the synchronized state of the chain, the voltage at its ends is $V = NV_0$, where V_0 is the stabilized voltage at one junction.

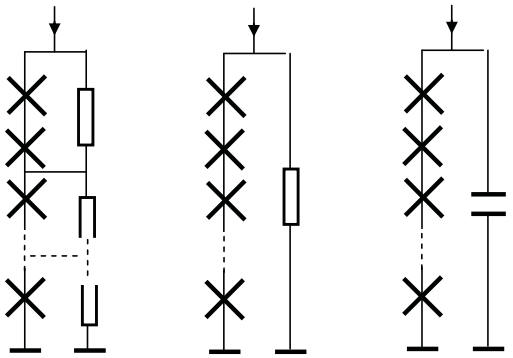

Fig. 3.7. An example of application of synchronized chains.

3.4. Regular and chaotic synchronization in a homogeneous chain of dynamical systems of "rotator – oscillator" type

Dynamics of the "rotator – oscillator" system have been studied in Section 1.5. In particular, we have established the existence of Lorenz and Feigenbaum chaotic attractors, as well as alternation of chaos in the phase space of this system. Below, we will consider dynamics of a chain of diffusively coupled systems of this type [164, 175, 182], i.e. synchronization of rotary motions of rotators, loaded by oscillatory links.

A physical example. Fig. 3.8 shows a chain of superconductive junctions, each of which is loaded by an oscillatory circuit. We assume that all junctions, as well as all similar elements of the electric schemes, are identical.

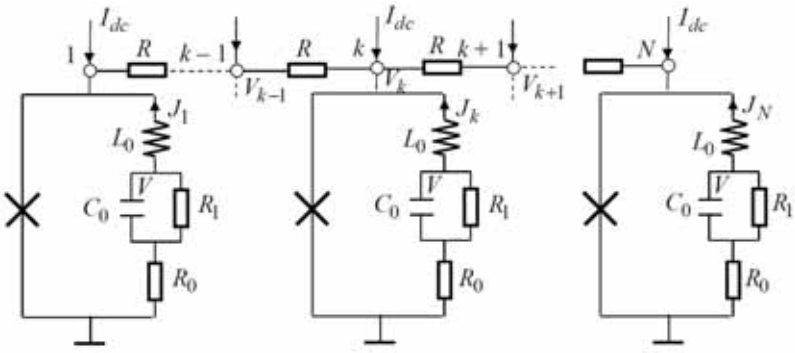

Fig. 3.8. A chain with superconductive junctions.

In dimensionless variables and parameters (see Section 1.5), the dynamics of the chain is governed by a system of equations of the form

$$\begin{aligned} &c\ddot{\varphi}_k + \dot{\varphi}_k + \sin\varphi_k = \gamma + \varepsilon\left(\dot{\varphi}_{k-1} - 2\dot{\varphi}_k + \dot{\varphi}_{k+1}\right) + J_k, \\ &\ddot{J}_k + \delta\dot{J}_k + \omega_0^2 J_k = b\ddot{\varphi}_k + d\dot{\varphi}_k, \\ &k = \overline{1, N}, \end{aligned} \tag{3.25}$$

with boundary conditions $\varphi_0 \equiv \varphi_1$, $\varphi_N \equiv \varphi_{N+1}$.

The relation of parameters of system (3.35) with dimensionless parameters of the above scheme is as follows:

$$\delta = \frac{c_0 r_0 r_1 + l_0}{c_0 l_0 r_1}, \quad \omega_0^2 = \frac{1}{c_0 l_0}\left(1 + \frac{r_0}{r_1}\right), \quad b = -\frac{1}{l_0}, \quad d = -\frac{1}{c_0 l_0 r_1}, \quad \varepsilon = \frac{1}{r}.$$

The study of synchronization will be carried out using the technique of averaging that has been discussed in Section 1.5. Consider parameter domain

$$D_\mu = \left\{ c^{-1} = \mu \ll 1,\ \delta = \mu h,\ \gamma + \frac{d}{\omega_0} - \omega_0 = \mu\Delta \right\},$$

for which system (3.25) is a chain of diffusive-coupled quasilinear rotators loaded with high-Q resonant oscillators. It is not difficult to prove that Eqs. (3.25) are equivalent to a system of the form:

$$\begin{aligned} &c\ddot{\varphi}_k + \dot{\varphi}_k + \sin\varphi_k = \gamma + J_k + \varepsilon\left(\dot{\varphi}_{k-1} - 2\dot{\varphi}_k + \dot{\varphi}_{k+1}\right), \\ &\dot{J}_k = W_k + b\dot{\varphi}_k - \mu h J_k, \\ &\dot{W}_k = -\omega_0^2 J_k + d\dot{\varphi}_k. \end{aligned} \tag{3.26}$$

In turn, equations (3.26) by the change of variables (see Appendix)

$$\begin{aligned} &J_k = \theta_k \sin\varphi_k + \eta_k \cos\varphi_k + \frac{d}{\omega_0}, \\ &W_k = \left(\theta_k \cos\varphi_k - \eta_k \sin\varphi_k\right)\omega_0 - b\omega_0, \\ &\dot{\varphi}_k = \omega_0 + \mu\Phi_k\left(\theta_k, \eta_k, \varphi_k, \xi_k\right), \\ &\eta_k = \varphi_k - \varphi_1, \end{aligned}$$

where $\Phi_k = \dfrac{1-\theta_k}{\omega_0}\cos\varphi_k + \dfrac{\eta_k}{\omega_0}\sin\varphi_k + \xi_k$, are reduced to an equivalent system in a standard form:

$$\begin{aligned}
&\dot{\theta}_k = \mu\Theta_k\left(\theta_k, \eta_k, \varphi_k, \xi_k\right),\\
&\dot{\eta}_k = \mu\mathrm{T}_k\left(\theta_k, \eta_k, \varphi_k, \xi_k\right),\\
&\dot{\xi}_k = \mu\Xi_k\left(\theta_k, \eta_k, \varphi_k, \xi_{k-1}, \xi_k, \xi_{k+1}\right),\\
&\dot{\psi}_k = \mu\left(\Phi_\kappa - \Phi_1\right),\\
&\dot{\varphi}_1 = \omega_0 + \mu\Phi_1\left(\theta_1, \eta_1, \varphi_1, \xi_1\right)
\end{aligned} \tag{3.27}$$

The functions on the right-hand sides have the form:

$$\Theta_k = \left(\eta_k + b\sin\varphi_k + \frac{d}{\omega_0}\cos\varphi_k\right)\Phi_k -$$

$$- h\left(\theta_k\sin\varphi_k + \eta_k\cos\varphi_k\right)\sin\varphi_k + \frac{d}{\omega_0}\sin\varphi_k,$$

$$\mathrm{T}_k = \left(b\cos\varphi_k - \theta_k - \frac{d}{\omega_0}\sin\varphi_k\right)\Phi_k -$$

$$- h\left(\theta_k\sin\varphi_k + \eta_k\cos\varphi_k\right)\cos\varphi_k + \frac{d}{\omega_0}\cos\varphi_k,$$

$$\Xi_k = \Delta - \left(\frac{\partial\Phi_k}{\partial\theta_k}\Theta_k + \frac{\partial\Phi_k}{\partial\eta_k}\mathrm{T}_k + \frac{\partial\Phi_k}{\partial\varphi_k}\Phi_k + \Phi_k\right) + \varepsilon\left(\Phi_{k-1} - 2\Phi_k + \Phi_{k+1}\right).$$

The averaged system for system (3.27) has the form:

$$\begin{aligned}
&\dot{\xi}_k = \mu\left(-b_1\xi_k + b_2\theta_k + b_3\eta_k + \Delta + \beta\left(\xi_{k-1} - 2\xi_k + \xi_{k+1}\right)\right),\\
&\dot{\theta}_k = \mu\left(-b_4\theta_k + b_5\eta_k + \eta_k\xi_k + b_6\right),\\
&\dot{\eta}_k = \mu\left(-b_4\eta_k - b_5\theta_k - \theta_k\xi_k + b_7\right),\\
&\dot{\psi}_k = \mu\left(\xi_k - \xi_1\right),\\
&\dot{\varphi}_1 = \omega_0 + \mu\xi_1
\end{aligned} \tag{3.28}$$

with boundary conditions $\xi_0 \equiv \xi_1,\ \xi_N \equiv \xi_{N+1}$ and parameters:

$$b_1 = 1 - \frac{d}{\omega_0^2},\ b_2 = 0,\ b_3 = \frac{1}{2\omega_0^2},\ b_4 = \frac{1}{2}\left(h + \frac{d}{\omega_0^2}\right),\ b_5 = \frac{b}{2\omega_0},$$
$$b_6 = \frac{d}{2\omega_0^2},\ b_7 = \frac{b}{2\omega_0}.$$

A change of the variables of the form

$$\begin{aligned}
&x_k = b_4^{-1}\left(\xi_k + b_5\right), y_k = \left(b_3\eta_k + b_2\theta_k\right)/b_1b_4 - \Lambda,\\
&z_k = \left(b_3\theta_k - b_2\eta_k\right)/b_1b_4 + R, \quad \mu b_4\tau = \tau_{\text{н}}
\end{aligned}$$

reduces the first $3N$ equations of the averaged system (3.28) to a chain of diffusive-coupled systems of the Lorenz type:

$$\begin{aligned}
&\dot{x}_k = -\sigma\left(x_k - y_k\right) + \rho + \varepsilon\left(x_{k-1} - 2x_k + x_{k+1}\right),\\
&\dot{y}_k = -y_k + Rx_k - x_kz_k,\\
&\dot{z}_k = -z_k + x_ky_k + \Lambda x_k,\\
&k = \overline{1,N},
\end{aligned} \tag{3.29}$$

with boundary conditions $x_0 \equiv x_1,\ x_N \equiv x_{N+1}$. Parameters in (3.29) are expressed as follows:

$$\sigma = b_1/b_4, \quad R = \frac{b_2 b_7 - b_3 b_6}{b_1 b_4^2}, \quad \Lambda = \frac{b_3 b_7 + b_2 b_6}{b_1 b_4^2},$$

$$\rho = \left(\Delta + \left(b_1 b_4 b_5 + b_3 b_7 + b_2 b_6\right) b_4^{-1}\right) b_4^{-2}, \quad \varepsilon = \frac{\beta}{b_4}.$$

In what follows, we will investigate isochronous synchronization in the chain (3.29) to interpret the results for the original system (3.25).

Dynamical properties of the partial system in (3.29) have been studied in Section 1.5; in particular, its dissipativity has been shown. The dissipation sphere is set using a quadratic form

$$V_k = \frac{1}{2}\left(x_k^2 + \left(y_k + \Lambda\right)^2 + \left(z_k - \sigma - R\right)^2\right).$$

The derivative of this quadratic form, taken along the vector field of the partial system, has the form

$$\dot{V} = -\sigma x^2 - \left(\rho - \sigma\Lambda\right)x - y^2 - \Lambda y - z^2 + \left(\sigma + R\right)z.$$

Outside of the sphere $U_k : x_k^2 + \left(y_k + \Lambda\right)^2 + \left(z_k - \sigma - R\right)^2 \le L^2$, the derivative of the quadratic form $\dot{V}_k < 0$. L is a constant that depends on parameters σ, R, Λ and ρ. Using this property of the partial system, let us formulate the dissipative proper-ty of the coupled system (3.25) in the form of a lemma.

Lemma 3.4.1. System (3.29) is dissipative into sphere $U = \bigcup_{k=1}^{N} U_k$.

Proof. Consider the quadratic form $V = \sum_{k=1}^{N} V_k$. Its derivative taken along the vector field of system (3.29) has the form and estimate

$$\dot{V} = \sum_{k=1}^{N} \left(x_k^2 + \left(y_k + \Lambda \right)^2 + \left(z_k - \sigma - R \right)^2 \right) - \varepsilon \sum_{k=1}^{N} \left(x_{k-1} - x_k \right)^2 \le \sum_{k=1}^{N} \dot{V}_k .$$

Since each of the terms of the last sum is negative outside the sphere U_k, then $\dot{V} \le 0$ outside of the sphere of dissipation $U = \bigcup_{k=1}^{N} U_k$ of system (3.29).

This lemma allows us to formulate sufficient conditions for the global asymptotic stability of synchronization in system (3.29) in a form of the following theorem.

Theorem 3.4.1. If $\varepsilon > \alpha/2$, where

$$\alpha = \sup_{\forall (x_k, y_k, z_k) \in V_k} \left(\frac{\left(\sigma + R - z_k \right)^2 + \left(y_k + \Lambda \right)^2}{4} - \sigma \right),$$

then integral manifold $M_0 = \left(x_k = x_{k+1}, y_k = y_{k+1}, z_k = z_{k+1} \right)$, $k = \overline{1, N}$ in chain (3.29) with the number of oscillators

$N \le N_0 = [\pi/\arccos\nu]$, where $\nu = (2\varepsilon - \alpha)/2\varepsilon$, is globally asymptotically stable.

Proof. Let us write system (3.29) with respect to variables $u_k = x_k - x_{k+1}$, $v_k = y_k - y_{k+1}$, $w_k = z_k - z_{k+1}$ that represent transversals to manifold M_0:

$$\begin{aligned}
&\dot{u}_k = -\sigma(u_k - v_k) + \varepsilon(u_{k-1} - 2u_k + u_{k+1}),\\
&\dot{v}_k = -v_k + (R - z_k)u_k - x_k w_k + u_k w_k,\\
&\dot{w}_k = -w_k + (y_k + \Lambda)u_k + x_k v_k - u_k v_k,\\
&k = \overline{1, N-1}, \quad u_0 \equiv 0.
\end{aligned} \tag{3.30}$$

Consider the Lyapunov function $V = \frac{1}{2}\sum_{k=1}^{N-1} V_k$, $V_k = u_k^2 + v_k^2 + w_k^2$. Its derivative taken along the vector field of system (3.30) has the form

$$\begin{aligned}
&\dot{V} = -\sum_{k=1}^{N-1}\left((\sigma+\alpha)u_k^2 + v_k^2 + w_k^2 + (\sigma + R - z_k)u_k v_k + (y_k + \Lambda)u_k w_k\right) - \varepsilon\Phi,\\
&\Phi = \sum_{k=1}^{N-1}\left(2\nu u_k^2 - 2u_k u_{k+1}\right),
\end{aligned} \tag{3.31}$$

where $\nu = 1 - \alpha/2\varepsilon$, and α is a parameter that is to be chosen.

According to the Lemma, all phase trajectories of (3.29) reach inside sphere $U = \bigcup_{k=1}^{N} U_k$ and stay there forever, i.e. for $t \to \infty$. For

this reason, the expression under the sign of the first sum is considered inside of the sphere dissipation. Let us select the value of parameter α as follows:

$$\alpha = \sup_{\forall(x_k, y_k, z_k)\in V_k} \left(\frac{(\sigma + R - z_k)^2 + (y_k + \Lambda)^2}{4} - \sigma \right).$$

In this case, each of the quadratic forms under the first sum sign is positive. Further, as in Theorem 3.2.1, we establish that the quadratic form Φ is positive if the inequalities indicated under the conditions of the Theorem are satisfied. That is, under the conditions of the theorem, manifold M_0, and, therefore, the synchronization in chain (3.29) are globally stable.

To determine the conditions for local stability of isochronous synchronization of oscillators in chain (3.29), one should refer to Theorem 3.1.1. The coupling matrix of oscillators in a chain: $\mathbf{C} = \mathrm{diag}(1,0,0)$ is admissible, and the local stability condition in this case is determined by inequality $\varepsilon > \varepsilon^* \Big/ 4\sin^2 \frac{\pi}{2N}$.

The method of the averaging, within the accuracy of $\sim \mu$ guarantees the fulfillment of the obtained conditions of global stability and of conditions of local stability of synchronization in the original chain (3.25) with one caveat: when using the method of averaging over the fast phase (φ_1 in equations (3.27)) it is assumed that the

parameters of the system are in the range of existence of rotator's rotations. That is, if the rotational motions (the nature of the rotations is unimportant) of the rotators are realized for any initial condition of system (3.25), then the conditions of the global stability in chain (3.29) are the conditions of the global stability of the corresponding synchronization in the initial chain (3.25). If, in addition to the limit sets of rotational trajectories in the phase space (3.25), there are oscillatory limit sets, including equilibria, then the conditions of global stability in chain (3.29) should be interpreted as the conditions for the stability of synchronization for the most part for the chain (3.11).

As for the physical interpretation of the results, for example, in relation to a chain of superconductive junctions, then, it is easy to provide it using the results of Section 1.5. In a synchronized state, the dynamics of all superconductive junctions is identical and coincides with the dynamics of one junction loaded by an oscillatory system. All types of rotation characteristic and resonance characteristic, as well as their properties described in Section 1.5, are types of volt-ampere characteristics of this junction and types of resonance characteristics of an oscillatory system including all their nontrivial features.

3.5. Synchronization of oscillators in an inhomogeneous chain and in a ring with diffusion

In this section, we will extend the asymptotic theory, presented in Section 2.2 for two oscillators, for a chain and for a ring. Just as in the case of a pair of oscillators, we consider two cases: 1) weakly non-identical oscillators with moderate diffusive coupling, 2) strongly non-identical oscillators with strong diffusion.

A chain and a ring of weakly non-identical oscillators.

Consider a dynamical system of the form

$$\dot{\mathbf{X}}_i = \mathbf{F}(\mathbf{X}_i) - \varepsilon \mathbf{C}(-\mathbf{X}_{i-1} + 2\mathbf{X}_i - \mathbf{X}_{i+1}) + \mu \mathbf{F}_i^*(\mathbf{X}_i, \mu), \quad i = \overline{1, N}, \tag{3.32}$$

with boundary conditions $\mathbf{X}_0 \equiv \mathbf{X}_1$, $\mathbf{X}_N \equiv \mathbf{X}_{N+1}$ for a chain and $\mathbf{X}_0 \equiv \mathbf{X}_N$, $\mathbf{X}_1 \equiv \mathbf{X}_{N+1}$ for a ring; μ is some small parameter associated with the non-identity of the parameters of the oscillators.

If $\mu = 0$ (the generating case is a system of identical oscillators), then system (3.32) has a generating integral manifold $M_0 = \{\mathbf{X}_1 = \mathbf{X}_2 = ... = \mathbf{X}_{N-1} = \mathbf{X}_N\}$, filled by trajectories of the generalized oscillator. The attractor of this oscillator $A_0(1) \subset M_0$. We will assume that the stability conditions for the manifold are satisfied (Theorem 3.1.1) and that all characteristic exponents of the respective linear system in variations of the form (3.3) are strictly

negative. In this case, the theorems [17 – 19] guarantee the existence in system (3.32) of a smooth, stable and one-to-one invariant manifold M_μ, containing attractor $A_\mu(1)$. In this case, M_μ turns in M_0, and $A_\mu(1)$ turns in $A_0(1)$ for $\mu = 0$. The conditions for stability of synchronization of oscillators in system (3.32) coincide with the corresponding conditions for isochronous synchronization in a chain of identical oscillators within the accuracy of μ.

Thus, the problems of existence and stability of synchronization in the inhomogeneous chain (3.32) are considered solved. Further, we will be interested in the features of this synchronization, defined by the nature of the mistuning of the parameters and by the nature of the coupling of the oscillators. In this case, we will appeal to the definition of synchronization given in Section 2.1.

Using in the technique outlined in Section 2.2, we define the parametric coupling of the variables of oscillators in the regime of synchronization (the parametric representation of manifold M_μ) as a power series by parameter μ:

$$\mathbf{X}_i = \mathbf{X} + \mu \mathbf{X}_{i1}(\mathbf{X}) + \mu^2 \mathbf{X}_{i2}(\mathbf{X}) + \ldots . \tag{3.33}$$

Moreover, we assume that manifold M_μ is decomposed into trajectories by phase trajectories of a dynamic system of the form

$$\dot{\mathbf{X}} = \mathbf{F}(\mathbf{X}) + \mu\mathbf{F}_*(\mathbf{X}) + \mu^2\mathbf{F}_{**}(\mathbf{X}) + \ldots . \tag{3.34}$$

The task is to define function $\mathbf{F}_*(\mathbf{X})$, $\mathbf{F}_{**}(\mathbf{X})$, ..., $\mathbf{X}_{i1}(\mathbf{X})$, $\mathbf{X}_{i2}(\mathbf{X})$, ... The choice of $\mathbf{F}_*(\mathbf{X})$, $\mathbf{F}_{**}(\mathbf{X})$, ... is carried out from the condition of independence of these functions from the number of the oscillator (index i), and also from the requirement of boundedness of the solutions of equations defining functions $\mathbf{X}_{ij}(\mathbf{X})$.

We consider the expansion of functions $\mathbf{F}(\mathbf{X}_i)$ and $\mathbf{F}_i^*(\mathbf{X}_i)$, $i = 1, 2,$ into a power series by a small parameter:

$$\mathbf{F}\left(\mathbf{X} + \mu\mathbf{X}_{i1}(\mathbf{X}) + \ldots\right) = \mathbf{F}(\mathbf{X}) + \mu\mathbf{F}'\mathbf{X}_{i1} + \ldots ,$$

$$\mathbf{F}_i^*\left(\mathbf{X} + \mu\mathbf{X}_{i1}(\mathbf{X}) + \ldots\right) = \mathbf{F}_i^*(\mathbf{X}) + \ldots .$$

Expression $\mathbf{F}'(\mathbf{X}) \equiv \dfrac{\partial \mathbf{F}}{\partial \mathbf{X}}$ is the Jacobi matrix.

Substituting equations (3.33) into (3.32) and equating terms of the same orders by μ, we obtain a system of equations defining the required functions. In particular, equations for the functions of the first approximation have the form

$$\mathbf{F}_* + \dot{\mathbf{X}}_{i1} = \mathbf{F}'\mathbf{X}_{i1} - \varepsilon\mathbf{C}\left(-\mathbf{X}_{i-1,1} + 2\mathbf{X}_{i1} - \mathbf{X}_{i+1,1}\right) + \mathbf{F}_i^* \tag{3.35}$$

with boundary conditions $\mathbf{X}_{01} \equiv \mathbf{X}_{11}$, $\mathbf{X}_{N+1,1} \equiv \mathbf{X}_{N1}$ for a chain and $\mathbf{X}_{N+1,1} \equiv \mathbf{X}_{11}$, $\mathbf{X}_{01} \equiv \mathbf{X}_{N1}$ for a ring.

Summing up all equations (3.35), we obtain

$$\begin{aligned} N\mathbf{F}_* + \dot{\mathbf{V}} &= \mathbf{F}'\mathbf{V} + \sum_{i=1}^{N} \mathbf{F}_i^*, \\ \mathbf{V} &= \sum_{i=1}^{N} \mathbf{X}_{i1}. \end{aligned} \tag{3.36}$$

Let us choose the required function in equation (3.36) in the form

$$\mathbf{F}_* = \frac{1}{N}\sum_{i=1}^{N} \mathbf{F}_i^* + \frac{\varepsilon\lambda_0}{N}\mathbf{C}\mathbf{U},$$

where $\lambda_0 > 0$ is a constant. Let us show that with this choice $\mathbf{X}_{i1}(t)$ are the bounded functions of time.

An equation with respect to variable $\mathbf{V}$ has the form

$$\dot{\mathbf{V}} = \mathbf{F}'\mathbf{V} - \varepsilon\lambda_0\mathbf{C}\mathbf{V}. \tag{3.37}$$

By defining constant λ_0 as the minimum root of matrix $\mathbf{D}_{N-1}$ from Section 3.1 $\lambda_0 = \lambda_{\min}$, where $\lambda_{\min} = 4\sin^2\frac{\pi}{2N}$ for a chain $\lambda_{\min} = 4\sin^2\frac{\pi}{N}$ for a ring, we obtain that the trivial solution $\mathbf{V} = 0$

of Eq. (3.37) is stable for $\varepsilon > \frac{\varepsilon^*\left(\lambda(1)\right)}{\lambda_{\min}}$. Here $\lambda(1)$ is the maximum Lyapunov exponent of the attractor $A_0(1)$ (see Section 3.1).

On the other hand, introducing variables $\mathbf{U}_i = \mathbf{X}_{i1} - \mathbf{X}_{i+1,1}$, $i = \overline{1, N-1}$ in system (3.35), we obtain an equation for the vector $\mathbf{U} = \left(\mathbf{U}_1, \mathbf{U}_2, \mathbf{U}_{N-1}\right)^T$:

$$\dot{\mathbf{U}} = \left(\mathbf{I}_{N-1} \otimes \mathbf{F}'\right)\mathbf{U} - \varepsilon\left(\mathbf{D}_{N-1} \otimes \mathbf{C}\right)\mathbf{U} + \mathbf{F}^*, \tag{3.38}$$

where $\mathbf{F}^* = \left(\mathbf{F}_{11}^* - \mathbf{F}_{21}^*, \mathbf{F}_{21}^* - \mathbf{F}_{31}^*, ..., \mathbf{F}_{N-1,1}^* - \mathbf{F}_{N1}^*\right)^T$, and $\mathbf{D}_{N-1}$ is the matrix from section 3.1, corresponding either to a chain or to a ring.

According to Theorem 3.1.1, the solution $\mathbf{U} = 0$ the homogeneous equation corresponding to (3.38) is stable for all $\varepsilon > \frac{\varepsilon^*\left(\lambda(1)\right)}{\lambda_{\min}}$.

Therefore, due to the boundedness of the vector $\mathbf{F}^*$, solutions of the inhomogeneous equation (3.38) are bounded. The boundedness of these solutions and the stability of equation (3.37) imply the boundedness of the functions $\mathbf{X}_{i1}\left(\mathbf{X}(t)\right)$.

Equations (3.35) are equivalent to a system of partial differential equations of the form

$$\frac{\partial \mathbf{X}_{i1}}{\partial \mathbf{X}}\mathbf{F} - \frac{\partial \mathbf{F}}{\partial \mathbf{X}}\mathbf{X}_{i1} + \varepsilon \mathbf{C}\left(-\mathbf{X}_{i-1,1} + 2\mathbf{X}_{i1} - \mathbf{X}_{i+1,1}\right) = \mathbf{F}_i^* - \mathbf{F}_*, \quad i = \overline{1,N}, \tag{3.39}$$

with boundary conditions $\mathbf{X}_{01} \equiv \mathbf{X}_{11}$, $\mathbf{X}_{N+1,1} \equiv \mathbf{X}_{N1}$ for a chain $\mathbf{X}_{N+1,1} \equiv \mathbf{X}_{11}$, $\mathbf{X}_{01} \equiv \mathbf{X}_{N1}$ for a ring.

Let us assume that for the given perturbations $\left(\mathbf{F}_i^* - \mathbf{F}_*\right)$, system (3.39) has been solved by us. In this case, within the accuracy of μ^2 we obtain the equation of the oscillator, the attractor of which determines the synchronous oscillation regime of the oscillators of the chain or of a ring:

$$\dot{\mathbf{X}} = \frac{1}{N}\sum_{i=1}^{N}\mathbf{F}_i\left(\mathbf{X}\right), \tag{3.40}$$

as well as parametric expressions for variables of the oscillators in the regime of synchronization:

$$\mathbf{X}_i = \mathbf{X} + \mu \mathbf{X}_{i1}\left(\mathbf{X}\right). \tag{3.41}$$

By excluding parameter **X** from equations (3.40), we obtain an explicit relation between the variables of the oscillator in the regime of synchronization – the mapping of the partial phase portraits of the oscillators (see the definition of synchronization given in Sec-

tion 2.1). Note that for $N = 2$, Eq. (3.39) coincides with equation (2.21).

Let us solve the problem of the relation between the synchronized motions of the oscillators in a specific case. We assume that perturbations of the right-hand sides of equations of the oscillators have the following expressions: $\mathbf{F}_i^*(\mathbf{X}) = \alpha_i^* \mathbf{C}\mathbf{F}(\mathbf{X})$, $i = \overline{1, N}$. In this case, the solutions of system (3.39) have the form $\mathbf{X}_{i1} = \Delta_i \mathbf{F}(\mathbf{X})$, where Δ_i are undefined coefficients. Their physical meaning for the case of two oscillators is explained in Section 2.2. In this case, it is the same.

We write down the equations of the first approximation relating the variables of arbitrary oscillators: $\mathbf{X}_i = \mathbf{X} + \mu\Delta_i \dot{\mathbf{X}}$ and $\mathbf{X}_j = \mathbf{X} + \mu\Delta_j \dot{\mathbf{X}}$. From these equations, within the accuracy of μ^2 we obtain $\mathbf{X}_i(t) = \mathbf{X}_j(t + \varphi_{ij})$, where $\varphi_{ij} = \mu(\Delta_i - \Delta_j)$ is the phase difference of oscillations of *j*-th oscillator with respect to the oscillations of *i*-th one. The fact that only parameter differences have a physical meaning Δ_k (phase difference) is quite natural for the mutual synchronization. This is a reflection of the fact that in the reciprocal case, any oscillator can be taken as a reference (standard) one.

Substituting expressions $\mathbf{X}_{i1} = \Delta_i \mathbf{F}(\mathbf{X})$ into equations (3.39), we obtain the following system with respect to the parameters Δ_k :

$$\varepsilon\left(\Delta_{i-1} - 2\Delta_i + \Delta_{i+1}\right) = \alpha_* - \alpha_i^* \tag{3.42}$$

with boundary conditions $\Delta_0 = \Delta_1,\ \ \Delta_{N+1} = \Delta_N$ for a chain and $\Delta_{N+1} = \Delta_1,\ \ \Delta_0 = \Delta_N$ for a ring. Here $\alpha_* = \frac{1}{N}\sum_{i=1}^{N}\alpha_i^*$ and for simplicity it is assumed that $\mathbf{C} = \mathbf{I}$.

System (3.40) with respect to parameters Δ_i is undefined (the rank of the system matrix is $N-1$). It can be solved in different ways, depending on this, resulting in a different meaning of parameters Δ_i. For example, if we set $\Delta_1 = 0,$ then all other parameters will be the phase differences of the oscillations of the respective oscillators with respect to the first one. System (3.39) can be considered as defined with respect to the differences of parameters $\Delta_k - \Delta_j$ (phase difference), having previously discarded one of the equations. Finally, one of the equations can be replaced by a new equation, for example by: $\sum_{i=1}^{N}\Delta_i = 0.$ In this case, parameters Δ_i will make sense of the phase differences of oscillators of a chain (ring) and the "arithmetic mean" oscillator (3.40).

The chain. Consider a system of $N-1$ equations of system (3.42) with respect to variables $\theta_k = \Delta_k - \Delta_{k-1}$ (up to a factor – the phase difference of neighboring oscillators) of the form

$$\theta_{i+1} - \theta_i = \frac{1}{\varepsilon}\left(\alpha_* - \alpha_i^*\right), \quad i = \overline{1, N-1}, \tag{3.43}$$

with the initial condition $\theta_1 = 0.$

From (3.43), we obtain expressions for the phase differences of any neighboring oscillators:

$$\Delta_{k+1} - \Delta_k = \frac{k}{\varepsilon}\left(\frac{1}{N}\sum_{i=1}^{N}\alpha_i^* - \frac{1}{k}\sum_{i=1}^{k}\alpha_i^*\right), \quad k = \overline{1, N-1}.$$

Expressions for phase differences of arbitrary oscillators (n-th and j-th, $1 \le j < n$):

$$\Delta_n - \Delta_j = \\ = \frac{1}{\varepsilon}\left(\frac{(n-j)(n+j-1)}{2N}\sum_{i=1}^{N}\alpha_i^* - (n-j)\sum_{i=1}^{j}\alpha_i^* - \sum_{i=1}^{n-j-1}(n-j-i)\alpha_{j+i}^*\right).$$

In particular, the expressions for the phase differences of arbitrary (n-th) and first oscillators have the form:

$$\Delta_n - \Delta_1 = \frac{1}{\varepsilon}\left(\frac{n(n-1)}{2N}\sum_{i=1}^{N}\alpha_i^* - \sum_{i=1}^{n}(n-i)\alpha_i^*\right).$$

The ring. Solving system (3.43) with the boundary conditions of the ring $\theta_1 = \Delta_1 - \Delta_N,\ \sum_{i=1}^{N}\theta_i = 0,$ we obtain

$$\theta_1 = \Delta_1 - \Delta_N = \frac{1}{\varepsilon N}\left(\sum_{i=1}^{N-1} (N-i)\alpha_i^* - \frac{N-1}{2}\sum_{i=1}^{N} \alpha_i^* \right),$$

$$\theta_{k+1} = \Delta_{k+1} - \Delta_k = \frac{k}{\varepsilon}\left(\frac{1}{N}\sum_{i=1}^{N} \alpha_i^* - \frac{1}{k}\sum_{i=1}^{k} \alpha_i^* \right) +$$

$$+ \frac{1}{\varepsilon N}\left(\sum_{i=1}^{N-1} (N-i)\alpha_i^* - \frac{N-1}{2}\sum_{i=1}^{N} \alpha_i^* \right),$$

$$k = \overline{1, N-1}.$$

A chain and a ring of strongly non-identical oscillators.

As in the case of two oscillators (see Section 2.3), we subdivide equations of each of the oscillators of the chain into groups of equations: one group represents equations with strongly non-identical respective parameters, while the second one represents equations containing weakly non-identical or identical right-hand sides. Then, we consider a system of the form

$$\begin{aligned} \dot{\mathbf{X}}_i &= \mathbf{F}_i(\mathbf{X}_i, \mathbf{Y}_i) - \mu^{-1}\mathbf{C}(-\mathbf{X}_{i-1} + 2\mathbf{X}_i - \mathbf{X}_{i+1}), \\ \dot{\mathbf{Y}}_i &= \mathbf{\Phi}(\mathbf{X}_i, \mathbf{Y}_i) - \mathbf{D}(-\mathbf{Y}_{i-1} + 2\mathbf{Y}_i - \mathbf{Y}_{i+1}) + \mu\mathbf{\Phi}_i^*(\mathbf{X}_i, \mathbf{Y}_i) \end{aligned} \qquad (3.44)$$

with boundary conditions $\mathbf{X}_0 \equiv \mathbf{X}_1$, $\mathbf{X}_N \equiv \mathbf{X}_{N+1}$, $\mathbf{Y}_0 \equiv \mathbf{Y}_1$, $\mathbf{Y}_N \equiv \mathbf{Y}_{N+1}$ for a chain and $\mathbf{X}_0 \equiv \mathbf{X}_N$, $\mathbf{X}_1 \equiv \mathbf{X}_{N+1}$, $\mathbf{Y}_0 \equiv \mathbf{Y}_N$, $\mathbf{Y}_1 \equiv \mathbf{Y}_{N+1}$ for a ring. Here $\mathbf{X}_i \in R^k$, $\mathbf{Y}_i \in R^{m-k}$, $\mathbf{C} = \operatorname{diag}(c_1, c_2, ..., c_k)$, $\mathbf{D} = \operatorname{diag}(d_1, d_2, ..., d_{m-k})$, $c_i > 0$, $d_j \geq 0$, $\mu = \varepsilon^{-1}$ is a small parameter.

System (3.44) is a system with singularly-regular perturbations (multiplying the first equations by μ, we obtain a small parameter in front of the respective derivatives). As in the case of a pair of oscillators, it is easy to reduce this system to a special form [17], thereby demonstrating that it has a unique and stable integral manifold M_μ, which is asymptotically close to manifold M_0. That is, the problem of the existence and stability of synchronization is considered resolved.

Next, we proceed by analogy with the case of a pair of oscillators: we search for a parametric representation of manifold M_μ, in the form of power series by a small parameter of the form

$$\begin{aligned}\mathbf{X}_i &= \mathbf{X} + \mu\mathbf{X}_{i1}(\mathbf{X},\mathbf{Y}) + \mu^2\mathbf{X}_{i2}(\mathbf{X},\mathbf{Y}) + \dots,\\ \mathbf{Y}_i &= \mathbf{Y} + \mu\mathbf{Y}_{i1}(\mathbf{X},\mathbf{Y}) + \mu^2\mathbf{Y}_{i2}(\mathbf{X},\mathbf{Y}) + \dots.\end{aligned} \tag{3.45}$$

We assume that our dynamical system on the manifold has the form

$$\begin{aligned}\dot{\mathbf{X}} &= \mathbf{F}(\mathbf{X},\mathbf{Y}) + \mu\mathbf{F}_*(\mathbf{X},\mathbf{Y}) + \mu^2\mathbf{F}_{**}(\mathbf{X},\mathbf{Y}) + \dots,\\ \dot{\mathbf{Y}} &= \mathbf{\Phi}(\mathbf{X},\mathbf{Y}) + \mu\mathbf{\Phi}_*(\mathbf{X},\mathbf{Y}) + \mu^2\mathbf{\Phi}_{**}(\mathbf{X},\mathbf{Y}) + \dots.\end{aligned} \tag{3.46}$$

Substituting expressions (3.45) into system (3.44), expanding the functions into power series and equating terms of the same orders, we obtain equations that determine the functions of the right-hand side of system (3.44) and functions (3.45). In particular, the equations of the first approximation have the form

$$\mathbf{F} + \mu\mathbf{F}_* + \mu\dot{\mathbf{X}}_{i1} =$$

$$= \mathbf{F}_i + \mu\left(\frac{\partial \mathbf{F}_i}{\partial \mathbf{X}}\mathbf{X}_{i1} + \frac{\partial \mathbf{F}_i}{\partial \mathbf{Y}}\mathbf{Y}_{i1}\right) - \mathbf{C}\left(-\mathbf{X}_{i-1} + 2\mathbf{X}_i - \mathbf{X}_{i+1}\right), \tag{3.47}$$

$$\mathbf{\Phi}_* + \dot{\mathbf{Y}}_{i1} = \frac{\partial \mathbf{\Phi}}{\partial \mathbf{X}}\mathbf{X}_{i1} + \frac{\partial \mathbf{\Phi}}{\partial \mathbf{Y}}\mathbf{Y}_{i1} - \mathbf{D}\left(-\mathbf{Y}_{i-1,1} + 2\mathbf{Y}_{i1} - \mathbf{Y}_{i+1,1}\right) + \mathbf{\Phi}_i^*. \tag{3.48}$$

Summing up all the equations of system (3.47) and choosing the functions $\mathbf{F}$, $\mathbf{F}_*$ using the same considerations as above, we obtain expressions

$$\mathbf{F} = \frac{1}{N}\sum_{i=1}^{N}\mathbf{F}_i + \frac{1}{N}\mathbf{C}\mathbf{U}, \quad \mathbf{U} = \sum_{i=1}^{N}\mathbf{X}_{i1}, \quad \mathbf{F}_* = \frac{1}{N}\sum_{i=1}^{N}\left(\frac{\partial \mathbf{F}_i}{\partial \mathbf{X}}\mathbf{X}_{i1} + \frac{\partial \mathbf{F}_i}{\partial \mathbf{Y}}\mathbf{Y}_{i1}\right)$$

and the equation for variable $\mathbf{U}$: $\mu\ddot{\mathbf{U}} = -\mathbf{C}\mathbf{U}$. Since $\mathbf{C}$ is a non-degenerate matrix, then solution $\mathbf{U} = 0$ of this equation is stable. Summing up all equations (3.48) and taking into account condition $\mathbf{U} = 0$, we choose function $\mathbf{\Phi}_*$ in the form

$$\mathbf{\Phi}_* = \frac{1}{N}\sum_{i=1}^{N}\mathbf{\Phi}_i^* + \mathbf{D}\mathbf{V}, \quad \mathbf{V} = \frac{1}{N}\sum_{i=1}^{N}\mathbf{Y}_{i1}.$$

As a result, we obtain an equation for variable $\mathbf{V}$:

$$\dot{\mathbf{V}} = \frac{\partial \mathbf{\Phi}}{\partial \mathbf{Y}}\mathbf{V} - \mathbf{D}\mathbf{V}.$$

There are two possibilities regarding the stability of solution $\mathbf{V} = 0$ of this equation:

a) if matrix $\dfrac{\partial \mathbf{\Phi}}{\partial \mathbf{Y}}$ is stable, then solution $\mathbf{V} = 0$ is stable for any matrix of the number of possible diagonal matrices $\mathbf{D}$, including $\mathbf{D} = 0$. In this case, dissipative couplings in the respective variables are not decisive for ensuring the regime of synchronization;

b) a trivial solution to this equation with the matrix $\mathbf{D} = 0$ is unstable. In this case, obviously, there is always such a matrix $\mathbf{D}$ (structure of couplings), in which the mentioned solution will be stable.

Thus, the stability of solution $\mathbf{V} = 0$ can always be realized. The stability conditions will be considered satisfied.

Singularly perturbed equations (3.47) have a unique stable surface of slow motions [17]. Assuming the condition $\sum_{i=1}^{N} \mathbf{X}_{i1} = 0$ fulfilled for selected functions $\mathbf{F}$ and $\mathbf{F}_*$, its equations in the zero approximation have the form

$$\begin{aligned} &-\mathbf{X}_{i-1,1} + 2\mathbf{X}_{i1} - \mathbf{X}_{i+1,1} = \mathbf{C}^{-1}\left(\mathbf{F}_i - \mathbf{F}\right), \\ &\sum_{i=1}^{N} \mathbf{X}_{i1} = 0, \\ &i = \overline{1, N}. \end{aligned} \tag{3.49}$$

Let us point out one of the simple solutions of (3.49). Let us assume that $\mathbf{F}_i = \nu_i \mathbf{F}$ and $\mathbf{C} = \mathbf{I}$. In this case, $\mathbf{X}_{i1} = \Delta_i \mathbf{F}$, where Δ_i are the undefined coefficients, is a solution for (3.49). The equations for determining the coefficients look familiar:

$$\Delta_{i-1} - 2\Delta_i + \Delta_{i+1} = 1 - \nu_i.$$

Obtained equation turns into (3.42) by a simple transformation of the form $\nu_i = \alpha_i / \alpha_0$, $\varepsilon \to \alpha_0$, where $\alpha_0 = \sum_{i=1}^{k} \alpha_i$. Therefore, we immediately obtain expressions for the phase differences of our interest (up to a factor $\mu = 1/\varepsilon$):

– expressions for the phase differences of any neighboring oscillators:

$$\Delta_{k+1} - \Delta_k = \frac{k}{\alpha_0}\left(\frac{1}{N}\sum_{i=1}^{N} \alpha_i - \frac{1}{k}\sum_{i=1}^{k} \alpha_i \right), \quad k = \overline{1, N-1}; \tag{3.50}$$

– expressions for the phase differences of arbitrary oscillators (n-th and j-th, $1 \le j < n$):

$$\Delta_n - \Delta_j =$$

$$= \frac{1}{\alpha_0}\left(\frac{(n-j)(n+j-1)}{2N}\sum_{i=1}^{N} \alpha_i - (n-j)\sum_{i=1}^{j} \alpha_i - \sum_{i=1}^{n-j-1} (n-j-i)\alpha_{j+i} \right); \tag{3.51}$$

– expressions for the phase differences of an arbitrary (n-th) and first oscillator:

$$\Delta_n - \Delta_1 = \frac{1}{\alpha_0}\left(\frac{n(n-1)}{2N}\sum_{i=1}^{N}\alpha_i - \sum_{i=1}^{n}(n-i)\alpha_i \right). \tag{3.52}$$

Suppose that the linear algebraic system (3.49) is solved. In this case, for the selected $\mathbf{\Phi}_*$ and condition $\sum_{i=1}^{N}\mathbf{Y}_{i1} = 0$, equations (3.48) define limited functions $\mathbf{Y}_{i1}$. Within the accuracy of μ these equations are equivalent to a system of partial differential equations of the form

$$\frac{\partial \mathbf{Y}_{i1}}{\partial \mathbf{X}}\mathbf{F} + \frac{\partial \mathbf{Y}_{i1}}{\partial \mathbf{Y}}\mathbf{\Phi} + \frac{\partial \mathbf{\Phi}}{\partial \mathbf{Y}}\mathbf{Y}_{i1} - \mathbf{D}\left(-\mathbf{Y}_{i-1,1} + 2\mathbf{Y}_{i1} - \mathbf{Y}_{i+1,1}\right) = \\ = \frac{\partial \mathbf{\Phi}}{\partial \mathbf{X}}\mathbf{X}_{i1} + \mathbf{\Phi}_i^* - \mathbf{\Phi}_*. \tag{3.53}$$

Solving equations (3.53), we find functions $\mathbf{Y}_{i1}$.

Thus, in the stable synchronization mode, the phase variables of the oscillators are coupled (accuracy μ^2) by parametric equations of the form

$$\mathbf{X}_i = \mathbf{X} + \mu\mathbf{X}_{i1}, \quad \mathbf{Y}_i = \mathbf{Y} + \mu\mathbf{Y}_{i1}.$$

In this case, the properties of the synchronous regime, within the accuracy of μ^2 are determined by the properties of the chaotic attractor A_μ of a dynamical system of the form

$$\dot{\mathbf{X}} = \frac{1}{N}\sum_{i=1}^{n} \mathbf{F}_i\left(\mathbf{X}, \mathbf{Y}\right) + \mu \mathbf{F}_*,$$
$$\dot{\mathbf{Y}} = \frac{1}{N}\sum_{i=1}^{n} \mathbf{\Phi}_i .$$

Note that if $\mathbf{F}_i \equiv \mathbf{F}_j = \mathbf{F}$, $\mathbf{\Phi}_i \equiv \mathbf{\Phi}_j = \mathbf{\Phi}$, then $\mathbf{F}_* = 0$, and solutions $\mathbf{X}_{i1} = \mathbf{X}_{j1} = 0$, $\mathbf{Y}_{i1} = \mathbf{Y}_{j1} = 0$ are stable, i.e., we have a transition to isochronous synchronization in a homogeneous chain.

Example. Consider synchronization in a chain of non-identical Lurie oscillators:

$$\begin{aligned} \dot{x}_i &= \alpha_i\left(-f\left(x_i\right) + \mathbf{a}^T \mathbf{y}_i\right) + \varepsilon\left(x_{i-1} - 2x_i + x_{i+1}\right), \\ \dot{\mathbf{y}}_i &= \mathbf{B}\mathbf{y}_i + \mathbf{b}x_i . \end{aligned} \tag{3.54}$$

Suppose that parameters α_i in (3.54) are strongly different. For $\varepsilon^{-1} = \mu \ll 1$ we have the considered asymptotic case. Since the equations for vector $\mathbf{y}$ are identical, then $\mathbf{C} = 1$. The dynamical properties of the regime of synchronization in the chain are determined by an attractor of the system of the form (zero approximation)

$$\dot{x} = \left(\frac{1}{N} \sum_{i=1}^{N} \alpha_i \right) \left(-f(x) + \mathbf{a}^T \mathbf{y} \right),$$
$$\dot{\mathbf{y}} = \mathbf{B}\mathbf{y} + \mathbf{b}x.$$

The functions of the first approximation that determine the relationship of dynamical variables in the regime of synchronization are determined by equations (5.49).

Note that the form of the right-hand sides refers to the case of equation (3.49) considered above.

Numerical experiment. The experiment has been carried out for a chain of six Chua's oscillators with parameters $\{\beta, \gamma, m_2, m_1, \varepsilon\} =$ $= \left\{ 14, 0.1, -\frac{1}{7}, \frac{2}{7}, 3 \right\}$ and $\left\{ \alpha_i,\ i = \overline{1-6} \right\} = \{4,14,14,4,4,14\}$. The synchronization in the chain is stable. Fig. 3.9 shows partial phase portraits of synchronized oscillators. They represent projections of the attractor of the "effective" Chua's oscillator with parameter $\alpha = \alpha_0 = 9$ onto the respective subspaces. This oscillator is set on manifold M_μ and determines properties of the synchronization in the chain oscillators.

It is easy to see that there are two groups (two clusters) of oscillators. In each group, the phase portraits of the oscillators are identical. The first group: $(\mathbf{X}_1, \mathbf{X}_4, \mathbf{X}_5)$, the second one: $(\mathbf{X}_2, \mathbf{X}_3, \mathbf{X}_6)$.

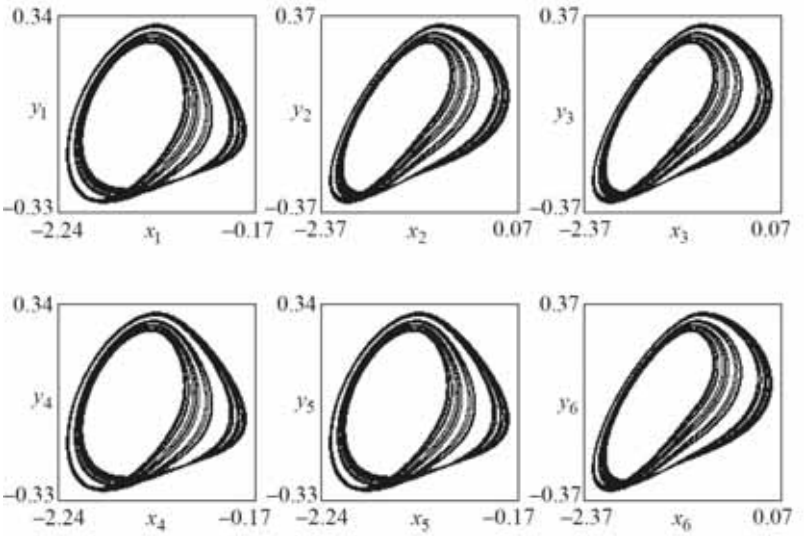

Fig. 3.9. Partial phase portraits of synchronized oscillators of the chain.

In the regime of synchronization $\mathbf{X}_1 = \mathbf{X}_4 = \mathbf{X}_5$ and $\mathbf{X}_2 = \mathbf{X}_3 = \mathbf{X}_6$. It must be said that the formation of these groups is not accidental, but is a consequence of the specially selected parameters of the oscillators of the chain. A separate chapter will be devoted to the cluster dynamics of systems of coupled oscillators. In this case, our interest is concerned with testing of results of the theory. Fig. 3.10 shows the segments of the time-histories of variables $x_i(t)$ of oscillators of the chain. As one can see, the oscillograms of oscillators from different groups have a phase shift. The fact that this shift is insignificant is not important, it is important that it exists. For the phase difference of arbitrary oscillators, we have expression

$\varphi_{ij} = \mu\left(\Delta_i - \Delta_j\right)$. Using formula (3.50), we obtain $\varphi_{21} = 5/27$, $\varphi_{32} = 0$, $\varphi_{43} = 5/27$, $\varphi_{54} = 0$, $\varphi_{65} = 5/27$. From formula (3.51), we obtain $\varphi_{21} = 5/27$, $\varphi_{31} = 5/27$, $\varphi_{41} = 0$, $\varphi_{51} = 0$, $\varphi_{61} = 5/27$ that is, we observe a complete qualitative agreement between the results of theory and experiment. Note that there is also a quantitative similarity of the results: according to Fig. 3.10, the phase shift is close to value 5/27.

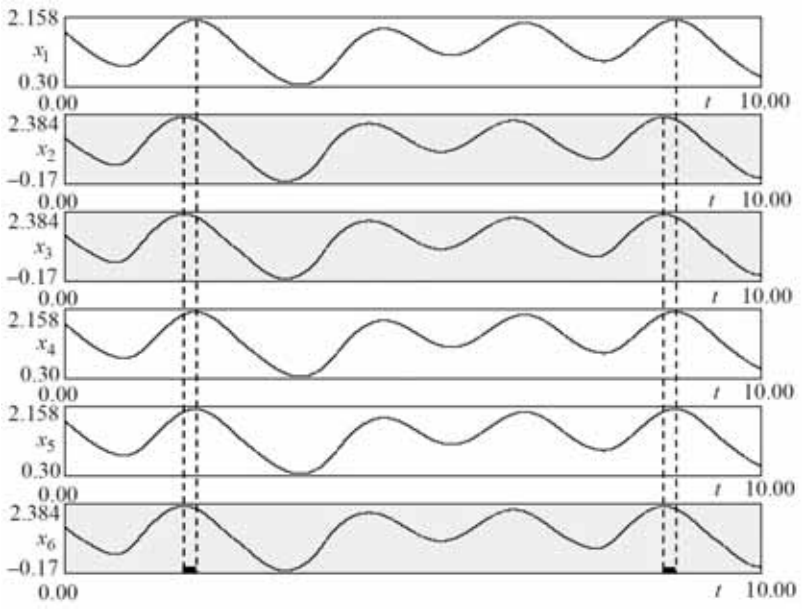

Fig. 3.10. Time-histories of oscillators in the regime of chaotic synchronization.

3.6. Dynamics of a homogeneous and of a heterogeneous flow chain

The study of the nonlinear dynamics of oscillator lattices began from the flow chains [183 – 186, etc.], the reason for which was their convenience in studying the mechanisms of transition from regular movements to chaos as the spatial coordinate of the chain (oscillator number) changes and thus obtaining a clear picture of the processes of nucleation and development of turbulence in flow systems (in particular, this concerns the nucleation of turbulence in hydrodynamic flows).

Consider the dynamics of the flow chain: system (3.12) for $\varepsilon_2 = 0$:

$$\begin{aligned} \dot{x}_k &= -f(x_k) + \mathbf{a}^T \mathbf{y}_k + \varepsilon_1 (x_{k-1} - x_k) + g(t), \\ \dot{\mathbf{y}}_k &= \mathbf{B}\mathbf{y}_k + \mathbf{b}x_k + \mathbf{q}(t) \end{aligned} \tag{3.55}$$

with boundary condition $x_0 \equiv x_1$. Our interest is concerned with the case of a chain segment $k = \overline{1, N}$ with boundary condition $x_N \equiv x_{N+1}$, and also the case of a chain, which is non-bounded from the right-hand side.

The conditions of the global stability for a spatially homogeneous state (isochronous synchronization for a segment of the chain of oscillators (3.55)) are formulated as a theorem.

Theorem 3.6.1. Suppose $\lambda_0 = \inf\limits_{\forall x \in R} f'(x)$, $xf(x) \geq mx^2 - l$, $x \in R$, and conditions *a* and *b* for system (1.4) (Lurie oscillator) are fulfilled. Then for $\varepsilon_1 > m - \lambda_0$, an isochronous synchronization in system (3.55) is a globally stable.

Proof. We transform system (3.55) to variables $U_k = x_k - x_{k+1}$, $\mathbf{W}_k = \mathbf{y}_k - \mathbf{y}_{k+1}$:

$$\begin{aligned} &\dot{U}_k = -\lambda_k(\xi_k)U_k + \mathbf{a}^T\mathbf{W}_k + \varepsilon_1(U_{k-1} - U_k), \\ &\dot{\mathbf{W}}_k = \mathbf{B}\mathbf{W}_k + \mathbf{b}U_k, \\ &k = \overline{1, N-1}. \end{aligned} \tag{3.56}$$

Here $\lambda_k = f'(\xi_k)$, $\xi_k \in [x_k, x_{k+1}]$ (Lagrange's theorem) and boundary conditions $U_0 = 0$, $U_N = 0$. Due to the boundary condition $U_0 = 0$, the first subsystem in (3.56) $(k = 1)$ is independent. Its solution $U_1 = 0$, $\mathbf{W}_1 = 0$ is globally stable for $\varepsilon_1 > m - \lambda_0$. This is established using the Lyapunov function $V = \frac{1}{2}\left(U_1^2 + \mathbf{W}_1^T\mathbf{H}\mathbf{W}_1\right)$. Its derivative, calculated by virtue of the first two equations of Eqs. (3.56), has the expression and estimate:

$$\dot{V} = -Q(U_1, \mathbf{W}_1) - (\lambda_1 - m + \varepsilon_1)U_1^2 \leq -\left[Q(U_1, \mathbf{W}_1) + (\lambda_0 - m + \varepsilon_1)U_1^2\right].$$

It is negative if $\varepsilon_1 > m - \lambda_0$. It means that $\|U_1\| < M_1 \varepsilon^{-\mu_1 \tau}$, $\|\mathbf{W}_1\| < M_1 \varepsilon^{-\mu_1 \tau}\ M_1,\ \mu_1 > 0.$

For any $k \geq 2$ we rewrite system (3.56) in the form

$$\begin{aligned} &\dot{\mathbf{Z}}_k = \mathbf{A}_k(\tau)\mathbf{Z}_k + \varepsilon \mathbf{Z}_{k-1}(\tau), \\ &k = \overline{2, N-1}, \end{aligned} \tag{3.57}$$

where $\mathbf{Z}_k = (U_k, \mathbf{W}_k)^T$, $\mathbf{A}_k = \begin{pmatrix} -\lambda_k(\tau) - \varepsilon_1 & \mathbf{a}^T \\ \mathbf{b} & \mathbf{B} \end{pmatrix}$, $\varepsilon = \begin{pmatrix} \varepsilon_1 & \mathbf{0}_{1\times n} \\ \mathbf{0}_{n\times 1} & \mathbf{0}_{n\times n} \end{pmatrix}$.

Note that all matrices $\mathbf{A}_k(\tau)$ are stable for $\varepsilon_1 > m - \lambda_0$.

If $k = 2,$ then, due to the stability of $\mathbf{A}_2(\tau)$ and of the and indignation norm $\|\mathbf{Z}_1\| < M_1 \varepsilon^{-\mu\tau}$, we obtain that $\|\mathbf{Z}_k\|_{k=2} < M_2 \varepsilon^{-\mu\tau}$ [187], i.e. solution $\mathbf{Z}_2 = 0$ is globally stable. Further, the reasoning is repeated for all $k \geq 3$. Thus, the trivial solution of equation (3.57) (isochronous synchronization of oscillators) is globally stable.

It seems that this theorem can be extended to the case of an unbounded chain. This would be true if it were possible to show that constants M_k in the estimates of the norms of solutions do not have unlimited growth as the number of the oscillator increases. If the named constants grow exponentially with the number of the oscillators, then, obviously, one will be dealing with convective instability [188] of a spatially-homogeneous state.

Let us investigate the stability of a spatially homogeneous state of a semi-infinite chain with respect to perturbations at the boundary – perturbations of equations of the first oscillator (the right-hand sides of its equations). Note that if a larger number of oscillators is disturbed in the chain, then the entire "disturbed" segment, from the beginning to the penultimate disturbed oscillators, can be discarded. The last perturbed oscillator can be taken as the beginning of the chain, thereby reducing the problem under consideration to a problem with perturbations on the chain's boundary.

Fully tracing the downstream evolution of attractors of individual oscillators (all components of attractors) is an analytically difficult task. Let us study the evolution of equilibriums, more precisely, the coordinates of equilibriums of partial oscillators along the chain under perturbations of these coordinates in the first oscillator. This will provide some idea of the evolution of the downstream attractors. For simplicity, we assume the chain to be autonomous. The equations for the equilibriums of system (3.55) have the form

$$\begin{aligned} &-f\left(x_k\right)+\mathbf{a}^T\mathbf{y}_k+\varepsilon\left(x_{k-1}-x_k\right)=0,\\ &\mathbf{B}\mathbf{y}_k+\mathbf{b}x_k=0,\\ &k=\overline{1,N}. \end{aligned}$$

Eliminating vector $\mathbf{y}_k$ from these equations, we obtain an implicit form of the recurrent equation relating the coordinates of the equi-

libriums of the previous oscillator with the coordinates of the next one: a one-dimensional mapping of the form

$$x_k = F^{-1}\left(x_{k-1}\right), \qquad (3.58)$$
$$F\left(x_{k-1}\right) = x_{k-1} + \frac{1}{\varepsilon}\left(f\left(x_{k-1}\right) + \mathbf{a}^T\mathbf{B}^{-1}\mathbf{b}x_{k-1}\right)$$

with the initial condition $x_0 = x_1$. The fixed points of mapping (3.58) $\left(x_k = x_{k-1} = x^*\right)$ are the roots of equation

$$f\left(x\right) + \mathbf{a}^T\mathbf{B}^{-1}\mathbf{b}x = 0.$$

It is easy to see that the coordinates of the fixed points coincide with the coordinates of the equilibriums of isolated oscillators (for $\varepsilon = 0$) .

For simplicity, we assume that the nonlinearity has the form of a cubic parabola. In this case, two qualitatively different types of mapping (3.58) are shown in Fig. 3.11.

In the first case (see Fig. 3.11a), each of the partial self-oscillators is under-excited and their stable equilibrium at the origin is globally stable. At the same time, as one be seen from the Figure, the non-moving point at the origin is also stable. It's obvious that in this case, the dynamics of the chain is trivial: for any disturbance of the equilibriums at the boundary of the chain, an equilibrium is established, which in the limit by the number of elements coincides with

the equilibrium of the unexcited partial oscillator. In other words, in this case, there is an absolute stability (in space and time) of the discrete environment of the oscillators. In the second case (see Fig. 3.11b), the partial self-oscillators are perturbed. In particular, if one deals with a chain of Chua's oscillators, then, depending on the parameters in the partial oscillator, either a periodic oscillatory regime, or a chaotic oscillation regime on one of Chua's attractors, or, finally, on a combined double-scroll attractor can be observed (see Section 1.1). The evolution of the coordinates of the equilibriums of the partial attractors of each of the oscillators of the chain under the perturbation of the coordinates in the first oscillator is shown in the Figure.

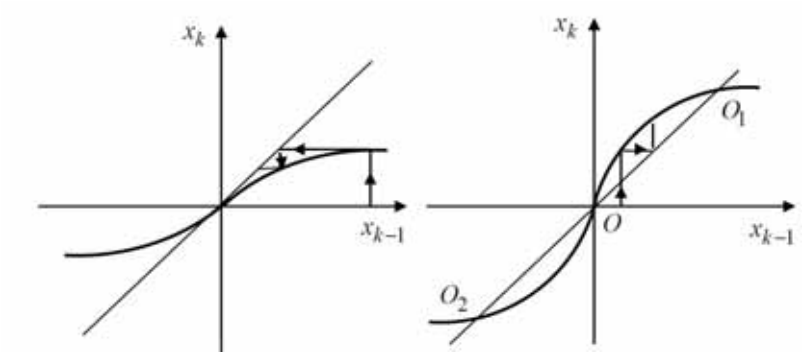

a b

Fig. 3.11. Different types of mapping (3.58) depending on the parameters of the oscillator.

In this case, the fixed point O is unstable. From the instability condition $\left|\left(F^{-1}(x)\right)'\right|_{x=x^*} > 1$ we obtain inequality

$$0 < -\frac{1}{2}\left(f'\left(x^*\right) + \mathbf{a}^T\mathbf{B}^{-1}\mathbf{b}\right) < \varepsilon.$$

In particular, for the Chua's oscillator we have the expressions:

$$\mathbf{a}^T = (\alpha, 0),\ \ \mathbf{b} = \begin{pmatrix} -1 \\ 0 \end{pmatrix},\ \ \mathbf{B}^{-1} = \frac{1}{\beta+\gamma}\begin{pmatrix} -\gamma & -1 \\ \beta & -1 \end{pmatrix},\ \ \mathbf{a}^T\mathbf{B}^{-1}\mathbf{b} = \frac{\alpha\gamma}{\gamma+\beta}.$$

Equilibrium $O(0,0,0)$ of the isolated oscillator, which for these parameters represents a saddle, corresponds to the fixed point O. For this point $f(0) = 0,\ \ f'(0) = \inf_{\forall x \in R} f'(x) = \lambda_0 = \alpha m_0 < 0.$ The condition for its instability has the form

$$0 < \frac{\alpha}{2}\left(|m_0| - \frac{\gamma}{\gamma+\beta}\right) < \varepsilon.$$

It is easy to establish that the condition of global stability for a segment of a chain $\varepsilon > \alpha|m_0| + m$ and the resulting condition of spatial instability (along the chain) are compatible.

Thus, if an individual oscillator had a single equilibrium $O(0, 0, 0)$, then the chain would exhibit pure convective instability. In reality, nonlinear dissipation suppresses this instability rather

quickly, which together leads only to a deformation of local attractors downstream from point to point. This fact is reflected in the diagram of the evolution of equilibriums shown in Fig. 3.3b.

Since the fixed points of the mapping O_1 and O_2 are stable, then the perturbed equilibrium of the individual oscillator O^k (k is it's number) approaches without limit O_1 or O_2 depending on the sign of the perturbation at the boundary. Consequently, $O_1^k \to O_1$, and $O_2^k \to O_2$, i.e., in the limit (for $k \to \infty$) equilibrium O^k merges with one of the equilibriums O_1 or O_2 Without further research, it can be predicted that or $k \to \infty$, a spatially homogeneous dynamic regime will be established in the chain; however, it will not be associated with the attractor of the partial oscillator, although it may contain some of its visual outlines.

Numerical experiment. Note that numerical and full-scale experiments with flow chains are associated with a number of difficulties, including the long-term establishment of stationary states of the chain, the high sensitivity of dynamical regimes to changes in the initial conditions arising from the existence of numerous attractors in the phase space of the system (a large number of potentially possible regimes), high sensitivity of dynamical regimes with respect to spatial perturbations, etc. Below are the results of a numerical experiment studying the evolution of dynamical regimes of a chain (flows) along the chain under various perturbations at the boundary.

The experiment was carried out for a chain of a small number $(N=6)$ of Chua's oscillators. This is sufficient for general conclusions regarding the established limiting regimes. The results of studying quasiperiodic wave motions in a flow chain of 120 elements are presented in [186].

We consider a constantly acting disturbance on the boundary: in the first oscillator, whose equations have the form

$$\begin{aligned} \dot{x} &= \alpha\left(y - h(x) + c\right), \\ \dot{y} &= -y + z - x, \\ \dot{z} &= -\beta y - \gamma z. \end{aligned} \tag{3.59}$$

Note that the change in the perturbing parameter c (shift of the nonlinearity) physically corresponds to the shift of the operating point on the volt-ampere characteristic of the nonlinear element. Note also that for $c \neq 0$, the equations of the oscillator lose their symmetry, which is reflected in its attractors.

The coupling between the oscillators is naturally interpreted as the flow rate, α – as a parameter of the environment's activity, αc according to equations (3.59) – as an excitation parameter. In the experiment, the choice of parameters is made such that the coordinates of the equilibriums of individual oscillators would approach their limiting values (see Fig. 3.11) close enough for a small number of iterations. At a low flow rate and low excitation, the flow chaoticity develops through a certain number of spatial bifurcations

that occur in individual oscillators as their number increases. The number of period doubling bifurcations of the limit cycle is always finite [178] (see Fig. 3.12).

The fact that the beginning of the doubling of the cycle period should end up in a spatial chaos is not a rule in this case. There are parameter values at which, after several doublings of the limit cycle's period, there is a return to a cycle of the single period with a further establishment of a spatially-homogeneous periodic motion (see Fig. 3.13).

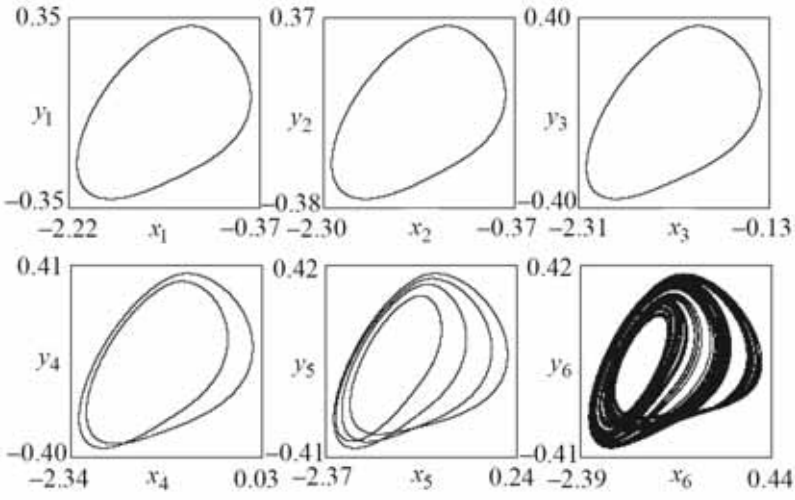

Fig. 3.12. Bifurcation diagrams for parameters

$$(\alpha, \beta, \gamma, m_0, m_1, \varepsilon, c) = (8.51, 14, 0.1, -1/7, 2/7, 0.2, 0.01),$$

$$\mathbf{C} = \mathrm{diag}(1, 0.1, 0.1).$$

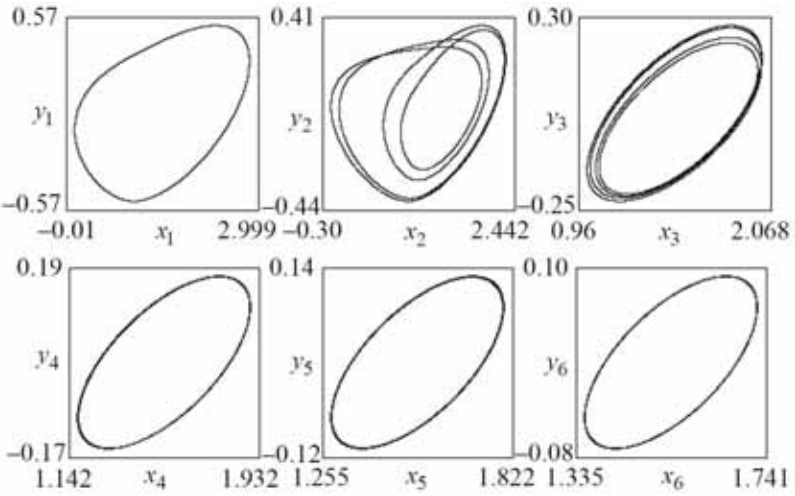

Fig. 3.13. Bifurcation diagrams for parameters

$$(\alpha, \beta, \gamma, m_0, m_1, \varepsilon, c) = (8.45, 14, 0.1, -1/7, 2/7, 0.2, 0.08),$$

$$\mathbf{C} = \mathrm{diag}(1, 1, 1).$$

A cascade of spatial bifurcations is not a prerequisite for the emergence of a chaotic regime. With an increase in excitation, the periodic movement of the first oscillator can immediately lead to chaotic movements of the second one (see Fig. 3.14) with a further establishment of spatially-homogeneous chaos.

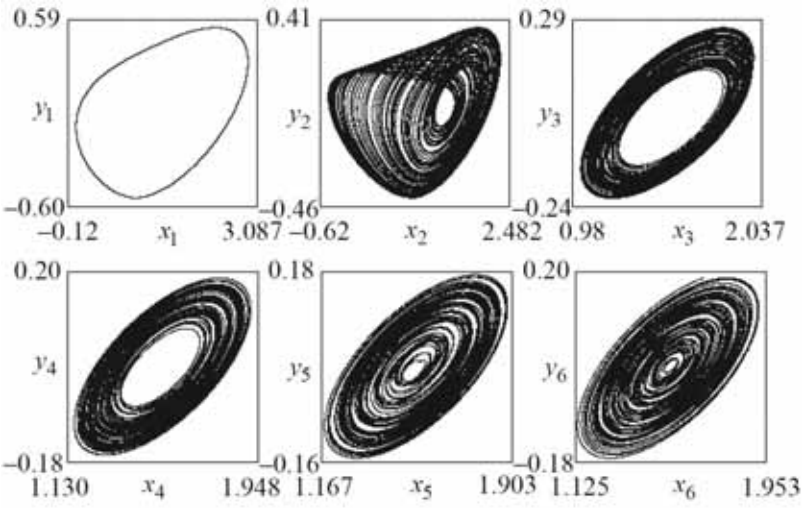

Fig. 3.14. Bifurcation diagrams for parameters

$$(\alpha, \beta, \gamma, m_0, m_1, \varepsilon, c) = (8.57{,}14, 0.1, -1/7, 2/7, 0.2, 0.09),$$

$$\mathbf{C} = \mathrm{diag}(1, 1, 1).$$

Note that at small values of the coupling parameter, there exists such a phenomenon as the stabilization of the dimension of (fractal) chaotic motion on separate segments of the chain of oscillators, which was first discovered in a numerical experiment [189]. The effect is explained by a partial synchronization of the oscillators with the numbers on these segments. In this case, on the graph of the dependence of the dimension of the chaotic motion of an individual oscillator on its number, there are almost horizontal "shelves", similar to the resonant "shelves" on the previously studied rotation characteristics.

If the level of the excitation at the boundary is significant, then, depending on the initial conditions, various spatially-homogeneous dynamical regimes can be realized in the chain. For example, Fig. 3.15 and 3.16 show the order of establishing of spatially homogeneous regimes in the chain with different initial conditions. Starting from the sixth one, the dynamics of the oscillators of the chain with subsequent numbers is almost the same.

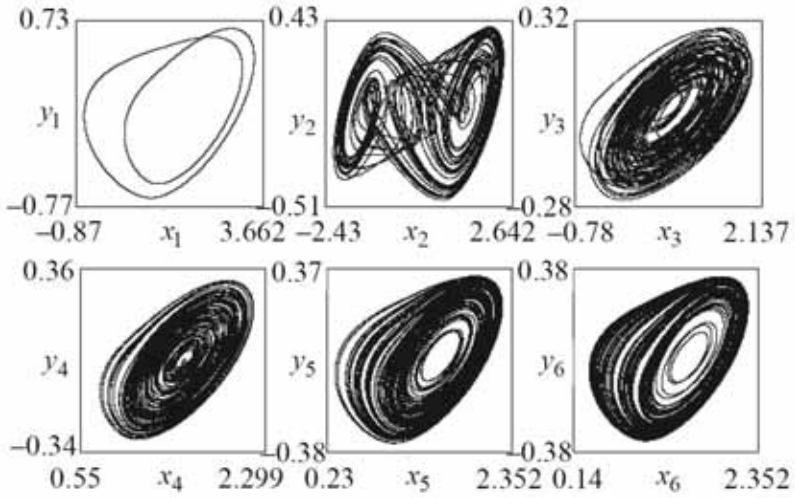

Fig. 3.15. Bifurcation diagrams for parameters

$$(\alpha, \beta, \gamma, m_0, m_1, \varepsilon, c) = (8.7; 14; 0.1; -1/7; 2/7; 0.2; 0.141),$$

$$\mathbf{C} = \mathrm{diag}(1, 1, 1).$$

Switching waves. The spatially-homogeneous chaotic regime, which is established in the flow system at a sufficient distance from its boundary, is sensitive to the magnitude and type of perturbations

applied to the boundary. In this case, the observed phenomena are in many respects similar to those occurring in potentially unstable (excitable) media when an external pulse is triggered. In this case, a switching wave can arise in the excitable medium, which corresponds to the transition of the medium from one state to another. Similar transitions – switching waves of the "order/chaos" type and vice versa – can be observed in the flow chain under consideration. In particular, the "switch" of the state of the medium from chaotic to laminar can be a periodic perturbation that synchronizes the master oscillator and acts during the required time. In this case, if the first state of the master oscillator is described by equations (3.59), then the second one is described by equations of the form

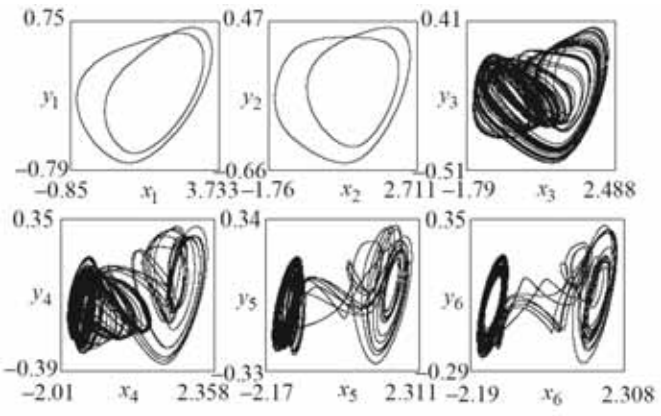

Fig. 3.16. Bifurcation diagrams for parameters

$$(\alpha, \beta, \gamma, m_0, m_1, \varepsilon, c) = (8.7; 14; 0.1; -1/7; 2/7; 0.2; 0.141),$$

$$\mathbf{C} = \mathrm{diag}(1, 1, 1).$$

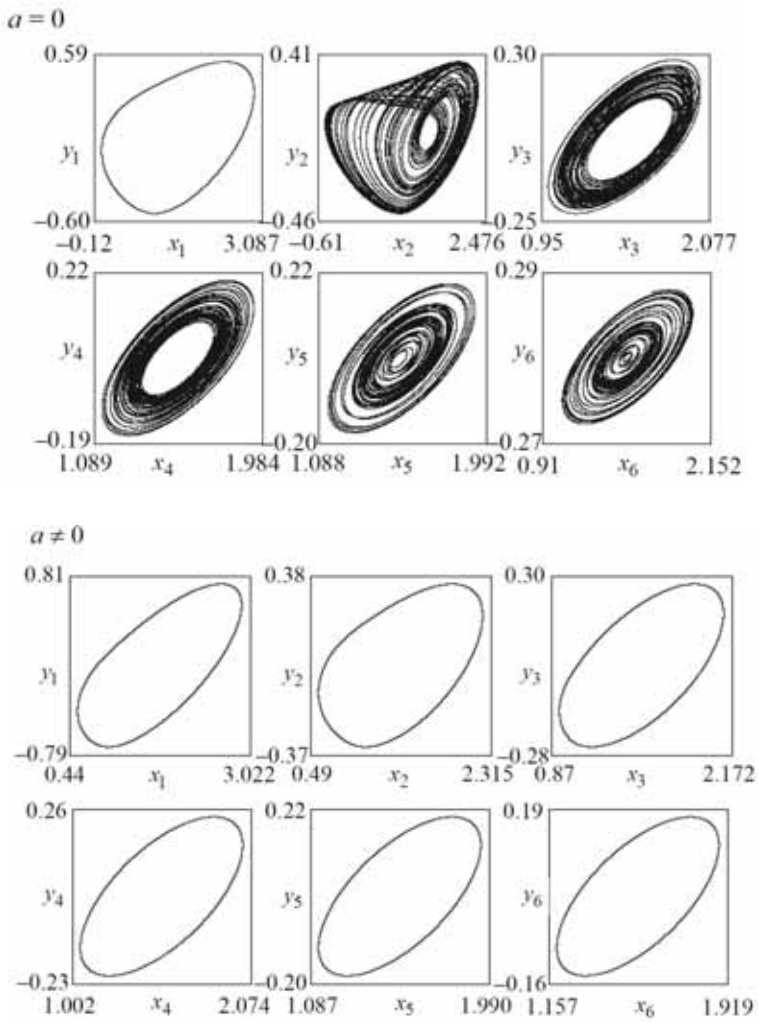

Fig. 3.17. Bifurcation diagrams for parameters

$$(\alpha, \beta, \gamma, m_0, m_1, \varepsilon, c, a, \omega) = (8.56, 14, 0.1, -1/7, 2/7, 0.2, 0.09, 0.25, 3.21),$$

$$\mathbf{C} = \mathrm{diag}(1,1,1).$$

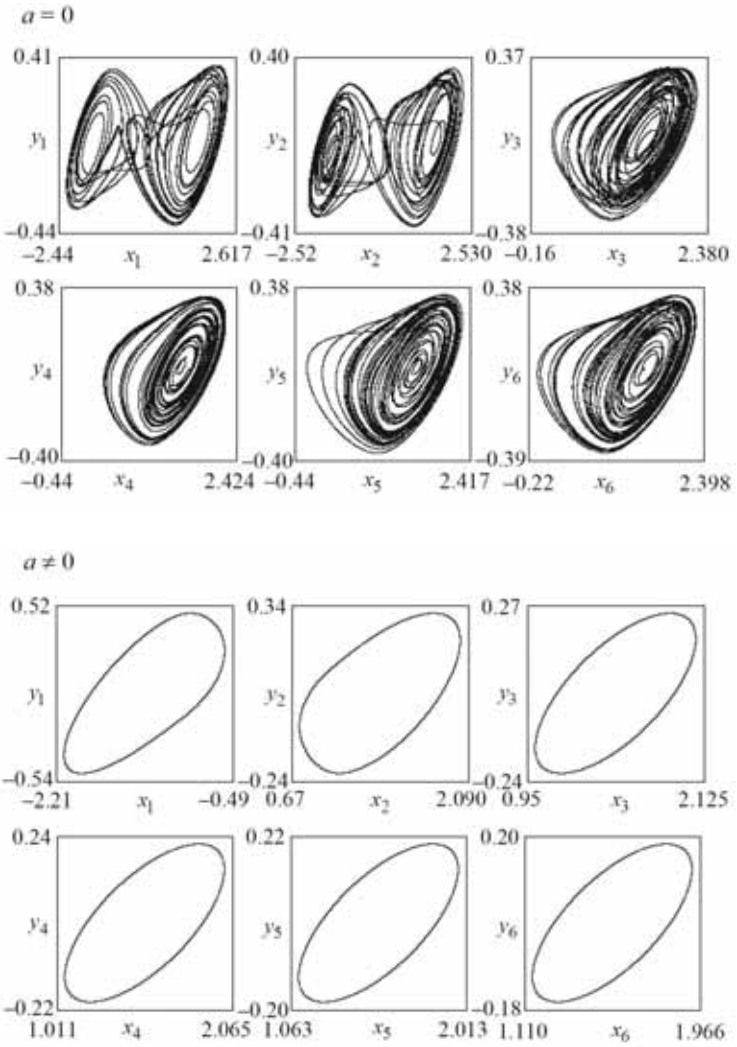

Fig. 3.18. Bifurcation diagrams for parameters

$$(\alpha, \beta, \gamma, m_0, m_1, \varepsilon, c, a, \omega) = (9.268, 14, 0.1, -1/7, 2/7, 0.2, 0.01, 0.2, 3.21),$$

$$\mathbf{C} = \mathrm{diag}(1,1,1).$$

$$\dot{x} = \alpha\left(y - h\left(x\right) + c + a\sin\omega\tau\right),$$
$$\dot{y} = -y + z - x,$$
$$\dot{z} = -\beta y - \gamma z.$$

Figs. 3.17 and 3.18 show the results of a numerical experiment with a chain for the various parameters, with constant and periodic excitations at the boundary. When perturbations change, there exists a wave of switching the state of the medium (the chain) from turbulent to laminar and vice versa.

Further, we will consider the properties of synchronization of oscillators, extending the theory outlined in Section 2.5 for a pair of oscillators to an inhomogeneous chain.

A chain of weakly non-identical oscillators. Consider a coupled system of the form

$$\begin{aligned}
&\dot{\mathbf{X}} = \mathbf{F}\left(\mathbf{X}\right),\\
&\dot{\mathbf{X}}_i = \mathbf{F}\left(\mathbf{X}_i\right) - \varepsilon\mathbf{C}\left(\mathbf{X}_i - \mathbf{X}_{i-1}\right) + \mu\mathbf{F}_i^*\left(\mathbf{X}_i\right),\\
&i = \overline{1, N},
\end{aligned} \tag{3.60}$$

with boundary condition $\mathbf{X}_0 \equiv \mathbf{X}$. Here μ is a certain small parameter that determines the small mistuning of parameters of the oscillators of the chain in relation to the respective parameters of the master oscillator. As before, we assume that each oscillator is a dissipative system, which is also the case for the coupled system (3.60),

i.e., all its phase trajectories are bounded by a sphere as well as the corresponding to them solutions.

We consider the conditions for the stability of a spatially-homogeneous state in the respective homogeneous chain to be fulfilled, and the synchronization regime of the oscillators to be realized. As in the case of two oscillators, we determine the relations of the variables of oscillators of the chain with the variables of the master oscillator in the form of power series by a small parameter:

$$\mathbf{X}_i = \mathbf{X} + \mu \mathbf{X}_{i1}(\mathbf{X}) + \mu^2 \mathbf{X}_{i2}(\mathbf{X}) + \ldots .$$

Performing the same procedures with the series as in the case of mutual synchronization, we obtain the equations defining functions $\mathbf{X}_{ij}$. In particular, for the function of the first approximation, we obtain equations of the form

$$\dot{\mathbf{X}}_{i1} - \frac{\partial \mathbf{F}}{\partial \mathbf{X}} \mathbf{X}_{i1} - \varepsilon \mathbf{C} \mathbf{X}_{i1} = \varepsilon \mathbf{C} \mathbf{X}_{i-1,1} + \mathbf{F}_i^*(\mathbf{X}) \tag{3.61}$$

with boundary condition $\mathbf{X}_{01} \equiv 0$.

Note that for $\varepsilon = 0$ and $\mathbf{F}_i^*(\mathbf{X}) = 0$, $\mathbf{X}_{i-1,1} = 0$ each of equations (3.61) coincides with the variational equation for the master oscillator. Moreover, the Jacobi matrix $\frac{\partial \mathbf{F}}{\partial \mathbf{X}}$ is considered with respect to the solution corresponding to the trajectory of its attractor $A_0(1)$.

And if $\lambda(1) > 0$ is the maximum Lyapunov exponent of solutions of this equation, then, by Theorem 2.1.1, for $\varepsilon > \varepsilon^*(\lambda(1))$ the trivial solution of the homogeneous equation corresponding to Eqs. (3.61) is stable. Due to the assumed dissipativity of system (3.60) and the aforementioned stability, the solution of each inhomogeneous equation of system (3.61) is bounded, which means that functional power series by a small parameter will converge.

The partial differential equation corresponding to equation (3.61) has the form

$$\frac{\partial \mathbf{X}_{i1}}{\partial \mathbf{X}}\mathbf{F} - \frac{\partial \mathbf{F}}{\partial \mathbf{X}}\mathbf{X}_{i1} + \varepsilon \mathbf{C}\mathbf{X}_{i1} = \varepsilon \mathbf{C}\mathbf{X}_{i-1,1} + \mathbf{F}_i^*(\mathbf{X}). \tag{3.62}$$

We recall that in order to pass from (3.61) to (3.62), the terms $\sim \mu$ are discarded. More precisely, they move to the next approximation by a small parameter.

For given vectors of disturbances $\mathbf{F}_i^*(\mathbf{X})$ functions $\mathbf{X}_{i1}$ are found by successive solution of equations (3.62).

Example 1. Consider the already familiar form of perturbations of vectors $\mathbf{F}_i^*(\mathbf{X}) = \alpha_i^* \mathbf{C}\mathbf{F},$ corresponding (according to Section 2.5) to phase synchronization. In this case, the change in the phase shift of the oscillations downstream is of our interest.

In this class of perturbations, the solution to system (3.62) has the form $\mathbf{X}_{i1} = \Delta_i \mathbf{F}(\mathbf{X})$, where constants Δ_i are a solution to a simple recurrent equation of the form

$$\Delta_i = \Delta_{i-1} + \varepsilon^{-1}\alpha_i^*$$

with initial condition $\Delta_0 = 0$. Parameter Δ_i has a sense of the phase difference between the *i*-th and the master oscillators.

Solving the recurrent equation, we obtain $\Delta_n = \frac{1}{\varepsilon}\sum_{i=1}^{n}\alpha_i^*$.

Similarly to Example 1 from Section 2.5 for a chain of Chua's oscillators that differs in parameter α, the relation of the variables of *n*-th oscillator with variables of the master oscillator is determined by the vector equation $\mathbf{X}(t) = \mathbf{X}_n(t + \varphi_n)$, where the difference between their phases φ_n expressed by formula $\varphi_n = \frac{1}{\varepsilon}\sum_{i=1}^{n}\left(\frac{\alpha_i - \alpha}{\alpha}\right)$.

A chain of strongly non-identical strongly coupled oscillators. As in the case of two oscillators, we define different groups of oscillator equations with different degrees of non-identity. Let us assume that the right-hand sides of *k* equations of each of the oscillators of the chain are "strongly" different and contain a strong coupling, while parameters of $m - k$ equations have a "weak" non-identity and contain a "moderate" coupling, or no coupling at all. Combining the

respective equations into groups, we consider a coupled system of the form

$$\begin{aligned}
&\dot{\mathbf{X}} = \mathbf{F}\left(\mathbf{X}, \mathbf{Y}\right), \\
&\dot{\mathbf{Y}} = \mathbf{\Phi}\left(\mathbf{X}, \mathbf{Y}\right), \\
&\dot{\mathbf{X}}_i = \mathbf{F}_i\left(\mathbf{X}_i, \mathbf{Y}_i\right) - \varepsilon\mathbf{C}\left(\mathbf{X}_i - \mathbf{X}_{i-1}\right), \\
&\dot{\mathbf{Y}}_i = \mathbf{\Phi}\left(\mathbf{X}_i, \mathbf{Y}_i\right) - \mathbf{D}\left(\mathbf{Y}_i - \mathbf{Y}_{i-1}\right) + \mu\mathbf{\Phi}_i^*\left(\mathbf{X}_i, \mathbf{Y}_i\right).
\end{aligned} \tag{3.63}$$

Here $\mathbf{X}_{1,2} \in R^k$, $\mathbf{Y}_{1,2} \in R^{m-k}$, $\mathbf{C} = \operatorname{diag}\left(c_1, c_2, ..., c_k\right)$, $\mathbf{D} = \operatorname{diag}\left(d_1, d_2, ..., d_{m-k}\right)$, $c_i > 0$, $d_j \geq 0$, $\varepsilon^{-1} = \mu$ is a small parameter.

As in the case of a pair of oscillators, we search for a representation of the manifold M_μ in the form of power series by a small parameter of the form

$$\begin{aligned}
&\mathbf{X}_i = \mathbf{X} + \mu\mathbf{X}_{i1}\left(\mathbf{X}, \mathbf{Y}\right) + \mu^2\mathbf{X}_{i2}\left(\mathbf{X}, \mathbf{Y}\right) + ..., \\
&\mathbf{Y}_i = \mathbf{Y} + \mu\mathbf{Y}_{i1}\left(\mathbf{X}, \mathbf{Y}\right) + \mu^2\mathbf{Y}_{i2}\left(\mathbf{X}, \mathbf{Y}\right) + ...
\end{aligned}$$

Performing the procedure with power series, we obtain equations for the functions of the first approximation

$$\begin{aligned}
&\mu\dot{\mathbf{X}}_{i1} = \mathbf{F}_i - \mathbf{F} - \mathbf{C}\mathbf{X}_{i1} + \mathbf{C}\mathbf{X}_{i-1,1} + \mu\left(\frac{\partial\mathbf{F}_i}{\partial\mathbf{X}}\mathbf{X}_{i1} + \frac{\partial\mathbf{F}_i}{\partial\mathbf{Y}}\mathbf{Y}_{i1}\right), \\
&\dot{\mathbf{Y}}_{i1} - \frac{\partial\mathbf{\Phi}}{\partial\mathbf{Y}}\mathbf{Y}_{i1} + \mathbf{D}\,\mathbf{Y}_{i1} = \frac{\partial\mathbf{\Phi}}{\partial\mathbf{X}}\mathbf{X}_{i1} + \mathbf{\Phi}_i^* + \mathbf{D}\,\mathbf{Y}_{i-1,1}
\end{aligned} \tag{3.64}$$

with boundary conditions $\mathbf{X}_{01} = 0, \ \mathbf{Y}_{01} = 0.$

We remind that, by condition, all solutions of a dynamic system representing a chain, regardless of parameters of the oscillators and the coupling parameter, are bounded. This means that all partial derivatives in system (3.64) are bounded. System (3.64) is a system with singular perturbations.

In another words, it is a system with "fast" and "slow" motions. The first equation determines the fast motion of the system to a certain surface (more precisely, a hypersurface) in the phase space of Eqs. (3.64), while the second equation determines the "slow" motion of the affix on this surface. Since matrix **C** is nondegenerate by hypothesis, then, according to [17], the surface of slow motions is stable. The equation of the "zero" approximation for this surface is found from the first equation in (3.64) by setting $\mu = 0$:

$$\mathbf{X}_{i1} = \mathbf{X}_{i-1,1} + \mathbf{C}^{-1}\left(\mathbf{F}_i - \mathbf{F}\right), \ \mathbf{F}_0\left(\mathbf{X}, \mathbf{Y}\right) = \mathbf{F}\left(\mathbf{X}, \mathbf{Y}\right), \ \mathbf{X}_{0,1} = 0. \quad (3.65)$$

This approximation is the main one for us. All functions $\mathbf{X}_{i1}$ are found by solving the simple recurrent equation (3.65), so this problem will be considered solved. In this case, the remaining problem to find function $\mathbf{Y}_{i1}$.

Let us justify the boundedness of the solutions of the second equation (3.64).

Since $\mathbf{Y}_{01} = 0,$ then (3.64) can be considered as a sequence of non-autonomous equations: for each number *i*, the right side of the respective equation can be interpreted as an external perturbation. On the other hand, the respective homogeneous equation for $\mathbf{D} = 0$ accurate within notations, is part of the system in variations for the master oscillator. If this equation is stable, then the complete equation (non-autonomous) has a bounded solution for any matrix **D** (by hypothesis, it is non-negative). If the above equation in variations is unstable, then the Lyapunov exponent of its solutions at least does not exceed the Lyapunov exponent of the chaotic attractor of the master oscillator. As it is known, in this case there is always a positive matrix **D**, "shifting" the exponents of solutions of the corresponding homogeneous equation (3.65) into the left half-plane. In other words, the case of a stable homogeneous equation is always realized, which means that all solutions of inhomogeneous equations of sequence (3.64) are bounded. This condition is necessary for the convergence of power series, representing the relation of variables of oscillators in the regime of synchronization.

For known $\mathbf{X}_{i1}$, functions $\mathbf{Y}_{i1}$ are found by solving the "flow" chain of partial differential equations of the form

$$\frac{\partial \mathbf{Y}_{i1}}{\partial \mathbf{X}}\mathbf{F} + \frac{\partial \mathbf{Y}_{i1}}{\partial \mathbf{Y}}\mathbf{\Phi} - \frac{\partial \mathbf{\Phi}}{\partial \mathbf{Y}}\mathbf{Y}_{i1} + \mathbf{D}\mathbf{Y}_{i1} = \frac{\partial \mathbf{\Phi}}{\partial \mathbf{X}}\mathbf{X}_{i1} + \mathbf{\Phi}_i^* + \mathbf{D}\,\mathbf{Y}_{i-1,1} \tag{3.66}$$

with boundary condition $\mathbf{Y}_{01} = 0.$

Example 2. Consider a Chua's oscillator stream chain with strongly different parameters α_i, while other parameters are identical. In this case, the sought vectors and matrices have the form: $\mathbf{X} = x$, $\mathbf{Y} = \left(y,\ z\right)^T$, $F\left(x, y\right) = \alpha\left(y - h\left(x\right)\right)$, $\mathbf{\Phi}\left(x, y, z\right) =$ $= \left(-y + z - x,\ -\beta y - \gamma z\right)^T$, $F_i\left(x, y\right) = \alpha_i\left(y - h\left(x\right)\right)$, $\mathbf{\Phi}_i^* = 0$, $\mathbf{D} = 0$, $\mathbf{C} = 1$ (scalar). It is easy to see that $F_i\left(x, y\right) = \left(\alpha_i/\alpha\right)F\left(x, y\right) = \left(\alpha_i/\alpha\right)\dot{x}$. Solving the recurrent equation (3.65), we obtain $\mathbf{X}_{n1} = \Delta_n \dot{x}$, where $\Delta_n = \sum_{i=1}^{n}\left(\alpha_i - \alpha\right)/\alpha$. Moreover, it is easy to prove that $\mathbf{Y}_{n1} = \Delta_n \dot{\mathbf{Y}}$ is a solution of equation (3.66). It means that $x_n\left(t\right) = x\left(t + \varphi_n\right)$, $\mathbf{Y}_n\left(t\right) = \mathbf{Y}\left(t + \varphi_n\right)$, that is, in this case, again, we are dealing with the phase chaotic synchronization of oscillators. The phase incursion between the oscillations of the master and arbitrary oscillators of the chain is $\varphi_n = \varepsilon^{-1}\Delta_n$ (see Fig. 3.19).

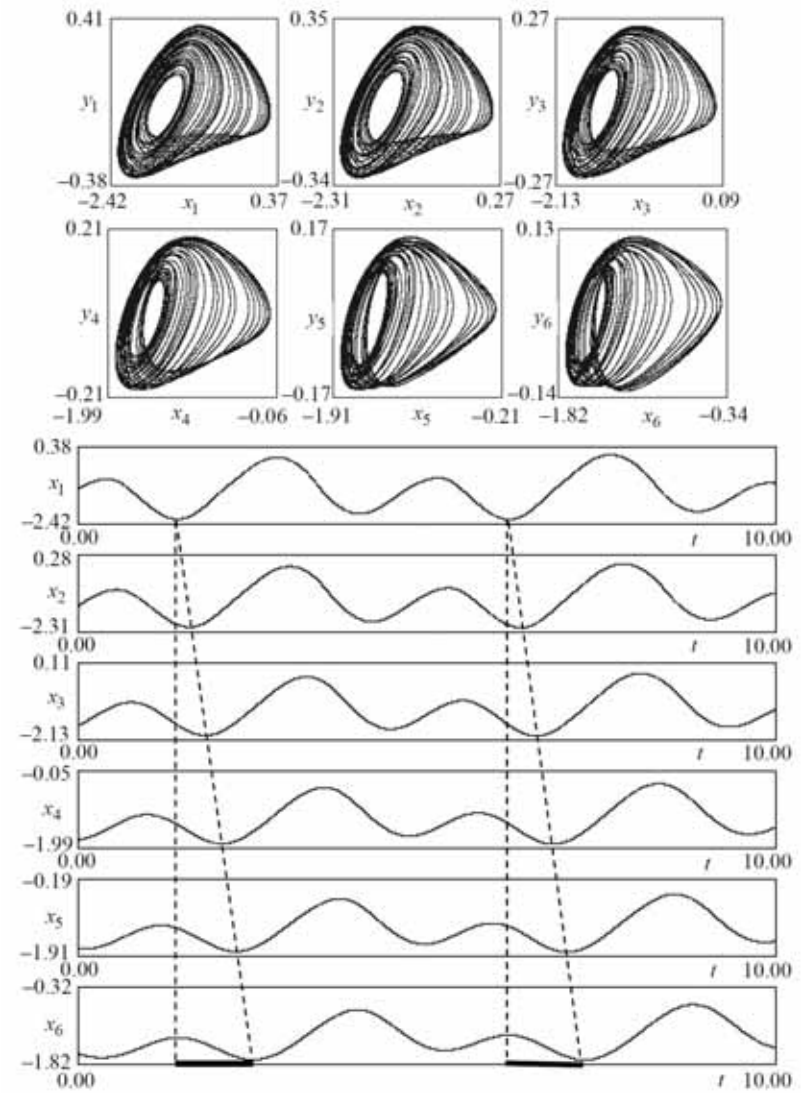

Fig. 3.19. Bifurcation diagrams for parameters $\{\beta, \gamma, m_2, m_1, \varepsilon\} =$

$= \{14, 0.1, -1/7,\ 2/7, 3\}$, $\{\alpha_i, i = \overline{1-6}\} = \{9.1,\ 4.0, 1.34, 1.0,\ 2.44,\ 0.4\}$.

CHAPTER 4

EXISTENCE, FUSION AND STABILITY OF CLUSTER STRUCTURES IN LATTICES OF OSCILLATORS

We come across pictures of cluster structures quite often, including in our everyday life. Such examples are, for instance, are multi-colored or patterned parquets and borders, when one somehow colored “piece” of the object's surface is connected to its own copy and this is repeated over and over. As a result of a certain number of iterations, the entire surface of the object acquires a periodic coloring. An attentive observer would find many examples of structured objects in the surrounding world. Similar patterns, however, already dynamic ones arise, in particular, in hydrodynamic flows, when secondary flows appear against the background of the main flow, forming a complex ordered structure. Similar phenomena of interest arise in the lattices of active oscillators (self-oscillators), when individual oscillators are combined into groups, and then these groups, as new subjects, organize a new dynamic order. At the same time, the synchronization of motions of the subjects is the cause and basis of the emerging “cluster” dynamic pictures.

This chapter is devoted to various aspects of the structural dynamics (cluster dynamics) of lattices of various geometric dimensions and shapes. We will try to answer the following questions: how are group oscillators (cluster oscillators) formed and what cluster structures do they generate in a given lattice? What types of structures can exist depending on the geometric dimension and shape of the lattices? What are their properties and their number depending on the size of the lattice? Are these structures stable? And many other questions like that.

4.1. Physics of cluster structures

Consider already known to us chain of the oscillators whose equations, for reasons of convenience, we rewrite as follows:

$$\begin{aligned} &\dot{\mathbf{X}}_i = \mathbf{F}\left(\mathbf{X}_i,\, t\right) + \varepsilon\mathbf{C}\left(\mathbf{X}_{i-1} - 2\mathbf{X}_i + \mathbf{X}_{i+1}\right), \\ &i = \overline{1, N},\ \ \mathbf{X}_0 \equiv \mathbf{X}_1,\ \ \mathbf{X}_N \equiv \mathbf{X}_{N+1}. \end{aligned} \tag{4.1}$$

As stated before, system (4.1) has integral manifold $M_0 = \left\{\mathbf{X}_i = \mathbf{X}_{i+1},\ \ i = \overline{1, N}\right\}$. Its existence is obvious, and it has played a role in the study of the synchronization of oscillators (rotators), which generated a spatially uniform state of the lattice. It is less obvious that in equations (4.1), apart from M_0, there are other so-called “cluster” invariant manifolds [94 – 101]. In particular, if $N = 6,$ then there are two such manifolds

$$M_{6,3=}\left\{=\mathbf{X}_{6=}=\mathbf{X}_1,=\mathbf{X}_{5=}=\mathbf{X}_2,=\mathbf{X}_{4=}=\mathbf{X}_3\right\}$$

and $M_{6,2}=\left\{\mathbf{X}_1=\mathbf{X}_4=\mathbf{X}_5,\ \ \mathbf{X}_2=\mathbf{X}_3=\mathbf{X}_6\right\}.$

This means that by controlling the initial conditions (if such control is possible), the dynamical regimes of the oscillators corresponding to these manifolds can be realized in the lattice. These regimes are shown symbolically in Fig. 4.1.

a b

Fig. 4.1. Cluster structures in a chain of $N=6$ oscillators.

[oscillators of the chain. Note that due to the homogeneity of the lattice, their dynamics is identical by all parameters. The order of numbers of the synchronized oscillators is determined by the presented manifolds. The nature of the dynamical regimes of individual oscillators is not yet important for us. Thus, we have two "borders": two cluster dynamic structures. In what follows, such images will be referred to as schemes of cluster structures.

The dynamics of lattices on manifolds was studied in papers [94 – 101] and called "cluster synchronization". Below we will formulate the cluster dynamics of lattices using the common language of classical synchronization [190 – 192], without appealing to their cluster

manifolds, and the latter will be obtained, if necessary, as consequences.

Subjects of cluster structures. To define group oscillators (hereinafter we will say “cluster oscillators”), we will forget for a while the formalism of integral manifolds and use elementary knowledge about the synchronization of self-oscillators as well as the information about equivalent transformations of electrical circuits.

Equivalent transformations of electrical circuits. We remind that transformations of electrical circuits are called equivalent if they do not change the currents and potentials of all points outside of the converted part of the circuit. In what follows, we will need only three mental operations: connecting the equipotential points of cluster circuits into a node (short circuits), cutting equipotential points (removing the connection between them) and, as the opposite one, connecting the “pieces” of circuits at equipotential points. Note that in other areas of physics, biology and other sciences there are always analogs of currents and potentials.

In the inductive order, we start with a pair of interacting oscillators, whose equations have the form

$$\begin{aligned}\dot{\mathbf{X}}_1 &= \mathbf{F}\left(\mathbf{X}_1\right) + \varepsilon\mathbf{C}\left(\mathbf{X}_2 - \mathbf{X}_1\right),\\ \dot{\mathbf{X}}_2 &= \mathbf{F}\left(\mathbf{X}_2\right) + \varepsilon\mathbf{C}\left(\mathbf{X}_1 - \mathbf{X}_2\right),\end{aligned} \tag{4.2}$$

where **C** is a matrix that determines the structure of coupling of the elementary oscillators, and, ε is a scalar parameter.

It is clear that in the usual case all stationary dynamic modes of this system can be divided into two types:

a) a regime of isochronous regular or chaotic mutual synchronization. This regime corresponds to the solution $\mathbf{X}_1(t) = \mathbf{X}_2(t) = \mathbf{X}(t)$. The form of the synchronous movements of the oscillators is determined by the parameters and type of the attractor (regular, chaotic) of a single oscillator $A(1)$. Important: in this case, coupled system (4.2) decomposes into a pair of synchronized oscillators;

b) a regime of non-isochronous dynamics that corresponds to attractor $A_s(2)$. This regime can represent either stationary beatings (regular or chaotic), or non-isochronous synchronization. In case when the affix moves over attractor $A_s(2)$ $\mathbf{X}_1(t) \neq \mathbf{X}_2(t)$. We note that, in this case, system (4.2) is a single object that is indivisible in this sense.

To illustrate what has been said, Fig. 4.2 shows the regime of chaotic synchronization and the regime of beatings of chaotic Chua self-oscillators [89, 90]. A single Chua's oscillator is described by a dynamical system of the form

$$\dot{x} = \alpha\left(y - h\left(x\right)\right),$$
$$\dot{y} = -y + z - x,$$
$$\dot{z} = -\beta y - \gamma z,$$

where $h\left(x\right) = m_1 x + \frac{m_0 - m_1}{2}\left(\left|x+1\right| - \left|x-1\right|\right)$, $m_0 < 0$; α, β, γ, $m_1 > 0$ are the parameters. Parameters of the experiment: $\left(\alpha, \beta, \gamma, m_0, m_1, \varepsilon\right) = \left(9.5, 14, 0.1, -1/7, 2/7, 1.0\right)$, the matrix of couplings of oscillators: $\mathbf{C} = \mathrm{diag}\left(1, 0, 0\right)$.

Figure shows in the first case, the phase portraits are completely identical, and this is additionally confirmed by the diagonal in the phase plane of the same-titled variables (the third one in the upper row). This is the projection of attractor $A\left(1\right)$ of the system onto the given plane. In the second case, the projection of $A_s\left(2\right)$ is different from the diagonal.

Schematically, the dynamics of system (4.2) in the indicated regimes are shown in Fig, 4.3.

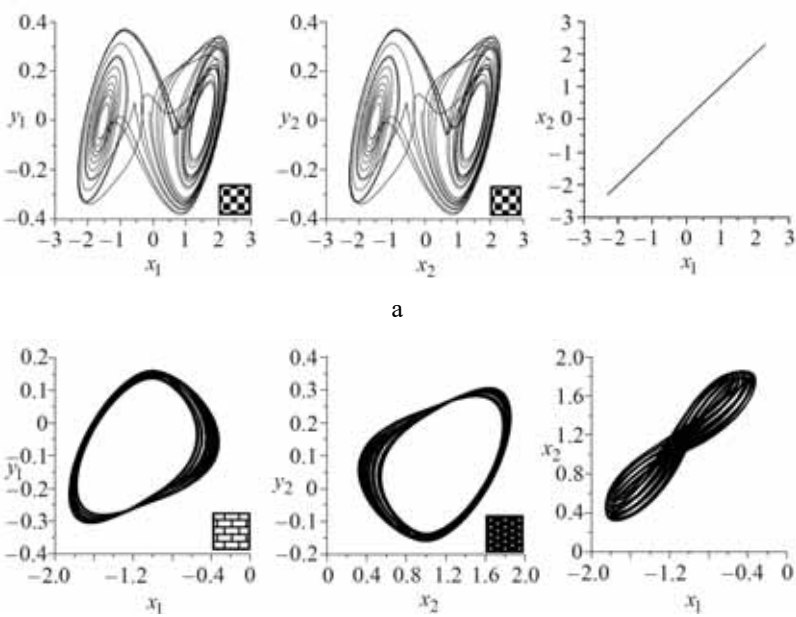

Fig. 4.2. Dynamical regimes of system (4.2): (a) attractor $A\,(1)$ of the regime of isochronous synchronization; (b) attractor $A_s\,(2)$, which corresponds to the regime of chaotic beatings in projections onto the coordinate planes of the oscillators.

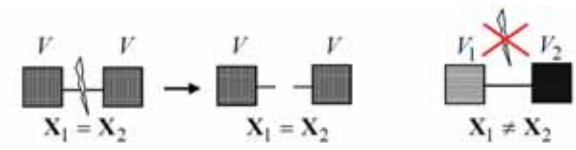

Fig. 4.3. Stationary dynamical regimes *a* and *b* of the coupled system. A symbolic knife is shown above the coupling of the oscillators.

As was previously said, in the regime of synchronization, system (4.2) decomposes into a pair of synchronized oscillators (by the condition of exact synchronism). Physically, this fact corresponds to the removal of the coupling between the corresponding oscillators without violating their dynamic regime. In particular, if the oscillators physically represent radio-frequency self-generators, then this procedure corresponds to cutting the connections between equipotential points, which represents one of the methods of equivalent transformations of electric circuits. We note that a spatially homogeneous structure is cut into individual oscillators, while the cluster structure (see Fig. 4.1) is cut into identical blocks. In the future, such a procedure of cutting the schemes of cluster structures (couplings between "same-colored" oscillators) will be used as a method for their equivalent transformations, as well as, on the contrary, connection of oscillator blocks through the corresponding points (connection of "same-colored" oscillators) during the fusion of cluster structures.

Let us turn again to system (4.2). Suppose there is attractor $A_s(2)$ in this system and its motions take place along this attractor. In this case, the system represents an indivisible object, i.e. a generalized oscillator, the dynamics of which are described by a vector equation of the form (system (4.2) rewritten in vector form)

$$\dot{\mathbf{X}} = \mathbf{H}(\mathbf{X}), \tag{4.3}$$

where $\mathbf{X} = (\mathbf{X}_1, \mathbf{X}_2)^T$, $\mathbf{H}(\mathbf{X}) = (\mathbf{F}(\mathbf{X}_1), \mathbf{F}(\mathbf{X}_2))^T + \varepsilon \mathbf{B}_s \otimes \mathbf{C}\mathbf{X}$, $\mathbf{B}_s = \begin{pmatrix} -1 & 1 \\ 1 & -1 \end{pmatrix}$.

We will call (4.3) the *cluster forming oscillator* (or C-oscillator) and denote it as $O_s(2)$. Index s reflects the symmetry of cluster matrix $\mathbf{B}_s$, and 2 is the number of elementary oscillators in the C-oscillator that produces clusters (the exact definition of the C-oscillator will be given below). Schematically, the C-oscillator in the stationary "operational" mode is shown in Fig. 4.3b. Note that the vector coordinates $\mathbf{X}_1$, $\mathbf{X}_2$ play the same role as scalar coordinates of the elementary oscillator.

Suppose now that we have an exact dynamic copy of a given C-oscillator, which is described by a vector variable $\mathbf{Y} = (\mathbf{Y}_1, \mathbf{Y}_2)^T$ (dynamic processes in the originals and in the copies happen synchronously). The answer to the question of how these two C-oscillators should be connected in an order not violating their dynamic regimes is contained in the previous reasoning regarding the cutting/connecting of equipotential points that correspond to the same coordinates. In other words, the couplings of a C-oscillator in the synthesized lattice should have the form $(\mathbf{C}^* \otimes \mathbf{C})(\mathbf{X} - \mathbf{Y})$ or $(\mathbf{C}_* \otimes \mathbf{C})(\mathbf{X} - \mathbf{Y})$, where $\mathbf{C}$ is an already known matrix that deter-

mines the number of coupled scalar variables of elementary oscillators, $\mathbf{C}^* = \mathrm{diag}(1, 0)$, $\mathbf{C}_* = \mathrm{diag}(0, 1)$ are the matrices that determine the number of coupled oscillators themselves that belong to one and to another C-oscillator (matrices of fusion). The first matrix determines a coupling along the first coordinates $(\mathbf{X}_1, \mathbf{Y}_1)$, while the second one determines a coupling along the second coordinates $(\mathbf{X}_2, \mathbf{Y}_2)$.

Taking the aforesaid matters into account, we consider a system of two coupled C-oscillators of the form

$$\begin{aligned} \dot{\mathbf{X}} &= \mathbf{H}(\mathbf{X}) + \varepsilon(\mathbf{C}_* \otimes \mathbf{C})(\mathbf{Y} - \mathbf{X}), \\ \dot{\mathbf{Y}} &= \mathbf{H}(\mathbf{Y}) + \varepsilon(\mathbf{C}_* \otimes \mathbf{C})(\mathbf{X} - \mathbf{Y}). \end{aligned} \tag{4.4}$$

First, we note that Eqs. (4.2) and (4.4) do not differ in form. Second, if system (4.4) is written coordinate-wise (with respect to elementary oscillators), assuming in this case that $\mathbf{Y}_1 = \mathbf{X}_4$, $\mathbf{Y}_2 = \mathbf{X}_3$, then it represents a chain of 4 elements. Third, this system, in the case of classical synchronization of C-oscillator that is expressed by equality $\mathbf{X} = \mathbf{Y}$, defines the cluster structure shown in Fig. 4.1b ($(\mathbf{X}_1, \mathbf{X}_2)^T = (\mathbf{Y}_1, \mathbf{Y}_2)^T$ or $\mathbf{X}_1 = \mathbf{X}_4$, $\mathbf{X}_2 = \mathbf{X}_3$), for which the oscillators with numbers 5 and 6 are removed. For a complete picture, one should couple an extra C-oscillator to system (4.4).

Suppose that we have one more dynamical copy of C-oscillator $O_s(2)$, described by vector $\mathbf{Z} = (Z_1, Z_2)^T$. By coupling this C-oscillator with the second C-oscillator in system (4.4), we obtain a system of the form

$$\begin{aligned}
\dot{\mathbf{X}} &= \mathbf{H}(\mathbf{X}) + \varepsilon(\mathbf{C}_* \otimes \mathbf{C})(\mathbf{Y} - \mathbf{X}),\\
\dot{\mathbf{Y}} &= \mathbf{H}(\mathbf{Y}) + \varepsilon(\mathbf{C}_* \otimes \mathbf{C})(\mathbf{X} - \mathbf{Y}) + \varepsilon(\mathbf{C}^* \otimes \mathbf{C})(\mathbf{Z} - \mathbf{Y}),\\
\dot{\mathbf{Z}} &= \mathbf{H}(\mathbf{Z}) + \varepsilon(\mathbf{C}^* \otimes \mathbf{C})(\mathbf{Y} - \mathbf{Z}).
\end{aligned} \tag{4.5}$$

The same can be repeated for (4.5) as has been done for (4.4). Then, supposing that $Z_1 = \mathbf{X}_5$, $Z_2 = \mathbf{X}_6$, we can see that this system represents a reformatted chain of 6 elements. Secondly, the classical synchronization of this triple C-oscillator generates the cluster structure depicted in Fig. 4.1b.

Consider one more example. Assume we have a C-oscillator of the type $O_s(3)$, composed of three elementary oscillators: $\mathbf{X} = (\mathbf{X}_1, \mathbf{X}_2, \mathbf{X}_3)^T$, as well as its copy with vector $\mathbf{Y} = (\mathbf{Y}_1, \mathbf{Y}_2, \mathbf{Y}_3)^T$. Equations for $O_s(3)$ have the same form as (4.3) with $\mathbf{B}_s = \begin{pmatrix} -1 & 1 & 0 \\ 1 & -2 & 1 \\ 0 & 1 & -1 \end{pmatrix}$.

A synthesized pair of such C-oscillators will have equations of the same form as (4.4), where the fusion matrix is replaced by $\mathbf{C}_* = \mathrm{diag}(0, 0, 1)$.

In the regime of synchronization of these C-oscillators, we obtain $(\mathbf{X}_1, \mathbf{X}_2, \mathbf{X}_3)^T = (\mathbf{Y}_1, \mathbf{Y}_2, \mathbf{Y}_3)^T$. Under the condition that $\mathbf{Y}_3 = \mathbf{X}_4$, $\mathbf{Y}_2 = \mathbf{X}_5$, $\mathbf{Y}_1 = \mathbf{X}_6$, we obtain equations $\mathbf{X}_1 = \mathbf{X}_6$, $\mathbf{X}_2 = \mathbf{X}_5$, $\mathbf{X}_3 = \mathbf{X}_4$, i.e. we obtain the cluster structure shown in Fig. 4.1a.

To illustrate the aforesaid scenario, Fig. 4.4 shows cluster attractor $A_s(3)$ of C-oscillator $O_s(3)$, obtained in a numerical experiment with a homogeneous chain of three Chua's oscillators for the following parameter set:

$$(\alpha, \beta, \gamma, m_0, m_1, \varepsilon) = (9.5, 14, 0.1, -1/7, 2/7, 0.37).$$

Fig. 4.5 shows a cluster structure in a chain of six Chua's oscillators as a result of classical synchronization of two C-oscillators $O_s(3)$.

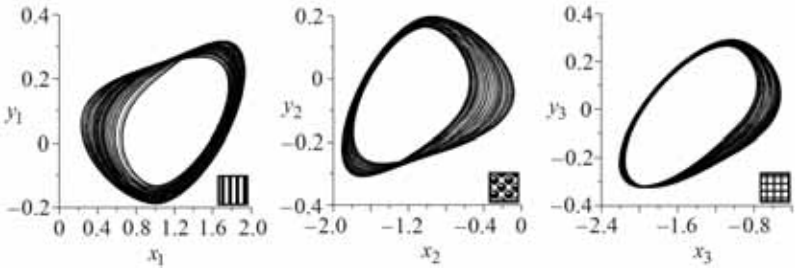

Fig. 4.4. Projections of cluster attractor $A_s(3)$ of C-oscillator $O_s(3)$ onto the coordinate planes.

As an intermediate conclusion, we state that in a chain of N elements, the number of cluster structures that can be synthesized, based on the $O_s(n)$ type of C-oscillators, is equal to the number of dividers of number N and, in each specific case, all of these structures are representable.

These types of C-oscillators do not exhaust the types of cluster structures in the chains. In particular, if number N is simple, then we can confidently say that the cluster structure in such a chain will belong to another type. Further we shall consider structures in chains with an odd number of oscillators $N = 2k + 1$.

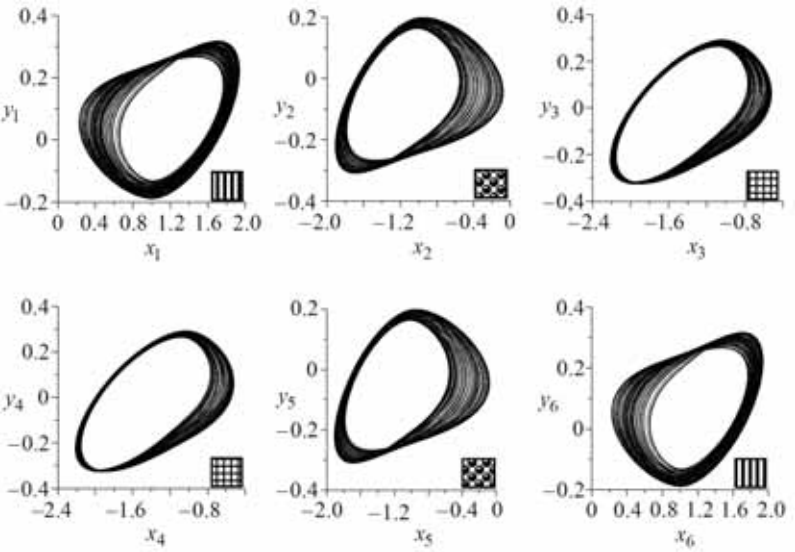

Fig. 4.5. Cluster structure in a homogeneous chain of $N = 6$ Chua's oscillators as a synchronization of two C-oscillators $O_s(3)$.

Let us consider the simplest case of a cluster structure in a chain of three elementary oscillators (see Fig. 4.6). As one can see from Fig. 4.6a, the structure is axisymmetric, as well as that in this case, the base C-oscillator, which determines this structure, is not clearly defined: like in the previous cases, the structure cannot be cut into blocks.

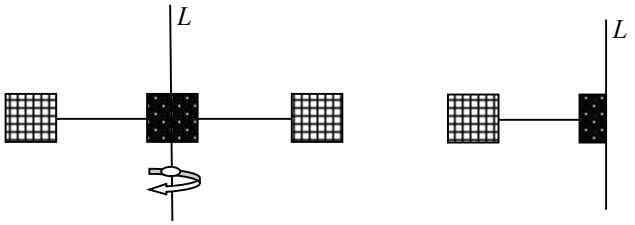

a b

Fig. 4.6. Schematic representation of a cluster structure of a simple cell (a) and C-oscillator $O_a(2)$ (b).

Let us imagine that this figure is printed on a sheet of paper and this paper is folded along line *L*. By rolling the sheet, we obtain the schematic representation shown in Fig. 4.6b. One can see that this figure can pretend to depict a C-oscillator under the condition that obtained "half-picture" of a central elementary oscillator would have a physical sense. To find out this physical sense, let us turn to the example of Froude pendula shown in Fig. 4.7, considering the process of rolling the figure in the opposite direction: from C-oscillator to the structure.

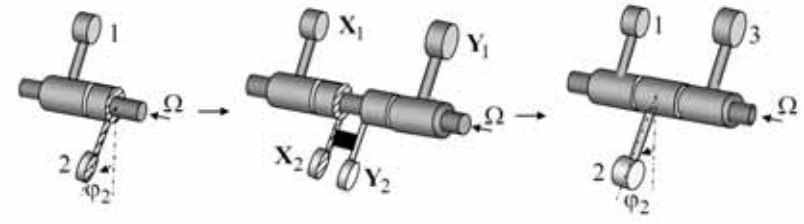

a b c

Fig. 4.7. Physical interpretation of C-oscillator $O_a(2)$ and simple cell based on this cluster forming oscillator.

Let us assume that there are two adjoining pendula that are placed on a rotating shaft. The second pendulum represents a "half" of the first "whole" pendulum (see Fig. 4.7a). One can imagine that such a "half-pendulum" is obtained as a result of "sawing" the "whole" pendulum in a plane perpendicular to the sleeve and passing through it in the middle. Suppose that there is viscous friction between the sleeves and the shaft. The same friction also exists between the sleeves of pendula. The equations of motion of the system have the form

$$ml^2\ddot{\varphi}_1 + d\dot{\varphi}_1 + mgl\sin\varphi_1 = R\left(\Omega - \dot{\varphi}_1\right) + \lambda\left(\dot{\varphi}_2 - \dot{\varphi}_1\right),$$
$$\frac{m}{2}l^2\ddot{\varphi}_2 + \frac{d}{2}\dot{\varphi}_2 + \frac{m}{2}gl\sin\varphi_2 = \frac{R}{2}\left(\Omega - \dot{\varphi}_2\right) + \lambda\left(\dot{\varphi}_1 - \dot{\varphi}_2\right).$$

Here $R\left(\Omega - \dot{\varphi}_1\right)$ is the moment of force of viscous friction acting on the first pendulum and, $\frac{R}{2}\left(\Omega - \dot{\varphi}_2\right)$ is the moment of force of viscous friction acting on the second pendulum (they are proportional to the contact area between the sleeve of the pendulum and the shaft); $\lambda\left(\dot{\varphi}_2 - \dot{\varphi}_1\right)$ and $\lambda\left(\dot{\varphi}_1 - \dot{\varphi}_2\right)$ are the mutual moments of the friction forces of the pendula; and d is the coefficient of the viscous friction of the medium. After the introduction of dimensionless time $\frac{mgl}{d+R}t = \tau$, we obtain the dynamical system for C-oscillator $O_a\left(2\right)$

$$\begin{aligned}\dot{\mathbf{X}}_1 &= \mathbf{F}(\mathbf{X}_1) + \varepsilon C(-\mathbf{X}_1 + \mathbf{X}_2),\\ \dot{\mathbf{X}}_2 &= \mathbf{F}(\mathbf{X}_2) + 2\varepsilon C(\mathbf{X}_1 - \mathbf{X}_2),\end{aligned} \tag{4.6}$$

where

$$\mathbf{X}_1 = (\varphi_1,\ \xi_1)^T,\ \ \mathbf{X}_2 = (\varphi_2,\ \xi_2)^T,$$

$$\mathbf{F}(\mathbf{X}_1) = \left(\gamma + I^{-1}\xi_1,\ -\xi_1 - \sin\varphi_1\right)^T,$$

$$\mathbf{F}(\mathbf{X}_2) = \left(\gamma + I^{-1}\xi_2,\ -\xi_2 - \sin\varphi_2\right)^T,\ \ \mathbf{C} = \mathrm{diag}(0,1),$$

$$I = \frac{l}{g}\left(\frac{mgl}{d+R}\right)^2,\ \ \gamma = \frac{R\Omega}{mgl},\ \ \varepsilon = \frac{\lambda I}{d+R}.$$

One can see that, in contrast to C-oscillator $O_s(2)$ (4.2), in which elementary oscillators are coupled by matrix $\mathbf{B}_s = \begin{pmatrix} -1 & 1 \\ 1 & -1 \end{pmatrix}$, and in the case of C-oscillator $O_a(2)$ (4.6), the matrix of couplings is an asymmetric matrix $\mathbf{B}_a = \begin{pmatrix} -1 & 1 \\ 2 & -2 \end{pmatrix}$. Naturally, the difference in the structure of the couplings fundamentally affects the conditions of existence and the character of cluster attractors of these C-oscillators. However, the main difference between $O_s(2)$ and $O_a(2)$ consists of the fact that if the first one is a full-fledged subject of cluster structures, then the role of the second in this sense is limited. Figs. 4.7b,c show the process of combining the original

$O_a(2)$ with its mirrored copy and the subsequent formation of a clustered and indivisible object of a new type, which we will hereinafter call the *simple cell*. The process of formation of the cluster structure of a simple cell can also be interpreted as follows: after establishing a rigid coupling between the half-oscillators (note the jumper in Fig. 4.7b), their synchronization occurs immediately (and, in fact, they become a "whole" oscillator). The side oscillators that indirectly interact with each other (through the central oscillator) synchronize their movements.

Let us repeat the aforesaid scenario using the language of equations. We rewrite system (4.6) in the form of one equation:

$$\dot{\mathbf{X}} = \mathbf{H}(\mathbf{X}), \tag{4.7}$$

where $\mathbf{X} = (\mathbf{X}_1, \mathbf{X}_2)^T$, $\mathbf{H}(\mathbf{X}) = (\mathbf{F}(\mathbf{X}_1), \mathbf{F}(\mathbf{X}_2))^T + \varepsilon \mathbf{B}_a \otimes \mathbf{C}\mathbf{X}$,

$\mathbf{B}_a = \begin{pmatrix} -1 & 1 \\ 2 & -2 \end{pmatrix}$.

Let us suppose that we have an exact copy of this C-oscillator described by vector $\mathbf{Y} = (\mathbf{Y}_1, \mathbf{Y}_2)^T$. Consider a system of a pair of C-oscillators of the form

$$\begin{aligned} \dot{\mathbf{X}} &= \mathbf{G}(\mathbf{X}) + \varepsilon \mathbf{D} \otimes \mathbf{C}(-\mathbf{X} + \mathbf{Y}), \\ \dot{\mathbf{Y}} &= \mathbf{G}(\mathbf{Y}) + \varepsilon \mathbf{D} \otimes \mathbf{C}(\mathbf{X} - \mathbf{Y}). \end{aligned} \tag{4.8}$$

Here $\mathbf{X}=\left(\mathbf{X}_1, \mathbf{X}_2\right)^T$, $\mathbf{Y}=\left(\mathbf{Y}_1, \mathbf{Y}_2\right)^T$, $\mathbf{D}=\begin{pmatrix} 0 & 0 \\ 1 & \lambda \end{pmatrix}$, $\lambda>0$ is a parameter responsible for the magnitude of couplings of "half-oscillators". If λ has moderate values, then system (4.8) is, in principle, similar to system (4.4), including the synchronization-generated cluster structure corresponding to solution $\mathbf{X}=\mathbf{Y}$ (without the fifth and sixth elements). However, if $\lambda \to \infty$ (a rigid "jumper" is installed between half-oscillators), then one can show that $\left\|\mathbf{X}_2-\mathbf{Y}_2\right\|=e^{-2\varepsilon\lambda t} \to 0$. That is, as expected, there is a degeneration of the number of degrees-of-freedom by one elementary oscillator in system (4.8) (the "halves" are glued together). Assuming now that $\mathbf{X}_2 \equiv \mathbf{Y}_2$, $\mathbf{Y}_1=\mathbf{X}_3$ and by introducing a new vector $\mathbf{X}=\left(\mathbf{X}_1,\ \mathbf{X}_2,\ \mathbf{X}_3\ \right)^T$, instead of system (4.8), we obtain a system of the form

$$\dot{\mathbf{X}}=\mathbf{S}(\mathbf{X}), \tag{4.9}$$

where

$$\mathbf{S}(\mathbf{X})=\left(\mathbf{F}\left(\mathbf{X}_1\right), \mathbf{F}\left(\mathbf{X}_2\right), \mathbf{F}\left(\mathbf{X}_3\right)\right)^T+\varepsilon \mathbf{B}_s \otimes \mathbf{C}\mathbf{X},\ \mathbf{B}_s=\begin{pmatrix} -1 & 1 & 0 \\ 1 & -2 & 1 \\ 0 & 1 & -1 \end{pmatrix}.$$

One can see that Eq. (4.9) coincides by its form with the equation of C-oscillator $O_s(3)$. However, its internal content is fundamentally

different. First, this equation is considered under the condition of the existence of attractor $A_a(2)$. Second, Eq. (4.6) is considered in a certain part of the phase space: either in the vicinity of attractor $A_a(2)$ (during the study of stability of structures), or on the attractor itself, as long as one deals with a fusion of schemes of the corresponding cluster structures. For these conditions, Eq. (4.9) represents a structured (or potentially structured, see Fig. 4.6a) and indivisible (in a sense) object: a simple cell. Considering the aforesaid matter, a simple cell can be interpreted as a limiting case of a system of two coupled C-oscillators of the type $O_a(n)$. Fig. 4.8 shows a "working" attractor of C-oscillator $O_a(2)$, which has been obtained during a numerical study of system (4.6) of two Chua's oscillators. The following parameter set has been used: $(\alpha, \beta, \gamma, m_0, m_1, \varepsilon) = (9.5, 14, 0.1, -1/7, 2/7, 0.215)$, as well as matrix $\mathbf{C} = \mathrm{diag}(1, 0, 0)$.

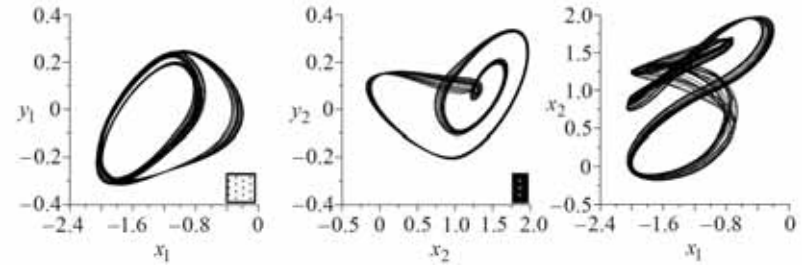

Fig. 4.8. Attractor $A_a(2)$ of C-oscillator $O_a(2)$ in projections onto coordinate planes.

Fig. 4.9 shows an "operational" regime of simple cell (4.9) that represents a dynamical cluster structure based on $O_a(2)$. The following parameter set has been used: $(\alpha, \beta, \gamma, m_0, m_1, \varepsilon) = (9.5, 14, 0.1, -1/7, 2/7, 0.215)$, $\mathbf{C} = \mathrm{diag}(1, 0, 0)$.

Thus, a simple cell, similarly to the C-oscillator of the type $O_s(n)$, is a subject in the formation of cluster structures in lattices. Moreover, due to the symmetry of its own cluster structure, the fusion matrix for one-dimensional lattices (chain, ring) with a cluster structure (as synchronization of simple cells) can be any of the matrices: $\mathbf{C}_*$ or $\mathbf{C}^*$. Let us illustrate this using the language of equations.

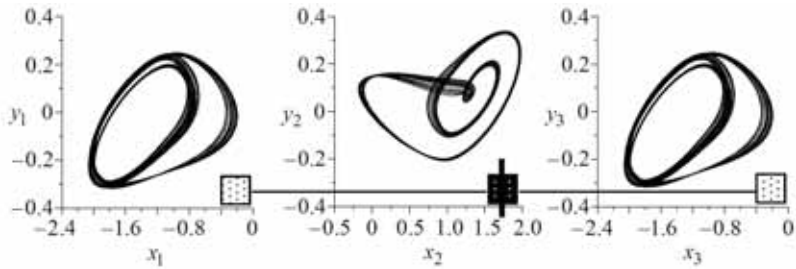

Fig. 4.9. Cluster structure of a simple cell based on $O_a(2)$

Suppose there is a simple cell (4.9) with a certain cluster structure and its dynamical copy is described by vector $\mathbf{Y} = (\mathbf{Y}_1, \mathbf{Y}_2, \mathbf{Y}_3)^T$. Consider a system of the form

$$\begin{aligned} \dot{\mathbf{X}} &= \mathbf{S}(\mathbf{X}) + \varepsilon(\mathbf{C}_* \otimes \mathbf{C})(\mathbf{Y} - \mathbf{X}), \\ \dot{\mathbf{Y}} &= \mathbf{S}(\mathbf{Y}) + \varepsilon(\mathbf{C}_* \otimes \mathbf{C})(\mathbf{X} - \mathbf{Y}), \end{aligned} \tag{4.10}$$

where $\mathbf{C}_* = \mathrm{diag}(0, 0, 1)$.

From the condition of synchronization in (4.10) and the form of the structure of the simple cell, we obtain $(\mathbf{X}_1, \mathbf{X}_2, \mathbf{X}_3)^T = (\mathbf{Y}_1, \mathbf{Y}_2, \mathbf{Y}_3)^T$ or $\mathbf{X}_1 = \mathbf{X}_3 = \mathbf{Y}_1 = \mathbf{Y}_3$, $\mathbf{X}_2 = \mathbf{Y}_2$. By reassigning coordinates of vector $\mathbf{Y}$ as $\mathbf{Y}_3 = \mathbf{X}_4$, $\mathbf{Y}_2 = \mathbf{X}_5$, $\mathbf{Y}_1 = \mathbf{X}_6$, we obtain the coordinate notation of the cluster structure in the chain of $N = 6$ elementary oscillators that appears based on synchronization of simple cells: $\mathbf{X}_1 = \mathbf{X}_3 = \mathbf{X}_4 = \mathbf{X}_6$, $\mathbf{X}_2 = \mathbf{X}_5$. Note that this notation also represents an integral manifold that occurs in the phase space of a lattice with 6 elements (see the beginning of this section).

Fig. 4.10 shows results of the numerical experiment performed for system (4.10), the elements of which represent chaotic Chua's oscillators. The following parameter set has been used: $(\alpha, \beta, \gamma, m_0, m_1, \varepsilon) = (9.5, 14, 0.1, -1/7, 2/7, 0.215)$, and matrix $\mathbf{C} = \mathrm{diag}(1, 0, 0)$.

As one can see, the cluster structure shown in Fig. 4.10 is "cut" into a pair of blocks – a pair of synchronized simple cells.

Let us summarize. First, the phenomenon of "cluster synchronization" represents the case of classical synchronization in the conventional understanding of this process and in this sense is not a new

physical phenomenon. Second, in the case of systems with a small number of oscillators, two types of subjects have been identified, the classical synchronization of which generates cluster structures in a chain of dynamical systems. The considered, particular cases of cluster structures with a small number of elements can be naturally generalized to a general case.

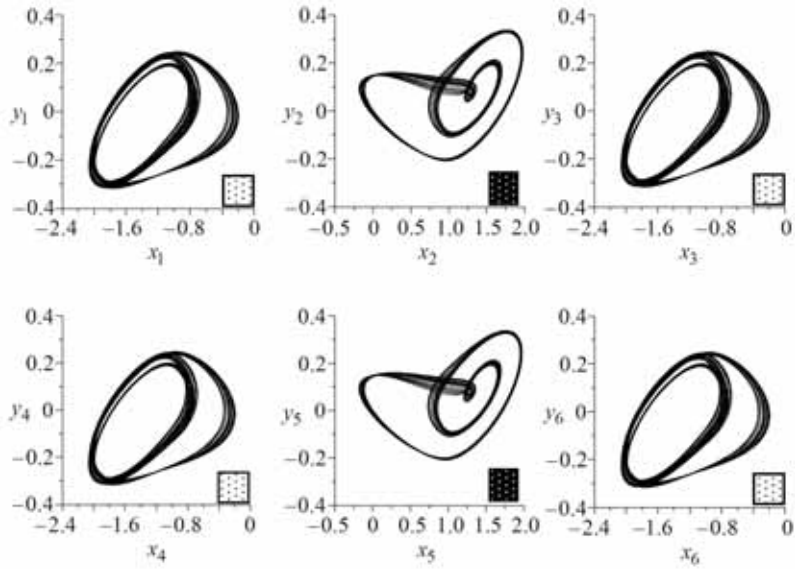

Fig. 4.10. Cluster structure in a chain of $N = 6$ elementary Chua's oscillators as a result of synchronization of two simple cells of $O_a(2)$ type.

Namely: the first subject of cluster structures in chains is a C-oscillator of the type $O_s(n)$; the second one is a simple cell, a structured object that appears as a result of synchronization of a pair of C-oscillators of the type $O_a(n)$. As it will be shown in the next

sections, these two types of subjects exhaust all possible types of cluster structures in chains of oscillators, which represent the simplest form of lattices.

Note. The structure and role of $O_s(n)$ and $O_a(n)$ in formation of cluster structures involuntarily impose an analogy with quantum-mechanical quasiparticles: bosons and fermions. It is known that the former ones play an independent role in interactions, and the latter ones, before becoming subjects of interactions, were previously combined into pairs (they are born and "die" in pairs). Within the framework of these representations, it is possible to propose a quantum-mechanical interpretation of cluster dynamics of lattices.

Using properties of number N (divisibility) and properties of $O_s(n)$ and $O_a(n)$ it is possible to establish all of the integral manifolds in the phase space of a lattice and, similarly to the energy levels, to order them according to the number of clusters. As it will be shown below, most of such levels (or all levels) are metastable. This means that (in a typical case) when a portion of energy is transferred to oscillators of the lattice (initial conditions), which corresponds to the upper energy level, the interaction of particles (elementary oscillators) will lead to the origination of an ensemble of interacting quasiparticles, i.e. a cluster structure of a certain type that corresponds to the "upper" manifold. Since the energy level is unstable, then, after a while, this state of the lattice disappears. Due to the

dissipative property of the system, a part of the energy is absorbed, i.e. the system goes from a lower energy level, to another metastable cluster structure and so on, up to the level that corresponds to integral manifold M_0. In general, such a scenario can resemble the process of transformation of a disturbed hydrodynamic flow into a laminar state through a sequence of successive structures.

4.2. Fusion and general properties of circuits of cluster structures

It must be said that the nature of the cluster structures that we have revealed (i.e. the synchronization of generalized oscillators (cluster forming oscillators) and simple cells) actually predetermines rules for the fusion of circuits of cluster structures, properties of these circuits, and their equivalent transformations, which are valid regardless of the geometric dimension of the lattices and their shape.

Let us provide a list of verbal definitions, general principles of the internal arrangement as well as elementary (equivalent) transformations of circuits of cluster structures.

1. Two directly connected, synchronized elementary oscillators, depicted in the diagram of the cluster structure using the same color, will be called the *cut pair*. The coupling between such oscillators can be removed by means of cutting (in the case of electric circuits, this corresponds to cutting the de-energized sections of the circuit representing equipotential points). On the contrary, any pas-

sive coupling can be established between same-colored schematic images and, in particular, a short-circuit can be made.

2. If a circuit has at least one cut pair, then we will call it the *cut circuit*, and otherwise the system is called the *non-cut circuit*.

3. The circuit of the cluster structure of a simple cell is non-cut.

4. If a certain circuit does not have any cut pairs, then it is either a circuit of a simple cell or a circuit of a separate cluster forming oscillator, or this circuit is not correct.

5. The procedure for combining two or more self-colored images by bending the circuit through the axes of symmetry or in another way will be called the *convolution of the circuit* (for the electric circuit, this corresponds to the procedure for connecting the equipotential points).

6. A circuit of a simple cell can be convoluted to the circuit of its basic cluster forming oscillator; that is, to a circuit that does not contain synchronized (same-colored) elementary oscillators.

7. Any circuit of a cluster structure, if it is not a circuit of a single cell or a circuit of a separate cluster forming oscillator, during the cutting of all cut pairs, is decomposed into identical blocks depicting the basic cluster forming oscillator (boson) or a circuit of the basic simple cell (fermion).

On the basis of these simple principles and equally simple elementary transformations of circuits (corresponding to the level of school physics), we will establish all possible types of cluster structures in a chain and in a ring of elementary oscillators. Also, mathematically non-trivial statements concerning the completeness of the aggregates of these types of structures will be proved.

Let us turn to the fusion of circuits of cluster structures. Like the connection of electric conductors, the connection of circuits of C-oscillators as parts of the complete circuit of the cluster structure, depicted in Fig. 4.11, we will call the *sequential coupling* (sequential fusion of a circuit of a cluster structure).

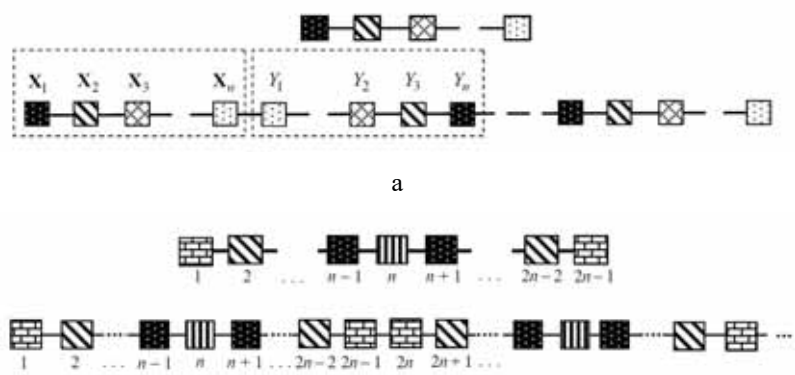

Fig. 4.11. A circuit (scheme) of C-oscillator $O_s(n)$ and sequential fusion of cluster structure on its basis (a); an image of a simple cell of C-oscillator $O_a(n)$ and sequential fusion of a cluster structure on its basis (b).

Matrix $\mathbf{D} = \mathrm{diag}\left(d_{11},\ d_{22}, ..., d_{ss}\right),$ in which the diagonal elements d_{ii} equal either 0 or 1, will be called the fusion matrix of the cluster structure. The subscripts of the unit elements determine the number of coupled elementary oscillators as elements of the C-oscillator or simple cell. The dimension of this matrix is equal to the number of oscillators forming the cluster forming oscillator $(m = n,$ see Fig. 4.11a) or simple cell $(m = 2n - 1,$ see Fig. 4.11b). By definition, the matrix of sequential fusion is matrix $\mathbf{D} = \mathbf{C}^{*} = \mathrm{diag}\left(1, 0, ..., 0\right)$ or $\mathbf{C}_{*} = \mathrm{diag}\left(0, 0, ..., 1\right).$

The coupling shown in Fig. 6.12 will be called the *parallel coupling*. In this particular case, the fusion matrix $\mathbf{D} = \mathrm{diag}\left(1, 1, ..., 1\right) = \mathbf{I}$ is a unit matrix.

All other types of fusion of block schemes from identical circuit-blocks (cluster forming oscillator or simple cell) are classified as a mixed type (see. Fig. 4.13).

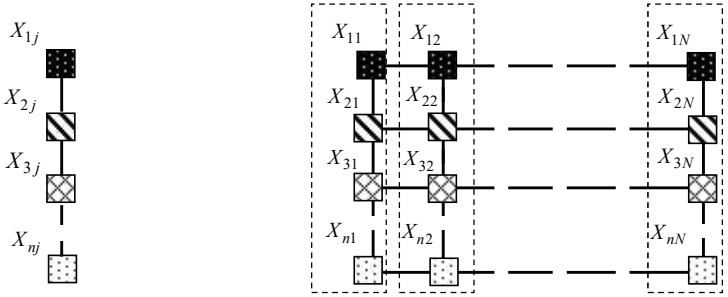

Fig. 4.12. A circuit (scheme) of C-oscillator $O_s(n)$ (a); a parallel fusion – tape-like cluster structure in a two-dimensional lattice (b).

Once again, we pay attention to the features of existence and coexistence of cluster structures in homogeneous lattices: if a synthesized circuit of the cluster structure uniquely determines the lattice itself, then, in a general case, this does not mean that the given structure will be unique in the resulting material lattice. A synthesized structure, as well as its accompanying structures, are associated with certain initial conditions of the obtained lattice. For example, for the circuit shown in Fig. 4.1a, in addition to this structure, in the corresponding lattice of six elements, accompanying structures can be observed, the circuits of which are shown in Figs. 4.1b and 4.10. In other words, cluster structures in homogeneous lattices, as a rule, are rigidly related to the initial conditions of the respective dynamical system, as well as with their stability. This means that in

order to implement structures in applications, one needs, among other things, to find a way to control the dynamical state of the system (initial conditions).

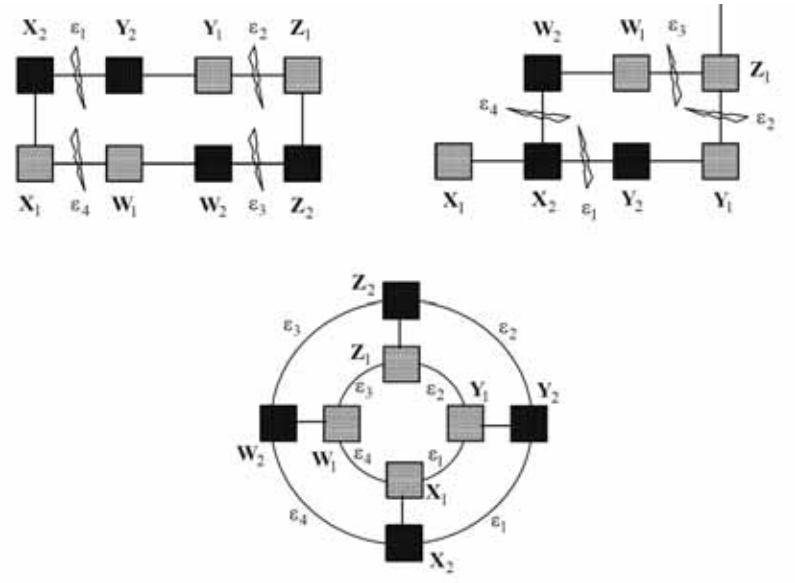

Fig. 4.13. Examples of a mixed type of fusion of cluster structure based on C-oscillator $O_s(2)$.

As a result of the aforesaid matter, questions arise about the fusion of structures in lattices by introducing a predetermined ordered inhomogeneity into the material part of the lattice. All problems of the fusion of orderly inhomogeneous lattices with the corresponding cluster dynamics have a positive solution, and it lies within the framework of the same principles and techniques as in the case of homogeneous lattices. It is sufficient to assume that the operating

mode of the cluster forming oscillator (attractor) is caused not by the initial conditions, but by the inhomogeneity of the parameters of the elementary oscillators that form it. A synthesized cluster structure in such a lattice may have global stability and controllability, including a remote control.

Here are two more examples of "clustering" of rather non-ordinary objects – objects with fractal properties. They represent one of the most outstanding directions of modern theoretical and applied research [193, 194].

The Cayley Tree. As a mathematical object, the Cayley tree is formed as follows. A figure is constructed in the form of an equilateral letter "H". Then a similar figure with a similarity factor of 1/2 is superimposed on each of the ends of this figure. The process of building is endless. Three iterations are shown in Fig. 4.14a. In practice, such a tree is produced by spraying or etching a thin film [193]. Naturally, in practice, the number of iterations is finite and is determined by the level of the technological process, i.e. physical objects have a pseudofractal structure, but their properties are close to the properties of the real fractals.

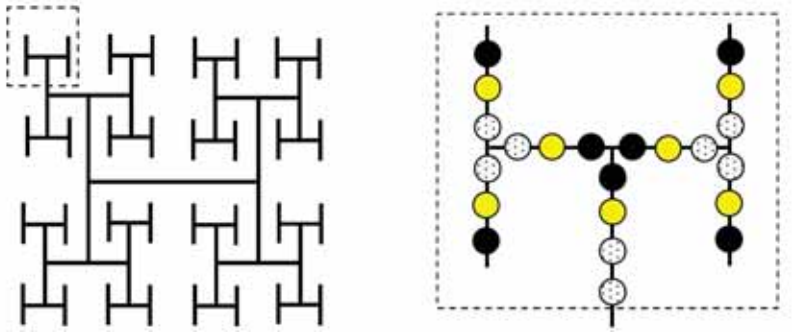

a b

Fig. 4.14. The Cayley tree (a); and a part of the clusterized tree (b).

Let us assume that technology allows us to construct some active nonlinear elements (conditional – oscillators) of sufficiently small sizes. In this case, taking as a basis a circuit of some C-oscillator of a chain with the number of elements n or a circuit of a simple cell with $2n-1,$ we "lay out" this circuit (according to the rules of the fusion) on each branch of the smallest element of the tree (in Fig. 4.14, it is indicated by a dashed line) the required number of times. Thus, we determine the necessary number of conditional oscillators to be placed on each branch of the tree. In the same way, the synthesis of the structure extends to the entire tree. As a result, we obtain a "clustered" tree, a segment of which is shown in Fig. 4.14b, which depicts the structure based on $O_s(3),$ However, other C-oscillators or simple cells could be chosen as well.

Now let us assume that all of the conditional oscillators are identical. In this case, we will deal with a homogeneous lattice, although

differently than for previous examples by its over-the-original form. The physics remains the same. We know that, along with the constructed cluster structure, other structures are potentially possible in this lattice. For this reason, in order to realize a necessary process, it is necessary to have the technical ability (a skill) to define specific initial conditions of the lattice (before it is put into operation). In addition, in the case of instability of this structure, additional measures are required to maintain its metastable state. Since control of the initial conditions represents an almost irresolvable task, it is most likely the case that the entire task is useless. A completely different situation can arise if the oscillators are controlled by some parameter like, for example, the frequency or phase of the oscillations. In this case, we will deal with an orderly inhomogeneous lattice, in which the cluster dynamic regime, on the one hand, will be stable, and on the other hand will have controllable parameters. In addition, controlling the parameters of the oscillators will create a possibility of switching the lattice from one cluster structure to another one. It could be possible to, in the case of antennas with a fractal lattice, obtain directional patterns with new unusual properties using the same approach.

The Sierpinsky carpet. This object is constructed as follows: a square is divided into nine equal squares; the middle square is removed, and with the remaining squares the division procedure is repeated. The process is endless. The resulting shape represents a so-called Sierpinsky carpet. Three iterations of a square are shown

in Fig. 4.15a. The unfinished carpet is marked by a black color, and a white color shows the removed parts of the square.

As in the previous example, we choose the smallest element of the carpet – the square, which is highlighted in Fig. 4.15 with a dotted line, as well as a diagram of the required C-oscillator or simple cell. The dimensions of the conditional oscillators as the "body" of the lattice, as determined by the possibilities of the manufacturing technology, must correspond to each other. Fig. 4.15b shows an example of the base element: a circuit of the square simple cell (3×3) with two clusters. Following the rules, we synthesize a circuit of the cluster structure, first in this element and then on the entire surface of the carpet. A fraction of the cluster structure is shown in Fig. 4.15b. The couplings of the elementary oscillators are represented by the contact of the sides of the squares. The properties of the obtained structures in homogeneous and non-homogeneous lattices are discussed above.

The principles of fusion of circuits of cluster structures do not exclude the fact that the elementary oscillators forming the C-oscillator can be different in their parameters, and also that they can be oscillators of different types. Let us provide an example illustrating what has been said above. Fig. 4.16 shows individual phase portraits of three oscillators representing "candidates" for C-oscillator $O_s(3)$. The first and the second ones are Chua's oscillators with parameters $(\beta, \gamma, m_0, m_1) = (14, 0.1, -1/7, 2/7)$ and $\alpha_1 = 9$,

$\alpha_2 = 9.5$, respectively. The third one is the Lorenz oscillator with parameters $\sigma = 10,\ r = 24$ and $b = 1$.

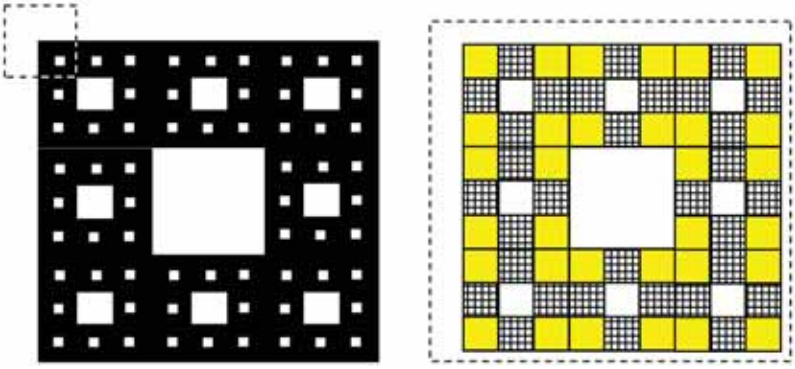

a b

Fig. 4.15. The Sierpinsky carpet (a) and a part of the clustered carpet (b).

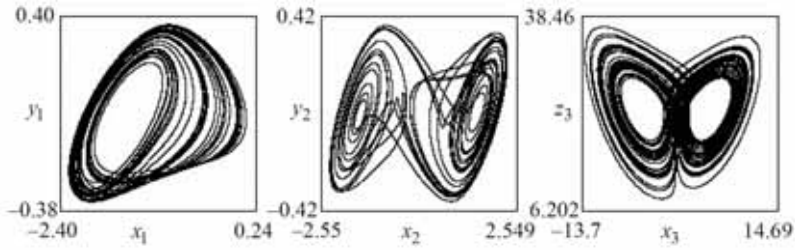

Fig. 4.16. Chaotic attractors of the oscillators before origination of C-oscillator $O_s(3)$.

Fig. 4.17 shows projections of a cluster attractor of C-oscillator $O_s(3)$ onto coordinate planes. The matrix of couplings of elementary oscillators has the form $\varepsilon \mathbf{C} = 0,5\mathbf{I}$.

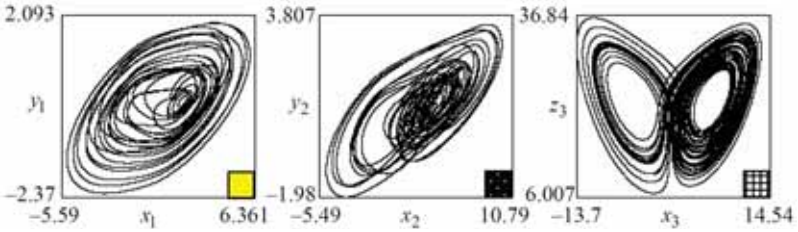

Fig. 4.17. Projections of cluster attractor onto the coordinate planes.

Fig. 4.18 shows a regime of synchronization of a pair of C-oscillators with matrix and scalar parameter of coupling $\varepsilon \mathbf{C}_* = 25\mathrm{diag}(0,0,1)$.

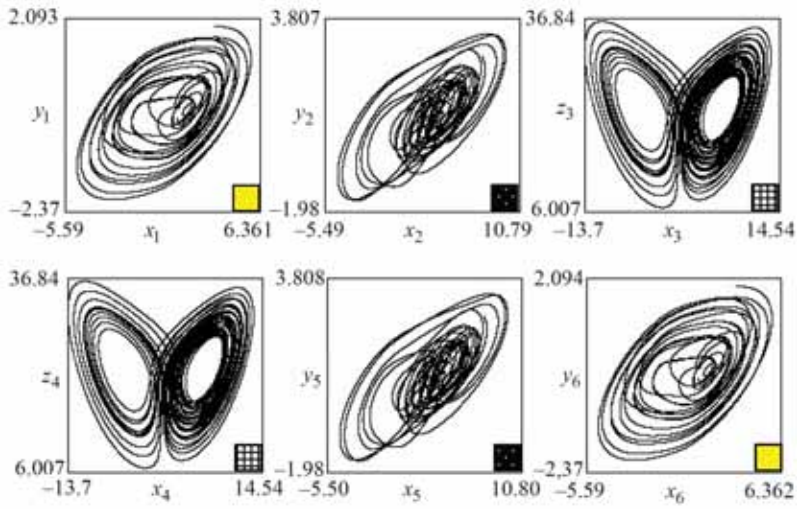

Fig. 4.18. Cluster structure as a synchronization of pair of C-oscillators of the type $O_s(3)$.

A visual comparison of the phase portraits of the oscillators is sufficient to state that we are dealing with the synchronization of a pair of C-oscillators. The synchronization is stable. Note that inhomogeneity in the circuit of a C-oscillator can be introduced through the magnitude of the couplings between its elementary oscillators.

In conclusion of this section, we would like to show an example from biology [194].

Being unfolded, a DNA molecule has the form of stairs consisting of separate links (in fact, it is twisted in a helix). The number of links is $\sim 10^5$. A segment of such a ladder is shown in Fig. 4.19a. In this figure, the following notations have been used: S denotes sugar molecules; F denotes molecules of phosphoric acid; T, A, G, and C denote nucleotides: thymine, adenine, guanine, and cytosine, respectively. In this case, nucleotides are assigned the role of conditional elementary oscillators. We classify sugars and phosphates as the "coupling" elements of the conditional oscillators T, A, G, and C. Under these conditions, a scheme of the cluster structure of a segment of the staircase is shown in Fig. 4.19b. One can see from the figure that the circuit of the structure does not have any cut pair. It means that it is uncut and, therefore, it can represent the circuit of the structure of a simple cell. In this case, after short-circuiting conditional equipotential points, it must contract to one C-oscillator. In this case, the procedure of convergence of a simple cell geometrically corresponds to the overlapping of two blocks after the rotation

of the second one by 180 degrees. Thus, the block (T, A, G, C) represents a C-oscillator, and the structure shown in Fig. 4.19a is the cluster structure of a simple cell.

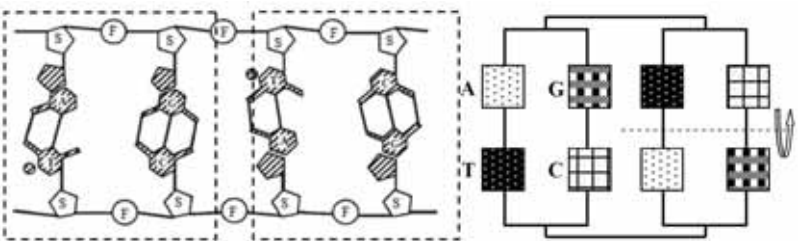

a b

Fig. 4.19. A segment of the unfolded DNA molecule.

4.3. C-oscillators of a chain and the fullness of types of their cluster structures

From the standpoint of cluster structures, a homogeneous chain is the simplest object. Numerous publications are devoted to its various applications for various physical systems and phenomena [96 – 98, 195 – 198]. Below, within the framework of the interpretation of cluster structures as mutual synchronization of generalized oscillators, we will show (we will prove) that all cluster structures in a chain are limited to only two types. And this applies to both homogeneous and orderly heterogeneous chains.

Let us formulate a general mathematical definition of the aforementioned C-oscillator of the type $O_s(n)$.

Definition 4.3.1. A dynamical system of n coupled elementary oscillators of the form

$$\begin{aligned}
&\dot{\mathbf{V}} = \mathbf{H}(\mathbf{V}), \\
&\mathbf{V} = (\mathbf{X}_1, \mathbf{X}_2, \ ..., \mathbf{X}_n)^T, \\
&\mathbf{H}(\mathbf{V}) = \left(\mathbf{F}_1(\mathbf{X}_1), \mathbf{F}_2(\mathbf{X}_2), ..., \mathbf{F}_n(\mathbf{X}_n)\right)^T - \varepsilon(\mathbf{B}_s \otimes \mathbf{C})\mathbf{V},
\end{aligned} \tag{4.11}$$

$$\mathbf{B}_s = \begin{pmatrix}
1 & -1 & 0 & \cdots & \cdots & 0 & 0 \\
-1 & 2 & -1 & \ddots & \cdots & 0 & 0 \\
0 & -1 & 2 & \ddots & \ddots & 0 & 0 \\
\vdots & \ddots & \ddots & \ddots & \ddots & \ddots & \vdots \\
\vdots & \vdots & \ddots & \ddots & 2 & -1 & 0 \\
0 & 0 & 0 & \ddots & -1 & 2 & -1 \\
0 & 0 & 0 & \cdots & 0 & -1 & 1
\end{pmatrix},$$

is called the C-oscillator of the type $O_s(n)$ conditioned that in the phase space there exists attractor $A_s(n)$, such that for $\forall(\mathbf{X}_1, \mathbf{X}_2, ..., \mathbf{X}_n) \in A_s(n), \quad \mathbf{X}_i \neq \mathbf{X}_j, \quad i \neq j, \quad i, \quad j = 1, 2, ..., n;$ $\mathbf{B}_s \otimes \mathbf{C}$ is the coupling matrix of elementary oscillators.

Elementary oscillators in Eq. (4.11) can be either identical, which corresponds to a homogeneous chain, or not identical by their parameters or even by their nature. The coupling of the oscillators in (4.11) is assumed to be homogeneous and local, although this cir-

cumstance is not fundamental and does not change the general essence of the matter.

By writing system (4.11) coordinate-wise, it is easy to verify that it corresponds to a segment of a chain with Neumann boundary conditions, which are satisfied "automatically" since they are embedded in the coupling matrix. For convenience, Fig. 4.20 shows once again a scheme of C-oscillator of the type $O_s(n)$ in its "operational" dynamical regime (on attractor $A_s(n)$), while Fig. 4.21 shows a process of fusion of a circuit of the cluster structure in a chain based on this C-oscillator.

Fig. 4.20. A circuit of $O_s(n)$

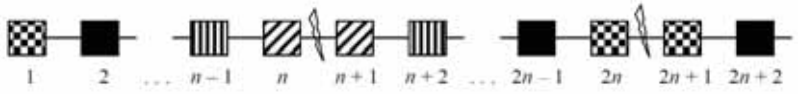

Fig. 4.21. The fusion of a circuit of cluster structure based on $O_s(n)$

By analogy, let us formulate the definition of a C-oscillator of the type $O_a(n)$

Definition 4.3.2. We call a system of coupled elementary oscillators of the form

$$\dot{\mathbf{V}} = \mathbf{H}(\mathbf{V}), \tag{4.12}$$

$$\mathbf{V} = (\mathbf{X}_1, \mathbf{X}_2, \ldots, \mathbf{X}_n)^T,$$

$$\mathbf{H}(\mathbf{V}) = \left(\mathbf{F}_1(\mathbf{X}_1), \mathbf{F}_2(\mathbf{X}_2), \ldots, \mathbf{F}_n(\mathbf{X}_n)\right)^T - \varepsilon(\mathbf{B}_a \otimes \mathbf{C})\mathbf{V},$$

$$\mathbf{B}_a = \begin{pmatrix} 1 & -1 & 0 & \cdots & \cdots & 0 & 0 \\ -1 & 2 & -1 & \ddots & \cdots & 0 & 0 \\ 0 & -1 & 2 & \ddots & \ddots & 0 & 0 \\ \vdots & \ddots & \ddots & \ddots & \ddots & \ddots & \vdots \\ \vdots & \vdots & \ddots & \ddots & 2 & -1 & 0 \\ 0 & 0 & 0 & \ddots & -1 & 2 & -1 \\ 0 & 0 & 0 & \cdots & 0 & -2 & 1 \end{pmatrix},$$

The C-oscillator of the type $O_a(n)$ is conditioned that in the phase space $G(\mathbf{V})$ there exists attractor $A_a(n)$, such that for $\forall(\mathbf{X}_1, \mathbf{X}_2, \ldots, \mathbf{X}_n) \in A_a(n), \quad \mathbf{X}_i \neq \mathbf{X}_j, \quad i \neq j, \quad i, \quad j = 1, 2, \ldots, n;$ $\mathbf{B}_a \otimes \mathbf{C}$ is the coupling matrix of elementary oscillators.

The sense of the variables and parameters of Eq. (4.12) is the same as explained above.

Recall that a C-oscillator of this type exists only in pairs. The mutual synchronization of such a pair in the limiting (rough) case of the connection of two C-oscillators to each other determines the cluster structure of the simple cell. In turn, the formed simple cells are the potential subjects of cluster structures in the chain. We note that

after a rigid coupling of the pair of terminal elementary oscillators of the C-oscillator, they actually merge and, as a consequence, degenerate in the number of degrees of freedom of the coupled system by the number of degrees of freedom of one elementary oscillator. In this case, the number of acting elementary oscillators in a simple cell becomes equal to $2n-1$. Equations of a simple cell are the equations of a segment of the chain with Neumann boundary conditions and number of elementary oscillators of $2n-1$. A fusion of a circuit of a cluster structure of a simple cell can be interpreted as an addition to circuit $O_a(n)$ of its mirrored image (Fig. 4.22). The bold vertical line in the figure symbolizes a mirror. Fig. 4.23 shows a fusion of a circuit of a cluster structure in a chain based on a circuit of the simple cell of the type $O_a(n)$.

Fig. 4.22. A circuit of the C-oscillator of type $O_a(n)$ and a fusion of a circuit of a cluster structure of a simple cell on its base.

Fig. 4.23. A fusion of the circuit of a cluster structure based on a circuit of a simple cell of the type $O_a(n)$.

As already mentioned regarding to the general principles of the theory of cluster structures, the division of systems into oscillators and rotators does not make a difference. The significance of this division appears only in the study of specific systems and their attractors, when systems of rotators exhibit specific features associated with the cylindricality of the phase space. For this reason, in what follows, we keep the adopted terminology and notation. Speaking of oscillators, we will bear in mind that the same applies to rotators as well. Let us just add to the aforesaid matter an illustration of a numerical experiment for cluster structures in a chain of rotators, a physical example of which is shown in Fig. 4.24.

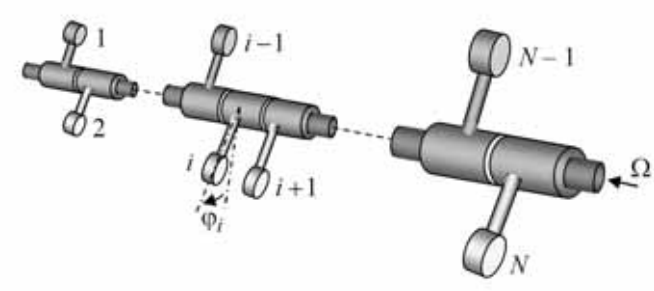

Fig. 4.24. A chain of Froude pendula with structured dynamics.

We have numerically studied a chain of rotators with the following vectors of dynamical state of elements: $\mathbf{X}_i = \left(\varphi_i, x_i\right)^T$ and $\mathbf{F}\left(\mathbf{X}_i\right) = \left(x_i, -\lambda x_i - \sin\varphi_i + \gamma + A\sin\omega_0\tau\right)^T$, with scalar coupling

parameter σ and matrix $\mathbf{C} = \begin{pmatrix} 0 & 0 \\ 0 & 1 \end{pmatrix}$, In particular, such a system models dynamics of a chain of Froude pendula shown in Fig. 4.24.

1. *Cluster structures of autonomous chain.* It is not difficult to demonstrate examples of cluster structures in a chain of rotators. For instance, in parameter domain (2) (see Fig. 1.7), a single rotator, depending on the initial conditions, may either be in equilibrium or in rotational motion. This means that, in the phase space of a pair of coupled rotators, there exists a stable oscillatory-rotational limit cycle (at least, for a weak coupling, this is guaranteed by the continuity of solutions by parameter). This limit cycle represents one of the cluster attractors of the system (see Fig. 4.25). The first of the coupled pendula rotates, while the second one experiences slight oscillations in the vicinity of the lower equilibrium.

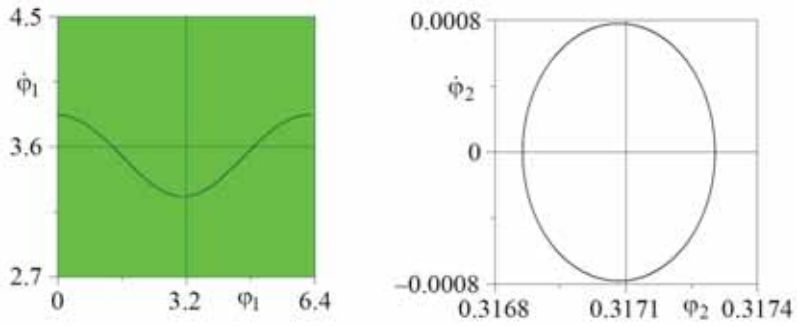

Fig. 4.25. Projections of attractor $A_s(2)$ onto coordinate planes of C-oscillator $O_s(2)$: $\lambda = 0.07$, $\gamma = 0.28$, $\sigma = 0.09$.

Further, we have studied a chain of 8 elements, for which, for the same parameters, the same cluster structure has been obtained (see Fig. 4.26). Looking ahead, we say that it is stable.

For parameters of the individual rotators from parameter domain (2) (see Fig. 1.7), a C-oscillator of the type $O_a(2)$ has been modeled according to Definition 4.3.2. Its attractor $A_a(2)$, with the parameters of the coupled system $\lambda = 0.07$, $\gamma = 0.28$, $\sigma = 0.29$, is shown in Fig. 4.27. The similarity with attractor $A_s(2)$ is only in appearance, but they are fundamentally different.

For parameters of the individual rotators from parameter domain (2) (see Fig. 1.7), a C-oscillator of the type $O_a(2)$ has been modeled according to Definition 4.3.2. Its attractor $A_a(2)$, with the parameters of the coupled system $\lambda = 0.07$, $\gamma = 0.28$, $\sigma = 0.29$, is shown in Fig. 4.27. The similarity with attractor $A_s(2)$ is only in appearance, but they are fundamentally different.

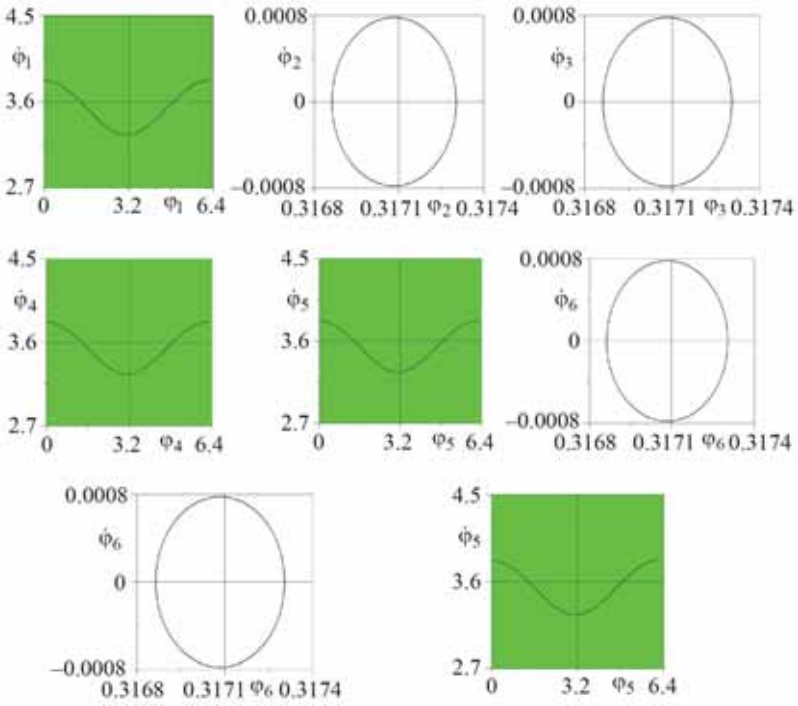

Fig. 4.26. Cluster structure based on synchronization of four C-oscillators of $O_s(2)$ type in a chain of $N = 8$ elementary rotators.

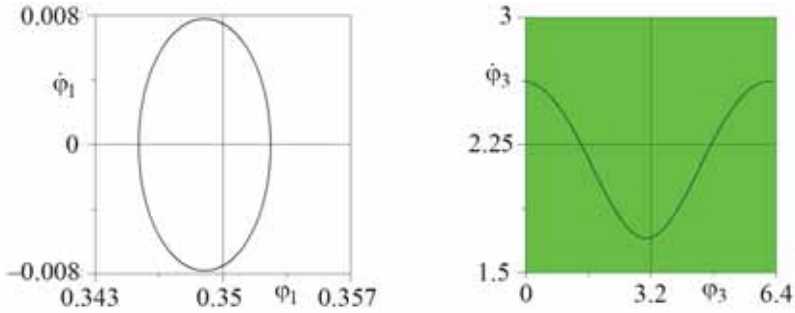

Fig. 4.27. Projections of attractor $A_a(2)$ into same-titled coordinate planes of the C-oscillator of the type $O_a(2)$.

Fig. 4.28 shows a cluster structure of a simple cell of C-oscillator $O_a(2)$ (stable), which has been obtained for the same parameters in a chain of three elements.

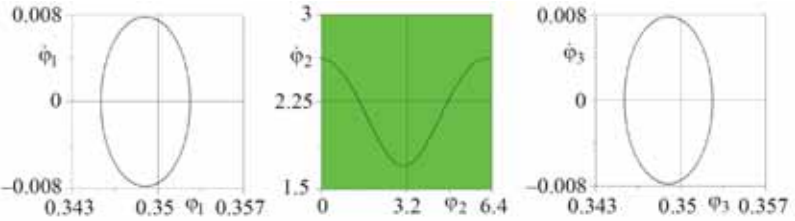

Fig. 4.28. Cluster structure of a simple cell of C-oscillator $O_a(2)$.

Further, for the same parameters, we have studied a chain of 6 elements, in which a cluster structure shown in Fig. 4.29 has been obtained.

2. *Cluster structures of non-autonomous chain*. In this case, to select parameters that are necessary for the existence of cluster attrac-

tors, we turn to the bifurcation diagram shown in Fig. 1.10a. As one can see from the figure, parameters from all domains suffice except for parameter domain (1): for these parameters a globally stable in-phase synchronization occurs, while we are looking for different partial dynamics of rotators.

An example of cluster attractor $A_s(2)$ is shown in Fig. 4.30. The following parameter set has been used: $\lambda = 0.07$; $\gamma = 0.51$; $\sigma = =0.079$; $A = 0.28$; $\omega = 0.56$.

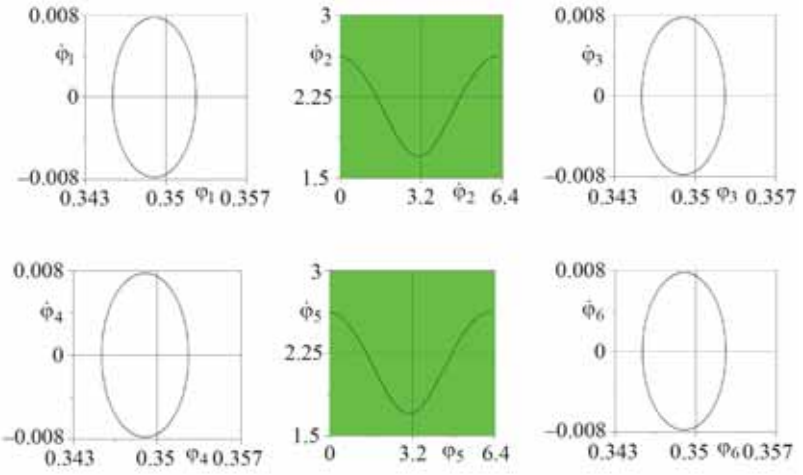

Fig. 4.29. Stable cluster structure as a synchronization of two simple cells of the type $O_s(2)$.

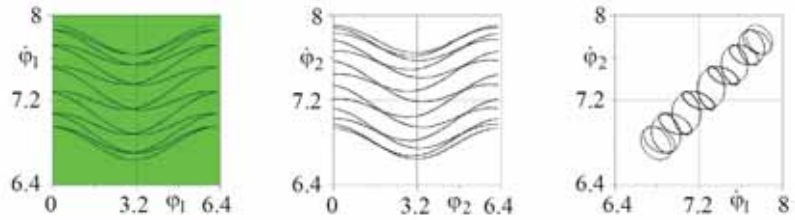

Fig. 4.30. Projections of attractor $A_s(2)$ into same-titled and cross-coordinate planes of C-oscillator $O_s(2)$.

In this case, a cluster attractor is a three-dimensional torus T^3, which corresponds to the regime of beatings of rotators with each other as well as with the periodic external force, which means the absence of both mutual and master-slave synchronization. In what follows, without going into much detail, we show results of the numerical experiment (Figs. 4.31 –4.34). All cluster structures are stable.

Now let us subdivide all cluster structures in a lattice into different types. A type of set of structures will be determined according to the type of basic C-oscillator that defines each structure of this set, i.e. the number of types of structures in a lattice is the number of all types C-oscillators that are possible in this lattice.

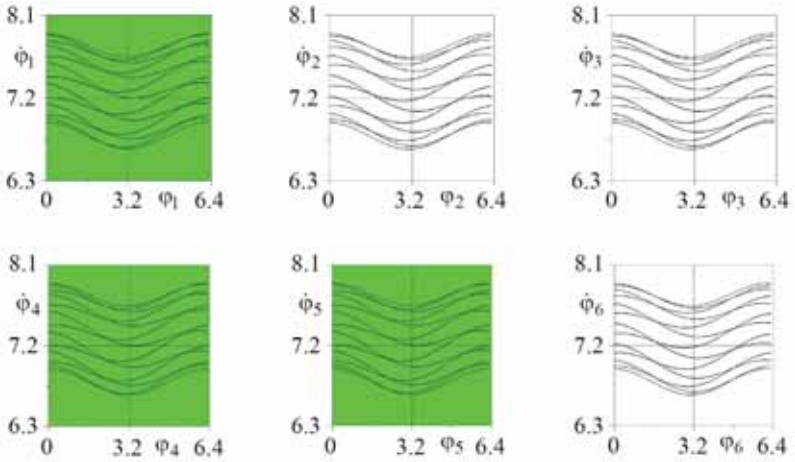

Fig. 4.31. Stable cluster structure based on the synchronization of three C-oscillators of the type $O_s(2)$.

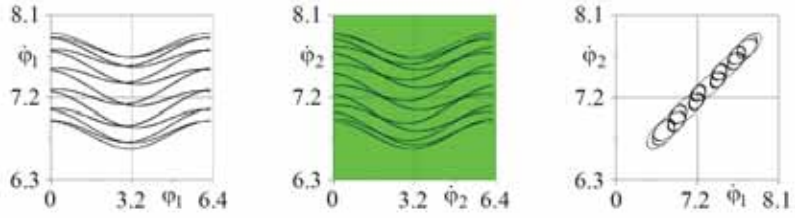

Fig. 4.32. Projections of attractor $A_a(2)$ onto the coordinate planes of C-oscillator $O_a(2)$. The following parameter set has been used: $\lambda = 0.07$, $\gamma = 0.51$, $\sigma = 0.079$, $A = 0.28$, $\omega = 0.56$.

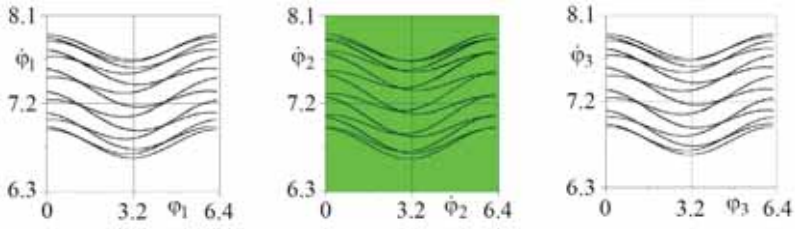

Fig. 4.33. Stable cluster structure of a simple cell $O_a(2)$.

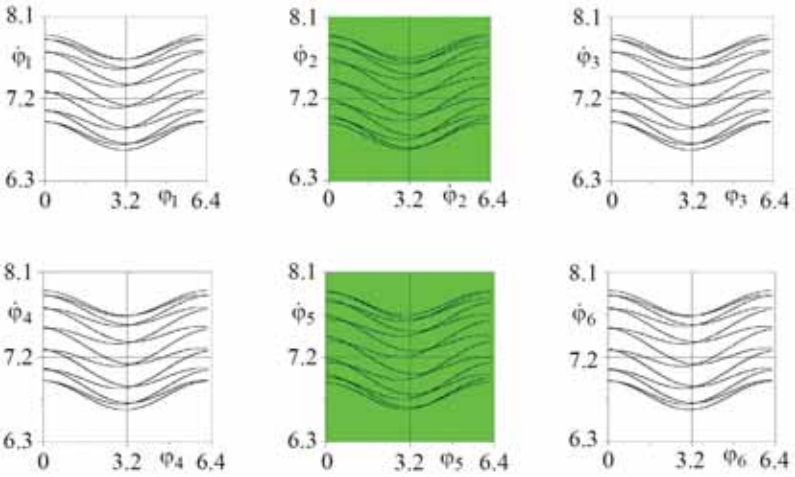

Fig. 4.34. Stable cluster structure based on the synchronization of two simple cells $O_a(2)$.

Theorem 4.3.1. $O_s(n)$ and $O_a(n)$ constitute the full set of types of cluster forming oscillators in a chain of elementary oscillators with Neumann boundary conditions. Synchronization of these C-oscillators and their simple cells defines all possible types of cluster structures existing in the chain [181].

Proof. We will use an electric scheme of the chain of oscillators (rotators) shown in Fig. 4.35. Let us rewrite equations for a chain in a common form

$$\dot{\mathbf{X}}_i = \mathbf{F}_i\left(\boldsymbol{X}_i,\, t\right) + \varepsilon\mathbf{C}\left(\mathbf{X}_{i-1} - 2\mathbf{X}_i + \mathbf{X}_{i+1}\right) \tag{4.13}$$

with the boundary condition at the left end $\mathbf{X}_0 = \mathbf{X}_1$. The boundary condition at the right end will be formulated during the proof. For the proof, we use equivalent transformations of circuits of structures as elementary transformations of this electrical circuit.

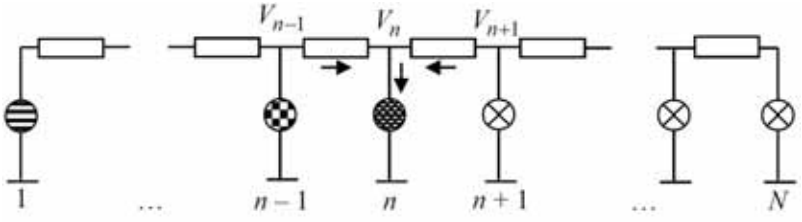

Fig. 4.35. A chain of oscillators (rotators).

Let us assume that a certain cluster structure is realized in the chain. Starting with the first one, we select all consecutive unsynchronized oscillators. Let us assume that their number is n (see Fig. 4.35). In this case, $(n + 1)$-th elementary oscillator is synchronized with one of the oscillators of the selected group.

Suppose that this oscillator is synchronized with some k-the one, where $k \le n-2$, elementary oscillator of the selected group. In this case, values of all same-titled variables of this pair of oscillators are identical at any moment of time. The points at their

"inputs" are equipotential: $V_k = V_{n+1}$. We perform equivalent circuit transformations that correspond to the transformation of the circuit of the cluster structure: after connecting (short-circuiting) equipotential points with a bridge, we perform a sequence of transformations, as shown in Fig. 4.36.

Let us write equations for the electric currents of synchronized oscillators in the first and last positions of the circuit, respectively:

$$V_n - 2V_{n+1} + V_{n+2} = IR,\ V_{k+1} - 2V_k + V_{n+2} = IR.$$

From these equations, we obtain $V_n = V_{k+1}$. Except for cases $k = n$ and $k = n-1$, this contradicts the condition of the non-synchronization of the first *n* oscillators. Thus, the (*n* + 1)-th oscillator cannot be synchronized with any $k \le n-2$ oscillator. Two remaining cases are: 1) $k = n$, 2) $k = n-1$.

1) Suppose that, $k = n$, so that we obtain $V_n = V_{n+1}$ and $I_n = I_{n+1}$. On the other hand, the following equations are valid for these oscillators: $V_{n-1} - V_n = I_n R$, $V_{n+2} - V_{n+1} = I_{n+1} R$. From here, we obtain $V_{n-1} = V_{n+2}$ i.e. the condition of the synchronization of the (*n* – 1)-th and (*n* + 2)-th oscillators. Writing the Kirchhoff equations for this pair of oscillators, we obtain: $V_{n-2} + V_n - 2V_{n-1} = I_{n-1} R$, $V_{n+3} + V_{n+1} - 2V_{n+2} = I_{n+2} R$, from which it follows that $V_{n-2} = V_{n+3}$ and the corresponding pair of oscillators is also synchronized.

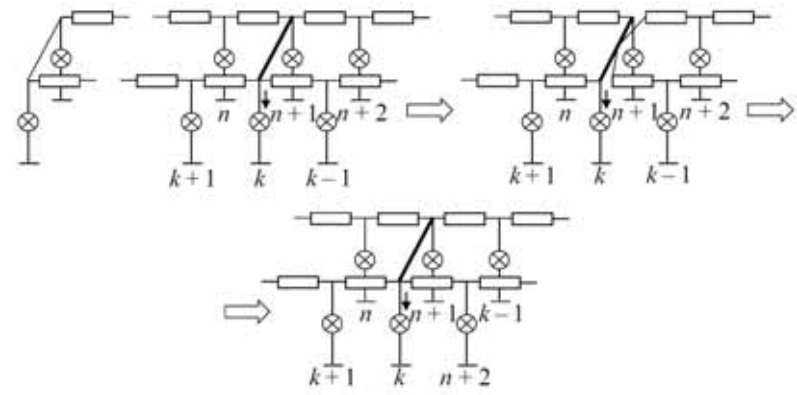

Fig. 4.36. Equivalent transformations of the chain of oscillators shown in Fig. 4.35.

Continuing the successive writing of equations for synchronized oscillators, we obtain $V_1 = V_{2n}$. Further, we obtain a "fork": the oscillator with number $(2n + 1)$ can be synchronized with the $2n$-th or with the $(2n - 1)$-th one. Let us assume that it is synchronized with the $(2n - 1)$-th, one, so that $V_{2n+1} = V_{2n-1}$. From the equations for the first and $2n$-th oscillators, we obtain: $V_2 - V_1 = I_1 R$, $V_{2n-1} + V_{2n} - 2V_{2n+1} = I_{2n} R$. Thus $V_2 = V_1$, but this contradicts the condition of absence of the synchronization for the first n oscillators.

Thus, the $(2n + 1)$-th oscillator is synchronized with the $2n$-th one. Repeating such kind of reasoning again and again, we obtain the order of synchronized oscillators in the chain, as shown in Fig. 4.21, i.e. the structure based on $O_s(n)$. We show that, in this case,

the cluster structure contains an integer number of images of C-oscillators $O_s(n)$, $N = mn$. Let us assume the opposite: the number of non-synchronized rotators in a finite interval is $k < n$. Let us remove all of C-oscillators from the chain (we cut the circuit) by leaving the penultimate cluster forming oscillator as well as the aforementioned segment. Then, we renumber the remaining oscillators from 1 to $k + n$. In this case, we obtain a scheme similar to one shown in Fig. 4.21 with the number of oscillators $n + k$. According to the condition, we have: $V_{n+k+1-i} = V_{n-k+i}$, $i = 1, 2, ..., k$. Let us write equations for the last and for the (n – k + 1)-th synchronized oscillators: $V_{n+k-1} - V_{n+k} = RI$, $V_{n-k} - 2V_{n-k+1} + V_{n-k+2} = RI$, $V_{n+k} = V_{n-k+1}$, $V_{n+k-1} = V_{n-k+2}$. From these equations and condition $V_{n+k} = V_{n-k+1}$, $V_{n+k-1} = V_{n-k+2}$ we obtain $V_{n-k} = V_{n-k+1}$. From here, it follows that if $k \neq n$, then the system of the first n rotators does not represent a C-oscillator, which is a contradiction, while if $k = n$, then $V_0 = V_1$, which represents a boundary condition.

Eventually, the final conclusion of this part of the proof is: if $\mathbf{X}_n = \mathbf{X}_{n+1}$, and if the first n oscillators are not synchronized, then the cluster structure is formed based on synchronization of C-oscillator of the type $O_s(n)$. Considering this equality in system (4.13), we find that it represents Eq. (4.11) in the expanded form. In contrast, by converging (4.13), we obtain Eq. (4.11) with cluster matrix $\mathbf{B}_s$.

2) Coming back to the beginning of the proof, we now assume that the $(n + 1)$-th oscillator is synchronized with the $(n - 1)$-th one, i.e. $V_{n-1} = V_{n+1}$. Writing the Kirchhoff equations for these oscillators, we obtain: $V_{n-2} - 2V_{n-1} + V_n = IR, \quad V_{n+2} - 2V_{n+1} + V_n = IR.$ From here it follows that $V_{n-2} = V_{n+2}$. From this equality, as well as from the equations for all subsequent oscillators, we obtain the general expression $V_i = V_{2n-i}, \ i = 1, 2, ..., n-1.$ Therefore, the conclusion is: in this case, the dynamical structure of the system of $2n-1$ oscillators represents a cluster structure of a simple cell (see Fig. 4.22). Taking into account condition $\mathbf{X}_{n-1} = \mathbf{X}_{n+1}$ in system (4.13), we find that it represents an extended form of the equation of C-oscillator $O_a(n)$ (4.12) with cluster matrix $\mathbf{B}_a$. The proof that, in this case, the complete circuit of the cluster structure of the chain consists of an integer number of simple cell's circuits (see Fig. 4.24) is carried out analogously to one considered in the first section of the Proof.

The final conclusion is: $O_s(n)$ and $O_a(n)$ constitute a full set of types of structure forming objects that cover all types of possible cluster structures that could be realized in a chain of oscillators.

Remark. In the proof of the theorem, the condition of chain homogeneity was not used. We have proceeded only from the condition that a certain structure in the chain is realized. This means that the theorem also holds for an inhomogeneous chain. It would have fol-

lowed from the proof that this heterogeneity should have a periodically ordered form; that is, to implement a particular structure in the chain, an individual order of non-identical oscillators should be organized in accordance with the circuit of the given cluster structure.

Conclusion 1. On a number of structures in a chain for a given number N. If p is the number of all even products (simple and composite) of number N, excluding the number itself and 1, then in a chain consisting of N elementary oscillators, there exist p cluster structures based on $O_s(n)$ for different n. If q is the number of all odd multipliers (simple and composite) of number N, including this number if it is odd, then there exist q cluster structures based on a simple cell of C-oscillator $O_a(n)$ for different n. The full number of cluster structures in a chain with a given number N equals $p+q$.

Proof. First, according to the theorem, all cluster structures in the chain are synthesized based on $O_s(n)$ or based on a simple cell of the type $O_a(n)$ Second, all cluster structures consist of an integer number of corresponding blocks (see Figs. 4.21, 4.24). For a cluster structure based on $O_s(n)$, the following equality is valid: $N = mn$, $m \geq 2$, $n \geq 2$. Hence, we obtain the number of cluster structures on its base that is equal to p. For structures based on simple cell, $O_a(n)$ $N = m(2n-1)$, $m \geq 1$, $n \geq 2$, and that means that the number of such structures equals q. The total number of structures

equals $p+q$. For an inhomogeneous chain, this means that such and only such a number of structures can be produced in a chain by manipulating its heterogeneity.

Example. Consider $N=100$, in this case, $p=7$, and $q=2$, i.e. 9 structures can be realized in the chain. Let us list these structures: $O_s(2)$ (the structure contains $m = 50$ pieces of such cluster forming oscillators), $O_s(4)$ (contains 25 pieces), $O_s(5)$ (contains 20 pieces), $O_s(10)$ (contains 10 pieces), $O_s(20)$ (contains 5 pieces), $O_s(25)$ (contains 4 pieces), $O_s(50)$ (contains 2 pieces), $O_a(13)$ (contains $m = 4$ simple cells $O_a(13)$),), $O_a(3)$ (contains 20 pieces).

Conclusion 2. *On integral manifolds of a chain of oscillators as a dynamical system.* Based on the arithmetic properties of the number of oscillators in the chain *N*, as well as on Conclusion 1 of Theorem 4.3.1, it is possible to obtain all integral manifolds of the chain presented in [97 – 99]. Their mathematical representations are obtained by equating the vectors of dynamic variables of synchronized oscillators. According to the theorem proven, it can be stated that there are no other than these “cluster” integral manifolds in the chain.

4.4. C-oscillators and cluster structures of a ring

Along with the chain, the ring of oscillators is one of the basic models of the theory of oscillations and waves [199]. In particular, the ring is a model for studying autowave processes in active media with periodic boundary conditions, for studies of the dynamics of collective phase synchronization systems, ring systems of superconducting transitions, and it is also used in modelling biological, chemical, and other systems [65, 96, 98, 200 – 203].

In the development of the theory of cluster structures, in what follows, we will consider cluster-forming objects of the ring and establish all existing types of cluster structures [204].

Cut cluster structures of the ring. Suppose that the circuit of the cluster structure of the ring contains a cut pair. Cutting this pair reduces the circuit in the ring to the equivalent circuit in the chain. This means that the basic, known-to-us C-oscillators of the chain, $O_s(n)$ and $O_a(n)$ are also the basic ones for the ring. Definitions of these cluster forming oscillators are provided in the previous section.

A fusion of the schemes of the cut cluster structures is carried out in a similar way as it was done for the chain, but with one remark: the number blocks of C-oscillators $O_s(n)$ in a circuit of the cluster structure is always even. This is not difficult to explain: first, if, as a result of cutting the cut pair, the circuit of the ring turns into a circuit of the chain, then conversely, the circuit of the chain turns into

a circuit of the ring as a result of connecting the oscillators. Second, since in this procedure the above oscillators are “same-coloured”, the corresponding structure in the chain is centrally symmetric. Hence, the conclusion: the number of circuit blocks $O_s(n)$ in a corresponding structure is always even. Fig. 4.37 shows a circuit of a cut cluster structure synthesized based on $O_s(n)$.

As an example, Fig. 6.38 shows a cut cluster structure as a synchronization of the pair of C-oscillators $O_s(3)$ in a homogeneous ring of $N=6$ diffusive coupled Chua’s oscillators. The following parameter set has been used: $\{\alpha, \beta, \gamma, m_0, m_1, \varepsilon\} = \{9.5, 14, 0.1, -1/7, 2/7, 0.34\}$. The first and sixth, as well as the third and fourth, elementary oscillators are two cut pairs of the cluster structure.

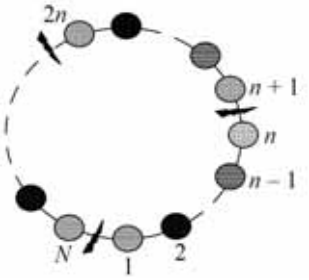

Fig. 4.37. A fusion of the cluster structure of a ring based on C-oscillator of the type $O_s(n)$.

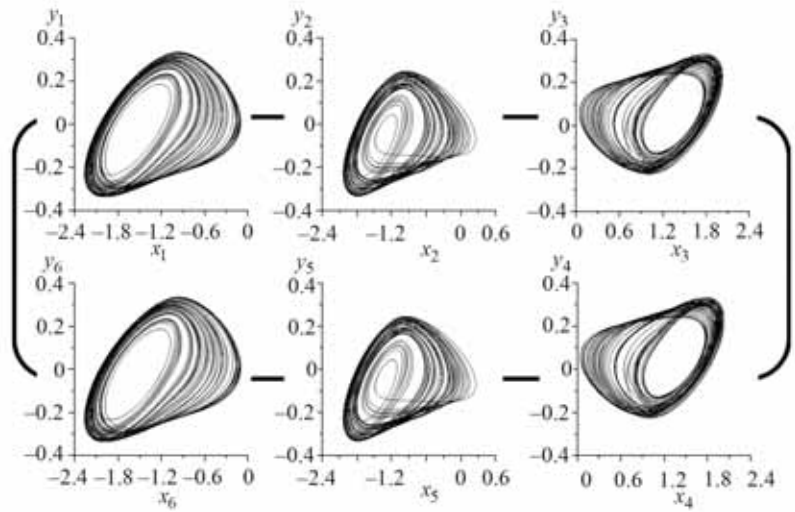

Fig. 4.38. Cut cluster structure based on a pair of C-oscillators of the type $O_s(3)$.

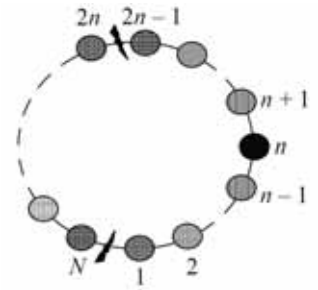

Fig. 4.39. A fusion of the cluster structure in a ring based on simple cell $O_a(n)$.

In contrast to structures based on $O_s(n)$ the number of simple cells based on $O_a(n)$ in the cluster structure of a ring can be arbitrary – even or odd. Fig. 4.39 shows a fusion of the circuit of a cut cluster structure based on simple cells $O_a(n)$.

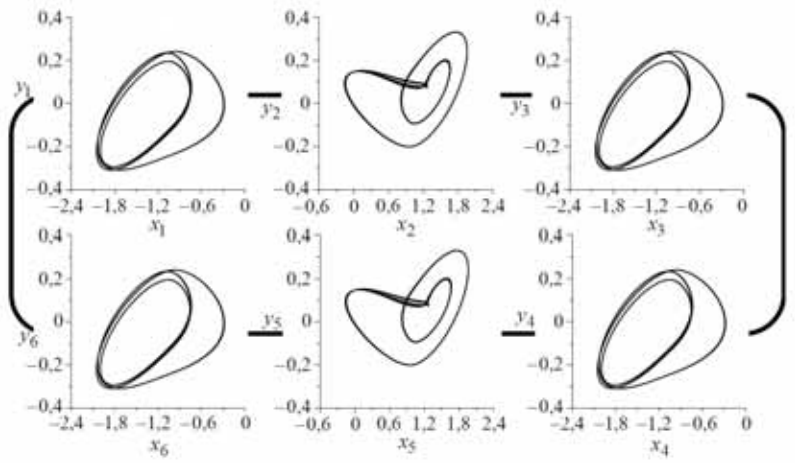

Fig. 4.40. Cut cluster structure as a synchronization of a pair of simple cells of the type $O_a(2)$.

To illustrate the aforesaid matter, Fig. 4.40 shows a result of the numerical experiment: it shows a cut cluster structure as a synchronization of two simple cells $O_a(2)$ in a homogeneous ring of $N = 6$ Chua's oscillators. The following parameter set has been used: $\{\alpha, \beta, \gamma, m_0, m_1, \varepsilon\} = \{9.5; 14; 0.1; -1/7; 2/7; 0.2175\}$.

Uncut cluster structures of the ring. Suppose that the structure of the ring contains no cut pairs. In this case, it represents a simple cell and, therefore, its circuit shall be converged to the circuit of a certain (sought) C-oscillator. In a homogeneous ring, it is natural to associate procedures of convergence with the different types of symmetry.

1. *Mirrored cluster structures of the ring*. According to our knowledge of a chain, one of the procedures of convergence – folding of a circuit of the structure of the simple cell along the its axis of symmetry, can be also considered as a mirroring. In the case of a ring, this axis is a diameter that passes through the centers of figures of the oscillators (we consider the ring as a circumference with a homogeneous distribution of oscillators). For another case of the axis of symmetry – diameter that passes through centers of couplings, the structure would be a cut structure, which has been already discussed above.

Suppose that the circuit of the cluster structure is symmetric with respect to a certain diameter AF. By folding the circuit over this diameter and aligning the same-coloured images, we obtain the case shown in Fig. 4.41a. Elementary oscillators are placed over a radial arc and the first and last ones are half-oscillators. The physical sense of these half-oscillators is clear. If all oscillators of the arc are not synchronized (have different colours), then their circuit is the sought C-oscillator and the procedure of convergence is finished.

Let us, however, suppose that there is a general case when there are synchronized oscillators among the oscillators of the arc (same-colored ones), see Fig. 4.41a. Then the circuit of oscillators of arc $\overset{\frown}{AF}$ represents an integer number of circuits of C-oscillators. The circuit of a basic C-oscillator shall be such that it would occupy the whole arc $\overset{\frown}{AF}$ (with half-oscillators at the ends). In the opposite

case, the transition to this case would be absent for the increased number of oscillators of the cluster forming oscillator.

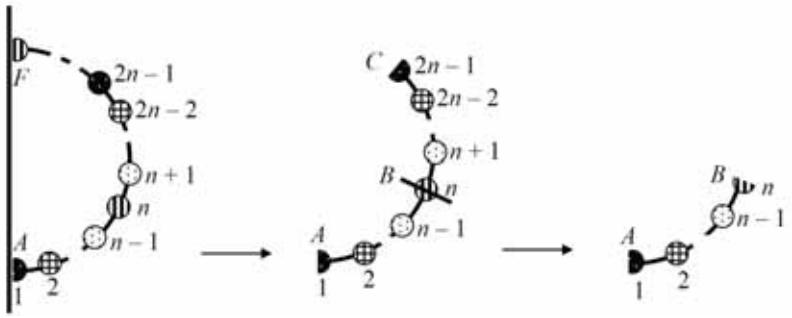

Fig. 4.41. Convergence of the circuit of a “mirrored” cluster structure of the simple cell.

Staring from oscillator F, we select all successive “multicolored” elementary oscillators – an arc of oscillators. Continuing to bend this and similar arcs through the middle of the final oscillator, we obtain the picture shown in Fig. 4.41c. Fig.46.41b shows the arc before the last iteration. Elementary oscillators on arc $\overset{\frown}{AF}$ represent the circuit of the sought C-oscillator, the basic one for the cluster structure, which we will call the mirror cluster structure. We denote it as $O_a^r(n)$.

Definition 4.4.1. A system of $n \geq 2$ coupled elementary oscillators of the form

$$\dot{\mathbf{X}} = \mathbf{G}(\mathbf{X}) - \varepsilon \mathbf{B}_a^r \otimes \mathbf{C}\mathbf{X}, \tag{4.14}$$

$$\mathbf{X}=\left(\mathbf{X}_1,\mathbf{X}_2,...,\mathbf{X}_n\right)^T,\ \ \mathbf{G}\left(\mathbf{X}\right)=\left(\mathbf{F}_1\left(\mathbf{X}_1\right),\ \mathbf{F}_2\left(\mathbf{X}_2\right),...,\mathbf{F}_n\left(\mathbf{X}_n\right)\right)^T,$$

$$\mathbf{B}_a^r=\begin{pmatrix} 2 & -2 & 0 & 0 & & & & \\ -1 & 2 & -1 & 0 & & & & \\ 0 & -1 & 2 & -1 & & \mathbf{0} & & \\ 0 & 0 & -1 & 2 & & & & \\ & & & & \ddots & & & \\ & & & & & 2 & -1 & 0 & 0 \\ & & \mathbf{0} & & & -1 & 2 & -1 & 0 \\ & & & & & 0 & -1 & 2 & -1 \\ & & & & & 0 & 0 & -2 & 2 \end{pmatrix},$$

is called the *mirror cluster oscillator* $O_a^r\left(n\right)$ and, conditioned that, in the phase space, there exists attractor $A_a^r\left(n\right)$, such that for $\forall\left(\mathbf{X}_1,\mathbf{X}_2,...,\mathbf{X}_n\right)\in A_a^r\left(n\right),\ \ \mathbf{X}_i\neq\mathbf{X}_j,\ \ i\neq j,\ \ i=\overline{1,n},\ \ j=\overline{1,n}.$
Eq. (4.14) can be obtained in different ways, and in particular, from Eq. (4.13), for which the following boundary conditions should be taken: $\mathbf{X}_2\equiv\mathbf{X}_0,\ \ \mathbf{X}_{n+1}\equiv\mathbf{X}_{n-1}.$

Fig. 4.42 shows a mirror cluster structure in a homogeneous ring of $N=6$ Chua's oscillators. The following parameter set has been used: $\left\{\alpha,\beta,\gamma,m_0,m_1,\varepsilon\right\}=\left\{9.11,14,0.1,-1/7,2/7,0.25\right\}.$ The surface of a "mirror" passes through the first and fourth oscillators.

The fusion of the circuit of the mirror structure is carried out in the order opposite of convergence: by a series of a chain of mirror reflections of the circuit of mirror cluster forming oscillator: its mir-

ror reflection is attached to the arc of the oscillators $\overset{\frown}{AB}$ and so on, up to the closure of the circuit of the structure into the ring.

It is not difficult to derive a formula for coupling the number of oscillators in the ring with the number of C-oscillators in the fusion of the structure and the number of elementary oscillators in the cluster forming oscillator itself: $N = 2m(n-1)$, where m is the number of C-oscillators that "cover" a half of the ring. From this formula, it follows that if r is the number of all multipliers of number $N/2$, including the number itself, then in the ring there exist r mirror cluster structures based on C-oscillator $O_a^r(n)$. For instance, for $N = 12$, there exist three structures based on $O_a^r(n)$: one consisting of two C-oscillators $O_a^r(7)$, one consisting of four C-oscillators $O_a^r(4)$, and one consisting of six C-oscillators $O_a^r(3)$. For $N = 6$, there exists one mirror structure in the ring based on the synchronization of $O_a^r(4)$ the example of which is shown in Fig. 4.42.

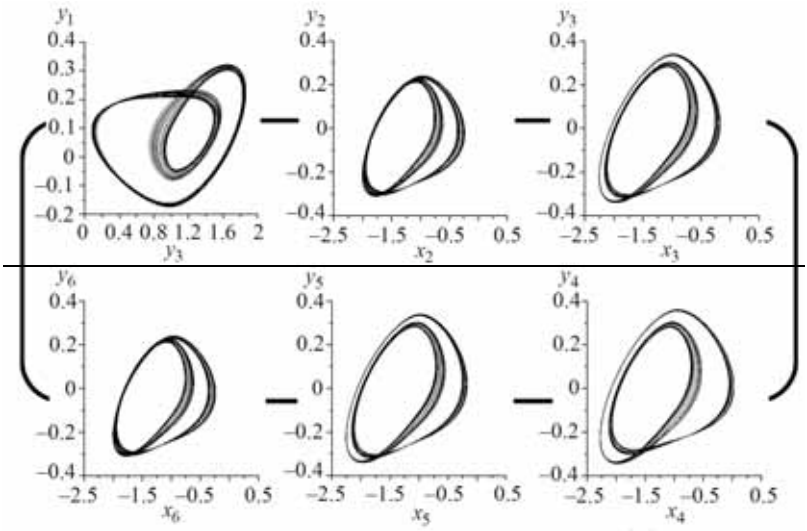

Fig. 4.42. Mirror cluster structure based on $O_a^r(4)$.

2. *Cyclic cluster structures of the ring.* This type of cluster structure is associated with the symmetry of the rotation of the ring. However, we come to the existence of such structures and define their base C-oscillator based on the physical principles reflected in the elementary transformations and the coagulability of circuits of the structures. Suppose that a certain uncut *n*-cluster structure is realized in the ring. We reduce all of the elementary oscillators of one cluster to a single node (by short circuiting, see Fig. 4.43a). As a result, we obtain a figure resembling an *m*-petal "rose" (see Fig. 4.43b).

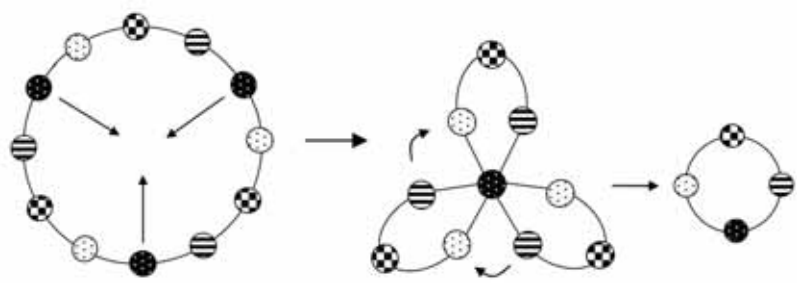

a b c

Fig. 4.43. Convergence of a circuit of the cyclic cluster structure.

Suppose that, among the oscillators of each petal, there are no single-coloured ones (from different clusters). Now we prove that, in this case, the order of the oscillators on the petals is the same: continue the convergence of the circuit of the cluster structure by turning the "petals" until the matching of same-coloured oscillators (short circuits). As a result, a ring of unsynchronized oscillators is formed (see Fig. 6.43c). This ring also represents the sought C-oscillator of "cyclic" structures.

The fusion of the circuit of the cyclic structure is carried out in the reverse order: we assume that there are m identical rings (cluster forming oscillators) superimposed on each other. Further, this system unfolds with respect to the image of any oscillator (more precisely, a node of m identical oscillators) into an m-petal "rose". Then the images of the oscillators located in the nodes blossom in their places. The same result is obtained as a result of successive rotations of the arc of "multi-coloured" oscillators.

We denote the basic cluster forming oscillator of cyclic cluster structures as $O_s^r(n)$.

Definition 4.4.2. A system of $n \geq 3$ coupled elementary oscillators of the form

$$\dot{\mathbf{X}} = \mathbf{G}(\mathbf{X}) - \varepsilon \mathbf{B}_s^r \otimes \mathbf{C}\mathbf{X}, \tag{4.15}$$

$$\mathbf{X} = (\mathbf{X}_1, \mathbf{X}_2, ..., \mathbf{X}_n)^T, \ \mathbf{G}(\mathbf{X}) = (\mathbf{F}_1(\mathbf{X}_1), \mathbf{F}_2(\mathbf{X}_2), ..., \mathbf{F}_n(\mathbf{X}_n))^T,$$

$$\mathbf{B}_s^r = \begin{pmatrix} 2 & -1 & 0 & 0 & \dots & 0 & 0 & 0 & -1 \\ -1 & 2 & -1 & 0 & \dots & 0 & 0 & 0 & 0 \\ 0 & -1 & 2 & -1 & \dots & 0 & 0 & 0 & 0 \\ 0 & 0 & -1 & 2 & \dots & 0 & 0 & 0 & 0 \\ \vdots & \vdots & \vdots & \vdots & \ddots & \vdots & \vdots & \vdots & \vdots \\ 0 & 0 & 0 & 0 & \dots & 2 & -1 & 0 & 0 \\ 0 & 0 & 0 & 0 & \dots & -1 & 2 & -1 & 0 \\ 0 & 0 & 0 & 0 & \dots & 0 & -1 & 2 & -1 \\ -1 & 0 & 0 & 0 & \dots & 0 & 0 & -1 & 2 \end{pmatrix},$$

is called the cyclic C-oscillator $O_s^r(n)$ and is conditioned that, in the phase space, there exists attractor $A_s^r(n)$ such that for $\forall(\mathbf{X}_1, \mathbf{X}_2, ..., \mathbf{X}_n) \in A_s^r(n), \ \mathbf{X}_i \neq \mathbf{X}_j, \ i \neq j, \ i = \overline{1,n}, \ j = \overline{1,n}.$

One can see that Eq. (4.15) represents a ring of *n* oscillators.

It is not difficult to see that Eq. (4.15) represents a ring of *n* oscillators. Fig. 4.44 shows a cyclic cluster structure obtained in a homogeneous ring of $N = 6$ Chua's oscillators. The following parameter set has been used: $\{\alpha, \beta, \gamma, m_0, m_1, \varepsilon\} =$ $= \{9.5, 14, 0.1, -1/7, 2/7, 0.08\}$.

It is evident that the number of synchronized C-oscillators and the number of clusters are related to the number of oscillators in the ring by a simple relation: $N = mn$. This allows formulation of a simple statement: if *s* is the number of all multipliers of number *N*, excluding *N* itself, then the number of cyclic structures in the ring equals *s*. For instance, for $N = 12$, there exist four cyclic structures based on $O_s^r(n)$: a structure of two C-oscillators of the type $O_s^r(6)$, a structure of three C-oscillators of the type $O_s^r(4)$, a structure of four C-oscillators of the type $O_s^r(3)$ and a structure of six C-oscillators of the type $O_s^r(2)$. For $N = 6$ and a structure of six C-oscillators of the type Fig. 4.44.

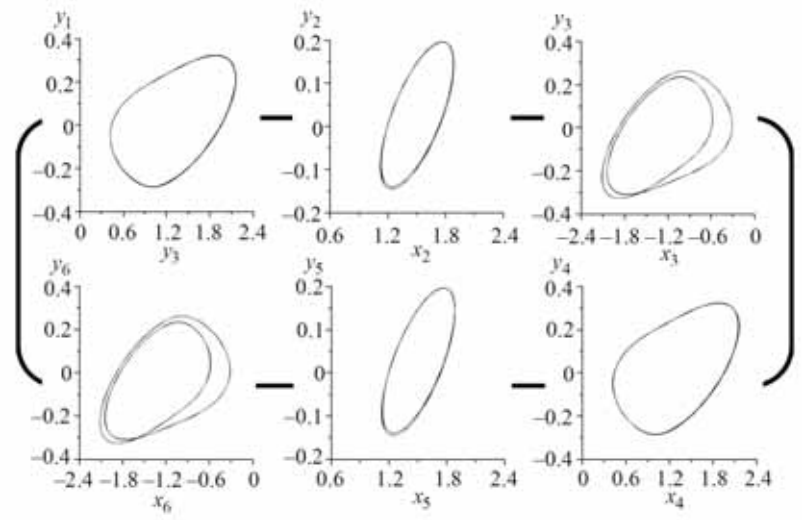

Fig. 4.44. Cyclic cluster structure based on $O_s^r(3)$

Above, we have defined four types of cluster structures of the ring. The inner conviction suggests (everything is taken into account, nothing else can be) that a complete group of cluster forming oscillators is found. Let us try to prove it. We formulate a simple lemma.

Lemma 4.4.1.

1) If the oscillators at the ends of two parallel chords are synchronized in pairs (see Fig. 4.45a), then the oscillators at the ends of all of the chords of the bundle are synchronized in pairs.

2) If the oscillators at the ends of two intersecting chords are synchronized in pairs (see Fig. 4.45b), then the oscillators at the ends

of all of the chords of the bundle are synchronized in pairs (oscillators are distributed along the ring in an appropriate way).

Proof.

1) Consider oscillators of chord *EF*. We write the Kirchhoff equations for oscillators *A* and *B*:

$$V_C + V_E - 2V_A = I_A R, \quad V_D + V_F - 2V_B = I_B R.$$

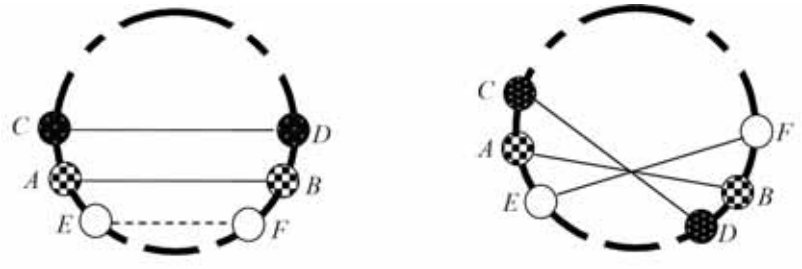

a b

Fig. 4.45. Example for Lemma 4.4.1.

According to condition $V_A = V_B$, $V_C = V_D$, $I_A = I_B$ (synchronization). Hence, we obtain the equality $V_E = V_F$, i.e. oscillators *E* and *F* are synchronized. Further, the reasoning is repeated for the oscillators of all other chords of the bundle.

2) The proof is similar to the first case. Consider oscillators of chord *EF*. The Kirchhoff equations for oscillators *A* and *B* have the form:

$$V_C + V_E - 2V_A = I_A R, = V_D + V_F - 2V_B = I_B R.$$

According to the condition $V_A = V_B$, $V_C = V_D$, $I_A = I_B$ (synchronization). Hence, we obtain equality $V_E = V_F$, i.e. oscillators *E* and *F* are synchronized. Further, the reasoning is repeated for the oscillators of all other chords of the bundle.

Theorem 4.4.1. Cluster forming oscillators $O_s(n)$, $O_a(n)$, $O_a^r(n)$ and $O_s^r(n)$ constitute a full set of types of C-oscillators in a ring of oscillators and define all types of cluster structures that can exist in the ring.

Proof. Let us assume that some cluster structure is realized in the ring. We select arc $\overset{\frown}{AF}$ with the maximum number *n* of unsynchronized oscillators and number them counter-clockwise, starting at one end (see Fig. 4.46).

By the condition, the oscillator *G* is synchronized with one of the oscillators of arc $\overset{\frown}{AF}$ We will consider various cases. If in each of them the cluster structure is represented by one of the four of these C-oscillators, then this will be a proof of the theorem, excluding, of course, physically impossible cases.

1) Suppose that oscillator *G* is synchronized with oscillator *F*. In this case, this pair of oscillators is a cut pair and, therefore, this

cluster structure is also a cut structure. The basic cluster forming oscillators of such structure are $O_s(n)$ or $O_a(n)$.

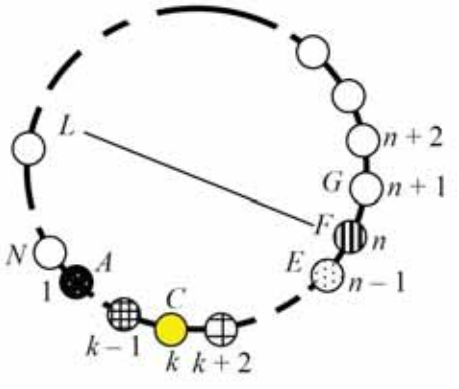

Fig. 4.46. For Theorem 4.4.1.

2) Suppose that oscillator *G* is synchronized with oscillator *E*. According to p.1 of Lemma 4.4.1 (a special case when one of the chords is tied to the point), oscillators at the ends of all chords that are parallel to *GE* are synchronized, and we have a structure that is symmetric with respect to the diameter passing through the oscillator *F*. If the number of oscillators in the ring is odd, then the last short chord of the bundle contracts the cut pair; that is, there is again a cut structure with the basic C-oscillator $O_a(n)$. If the number of oscillators is even, then diameter *FL* passes through the middle of the oscillators. Suppose that, among the oscillators of arc $\widetilde{LG}$, there is no cut pair (otherwise the structure is cut and its C-oscillator is $O_a(n)$). In such a case, this cluster structure (symmet-

ric with respect to diameter *FL*) is a "mirror" and its C-oscillator is $O_a^r(n)$.

3) Suppose that oscillator *G* is synchronized with oscillator *C*. We make equivalent transformations of the cluster structure: synchronized oscillators *C* and *G* are "tightened" into a node, and then we "move" them along different circles (see Fig. 4.47a,b).

We write the Kirchhoff equations for oscillators *G* and *C* in the first and second positions of the system:

$$V_{n+2} + V_n - 2V_G = I_G R, \quad V_{k-1} + V_{k+2} - 2V_C = I_C R,$$
$$V_{k-1} + V_{n+2} - 2V_C = I_C R, \quad V_{k+1} + V_n - 2V_G = I_G R.$$

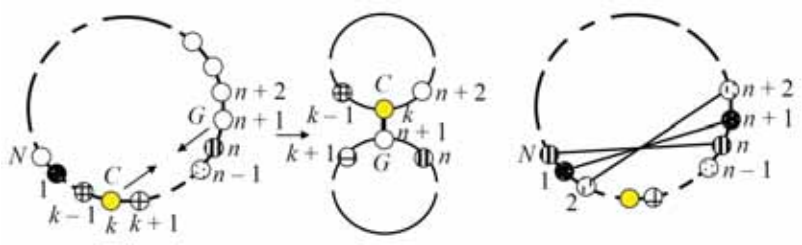

a b c

Fig. 4.47. Equivalent transformations of the circuit of a cluster structure.

Taking into account equalities $V_G = V_C$, $I_G = I_C$ (synchronization), we obtain $V_n = V_{k-1}$ and $V_{n+2} = V_{k+1}$. For any $k > 1$, these equations contradict the condition that the first *n* oscillators are not synchronized, and when $k = 1$, taking into account that $V_0 = V_N$, we

obtain equalities $V_n = V_N$, $V_{n+2} = V_2$. According to Lemma 6.1, the latter equations define a cyclic cluster structure with basic C-oscillator $O_s^r(n)$. (see Fig. 4.47c). The theorem is proven.

Conclusion. If p is the number of all multipliers (simple and composite) of number $N/2$, including the number itself, and q is the number of all odd multipliers of number N, including the number itself if it is odd, then the full number of cut structures in the ring equals $p+q$. If r is the number of all multipliers of number $N/2$, including the number itself, then in the ring there exist r "mirror" cluster structures based on C-oscillator $O_a(n)$ If s is the number of all multipliers N, excluding N, then the number of cyclic structures based on C-oscillator $O_s^r(n)$ equals s. The full number of cluster structures of all types equals $p+q+r+s$.

The proof of the conclusion is actually given above, during the investigation of types of cluster oscillators.

For example, if $N=12$, then, according to *Conclusion*, there are 11 cluster structures in the ring. Listing them is not difficult. Note that in the case of a simple N, there exists a unique simple cell (it is also a cut one) in the ring based on simple cell $O_a(n)$ with number of clusters $n=(N+1)/2$.

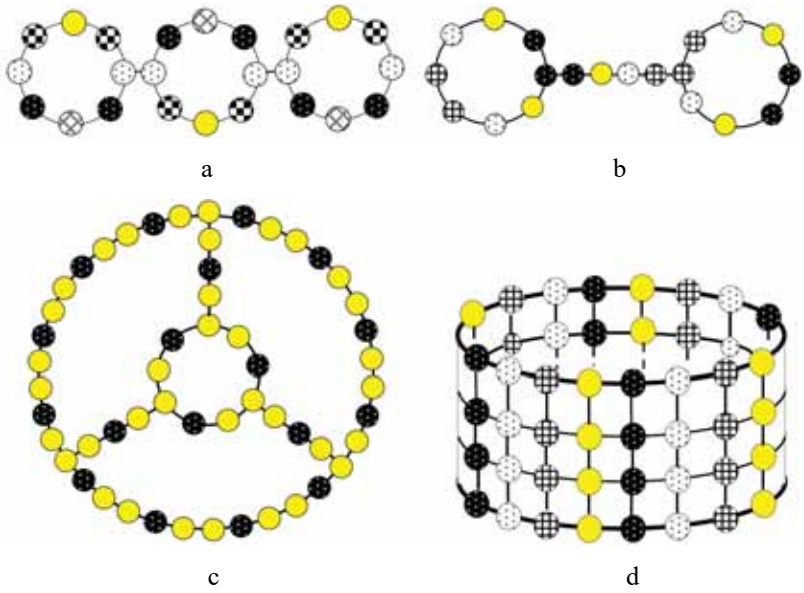

Fig. 4.48. Examples of cluster structures based on different cluster structures and based on the different C-oscillators of the ring:

a) structure based on C-oscillators $O_a^r(5)$, b) structure based on C-oscillators $O_s(4)$, c) structure based on C-oscillators $O_a(2)$, d) structure based on C-oscillators $O_s^r(4)$.

At the end of this section, we also note that the above types of cluster forming oscillators can serve as the basis for the circuits of structures, not only in the ring, but also in other lattices, for which the ring is an element of their construction (see Fig. 4.48).

4.5. C-oscillators, simple cells and cluster structures in two-dimensional lattices

Two-dimensional lattices of oscillators are common models of the theory of oscillations and waves. A lot of papers [100, 205 – 213, etc.] are devoted to the study of dynamic processes from various fields of natural science, modeled with the help of these objects. We are interested in studying the existence and systematization of various types of cluster structures in these lattices.

The study of structures will be carried out in the context of synchronization of C-oscillators and their simple cells [190, 191].

The equation of a two-dimensional oscillator lattice has the following form:

$$\dot{\mathbf{X}}_{ij} = \mathbf{F}_{ij}\left(\mathbf{X}_{ij}\right) + \varepsilon\mathbf{C}\left(\mathbf{X}_{i-1\,j} + \mathbf{X}_{i+1\,j} + \mathbf{X}_{ij-1} + \mathbf{X}_{ij+1} - 4\mathbf{X}_{ij}\right),$$
$$i = \overline{1, N_1}, \quad j = \overline{1, N_2}. \tag{4.16}$$

We define the boundary conditions in (4.16) later on.

One-dimensional C-oscillators of two-dimensional gratings.

1) Note that the chain is a special case of a two-dimensional lattice. Its equations are obtained from Eqs. (4.16) by imposing boundary conditions of the form $\mathbf{X}_{0j} \equiv \mathbf{X}_{1j} \equiv \mathbf{X}_j$, $\mathbf{X}_{10} \equiv \mathbf{X}_{11} \equiv \mathbf{X}_1$, $\mathbf{X}_{2j} \equiv \mathbf{X}_{1j} \equiv \mathbf{X}_j$, $\mathbf{X}_{1n+1} \equiv \mathbf{X}_{1n} \equiv \mathbf{X}_n$. For this reason, C-oscillators of the chain: $O_s\left(n\right)$ and $O_a\left(n\right)$ are the same for a two-dimensional

lattice. We denote $O_s(n)$ as $O_s(1\times n)$. Further under the notation "$m \times n$", we will mean both the dimensions of the respective lattice and the product mn. It is obvious that the denoted C-oscillator and $O_s(1\times n)$ physically identical and must be classified as one type: up to notation, they are represented by the same equations and have the same "working" attractors. However, structures based on one or the other, synthesized in the same lattice, will be different. This fact should be taken into account. An example is shown in Fig. 4.49. Hereinafter, the couplings between the images of elementary oscillators are depicted by joining the sides of the squares.

Let us formulate a statement about the number of structures of this type in the lattice $N_1 \times N_2$.

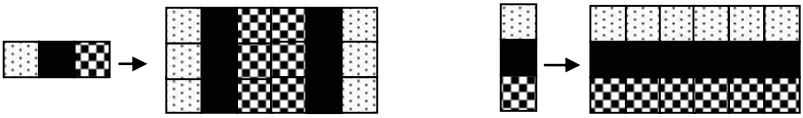

a b

Fig. 4.49. Examples of one-dimensional C-oscillators of two-dimensional lattices based on C-oscillators $O_s(1\times n)$ and $O_s(n\times 1)$.

Statement 1. Suppose p and q are the numbers of all multipliers of numbers N_1 and N_2 accordingly, including the numbers N_1 and N_2 themselves in the number of multipliers, then the total number

of structures based on C-oscillators $O_s(1\times n)$ and $O_s(n\times 1)$ in the lattice with dimension $N_1\times N_2$ equals to $p+q$.

2) The second type of C-oscillators of chains $O_a(n)$ is also a structure-forming C-oscillator of two-dimensional lattices. We denote it as $O_a(1\times n)$. The latter is defined by system of oscillators (4.16) for $i=1,\ \ j=\overline{1,n}$ and with boundary conditions $\mathbf{X}_{0j}\equiv\mathbf{X}_{1j}\equiv\mathbf{X}_j$, $\mathbf{X}_{10}\equiv\mathbf{X}_{11}\equiv\mathbf{X}_1,\ \ \mathbf{X}_{2j}\equiv\mathbf{X}_{1j}\equiv\mathbf{X}_j,\ \ \mathbf{X}_{1n+1}\equiv\mathbf{X}_{1n}\equiv\mathbf{X}_n$. It is assumed that the system contains a cluster attractor $A_a(n)$ in its phase space. Similarly to above, C-oscillator $O_a(n\times 1)$ is identified with C-oscillator $O_a(1\times n)$ with reservations made regarding the fusion of circuits based on them. Examples of circuit fusion based on this C-oscillator are shown in Fig. 4.50.

Statement 2. Suppose *p* and *q* are the numbers of all odd multipliers of numbers N_1 and N_2 accordingly, including the numbers N_1 and N_2 themselves in the number of multipliers, if they are odd. In this case, the total number of structures based on C-oscillators $O_a(1\times n)$ and $O_a(n\times 1)$ equals to $p+q$.

Two-dimensional C-oscillators.

Since we are dealing with a rectangular lattice, it is natural to assume that simple cells have the same form. This assumption is, ac-

tually, correct. If the circuit is not cut, then it entirely represents a rectangular circuit of a simple cell. If it is cut, then by simple means, one can prove that the cut line cannot be a broken (non-straight) line. When folding the simple cell, we will use various types of symmetry of rectangles (and/or squares) [214].

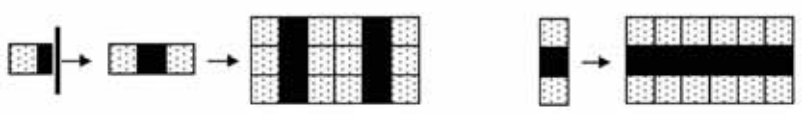

a b

Fig. 4.50. Cluster structures of simple cells of C-oscillators $O_a(1\times n)$ and $O_a(n\times 1)$.

3) Let us assume that a certain cluster structure is realized in the lattice under consideration and its circuit is cut into identical circuit blocks of simple cells. We will evaluate various options of how the cluster structure of the simple cell itself can be “arranged”. The first of the possible cases is the case of the maximum number of clusters, or, in other words, the case when all the oscillators of the simple cell are unsynchronized. In this case, the simple cell is special, and it also represents a special C-oscillator: a two-dimensional analogue of $O_s(n)$ in the chain. We denote it as $O_{ss}(m\times n)$ and define it as a system of oscillators (4.16) with boundary conditions $\mathbf{X}_{0j}\equiv\mathbf{X}_{1j}$, $\mathbf{X}_{i0}\equiv\mathbf{X}_{i1}$, $\mathbf{X}_{m+1j}\equiv\mathbf{X}_{mj}$, $\mathbf{X}_{in+1}\equiv\mathbf{X}_{in}$ (rectangular

$m \times n$ -lattice) provided there is a cluster attractor $A_{ss}(mn)$ in its phase space.

Statement 3. Suppose *p* and *q* are the numbers of all multipliers of numbers N_1 and N_2 accordingly, including the numbers themselves in the number of multipliers, then in a lattice with dimension $N_1 \times N_2$, there exist $pq-1$ of cluster structures based on C-oscillator $O_{ss}(m \times n)$, $m \geq 2$, $n \geq 2$.

Note that $O_s(n)$ can be considered as a special case $O_{ss}(m \times n)$, when one of the numbers equals to one.

An example of the fusion of a circuit of cluster structure based on C-oscillator $O_{ss}(2 \times 3)$ in a rectangular lattice with dimension (4×6) depicted in Fig. 4.51a, while Fig. 4.51b shows an example of a "free" fusion of a circuit of the cluster structure in an "irregular" lattice based on the same C-oscillator (as a by-product).

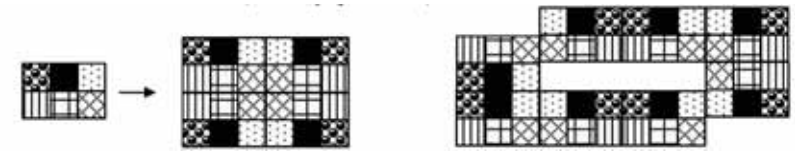

a b

Fig. 4.51. Fusion of a circuit of cluster structure based on C-oscillator $O_{ss}(2 \times 3)$: a) in a rectangular lattice; b) in the "irregular" lattice.

4) Suppose that a rectangular (or square) simple cell is not special, that is, there are synchronized oscillators among its elements. Consequently, its circuit in one or another way should be reduced to the circuit of C-oscillator. We will take into account the experience of folding simple cells of a chain and of a ring using different types of symmetry. We start with the case of one iteration of folding.

Suppose that the circuit is symmetric with respect to one of the symmetry planes (as one knows, there are two of them). In this case, the respective side of the rectangle contains an odd number of elements, and the trace of the mirror passes through the middle of images of the oscillators. Otherwise (the number of oscillators on the side is even), the trace of the mirror would be a cut line, which would contradict the property of the simple cell. Bending the cluster structure through the mirror's trace, we obtain the image of the C-oscillator (see Fig. 4.52). Suppose that an odd number of oscillators is located in a column (see Fig. 4.52a). In this case, the C-oscillator, which we denote is determined by system (4.16) for $i=\overline{1,m}$, $j=\overline{1,n}$ with boundary conditions $\mathbf{X}_{0j}\equiv\mathbf{X}_{1j}$, $\mathbf{X}_{i0}\equiv\mathbf{X}_{i1}$, $\mathbf{X}_{m-1\,j}\equiv\mathbf{X}_{m+1\,j}$, $\mathbf{X}_{in}\equiv\mathbf{X}_{in+1}$, which has a cluster attractor in the phase space $A_{as}\left(mn\right)$. A simple cell of this C-oscillator consists of a pair of rigidly coupled C-oscillators. Her size is $\left(2m-1\right)\times n$. As a check, one can make sure that the equations of the simple cell are represented by a pair of systems of coupled C-oscillators and de-

compose into a pair of these systems in the regime of data synchronization of C-oscillators. This is a formal criterion for the fact that the found object actually represents a C-oscillator.

The fusion of the circuit of the cluster structure of a simple cell occurs in the reverse order – by attaching its mirror image to the image of C-oscillator.

a b

Fig. 4.52. An example of a mirror transformation of cluster structure – the folding of simple cells based on C-oscillators $O_{as}\left(m\times n\right)$ and $O_{sa}\left(m\times n\right)$.

If the cluster structure of a simple cell is symmetric with respect to another plane (see Fig. 4.52b), then we come to the definition of C-oscillator $O_{sa}\left(m\times n\right)$. This will be system (4.16) for $i=\overline{1,m}$, $j=\overline{1,n}$ and with boundary conditions $\mathbf{X}_{0j}\equiv\mathbf{X}_{1j}$, $\mathbf{X}_{i0}\equiv\mathbf{X}_{i1}$, $\mathbf{X}_{in-1}\equiv\mathbf{X}_{in+1}$, $\mathbf{X}_{mj}\equiv\mathbf{X}_{m+1j}$. In this case, the size of the simple cell $m\times\left(2n-1\right)$. An example of C-oscillator $O_{sa}\left(2\times 3\right)$ and of the fusion of the simple cell is shown in Fig. 4.52b. Both C-oscillators belong to the same type. Note that C-oscillators $O_{a}\left(1\times n\right)$ and

$O_a(m\times 1)$ can be considered a special case of these two-dimensional C-oscillators.

Based on the size of simple cells and the size of the lattice $N_1\times N_2$, we obtain the following statement about the number of structures based on C-oscillators $O_{as}(m\times n)$ and $O_{sa}(m\times n)$.

Statement 4. Suppose *p* and *q* are the numbers of all odd multipliers of numbers N_1 and N_2, accordingly, including the numbers N_1 and N_2, themselves in the number of multipliers if they are odd. If n_1 and n_2 are the numbers of all odd multipliers of numbers N_1 and N_2, including the numbers themselves in the number of multipliers. Then in this lattice there exists pn_2 and qn_1 cluster structures based on C-oscillators $O_{as}(m\times n)$ and $O_{sa}(m\times n)$, respectively. The total number of structures of this type pn_2+qn_1. For example, in the lattice 3×6 $p=1,\ q=1,\ n_1=1,\ n_2=3,$ that is, there are four cluster structures of this type. All of their fusion diagrams are shown in Fig. 4.53.

Note, if N_1 and N_2 are integers, then in the lattice $N_1\times N_2$ there are only two cluster structures of this type. One of them has the number of clusters $N_1(N_2+1)/2$, while the second one – $N_2(N_1+1)/2.$

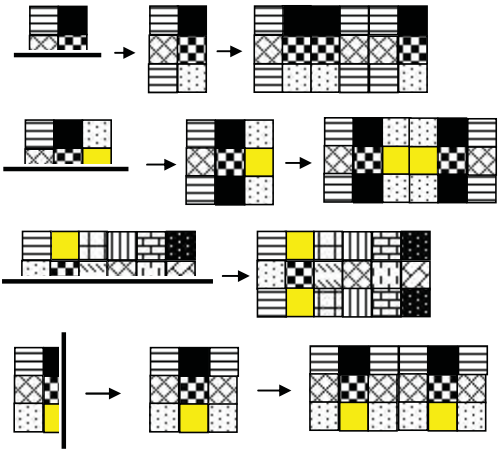

Fig. 4.53. An example of the fusion - cluster structures based on C-oscillators $O_{as}(m\times n)$ and $O_{sa}(m\times n)$ in the lattice with dimension 3×6.

5) Suppose that the circuit of a cluster structure of the simple cell obtained as a result of one iteration of folding (as a result of bending the circuit through one of the axes) contains synchronized oscillators. This figure is symmetric about the second plane of symmetry, the trace of which also passes through the middle of images of the oscillators. Otherwise, the cluster structure would be cut, which contradicts the condition. Performing the second bend of the circuit through the trace of the second mirror, we obtain the circuit of the desired C-oscillator. Such a procedure of folding a circuit that is mirrored with respect to two planes is shown in Fig. 4.54. Here the “quarter” of the image of an elementary oscillator has the same meaning as the “half”.

Writing the equations of a simple cell in the form of a quadruple of coupled systems, one can make sure that the resulting object indeed represents a circuit of the C-oscillator.

We denote the resulting C-oscillator $O_{aa}(m\times n)$ and define it as system (4.16) for $i=\overline{1,m}$, $j=\overline{1,n}$ (rectangular lattice of *mn* oscillators) with boundary conditions of the form $\mathbf{X}_{0j}\equiv\mathbf{X}_{1j}$, $\mathbf{X}_{i0}\equiv\mathbf{X}_{i1}$, $\mathbf{X}_{m-1j}\equiv\mathbf{X}_{m+1j}$, $\mathbf{X}_{in-1}\equiv\mathbf{X}_{in+1}$ under the condition of existence of a cluster attractor $A_{aa}(mn)$. A simple cell of this type consists of four coupled C-oscillators and has dimensions $(2m-1)\times(2n-1)$.

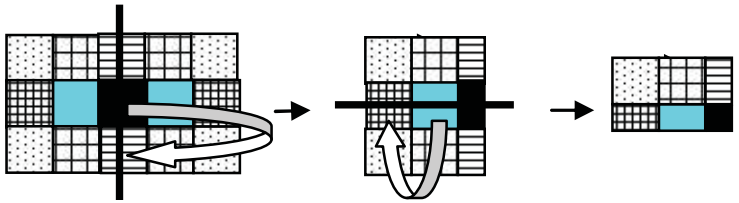

a b c

Fig. 4.54. The order of folding the circuit of the cluster structure with double axial symmetry.

From what has been said, we formulate a statement about the number of structures based on $O_{aa}(m\times n)$ in the lattice with dimension $N_1\times N_2$.

Statement 5. Suppose $\{p\}$, $\{q\}$ are all odd multipliers of numbers N_1 and N_2, including the numbers N_1 and N_2 themselves if they are odd. Then the number of cluster structures based on $O_{aa}(m \times n)$ in the lattice $N_1 \times N_2$ is equal to the number of all possible pairs (p_i, q_j). The number of clusters in each structure is $mn = (p_i + 1)(q_j + 1)/4$.

6) Let us turn to the circuits of simple cells with central symmetry. Suppose that in $m \times n$ cell, a cluster structure with central symmetry is implemented and at least one of its dimensions is an even number. The procedure for folding the circuit of the cluster structure in this case will look as follows. Let us mentally draw a straight line (perpendicular to the even side) dividing the circuit into two parts, containing identical sets of non-synchronized oscillators (see Fig. 4.55a). In this case, the circuits of both parts can be combined as a result of turning one of them by 180° relative to the center (see Fig. 4.55b). We assume that couplings of the oscillators adjoining along the named line are preserved. Carrying out this procedure, we obtain the diagram shown in Fig. 4.55c. The set of oscillators of this lattice represents a C-oscillator, which we denote $O_{2a}^{\pi r}(mn/2)$ and will call it the *π-rectangle*. Here $mn/2$ is the number of clusters in the cluster structure of the simple cell.

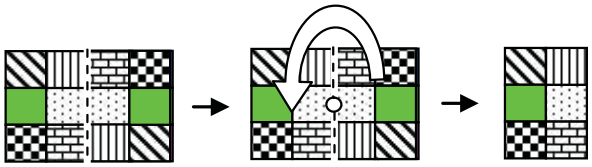

a b c

Fig. 4.55. The order of folding the circuit of the cluster structure with central symmetry based on $O_{2a}^{\pi r}(mn/2)$

Statement 6. Suppose p and q are the numbers of all even multipliers of numbers N_1 and N_2, including the numbers N_1 and N_2 themselves if they are odd. Suppose n_1 and n_2 are the numbers of all multipliers of numbers N_1 and N_2, including the numbers N_1 and N_2 themselves. Then in this lattice there exists $pn_2 + qn_1$ cluster structures based on $O_{2a}^{\pi r}(mn/2)$.

7) Let us assume that a simple cell with a centrally symmetric cluster structure has dimensions $m \times n$, where both numbers are odd. In this case, the center of the lattice is located on the image of the central elementary oscillator. The procedure for folding the circuit of the cluster structure scheme to the circuit of C-oscillator will be as follows. Let us mentally draw a three-link broken line, crossing the central oscillator and dividing the circuit into two identical blocks, composed of their "multi-colored" oscillators (see Fig. 4.56a). The resulting pair of circuits is united as a result of turning one of them

by 180° relative to the center of the lattice (see Fig. 4.56b). We assume that the couplings between all oscillators are preserved. As a result of rotation, we obtain an image of the C-oscillator (see Fig. 4.56c). We denote this C-oscillator $O_{2a}^{\pi f}\left(\left(mn+1\right)/2\right)$ and will call it *π-flag*. Here $\left(mn+1\right)/2$ is the number of clusters produced by this C-oscillator. The fusion of the circuit of the cell occurs in the reverse order.

Based on the size of the simple cell, we formulate the following statement about the number of cluster structures in the lattice $N_1 \times N_2$, whose circuits can be synthesized based on $O_{2a}^{\pi f}\left(\left(mn+1\right)/2\right)$.

Statement 7. Suppose $\{p\}$, $\{q\}$ are the numbers of odd multipliers numbers N_1 and N_2, including the numbers N_1 and N_2 themselves if they are odd. Then the number of cluster structures based on $O_{aa}\left(m \times n\right)$ in the lattice $N_1 \times N_2$ is equal to the number of all possible different pairs $\left(p_i,\, q_j\right)$.

The list of C-oscillators of two-dimensional lattices will be incomplete if we do not add to it the types of C-oscillators that define cluster structures in square simple cells and are associated with their additional diagonal symmetry.

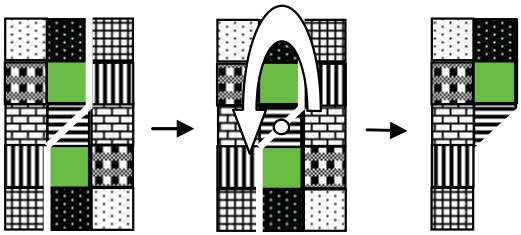

a b c

Fig. 4.56. Folding of the cluster structure with central symmetry based on $O_{2a}^{\pi f}\left((mn+1)/2\right)$.

8) Let us start with the case of the maximum number of clusters of a cluster structure in a square simple cell. Let us assume that the number of unsynchronized ("multi-colored") oscillators on the side of the square equals to n and the cluster structure is symmetric with respect to one of its diagonals. By over-bending the circuit of the structure via the diagonal (mirror trace, see Fig. 4.57a), we obtain the circuit of a C-oscillator (see Fig. 4.57, b). We denote this C-oscillator $O_{2a}^{f}\left(n(n+1)/2\right)$ and will call it *flag 2*. Here $n(n+1)/2$ is the number of cluster produced by the C-oscillator.

Based on the simple problem of the number of ways to cover the lattice $N_1 \times N_2$ by all possible squares, we will formulate a statement about the number of cluster structures, the base of which can be $O_{2a}^{f}\left(n(n+1)/2\right)$ for the different n.

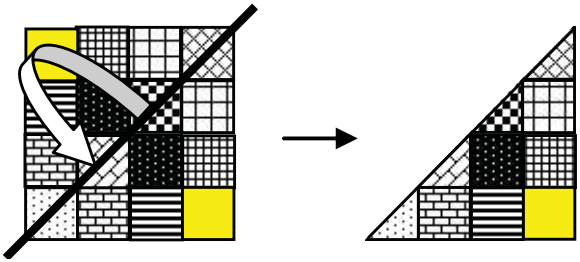

a b

Fig. 4.57. Folding of a circuit of a simple cell based on $O_{2a}^{f}\left(n(n+1)/2\right)$.

Statement 8. Suppose $\{p\}$, $\{q\}$ are the numbers of all multipliers of numbers N_1 and N_2, including these numbers themselves. Then the number of cluster structures based on $O_{2a}^{f}\left(n(n+1)/2\right)$ in the lattice $N_1 \times N_2$ equals to the number of possible pairs $\left(p_i,\ q_j = p_i\right)$ of identical multipliers.

9) To continue the study of the types of C-oscillators, it is necessary to separate the cases of an even and an odd number of oscillators located on the side of the square.

Suppose that the number of oscillators on the side of the square is even, $n = 2k$. Let us also assume that after the first iteration (the first bend via the diagonal), the resulting figure contains synchronized oscillators, symmetric with respect to the second diagonal (see Fig. 4.58a,b). Bending the last figure through the second diagonal, we get a figure filled with unsynchronized oscillators: a circuit

of C-oscillator. Let us denote this C-oscillator $O_{4a}^{f}\left(\left(n^2+2n\right)/4\right)$ and we will call it *flag 4*.

In this case, the simple cell consists of four coupled C-oscillators. The meaning of the halves of the oscillators is already known.

Let us formulate a statement about the number of structures of a given type in a lattice of given dimensions.

Statement 9. Suppose $\{p\}$, $\{q\}$ are the numbers of all even multipliers of numbers N_1 and N_2, including these numbers themselves if they are even. Then the number of cluster structures based on $O_{4a}^{f}\left(\left(n^2+2n\right)/4\right)$ in the lattice $N_1 \times N_2$ equals to the number of possible pairs $\left(p_i,\ q_j = p_i\right)$ of identical multipliers.

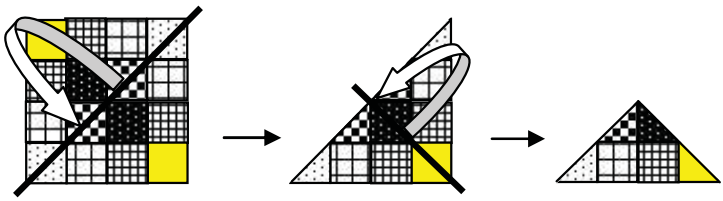

a b c

Fig. 4.58. The order of folding of a circuit of simple cell based on $O_{4a}^{f}\left(\left(n^2+2n\right)/4\right)$.

10) Suppose that the number of oscillators of the square is odd, $O_{4a}^{f}\left(\left(n^2+2n\right)/4\right)$. Let us also assume that after the first iteration (bending via the diagonal), synchronized oscillators, symmetrical with respect to the second diagonal, remain in the resulting figure (see Fig. 4.59b). Performing the second iteration, we obtain a figure filled with unsynchronized oscillator: a circuit of C-oscillator (see Fig. 4.59c). We denote this C-oscillator $O_{4a}^{p}\left(\left(n+1\right)^2/4\right)$ and we will call it *pyramid 4*. Simple cell consists of four coupled C-oscillators.

Let us formulate a statement about the number of structures of a given type in a lattice of given dimensions.

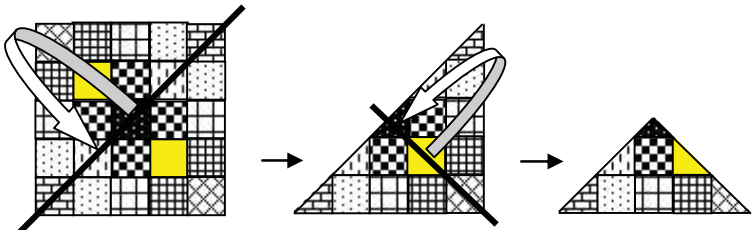

a b c

Fig. 4.59. The order of folding of a circuit of simple cell based on $O_{4a}^{p}\left(\left(n+1\right)^2/4\right)$.

Statement 10. Suppose $\{p\}$, $\{q\}$ are the numbers of all odd multipliers of numbers N_1 and N_2, including these numbers themselves if they are odd. Then the number of cluster structures based on

$O_{4a}^{p}\left(\left(n+1\right)^2/4\right)$ in the lattice $N_1 \times N_2$ equals to the number of possible pairs $\left(p_i,\ q_j = p_i\right)$ of identical multipliers.

11) The structure in a square with an odd number $\left(n = 2k+1\right)$ of oscillators has one more C-oscillator. Let us assume that after two iterations performed in paragraph 10, in the resulting circuit (see Fig. 4.59c), there remain synchronized oscillators, which are symmetric about its plane of symmetry. In this case, the folding of a circuit of the cell can be continued by bending through the respective axis. The sequence of iterations is shown in Fig. 4.60. We denote the resulting C-oscillator as $O_{8a}^{f}\left(\left(n+1\right)\left(n+3\right)/8\right)$ and will call it *flag 8*.

The fusion of the circuit of a cluster structure of the simple cell occurs in the reverse order. The simple cell consists of eight rigidly coupled C-oscillators. The meaning of 1/8 of the oscillator's image is the same as one for 1/2.

The number of structures based on $O_{8a}^{f}\left(\left(n+1\right)\left(n+3\right)/8\right)$ is defined by *Statement 10*.

Remark. There are no similar structures in a square with an even number of oscillators: when carrying out reverse iterations of the respective triangle shown in Fig. 4.60 (in the order: d, c, b, a) we

would obtain a cut structure (see Fig. 4.61). This contradicts the fact that a square lattice represents a simple cell.

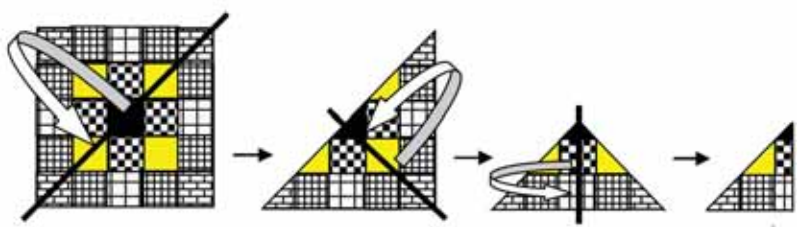

a b c d

Fig. 4.60. The order of folding of a circuit of simple cell based on $O_{8a}^{f}\left((n+1)(n+3)/8\right)$.

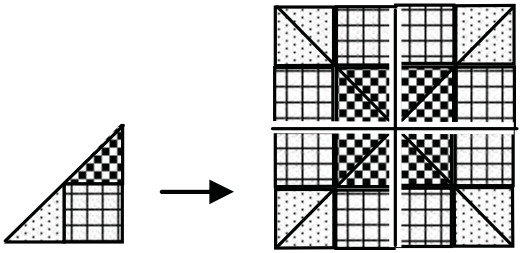

Fig. 4.61. Illustration for the *Remark*: (example of a cut structure).

Apparently, $(n+1)(n+3)/8$ is the minimum number of clusters in the structure, which is possible in a square oscillator lattice with an odd number of elementary oscillators and, $\left(n^2+2n\right)/4$ is the minimum number of clusters in the structure, which is possible in a

square oscillator lattice with an even number of elementary oscillators.

Above, we have considered all types of symmetries of structural schemes of rectangles and squares. The case of a special C-oscillator is also considered. Thus, there is enough confidence to believe that the presented set of types of C-oscillators is complete for a two-dimensional lattice. We omit the proof of this simple fact.

4.6. Stability of cluster structures

The phase space of homogeneous lattices of oscillators is complicated. In the general case, along with an attractor representing the cluster structure of interest (for example, $A_s(n)$, $A_a(n)$, etc.), there also exist other attractors in the phase space. These attractors can include attractor $A(1)$, which corresponds to spatially-homogeneous state of the lattice, which occurs always. This circumstance substantially complicates the problem of studying the stability of structures, including narrowing the set of research methods (excluding the second Lyapunov method). In addition, if the intrinsic properties of the main attractor $A(1)$, which we dealt with earlier, do not depend on parameter of the lattice ε, then this cannot be said of cluster attractors. Their properties, in particular the Lyapunov exponents, as well as the existence of these attractors, are determined by this parameter, which excludes the possibility of

formulating the stability conditions explicitly, like in the case of spatially homogeneous structures. This creates additional difficulties in the refinement of the analytical conditions of stability and suggests additional numerical or full-scale studies.

The stability of structures was considered from different positions in [94, 95, 98 – 101, 215 – 222, etc.]. We will solve this problem within the framework of the aforementioned concepts of structures as products of synchronization of group oscillators.

Further, we assume that attractors of the cluster structures of interest exist and their properties are known. In particular, we assume that the maximal Lyapunov exponents of attractors are known.

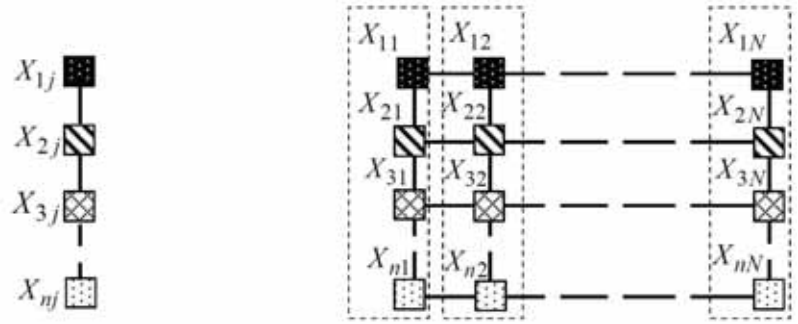

a b

Fig. 4.62. A circuit of C-oscillator $O_s(n)$, a); and tape cluster structure on its basis, b).

Stability of the simplest cluster structure based on $O_s(n)$ *during the parallel fusion.*

Fig. 4.62 shows a circuit of C-oscillator $O_s(n)$ as well as a circuit of a cluster structure on its base.

Equations of the lattice are composed using the experience from the previous sections. For vectors of the dynamical state of C-oscillator $\mathbf{Y}_j = \mathrm{col}\left(\mathbf{X}_{1j}, \mathbf{X}_{2j}, ..., \mathbf{X}_{nj}\right)$, $j = \overline{1, N_s}$, these equations take the form

$$\begin{aligned} &\dot{\mathbf{Y}}_j = \mathbf{G}\left(\mathbf{Y}_j\right) - \varepsilon\left(\mathbf{I}_n \otimes \mathbf{C}\right)\left(-\mathbf{Y}_{j-1} + 2\mathbf{Y}_j - \mathbf{Y}_{j+1}\right), \\ &j = 1, 2, ..., N. \end{aligned} \tag{4.17}$$

With boundary conditions: $\mathbf{Y}_0 = \mathbf{Y}_1$, $\mathbf{Y}_{N_s} = \mathbf{Y}_{N_s+1}$.

Let us study the local stability of attractor $A_s(n)$, by linearizing (4.17) in the vicinity of solution $\mathbf{Y}_1 = \mathbf{Y}_2 = ... = \mathbf{Y}_{N_s} = \xi(t) \in A_s(n)$.

With respect to vector $\mathbf{U} = \left(\mathbf{U}_1, \mathbf{U}_2, ..., \mathbf{U}_{N_s-1}\right)^T$, where $\mathbf{U}_i = \mathbf{Y}_i - \mathbf{Y}_{i+1}$, the corresponding linear system, written in a form of one equation, has the form

$$\dot{\mathbf{U}} = \left(\mathbf{I}_p \otimes \mathbf{J}\left(\xi\right) - \varepsilon \mathbf{D}_p \otimes \mathbf{I}_n \otimes \mathbf{C}\right)\mathbf{U}, \tag{4.18}$$

where $p = N_s - 1$, $\mathbf{J}_k(\xi_k)$ is the Jacobi matrix of the elementary oscillator, $\mathbf{J}(\xi) = \mathrm{diag}\left(\mathbf{J}_1(\xi_1), \mathbf{J}_2(\xi_2), ..., \mathbf{J}_n(\xi_n)\right) - \varepsilon \mathbf{B}_n \otimes \mathbf{C}$ is the Jacobi matrix of C-oscillator $O_s(n)$, and $\mathbf{D}_p$ is a matrix of the form

$$\mathbf{D}_p = \begin{pmatrix} 2 & -1 & 0 & 0 & & & & \\ -1 & 2 & -1 & 0 & & & & \\ 0 & -1 & 2 & -1 & & & & \\ 0 & 0 & -1 & 2 & & & & \\ & & & & \ddots & & & \\ & & & & & 2 & -1 & 0 & 0 \\ & & & & & -1 & 2 & -1 & 0 \\ & & & & & 0 & -1 & 2 & -1 \\ & & & & & 0 & 0 & -1 & 2 \end{pmatrix}.$$

Eq. (4.18) complies with Lemma 3.1.1, and, consequently, with Theorem 3.1.1 under the condition of replacement of matrix $\mathbf{C}$ (in Lemma and in Theorem) by matrix $\mathbf{I}_n \otimes \mathbf{C}$. Taking this into account and considering that eigenvalues of matrix $\mathbf{D}_p$ are known to us, we obtain conditions of stability of the cluster structure in a form of the following inequalities $\varepsilon > \lambda_s(n) \Big/ 4\sin^2 \dfrac{\pi}{2N_s}$, if $\mathbf{C} = \mathbf{I}_m$, and $\varepsilon > \varepsilon^*\left(\lambda_s(n)\right) \Big/ 4\sin^2 \dfrac{\pi}{2N_s}$ in a general case of matrix $\mathbf{C}$.

As we see, the inequalities obtained for the stability of a given cluster structure and the corresponding inequalities in the case of a spatially homogeneous structure in the chain are identical in their forms: the circuit shown in Fig. 4.63 can be interpreted as a "chain of chains", so the number of elementary oscillators is replaced by the number of blocks – C-oscillators. The principal difference is that, in this case, the Lyapunov exponent depends on number ε: $\lambda_s = \lambda_s(n, \varepsilon)$. That is, these parameters are implicit in the coupling parameter, which means that additional numerical or full-scale studies of the dependence of the Lyapunov exponent on this parameter are required for the completeness of the picture. In [172], circuits, mathematical justification, and a procedure for measuring the exponents in a full-scale experiment are described. This concerns the case of chaotic cluster attractors. In the case of regular attractors, the situation looks simple: if the cluster attractor is regular, i.e. if $\lambda_s(n, \varepsilon) \le 0$, then structure is stable for any corresponding values of ε including the arbitrary, small ones. Obviously, we will arrive at a result of the same form in the case of a three-dimensional cluster structure based on $O_{ss}(m \times n)$ in a parallel fusion (see Fig. 4.63).

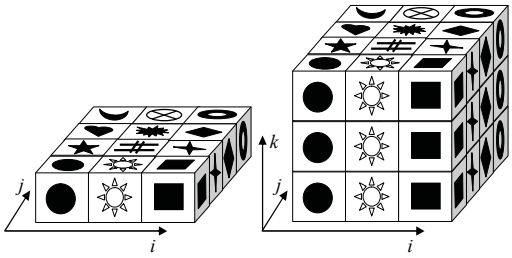

a b

Fig. 4.63. A circuit of a three-dimensional cluster structure in parallel synthesis of C-oscillator: a) a circuit of C-oscillator $O_{ss}(3\times 4)$, b) a diagram of a tape-mosaic cluster structure in a three-dimensional lattice $3\times 4\times 3$.

Stability of cluster structure based on $O_s(n)$ during the sequential fusion.

For the beginning, let us study the case of two C-oscillators (see Fig. 4.64).

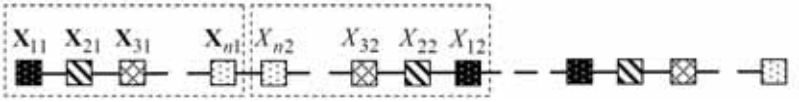

Fig. 4.64. A circuit of the cluster structure based on $O_s(n)$.

With respect to vectors $\mathbf{Y}_j = \mathrm{col}\left(\mathbf{X}_{1j}, \mathbf{X}_{2j}, ..., \mathbf{X}_{nj}\right)$, $j = 1, 2$, the dynamical system has the form

$$\begin{aligned} \dot{\mathbf{Y}}_1 &= \mathbf{G}\left(\mathbf{Y}_1\right) - \varepsilon\left(\mathbf{C}_* \otimes \mathbf{C}\right)\left(\mathbf{Y}_1 - \mathbf{Y}_2\right), \\ \dot{\mathbf{Y}}_2 &= \mathbf{G}\left(\mathbf{Y}_2\right) + \varepsilon\left(\mathbf{C}_* \otimes \mathbf{C}\right)\left(\mathbf{Y}_1 - \mathbf{Y}_2\right), \end{aligned} \tag{4.19}$$

where $\mathbf{C}_* = \mathrm{diag}(0, 0..., 0, 1)$ is the fusion matrix. A linearization of (4.19) by variable $\mathbf{U} = \mathbf{Y}_1 - \mathbf{Y}_2$ leads to the equation

$$\dot{\mathbf{U}} = \left(\mathbf{J}(\xi) - \varepsilon 2\mathbf{C}_* \otimes \mathbf{C}\right)\mathbf{U}. \tag{4.20}$$

Directly from Eq. (4.20), we find that a structure with regular internal dynamics is stable. This follows from the fact that matrix $\varepsilon 2\mathbf{C}_* \otimes \mathbf{C}$ is diagonal and can be considered as a perturbation of Jacobian $\mathbf{J}(\xi)$. Such perturbations do not increase the Lyapunov exponents of solutions [174, 223, 224]. In contrast to the parallel connection, where the fusion matrix was a unit matrix $(\mathbf{C}_* \to \mathbf{I}_n)$, in this case, it is impossible to formulate the stability conditions directly from Eq. (4.20) or, at least, it is difficult. To overcome technical difficulties, we formulate an additional lemma.

Lemma 4.6.1. Assume that the norm of variable matrix $A(t)$ is bounded: $\|A(t)\| = \mu$, and $\lambda_{\min} > 0$ is the least root of constant symmetric matrix B. Then, for $\varepsilon > \mu/\lambda_{\min}$, a trivial solution of equation

$$\dot{\mathbf{y}} = \left(\mathbf{A}(t) - \varepsilon\mathbf{B}\right)\mathbf{y} \tag{4.21}$$

is asymptotically stable.

Proof. Suppose that $\mathbf{Y}(t,t_0)$ is a matriciant of equation $\dot{\mathbf{y}} = -\varepsilon\mathbf{B}\mathbf{y}$. Then $\mathbf{Y}(t,t_0) = e^{-\varepsilon\mathbf{B}(t-t_0)}$ and $\left\|\mathbf{Y}(t,t_0)\right\| = e^{-\varepsilon\lambda_{\min}(t-t_0)}$. Taking expression $\mathbf{A}(t)\mathbf{y}$ as an external perturbation, we rewrite (4.21) in an integral form:

$$\mathbf{y}(t) = \int_{t_0}^{t} \mathbf{Y}(t,\tau)\mathbf{A}(\tau)\mathbf{y}(\tau)d\tau + \mathbf{Y}(t,t_0)\mathbf{c},$$

where **c** is an arbitrary constant vector. Estimating the norm of the right- and left-hand sides of this equation, we obtain the inequality

$$\left\|\mathbf{y}(t)\right\| \le \int_{t_0}^{t} \left\|\mathbf{Y}(t,\tau)\right\|\left\|\mathbf{A}(\tau)\right\|\left\|\mathbf{y}(\tau)\right\|d\tau + \left\|\mathbf{Y}(t,t_0)\right\|\left\|\mathbf{c}\right\|,$$

which, taking into account the proposed conditions, is transformed to the form

$$\left\|\mathbf{y}(t)\right\|e^{\varepsilon\lambda_{\min}t} \le \int_{t_0}^{t} \mu\left\|\mathbf{y}(\tau)\right\|e^{\varepsilon\lambda_{\min}\tau}d\tau + Ce^{\varepsilon\lambda_{\min}t_0},$$

where C is an arbitrary constant. After applying the well-known lemma (about the integral inequality) [225] to the given inequality, and after further minor transformations, we obtain $\left\|\mathbf{y}(t)\right\| \le Ce^{-(\varepsilon\lambda_{\min}-\mu)(t-t_0)}$. From this inequality, it follows that: if $\varepsilon > \mu/\lambda_{\min}$, then $\mathbf{y}(t) \to 0$ for $t \to \infty$. The Lemma is proven.

Let us establish relation of Eqs. (4.20) and (4.21). To do so, we select a variable part $\mathbf{A}(t) = \mathrm{diag}\left(\mathbf{J}_1(\xi_1), \mathbf{J}_2(\xi_2), ..., \mathbf{J}_n(\xi_n)\right)$ (truncated Jacobian) in the Jacobian of C-oscillator $\mathbf{J}(\xi) = \mathrm{diag}\left(\mathbf{J}_1(\xi_1), \mathbf{J}_2(\xi_2), ..., \mathbf{J}_n(\xi_n)\right) - \varepsilon \mathbf{B}_n \otimes \mathbf{C}$, while cluster matrix $\mathbf{B}_n$ will be merged with matrix $2\mathbf{C}_*$:

$$\mathbf{B} = \left(\mathbf{B}_n + 2\mathbf{C}_*\right) \otimes \mathbf{C} = \begin{pmatrix} 1 & -1 & 0 & 0 & & & & \\ -1 & 2 & -1 & 0 & & & & \\ 0 & -1 & 2 & -1 & & \mathbf{0} & & \\ 0 & 0 & -1 & 2 & & & & \\ & & & & \ddots & & & \\ & & & & & 2 & -1 & 0 & 0 \\ & & \mathbf{0} & & & -1 & 2 & -1 & 0 \\ & & & & & 0 & -1 & 2 & -1 \\ & & & & & 0 & 0 & -1 & 3 \end{pmatrix} \otimes \mathbf{C}.$$

In this case, Eq. (4.20) takes the form of Eq. (4.21). The norm of the truncated Jacobian:

$$\left\|\mathbf{A}(t)\right\| = \max\left(\left\|\mathbf{J}_1(\xi_1)\right\|, \left\|\mathbf{J}_2(\xi_2)\right\|, \ ..., \left\|\mathbf{J}_n(\xi_n)\right\|\right) = \left\|\mathbf{J}_0(\xi_0)\right\| = \mu.$$

Here we denote the "partial" Jacobian of the elementary oscillator with maximal norm $\mathbf{J}_0(\xi_0)$. It is known that the minimal eigenvalue of matrix $\mathbf{B}_n + 2\mathbf{C}_*$ equals $\lambda_{\min} = 4\sin^2\dfrac{\pi}{4n}$ (see Appendix). Summarizing the aforesaid matter, we formulate stability conditions for the trivial solution (4.20) (structure): the cluster structure, in the case of a pair of coupled C-oscillators, is stable if the following in-

equalities are satisfied: $\varepsilon > \mu \Big/ 4\sin^2 \frac{\pi}{4n}$, if $\mathbf{C} = \mathbf{I}_m$, and $\varepsilon > \varepsilon^*(\mu) \Big/ 4\sin^2 \frac{\pi}{4n}$ in a general case of matrix **C**. These conditions are sufficient.

Remark. The obtained stability conditions are known to be "rough". It may happen that when they are fulfilled, the "working" attractor of the C-oscillator has already ceased to exist, then the inequality reflects the stability of the respective integral manifold: the hypersurface, on which the mentioned attractor was located. In this case, the motion of the affix (phase) in the phase space of the lattice will be as follows: the phase point, starting from the neighborhood of the respective manifold, approaches it without limit, and then moves along the manifold to some of its stable submanifolds. With a large enough ε (area of global sustainability of $A(1)$), after passing through all the "empty" submanifolds, the affix approaches manifold M_0 and, therefore, attractor $A(1)$, that corresponds to the spatially homogeneous state of the lattice. If the process is recorded on the monitor in the form of a chain of phase portraits of elementary oscillators, then a kaleidoscope of alternating pictures of cluster structures will be observed as a result of the movement of the phase point "in the tracks" of the former cluster attractors.

Let us consider the case of an arbitrary number of C-oscillators of the type $O_s(n)$. With respect to vectors

$\mathbf{Y}_j = \mathrm{col}\left(\mathbf{X}_{1j}, \mathbf{X}_{2j}, ..., \mathbf{X}_{nj}\right)$, $j = 1, 2, ..., k$, we obtain the following system of equations:

$$\begin{aligned}
&\dot{\mathbf{Y}}_1 = \mathbf{G}\left(\mathbf{Y}_1\right) + \varepsilon\left(\mathbf{C}_* \otimes \mathbf{C}\right)\left(\mathbf{Y}_2 - \mathbf{Y}_1\right),\\
&\dot{\mathbf{Y}}_2 = \mathbf{G}\left(\mathbf{Y}_2\right) - \varepsilon\left(\mathbf{C}_* \otimes \mathbf{C}\right)\left(\mathbf{Y}_2 - \mathbf{Y}_1\right) + \varepsilon\left(\mathbf{C}^* \otimes \mathbf{C}\right)\left(\mathbf{Y}_3 - \mathbf{Y}_2\right),\\
&\dot{\mathbf{Y}}_3 = \mathbf{G}\left(\mathbf{Y}_3\right) - \varepsilon\left(\mathbf{C}^* \otimes \mathbf{C}\right)\left(\mathbf{Y}_3 - \mathbf{Y}_2\right) + \varepsilon\left(\mathbf{C}_* \otimes \mathbf{C}\right)\left(\mathbf{Y}_4 - \mathbf{Y}_3\right),\\
&\vdots\\
&\dot{\mathbf{Y}}_k = \mathbf{G}\left(\mathbf{Y}_k\right) + \varepsilon\left(\mathbf{C}^* \otimes \mathbf{C}\right)\left(\mathbf{Y}_{k-1} - \mathbf{Y}_k\right),
\end{aligned} \tag{4.22}$$

where $\mathbf{C}_* = \mathrm{diag}\left(0,0,...,0,1\right)$ and $\mathbf{C}^* = \mathrm{diag}\left(1,0,...,0,0\right)$ are the fusion matrices.

System (4.22) is written for odd k. In the case of even ones, in the last equation the following change is to be done $\mathbf{C}^* \to \mathbf{C}_*$. We study sufficient conditions of stability of the cluster structure.

With respect to vectors $\mathbf{U}_j = \mathbf{Y}_j - \mathbf{Y}_{j+1}$, the linearized system has the form:

$$\begin{aligned}
&\dot{\mathbf{U}}_1 = \mathbf{J}(\xi)\mathbf{U}_1 - \varepsilon\Big(2(\mathbf{C}_* \otimes \mathbf{C})\mathbf{U}_1 - \big(\mathbf{C}^* \otimes \mathbf{C}\big)\mathbf{U}_2\Big),\\
&\dot{\mathbf{U}}_2 = \mathbf{J}(\xi)\mathbf{U}_2 - \varepsilon\Big(-(\mathbf{C}_* \otimes \mathbf{C})\mathbf{U}_1 + 2\big(\mathbf{C}^* \otimes \mathbf{C}\big)\mathbf{U}_2 - (\mathbf{C}_* \otimes \mathbf{C})\mathbf{U}_3\Big),\\
&\dot{\mathbf{U}}_3 = \mathbf{J}(\xi)\mathbf{U}_3 - \varepsilon\Big(-\big(\mathbf{C}^* \otimes \mathbf{C}\big)\mathbf{U}_2 + 2(\mathbf{C}_* \otimes \mathbf{C})\mathbf{U}_3 - \big(\mathbf{C}^* \otimes \mathbf{C}\big)\mathbf{U}_4\Big),\\
&\vdots\\
&\dot{\mathbf{U}}_{k-1} = \mathbf{J}(\xi)\mathbf{U}_{k-1} - \varepsilon\Big(-\big(\mathbf{C}^* \otimes \mathbf{C}\big)\mathbf{U}_{k-2} + 2(\mathbf{C}_* \otimes \mathbf{C})\mathbf{U}_{k-1}\Big).
\end{aligned} \tag{4.23}$$

System (4.23), written in a form of one equation has the form

$$\dot{\mathbf{U}} = \mathbf{I}_{k-1} \otimes \Big(\operatorname{diag}\big(\mathbf{J}_1(\xi_1), \mathbf{J}_2(\xi_2), ..., \mathbf{J}_n(\xi_n)\big) - \varepsilon \mathbf{B}_n \otimes \mathbf{C}\Big)\mathbf{U} -$$

$$-\varepsilon\Big(\mathbf{D}_{n(k-1)} \otimes \mathbf{C}\Big)\mathbf{U}, \tag{4.24}$$

where $\mathbf{U} = \big(\mathbf{U}_1, \mathbf{U}_2, ..., \mathbf{U}_{k-1}\big)^T$, and matrix

$$\mathbf{D}_{n(k-1)} = \begin{pmatrix}
2\mathbf{C}_* & -\mathbf{C}^* & 0 & & & \\
-\mathbf{C}_* & 2\mathbf{C}^* & -\mathbf{C}_* & & \mathbf{0} & \\
0 & -\mathbf{C}^* & 2\mathbf{C}_* & & & \\
 & & & \ddots & & \\
 & \mathbf{0} & & & 2\mathbf{C}_* & -\mathbf{C}^* & 0 \\
 & & & & -\mathbf{C}_* & 2\mathbf{C}^* & -\mathbf{C}_* \\
 & & & & 0 & -\mathbf{C}^* & 2\mathbf{C}_*
\end{pmatrix}.$$

Applying Eq. (4.24) to Lemma 4.6.1, we obtain: $\mathbf{A}(t) = \mathbf{I}_{n(k-1)} \otimes$

$\otimes \operatorname{diag}\left(\mathbf{J}_1(\xi_1),\ \mathbf{J}_2(\xi_2), ..., \mathbf{J}_n(\xi_n)\right)$,

$\mathbf{B} = \left(\mathbf{I}_{k-1} \otimes \mathbf{B}_n + \mathbf{D}_{n(k-1)}\right) \otimes \mathbf{C}$. As we can see, the norm of the variable matrix remains the same. In addition, the minimum root of matrix $\mathbf{I}_{k-1} \otimes \mathbf{B}_n + \mathbf{D}_{n(k-1)}$ is $\lambda_{\min} = 4\sin^2 \frac{\pi}{2nk}$. Everything together gives stability conditions of the structure, which are formulated in the same form.

Stability of cluster structures based on simple cells $O_a(n)$.

For convenience, we reconstruct the cluster structure diagram in a simple cell based on $O_a(n)$ and a circuit of a structure based on simple cells in sequential fusion (see Fig. 4.64).

First of all, we investigate the stability of the structure of the very simple cell, considering its equations as the equations of a chain of elementary oscillators with number $N = 2n-1$:

$$\begin{aligned} &\dot{\mathbf{X}}_i = \mathbf{F}(\mathbf{X}_i) - \varepsilon \mathbf{C}(-\mathbf{X}_{i-1} + 2\mathbf{X}_i - \mathbf{X}_{i+1}), \\ &i = \overline{1, N},\ \mathbf{X}_0 = \mathbf{X}_1,\ \mathbf{X}_N = \mathbf{X}_{N+1}. \end{aligned} \tag{4.25}$$

Due to symmetry of the cluster structure, we carry out linearization of (4.25) by variables $\mathbf{U}_i = \mathbf{X}_i - \mathbf{X}_{N-i+1},\ \ i = \overline{1, n-1}$. A linearized system has the form

$$\dot{\mathbf{U}}_i = \mathbf{J}_i\left(\xi_i\right)\mathbf{U}_i - \varepsilon\mathbf{C}\left(-\mathbf{U}_{i-1} + 2\mathbf{U}_i - \mathbf{U}_{i+1}\right),$$
$$i = \overline{1, n-1}, \quad \mathbf{U}_0 = \mathbf{U}_1, \quad \mathbf{U}_n = 0. \tag{4.26}$$

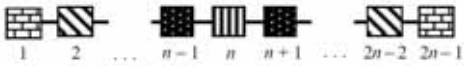

a

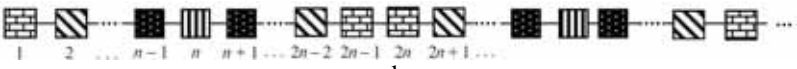

b

Fig. 4.65. A circuit of the cluster structure of a simple cell, a), and a circuit of the structure in the sequential fusion of simple cells, b).

System (4.26) written in a form of one equation

$$\dot{\mathbf{U}} = \left(\mathbf{J}^*\left(\xi\right) - \varepsilon\mathbf{D}_p \otimes \mathbf{C}\right)\mathbf{U}, \tag{4.27}$$

where $\mathbf{J}^*\left(\xi\right) = \mathrm{diag}\left(\mathbf{J}_1\left(\xi_1\right), \mathbf{J}_2\left(\xi_2\right), ..., \mathbf{J}_{n-1}\left(\xi_{n-1}\right)\right)$ is the truncated Jacobian of a C-oscillator of the type $O_a\left(n\right), \left(\xi_1, \xi_2, ..., \xi_n\right) \in A_a\left(n\right),$ and matrix $\mathbf{D}_p$ has the form

$$\mathbf{D}_p = \begin{Vmatrix} 1 & -1 & 0 & \cdots & \cdots & 0 & 0 \\ -1 & 2 & -1 & \ddots & \cdots & 0 & 0 \\ 0 & -1 & 2 & \ddots & \ddots & 0 & 0 \\ \vdots & \ddots & \ddots & \ddots & \ddots & \ddots & \vdots \\ \vdots & \vdots & \ddots & \ddots & 2 & -1 & 0 \\ 0 & 0 & 0 & \ddots & -1 & 2 & -1 \\ 0 & 0 & 0 & \cdots & 0 & -1 & 2 \end{Vmatrix}.$$

As one can see, Eq. (4.27) falls completely under Lemma 4.6.1. The norm of the variable matrix remains the same, and the minimal root of the matrix $\mathbf{D}_p$ has the form $\lambda_{\min} = 4\sin^2 \frac{\pi}{2(2n-1)}$. Thus, stability conditions of a cluster structure of the simple cell has an already known form: $\varepsilon > \mu/\lambda_{\min}$, if $\mathbf{C} = \mathbf{I}$, and $\varepsilon > \varepsilon^*(\mu)/\lambda_{\min}$ in the case of matrix $\mathbf{C}$ of the general form.

Consider structures based on simple cells in sequential fusion (see Fig. 4.64b). We will assume that the conditions for the stability of the structure of the simple cell itself are satisfied.

Compared to a structure in a chain based on $O_s(n)$, in this case, the situation is simplified due to the symmetry of the internal structure of the simple cell. At each step, the fusion matrix will be the same matrix $\mathbf{C}_* = \mathrm{diag}(0,0,...,0,1)$ or $\mathbf{C}^* = \mathrm{diag}(1,0,...,0,0)$ with dimension $2n-1$. it does not matter which one of them would it be exactly. Thus, one can use system (4.23) after the change $\mathbf{C}^* \to \mathbf{C}_*$. In this case, matrix $\mathbf{D}_{n(k-1)}$ (change $n \to 2n-1,$) takes the form $\mathbf{D}_{(2n-1)(k-1)} = \mathbf{D}_{k-1} \otimes \mathbf{C}_*,$ where

$$\mathbf{D}_{k-1} = \begin{Vmatrix} 2 & -1 & 0 & \cdots & \cdots & 0 & 0 \\ -1 & 2 & -1 & \ddots & \cdots & 0 & 0 \\ 0 & -1 & 2 & \ddots & \ddots & 0 & 0 \\ \vdots & \ddots & \ddots & \ddots & \ddots & \ddots & \vdots \\ \vdots & \vdots & \ddots & \ddots & 2 & -1 & 0 \\ 0 & 0 & 0 & \ddots & -1 & 2 & -1 \\ 0 & 0 & 0 & \cdots & 0 & -1 & 2 \end{Vmatrix}.$$

Taking into account the aforesaid matters, Eq. (4.24) takes the form

$$\dot{\mathbf{U}} = \mathbf{I}_{k-1} \otimes \mathbf{J}(\xi)\mathbf{U} - \varepsilon\left(\mathbf{D}_{k-1} \otimes \mathbf{C}_* \otimes \mathbf{C}\right)\mathbf{U}, \tag{4.28}$$

where $\mathbf{J}(\xi) = \operatorname{diag}\left(\mathbf{J}_1(\xi_1),\ \mathbf{J}_2(\xi_2), ..., \mathbf{J}_{2n-1}(\xi_1)\right) - \varepsilon\mathbf{B}_{2n-1} \otimes \mathbf{C}$ is the Jacobian of the simple cell. As one can see, Eq. (4.28) falls under Lemma 3.1.1, and, consequently, the stability problem (4.28) reduces to the corresponding problem for an equation of the form

$$\dot{\mathbf{U}} = \mathbf{J}(\xi)\mathbf{U} - \varepsilon\lambda_{\min}\mathbf{C}_* \otimes \mathbf{C}\mathbf{U}, \tag{4.29}$$

where $\lambda_{\min} = 4\sin^2\dfrac{\pi}{2k}$ is the minimal root of matrix $\mathbf{D}_{k-1}$.

Equation (4.29) is not an end of the problem solution since it has the same problem as one for Eq. (4.20). For this reason, we continue transformations (4.29) under Lemma 4.6.1, performing the same procedures as for Eq. (4.20). As a result, we obtain the norm for the variable matrix as the largest norm of the partial Jacobians of the oscillators of simple cells, as well as the minimum eigenvalue of

the constant matrix – the minimum root $\Lambda_{\min}$ of matrix $\mathbf{B}_{2n-1} + \lambda_{\min}\mathbf{C}_*$:

$$\mathbf{B}_{2n-1} + \lambda_{\min}\mathbf{C}_* = \begin{Vmatrix} 1 & -1 & 0 & \cdots & \cdots & 0 & 0 \\ -1 & 2 & -1 & \ddots & \cdots & 0 & 0 \\ 0 & -1 & 2 & \ddots & \ddots & 0 & 0 \\ \vdots & \ddots & \ddots & \ddots & \ddots & \ddots & \vdots \\ \vdots & \vdots & \ddots & \ddots & 2 & -1 & 0 \\ 0 & 0 & 0 & \ddots & -1 & 2 & -1 \\ 0 & 0 & 0 & \cdots & 0 & -1 & a \end{Vmatrix},$$

$$a = 1 + 4\sin^2\frac{\pi}{2k}.$$

In particular, if $k = 2$, then $\Lambda_{\min} = 4\sin^2\dfrac{\pi}{4(2n-1)}$; if $k = 3$, then $\Lambda_{\min} = 4\sin^2\dfrac{\pi}{2(4n-1)}$. The cluster structure (see Fig. 4.66) is stable for $\varepsilon > \mu/\Lambda_{\min}$, if $\mathbf{C} = \mathbf{I}$, and $\varepsilon > \varepsilon^*(\mu)/\Lambda_{\min}$ is the case of matrix $\mathbf{C}$ of a general form.

The solution of the problem of stability of structures, whose circuits are the result of parallel fusion of circuits of one-dimensional simple cells (see Fig. 4.66), will not differ from the respective problem with C-oscillator (see above).

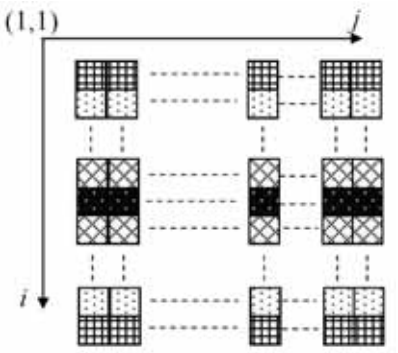

Fig. 4.66. Cluster structure obtained during a parallel fusion based on $\varepsilon > \varepsilon^{*}(\mu)/\Lambda_{\min}$.

To obtain the required matrices and stability conditions (inequalities) for the case under consideration, it suffices to replace $\lambda_s(n) \to \lambda_a(n), \quad n \to 2n-1$ in the respective matrices and inequalities. The same applies to the problem of stability of structures in three-dimensional lattices, the circuits of which are formed during the parallel fusion of circuits of two-dimensional simple cells. Such an example is shown in Fig. 4.67.

Studies of the stability of structures, the circuits of which are formed as a result of mixed fusion, ideologically will not differ from those carried out above. Difficulties that may arise along this path will be of a technical nature, associated with the problem of the dimension of dynamical systems.

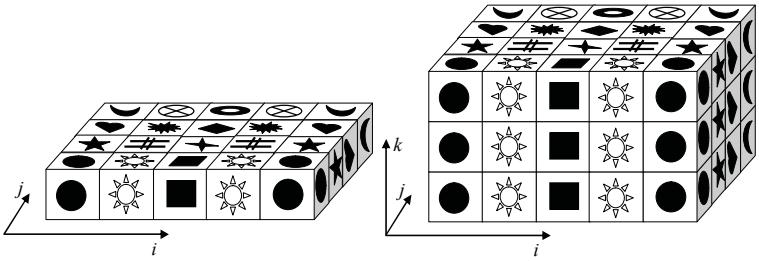

Fig. 4.67. A scheme of the cluster structure in a three-dimensional lattice based on the circuit of a simple cell of C-oscillator $O_{sa}\left(5\times 4\right)$ in parallel fusion.

APPENDIX I

ALGORITHMS OF TRANSFORMATION OF SYSTEMS OF COUPLED ROTATORS TO THE STANDARD FORM

AI.1. Systems of coupled rotators without additional loads

Consider a case when each of the rotators is not loaded by any additional aperiodic or oscillatory loads. In this case, system (F1) has the form

$$\begin{aligned} & I\ddot{\varphi}_k + \delta_k\left(1+F_{1k}\left(\varphi_k\right)\right)\dot{\varphi}_k + F_{2k}\left(\varphi_k\right) = \\ & = \gamma_k + \sum_{j=1}^{n} f_{kj}\left(\varphi_j\right) + \sum_{j=1}^{n}\beta_{kj}\dot{\varphi}_j + f_k\left(\psi\right) + \mu F_k^*\left(\boldsymbol{\varphi}\right), \\ & \dot{\psi} = \omega_0, \end{aligned} \tag{AI.1.1}$$

where $\left\langle f_{kj}\left(\varphi_j\right)\right\rangle_{\varphi_j} = 0$, $\left\langle f_k\left(\psi\right)\right\rangle_{\psi} = 0$, $\mu = I^{-1}$.

In other words, we consider a system of rotators coupled by angular speeds and angular accelerations that results in couplings by periodic functions and "other couplings" expressed by terms $\mu F_k^*\left(\boldsymbol{\varphi}\right)$.

We need to determine a form of transformation $\left(\boldsymbol{\varphi},\dot{\boldsymbol{\varphi}}\right)\to\left(\boldsymbol{\varphi},\boldsymbol{\xi}\right)$,

which reduces system (AI.1.1) to a system in a standard form with fast spinning phases

$$\begin{aligned}\dot{\xi}_k &= \mu\Xi_k\left(\boldsymbol{\varphi},\psi,\boldsymbol{\xi}\right),\\ \dot{\varphi}_k &= \omega_k + \mu\Phi_k\left(\boldsymbol{\varphi},\psi,\xi_k\right),\\ \dot{\psi} &= \omega_0,\end{aligned} \tag{AI.1.2}$$

where ω_k, $\Xi_k\left(\boldsymbol{\varphi},\psi,\boldsymbol{\xi}\right)$, $\Phi_k\left(\boldsymbol{\varphi},\psi,\xi_k\right)$ are the unknown parameters and functions to be determined.

Functions $\Xi_k\left(\boldsymbol{\varphi},\psi,\boldsymbol{\xi}\right)$ and $\Phi_k\left(\boldsymbol{\varphi},\psi,\xi_k\right)$ are bounded by all phase variables (there are no secular terms for $\boldsymbol{\varphi}$), which correspond to their periodicity by these variables.

Substitution of the second equation from system (AI.1.2) into (AI.1.1) leads to an equation that determines the sought parameters and functions of the transformation:

$$\begin{aligned}&\sum_{j=1}^{n}\frac{\partial\Phi_k}{\partial\varphi_j}\left(\omega_j+\mu\Phi_j\right)+\frac{\partial\Phi_k}{\partial\psi}\omega_0+\dot{\xi}_k+\delta_k\left(1+F_{1k}\right)\left(\omega_k+\mu\Phi_k\right)+F_{2k}=\\ &\qquad=\gamma_k+\sum_{j=1}^{n}f_{kj}+\sum_{j=1}^{n}\beta_{kj}\left(\omega_j+\mu\Phi_j\right)+f_k\left(\psi\right)+\mu F_k^{*}\left(\boldsymbol{\varphi}\right).\end{aligned} \tag{AI.1.3}$$

Using the condition of boundedness, we obtain the equations for normal frequencies of rotators:

$$\delta_k \omega_k - \sum_{j=1}^{n} \beta_{kj} \omega_j = \gamma_k , \; k = \overline{1,n.} \tag{AI.1.4}$$

These equations are obtained after the elimination of all constants from (AI.1.3). Taking into account the form of the first equation in system (AI.1.2) $\left(\dot{\xi} \sim \mu\right)$, we obtain equations for determining functions Φ_k (elimination of terms not proportional to μ):

$$\sum_{j=1}^{n} \frac{\partial \Phi_k}{\partial \varphi_j} \omega_j + \frac{\partial \Phi_k}{\partial \psi} \omega_0 + \delta_k \omega_k F_{1k}\left(\varphi_k\right) + F_{2k}\left(\varphi_k\right) =$$

$$= \sum_{j=1}^{n} f_{kj}\left(\varphi_j\right) + f_k\left(\psi\right). \tag{AI.1.5}$$

Linear system (AI.1.4) is easy to solve. Eq. (AI.1.5) is also simple. The sought solution has the form

$$\Phi_k = \sum_{j=1}^{n} \frac{1}{\omega_j} \int f_{kj}\left(\varphi_j\right) d\varphi_j + \frac{1}{\omega_0} \int f_k\left(\psi\right) d\psi - \delta_k \int F_{1k}\left(\varphi_k\right) d\varphi_k -$$

$$- \frac{1}{\omega_k} \int F_{2k}\left(\varphi_k\right) d\varphi_k + \xi_k .$$

These functions are bounded by phase variables (this is a result of the elimination of constants). For functions Ξ_k, we obtain expressions

$$\Xi_k = \sum_{j=1}^{n}\left(\beta_{kj} - \frac{\partial \Phi_k}{\partial \varphi_j}\right)\Phi_j - \delta_k \Phi_k \left(1 + F_{1k}\right) + F_k^*.$$

As it was already said, for the interacting quasi-linear systems, the "strong" resonances are the harmonic resonances corresponding to an integer ratio of the frequencies. By saying "strong", we mean that resonance takes place in an averaged system in the first approximation. According to this terminology, subharmonic resonances are "weak". Generally, the most significant is the first (main) resonance. We consider self-oscillating systems and, therefore, the main resonance corresponds to the "simple" mutual synchronization of oscillations and all other resonances correspond to a multiple ("divisible") synchronization. The same can be said with respect to the master-slave synchronization of a self-oscillatory system by an external force. To study harmonic resonances in system (AI.1.2), we introduce phase and frequency mistunings of the form $q_k\varphi_k - p_k\psi = \eta_k$, $q_k\omega_k - p_k\omega_0 = \mu\Delta_k$, where $p_k/q_k = n_k$ are integers. The value of $n_k = 1$ corresponds to the simple synchronization. As a result, we obtain a system with one fast spinning phase ψ of the form

$$\begin{aligned}
\dot{\xi}_k &= \mu\Xi_k\left(\boldsymbol{\eta}, \psi, \boldsymbol{\xi}\right),\\
\dot{\eta}_k &= \mu\left(\Delta_k + q_k\Phi_k\left(\boldsymbol{\eta}, \psi, \xi_k\right)\right),\\
\dot{\psi} &= \omega_0.
\end{aligned} \qquad \text{(AI.1.6)}$$

We apply the method of the averaging to obtain:

$$\Xi_k^*(\boldsymbol{\eta},\mathbf{x}) = \frac{1}{2\pi}\int_0^{2\pi}\Xi_k(\boldsymbol{\eta},\mathbf{x},\psi)\partial\psi,\ \frac{1}{2\pi}\int_0^{2\pi}(\Delta_k + q_k\Phi_k)\partial\psi = \Delta_k + q_k\xi_k$$

and an averaged system of the form

$$\begin{aligned}\dot{\xi}_k &= \Xi_k^*(\boldsymbol{\eta},\boldsymbol{\xi}),\\ \dot{\eta}_k &= \Delta_k + q_k\xi_k.\end{aligned} \qquad \text{(AI.1.7)}$$

In system (AI.1.7), we have kept old names for the averaged variables and transformed time $\mu\tau = \tau_n$. By studying system (AI.1.7), one can particularly obtain rotation characteristics of rotators in the resonance zones: $\langle\dot{\varphi}_k\rangle_\tau = \Omega_k = n_k\omega_0 + \frac{\mu}{q_k}\langle\dot{\eta}_k^*\rangle_\tau$.

During the interpretation of dynamical properties of averaged system (AI.1.7) onto the original system (F1), we take into account that if G is a limit set of trajectories of the averaged system, then $G\times S^1$ is a limit set of trajectories of the original system with some limitations described above. Also, one needs to remember the relation between the trajectories of the averaged system and the trajectories of the point mapping (Poincaré mapping) for the original system.

Remark 1. The choice of a "fast" phase for the averaging in system (AI.1.2) is normally done according to considerations of convenience. If a system is non-autonomous, then such phase is a phase of external force ψ. If systems (AI.1.1) and (AI.1.2), respectively, are

autonomous, then any phase can be chosen. If such phase is $\varphi_1 = \varphi$, then phase and frequency mistunings of the form $q_k\varphi_k - p_k\varphi = \eta_k$, $q_k\omega_k - p_k\omega_1 = \mu\Delta_k$, where p, q are integers, are to be introduced to study the synchronization.

Remark 2. If system (AI.1.1) is non-autonomous, then during the transformations it is convenient to choose a form of equations for the phases of rotators in the form $\dot{\varphi}_k = n_k\omega_0 + \mu\Phi_k\left(\boldsymbol{\varphi}, \psi, \xi_k\right)$. If the system is autonomous, then $\dot{\varphi}_k = n_k\omega + \mu\Phi_k\left(\boldsymbol{\varphi}, \xi_k\right)$, where ω is a normal frequency of the "averaging" rotator, and n_k are the integers. In this case, frequency mistunings pass into the equation for variable ξ. Note that the choice of the frequency does not affect the result, but reduces the procedure of transformations.

AI.2. Systems of coupled rotators with aperiodic loads

First we consider one rotator with an aperiodic load, the equations of which have an arbitrary dimension. Suppose that matrix **A** has real roots and, without loss of generality, we consider that it is diagonal. We also assume that the load has a small dissipation, i.e. $\mathbf{A} = \mu\mathbf{B}$, where **B** is a diagonal nondegenerate matrix. Under the above assumptions, we consider a dynamical system of the form

$$\begin{aligned} &I\ddot{\varphi} + \delta\left(1 + F_1\left(\varphi\right)\right)\dot{\varphi} + F_2\left(\varphi\right) = \gamma + \mathbf{a}^T\mathbf{z} + f\left(\psi\right) + \mu F^*\left(\varphi, \mathbf{z}\right), \\ &\dot{\mathbf{z}} = \mu\left(\mathbf{B}\mathbf{z} + \mathbf{b}\dot{\varphi} + \mathbf{c}f_1\left(\varphi\right) + \mathbf{d}f_2\left(\psi\right)\right), \end{aligned} \qquad \text{(AI.2.1)}$$

where **a**, **b**, **c**, and **d** are the constant vectors.

It is easy to see that a "generating" solution for the second equation (equation for the load; solution for $\mu = 0$) is solution $\mathbf{z} = \text{const}$. This means that if one would transform the equation for the rotator to the standard form directly from (AI.2.1), then variable **z** will be included in to the "generating" frequency of the rotator. This circumstance will complicate the entire procedure of the averaging. The ideal case is a case when a "generating" frequency does not depend on slow variables (i.e. it is a parameter). Due to this reason, let us perform the following transformation of the equation for the load:

$$\mathbf{z} = \boldsymbol{\beta} + \mu \boldsymbol{\Psi}(\varphi, \psi) + \mu \mathbf{y}, \tag{AI.2.2}$$

where constant vector $\boldsymbol{\beta}$ and vector-function $\boldsymbol{\Psi}(\varphi, \psi)$ are to be determined. Substituting Eq. (AI.2.2) into the second equation of (AI.2.1) and taking into account that the equation for phase φ has the form $\dot{\varphi} = \omega_0 + \mu\Phi,$ we obtain:

$$\frac{\partial \boldsymbol{\Psi}}{\partial \varphi}(\omega_0 + \mu\Phi) + \frac{\partial \boldsymbol{\Psi}}{\partial \psi}\omega_0 + \dot{\mathbf{y}} =$$

$$= \mu \mathbf{B}(\boldsymbol{\Psi} + \mathbf{y}) + \mathbf{B}\boldsymbol{\beta} + \mathbf{b}\omega_0 + \mu \mathbf{b}\Phi + \mathbf{c}f_1(\varphi) + \mathbf{d}f_2(\psi). \tag{AI.2.3}$$

Equations that determine $\boldsymbol{\beta}$ and $\boldsymbol{\Upsilon}(\varphi, \psi),$ are obtained using the following simple considerations: first, the equation for variable **y**

has to have a standard form; second, function $\mathbf{Y}(\varphi,\psi)$, has to be bounded. For these conditions, the sought equations have the form

$$\begin{aligned}&\frac{\partial\mathbf{\Psi}}{\partial\varphi}\omega_0+\frac{\partial\mathbf{\Psi}}{\partial\psi}\omega_0=\mathbf{c}f_1(\varphi)+\mathbf{d}f_2(\psi),\\&\mathbf{B}\boldsymbol{\beta}+\mathbf{b}\omega_0=0.\end{aligned}\qquad\text{(AI.2.4)}$$

Solving Eqs. (AI.2.4) is not difficult:

$$\begin{aligned}&\mathbf{\Psi}=\frac{\mathbf{c}}{\omega_0}\int f_1(\varphi)d\varphi+\frac{\mathbf{d}}{\omega_0}\int f_2(\psi)d\psi,\\&\boldsymbol{\beta}=-\mathbf{B}^{-1}\mathbf{b}\omega_0.\end{aligned}$$

For the found solutions, Eqs. (AI.2.1) take the form

$$\begin{aligned}&I\ddot{\varphi}+\delta\left(1+F_1(\varphi)\right)\dot{\varphi}+F_2(\varphi)=\gamma+\mathbf{a}^T\boldsymbol{\beta}+f(\psi)+\\&+\mu\mathbf{a}^T\left(\mathbf{\Psi}+\mathbf{y}\right)+\mu F^*(\varphi,\mathbf{z}),\\&\dot{\mathbf{y}}=\mu\left(\mathbf{B}\mathbf{y}+\mathbf{B}\mathbf{\Psi}-\frac{\partial\mathbf{\Psi}}{\partial\varphi}\Phi+\mathbf{b}\Phi\right).\end{aligned}\qquad\text{(AI.2.5)}$$

And now let us transform the equation for the rotator. Substituting into the first equation of (AI.2.5) the equation for the phase $\dot{\varphi}=\omega_0+\mu\Phi(\varphi,\psi,\xi)$, we obtain

$$\begin{aligned}&\frac{\partial\Phi}{\partial\varphi}(\omega_0+\mu\Phi)+\frac{\partial\Phi}{\partial\psi}\omega_0+\frac{\partial\Phi}{\partial\xi}\dot{\xi}+\delta\left(1+F_1(\varphi)\right)(\omega_0+\mu\Phi)+F_2(\varphi)=\\&=\gamma+\mathbf{a}^T\boldsymbol{\beta}+f(\psi)+\mu\mathbf{a}^T\left(\mathbf{\Psi}+\mathbf{y}\right)+\mu F^*(\varphi,\mathbf{z}).\end{aligned}\qquad\text{(AI.2.6)}$$

The equation for function $\Phi(\varphi,\psi,\xi)$ is obtained using the same considerations as those for (F1):

$$\frac{\partial\Phi}{\partial\varphi}\omega_0+\frac{\partial\Phi}{\partial\psi}\omega_0+\delta\omega_0F_1(\varphi)+F_2(\varphi)=f(\psi).$$

Its solutions are:

$$\Phi=-\delta\int F_1(\varphi)d\varphi-\frac{1}{\omega_0}\int F_2(\varphi)d\varphi+\frac{1}{\omega_0}\int f(\psi)d\psi+\xi.$$

Relation $\gamma+\mathbf{a}^T\boldsymbol{\beta}-\delta\omega_0=\mu\Delta$ determines the resonance zone of the parameters.

Eventually, we obtain system of equations in a standard form, which is equivalent to system (AI.2.1):

$$\begin{aligned}\dot{\xi}&=\mu\Xi,\\ \dot{\mathbf{y}}&=\mu\mathbf{Y},\\ \dot{\eta}&=\mu\Phi,\\ \dot{\varphi}&=\omega_0+\mu\Phi,\end{aligned}\qquad\text{(AI.2.7)}$$

where $\Xi=\Delta-\delta\left(1+F_1(\varphi)\right)\Phi-\dfrac{\partial\Phi}{\partial\varphi}\Phi+\mathbf{a}^T\left(\boldsymbol{\Psi}+\mathbf{y}\right)+F^*(\varphi,\mathbf{z}),$

$\mathbf{Y}=\mathbf{B}\mathbf{y}+\mathbf{B}\boldsymbol{\Psi}-\dfrac{\partial\boldsymbol{\Psi}}{\partial\varphi}\Phi+\mathbf{b}\Phi$, $\eta=\varphi-\psi$ is the phase mistuning.

Remark 3. We have considered the case of a non-autonomous system. Here, the generating frequency has been determined and it was

a frequency of external force ω_0. In the autonomous case, the generating frequency of the rotator is a priori unknown. Formally, it is found using the resonance relation. Namely, assuming $\Delta = 0$, we obtain the generating frequency of the rotator:

$$\omega_0 = \frac{\gamma}{\left(\mathbf{a}^T \mathbf{B}^{-1} \mathbf{b} + \delta\right)}.$$

Consider a system of an arbitrary number of coupled rotators with aperiodic loads. Suppose that the equations for all aperiodic loads are transformed in the aforementioned way and the system of coupled rotators has the form

$$\begin{aligned} &I\ddot{\varphi}_k + \delta\left(1 + F_{1k}\left(\varphi_k\right)\right)\dot{\varphi}_k + F_{2k}\left(\varphi_k\right) = \gamma_k + \mathbf{a}_k^T \boldsymbol{\beta}_\kappa + f_k\left(\psi\right) + \\ &+ \sum_{j=1}^{n} f_{kj}\left(\varphi_j\right) + \sum_{j=1}^{n} \beta_{kj}\dot{\varphi}_j + \mu \mathbf{a}_k^T\left(\boldsymbol{\Psi}_k + \mathbf{y}_k\right) + \mu F_k^*\left(\varphi, \mathbf{z}\right), \\ &\dot{\mathbf{y}}_k = \mu \mathbf{Y}_k, \\ &\dot{\psi} = \omega_0. \end{aligned} \tag{AI.2.8}$$

Transformation of the equations for the rotators in system (AI.2.8) is the same as that for system (AI.1.1). Moreover, since the impact of the loads on the rotators is “weak” in system (AI.2.8), then functions Φ_k will not depend on vectors y_k. They will have the same expressions as in (F1).

Performing transformations and determining the necessary functions, we obtain the system in a standard form equivalent to system

(AI.2.8) that has the form

$$\begin{aligned}
\dot{\xi}_k &= \mu \Xi_k \left(\boldsymbol{\varphi}, \psi, \boldsymbol{\xi}, \mathbf{y}_k \right), \\
\dot{\mathbf{y}}_k &= \mu \mathbf{Y}_k \left(\boldsymbol{\varphi}, \psi, \boldsymbol{\xi}, \mathbf{y}_k \right), \\
\dot{\varphi}_k &= \omega_k + \mu \Phi_k \left(\boldsymbol{\varphi}, \psi, \xi_k \right), \\
\dot{\psi} &= \omega_0 .
\end{aligned} \tag{AI.2.9}$$

The equations and, consequently, expressions for functions Φ_k are the same as those in (F1):

$$\Phi_k = \sum_{j=1}^{n} \frac{1}{\omega_j} \int f_{kj} \left(\varphi_j \right) d\varphi_j + \frac{1}{\omega_0} \int f_k \left(\psi \right) d\psi - \delta_k \int F_{1k} \left(\varphi_k \right) d\varphi_k - \\ - \frac{1}{\omega_k} \int F_{2k} \left(\varphi_k \right) d\varphi_k + \xi_k .$$

Expressions for Ξ_k and Y_k :

$$\Xi_k = \sum_{j=1}^{n} \left(\beta_{kj} - \frac{\partial \Phi_k}{\partial \varphi_j} \right) \Phi_j - \delta_k \Phi_k \left(1 + F_{1k} \right) + F_k^* + \mathbf{a}_k^T \left(\boldsymbol{\Psi}_k + \mathbf{y}_k \right),$$

$$\mathbf{Y}_k = \mathbf{B}_k \mathbf{y}_k + \mathbf{B}_k \boldsymbol{\Psi}_k - \frac{\partial \boldsymbol{\Psi}_k}{\partial \varphi_k} \Phi_k + \mathbf{b}_k \Phi_k$$

Consequently, expressions for the generating frequencies of the rotators have the form

$$\left(\delta_k + \mathbf{a}_k^T \mathbf{B}_k^{-1} \mathbf{b}_k \right) \omega_k - \sum_{j=1}^{n} \beta_{kj} \omega_j = \gamma_k ,$$
$$k = \overline{1, n}.$$

Further, taking into account Remarks 1 and 2, system (AI.2.9) is to be reduced to the system in a standard form with one fast spinning phase and the procedure of the averaging is to be carried out.

AI.3. Systems of coupled rotators with oscillatory loads

First, let us consider a case of one rotator interacting with a multifrequency oscillatory load.

As it was said above, a quasi-linear rotator effectively interacts with an oscillatory load only in the resonance case, when the oscillator has a high quality (small damping). We will suppose that all dissipative terms of oscillators are described by function $\mathbf{Z}(\mathbf{z},\varphi,\dot{\varphi},\psi)$ of system (F1). We will also assume that the ratio of all frequencies of oscillators to the least frequency (or to the frequency of external impact) is close to an integer, i.e. $\omega_j^2 = n_j^2\omega_0^2 + \mu\nu_j$, where n_j are integers. Suppose that all terms of the equation concerned with frequency mistunings $(\mu\nu_j)$, are also described by function $\mathbf{Z}(\mathbf{z},\varphi,\dot{\varphi},\psi)$. Also, we assume that the vector equation for an oscillatory system is transformed to the equilibrium in the origin. The named conditions are easy to fulfil using elementary transformations of equations of an oscillatory system and we assume that these transformations are performed. The systems considered throughout this work can serve as examples.

Taking these into account, consider a dynamical system of the form

$$I\ddot{\varphi}+\delta\left(1+F_1(\varphi)\right)\dot{\varphi}+F_2(\varphi)=\gamma+\mathbf{a}^T\mathbf{z}+f(\psi)+\mu F^*(\varphi,\mathbf{z}),$$
$$\dot{z}=\mathbf{A}\mathbf{z}+\mu\mathbf{Z}(\mathbf{z},\varphi),$$
$$\dot{\psi}=\omega_0, \qquad \text{(AI.3.1)}$$

where **a** is a constant vector and matrix **A** has imaginary eigenvalues and Jordan form with cells of the form $\mathbf{A}_j=\begin{pmatrix}0 & 1\\ -n_j^2\omega_0^2 & 0\end{pmatrix}$,

$j=\overline{1,m},\ \dim(\mathbf{z},\mathbf{Z})=2m.$

It is easy to see that the generating vector equation for the oscillatory system (equation for $\mu=0$) represents a system of independent harmonic oscillators. Let us rename the variables: $z_{2j-1}=x_j$, $Z_{2j-1}=X_j$, $z_{2j}=y_j$, $Z_{2j}=Y_j$.

According to Remark 2, let us determine the form of the equation for the phase of the rotator using the form $\dot{\varphi}=\omega_0+\mu\Phi$ and transform all quasi-linear equations of oscillators using a modified van der Pol change in the same manner. In each system of the form

$$\dot{x}=y+\mu X,\quad \dot{y}=-n^2\omega_0^2x+\mu Y$$

we perform a change of the variables of the form

$$x=\theta\sin n\varphi+\eta\cos n\varphi,\quad y=\left(\theta\cos n\varphi-\eta\sin n\varphi\right)n\omega_0,$$

As a result, we obtain the system in a standard form

$$\dot{\theta} = \mu\Theta, \quad \dot{\eta} = \mu T,$$

where

$$\Theta = n\eta\Phi + X \sin n\varphi + \frac{1}{n\omega_0} Y \cos n\varphi,$$

$$T = -n\theta\Phi + X \cos n\varphi - \frac{1}{n\omega_0} Y \sin n\varphi.$$

In the new variables, the equations for the oscillatory system have a standard form with respect to $\theta = (\theta_1, ..., \theta_m)^T$, and $\eta = (\eta_1, ..., \eta_m)^T$, while system (AI.3.1) takes the form

$$\begin{aligned} &I\ddot{\varphi} + \delta\left(1 + F_1(\varphi)\right)\dot{\varphi} + F_2(\varphi) = \gamma + b^T x + c^T y + f(\psi) + \mu F^*(\varphi, z), \\ &\dot{\boldsymbol{\theta}} = \mu\boldsymbol{\Theta}, \\ &\dot{\boldsymbol{\eta}} = \mu\mathbf{T}, \\ &\dot{\psi} = \omega_0, \end{aligned} \tag{AI.3.2}$$

where $\mathbf{b}^T\mathbf{x} = \sum_{i=1}^{m} b_i \left(\theta_i \sin n_i\varphi + \eta_i \cos n_i\varphi\right)$, $\mathbf{c}^T\mathbf{y} = \sum_{i=1}^{m} c_i \left(\theta_i \cos n_i\varphi - \right.$ $\left. - \eta_i \sin n_i\varphi\right) n_i\omega_0$; b_i, c_i are the odd and even coordinates of vector **a**.

Now, let us transform the equation for the rotator. Substituting the

expression for phase $\dot{\varphi} = \omega_0 + \mu\Phi(\varphi, \psi, \xi, \boldsymbol{\theta}, \boldsymbol{\eta})$ into the first equation of system (AI.3.2), we obtain:

$$\frac{\partial\Phi}{\partial\varphi}(\omega_0 + \mu\Phi) + \frac{\partial\Phi}{\partial\psi}\omega_0 + \sum_{j=1}^{m}\frac{\partial\Phi}{\partial\theta_j}\mu\Theta_j + \sum_{j=1}^{m}\frac{\partial\Phi}{\partial\eta_j}\mu\mathbf{T}_j + \dot{\xi} +$$

$$+\delta(1+F_1)(\omega_0 + \mu\Phi) + F_2 = \gamma + \mathbf{b}^T\mathbf{x} + \mathbf{c}^T\mathbf{y} + f(\psi) + \mu F^*(\varphi, \mathbf{z}). \tag{AI.3.3}$$

Keeping in mind requirements for function Φ, using (AI.3.3) we obtain the equation for determining this function

$$\frac{\partial\Phi}{\partial\varphi}\omega_0 + \frac{\partial\Phi}{\partial\psi}\omega_0 + \delta\omega_0 F_1 + F_2 = \mathbf{b}^T\mathbf{x} + \mathbf{c}^T\mathbf{y} + f(\psi) \tag{AI.3.4}$$

And the resonance zone of parameters $\gamma - \delta\omega_0 = \mu\Delta.$

The solution of Eq. (AI.3.4) has the form:

$$\Phi = -\delta\int F_1(\varphi)d\varphi - \frac{1}{\omega_0}\int F_2(\varphi)d\varphi + \frac{1}{\omega_0}\int f(\psi)d\varphi +$$

$$+ \frac{1}{\omega_0}\int \mathbf{b}^T\mathbf{x}(\varphi)d\varphi + \frac{1}{\omega_0}\int \mathbf{c}^T\mathbf{y}(\varphi)d\varphi + \xi,$$

where

$$\frac{1}{\omega_0}\int \mathbf{b}^T\mathbf{x}(\varphi)d\varphi = \frac{1}{\omega_0}\sum_{i=1}^{m}\frac{b_i}{n_i}(-\theta_i\cos n_i\varphi + \eta_i\sin n_i\varphi)\frac{1}{\omega_0}\int \mathbf{c}^T\mathbf{y}(\varphi)d\varphi =$$

$$= \sum_{i=1}^{m} c_i \left(\theta_i \sin n_i \varphi + \eta_i \cos n_i \varphi \right).$$

The expression for function Ξ:

$$\Xi = \Delta - \frac{\partial \Phi}{\partial \varphi} \Phi - \delta \left(1 + F_1\right) \Phi - \sum_{j=1}^{m} \frac{\partial \Phi}{\partial \theta_j} \Theta_j - \sum_{j=1}^{m} \frac{\partial \Phi}{\partial \eta_j} T_j + F^* \left(\varphi, \mathbf{z} \right).$$

Eventually, we obtain the system in a standard form, which is equivalent to system (AI.3.1):

$$\begin{aligned} \dot{\xi} &= \mu \Xi, \\ \dot{\boldsymbol{\theta}} &= \mu \boldsymbol{\Theta}, \\ \dot{\boldsymbol{\eta}} &= \mu \mathbf{T}, \\ \dot{\chi} &= \mu \Phi, \\ \dot{\varphi} &= \omega_0 + \mu \Phi, \end{aligned} \tag{AI.3.5}$$

where $\chi = \varphi - \psi$ is the phase mistuning.

Consider now the system of coupled rotators, where each of them is loaded by an oscillatory load. Equations for loads can have different dimensions and frequency spectra. We will suppose that all of the aforementioned conditions for oscillatory systems are satisfied and their equations are transformed to the standard form.

Consider a dynamical system of the form

$$
\begin{aligned}
&I\ddot{\varphi}_k + \delta_k\left(1 + F_{1k}\left(\varphi_k\right)\right)\dot{\varphi}_k + F_{2k}\left(\varphi_k\right) = \gamma_k + f_k\left(\psi\right) + \\
&+\sum_{j=1}^{n} f_{kj}\left(\varphi_j\right) + \sum_{j=1}^{n}\beta_{kj}\dot{\varphi}_j + \mathbf{b}_k^T\mathbf{x}_k + \mathbf{c}_k^T\mathbf{y}_k + \mu F_k^*\left(\varphi, \mathbf{z}\right), \\
&\dot{\boldsymbol{\theta}}_k = \mu\boldsymbol{\Theta}_k, \\
&\dot{\boldsymbol{\eta}}_k = \mu\mathbf{T}_k, \\
&\dot{\psi} = \omega_0,
\end{aligned}
\tag{AI.3.6}
$$

where

$\mathbf{b}_k^T\mathbf{x}_k = \sum_{i=1}^{m_k} b_{ki}\left(\theta_{ki}\sin n_{ki}\varphi + \eta_{ki}\cos n_{ki}\varphi\right)$, $\mathbf{c}_k^T\mathbf{y}_k = \sum_{i=1}^{m_k} c_{ki}\left(\theta_{ki}\cos n_{ki}\varphi - \right.$

$\left. - \eta_{ki}\sin n_{ki}\varphi\right) n_{ki}\omega_0$, φ is one of the phases of the rotators.

Having defined a form of the equations for the phases $\dot{\varphi}_k = \omega_0 + \mu\Phi_k\left(\boldsymbol{\varphi}, \psi, \boldsymbol{\theta}_k, \boldsymbol{\eta}_k, \xi_k\right)$ and substituting these expressions into the equations for rotators, we obtain equations for functions $\Phi_k\left(\boldsymbol{\varphi}, \psi, \boldsymbol{\theta}_k, \boldsymbol{\eta}_k, \xi_k\right)$, expressions for functions Ξ_k, and resonance zones of parameters

$$
\begin{aligned}
&\sum_{j=1}^{n}\frac{\partial\Phi_k}{\partial\varphi_j}\omega_0 + \frac{\partial\Phi_k}{\partial\psi}\omega_0 + \delta_k\omega_0 F_{1k}\left(\varphi_k\right) + F_{2k}\left(\varphi_k\right) = \\
&= \sum_{j=1}^{n} f_{kj}\left(\varphi_j\right) + f_k\left(\psi\right) + \mathbf{b}_k^T\mathbf{x}_k + \mathbf{c}_k^T\mathbf{y}_k, \\
&\gamma_k - \left(\delta_k + \mathbf{a}_k^T\mathbf{B}_k^{-1}\mathbf{b}_k - \sum_{j=1}^{n}\beta_{kj}\right)\omega_0 = \mu\Delta_k, \quad k = \overline{1, n.}
\end{aligned}
\tag{AI.3.7}
$$

The sought solution of Eq. (AI.3.7) is not difficult to find:

$$\Phi_k = \frac{1}{\omega_0}\sum_{j=1}^{n}\int f_{kj}\left(\varphi_j\right)d\varphi_j + \frac{1}{\omega_0}\int f_k\left(\psi\right)d\psi - \delta_k\int F_{1k}\left(\varphi_k\right)d\varphi_k -$$
$$- \frac{1}{\omega_0}\int F_{2k}\left(\varphi_k\right)d\varphi_k + \frac{1}{\omega_0}\int \mathbf{b}_k^T\mathbf{x}_k\left(\varphi\right)d\varphi + \frac{1}{\omega_0}\int \mathbf{c}_k^T\mathbf{y}_k\left(\varphi\right)d\varphi + \xi_k.$$

The expressions for functions Ξ_k :

$$\Xi_k = \Delta_k + \sum_{j=1}^{n}\left(\beta_{kj} - \frac{\partial\Phi_k}{\partial\varphi_j}\right)\Phi_j - \delta_k\Phi_k\left(1+F_{1k}\right) -$$
$$- \sum_{j=1}^{m}\frac{\partial\Phi_k}{\partial\theta_{kj}}\Theta_{kj} - \sum_{j=1}^{m}\frac{\partial\Phi_k}{\partial\eta_{kj}}T_{kj} + F_k^*.$$

Eventually, we obtain a system in a standard form with a fast spinning phase, which is equivalent to Eqs. (AI.3.6):

$$\dot{\xi}_k = \mu\Xi_k,$$
$$\dot{\boldsymbol{\theta}}_k = \mu\boldsymbol{\Theta}_k,$$
$$\dot{\boldsymbol{\eta}}_k = \mu\mathbf{T}_k,$$
$$\dot{\chi}_k = \mu\left(\Phi - \Phi_k\right),$$
$$\dot{\varphi} = \omega_0 + \mu\Phi,$$

where $\chi_k = \varphi - \varphi_k$ are the phase mistunings, and φ is one of the phases of rotators.

APPENDIX II

CALCULATION OF EIGENVALUES OF MATRICES

Consider matrix $\mathbf{A}_p$ and determinant Δ_p of the form

$$\mathbf{A}_p = \begin{pmatrix} 2\nu+\alpha & -1 & 0 & 0 & & & & & \\ -1 & 2\nu & -1 & 0 & & & & & \\ 0 & -1 & 2\nu & -1 & 0 & & & 0 & \\ 0 & 0 & -1 & 2\nu & & & & & \\ & 0 & & & \ddots & & & 0 & \\ & & & & & 2\nu & -1 & 0 & 0 \\ & & & & & -1 & 2\nu & -1 & 0 \\ & 0 & & & 0 & 0 & -1 & 2\nu & -1 \\ & & & & & 0 & 0 & -1 & 2\nu+\beta \end{pmatrix},$$

$$\Delta_p = \begin{vmatrix} 2\nu & -1 & 0 & 0 & & & & \\ -1 & 2\nu & -1 & 0 & 0 & & 0 & \\ 0 & -1 & 2\nu & -1 & & & & \\ 0 & 0 & -1 & 2\nu & & & & \\ & 0 & & & \ddots & & 0 & \\ & & & & & 2\nu & -1 & 0 & 0 \\ & & & & & -1 & 2\nu & -1 & 0 \\ & 0 & & & 0 & 0 & -1 & 2\nu & -1 \\ & & & & & 0 & 0 & -1 & 2\nu \end{vmatrix}.$$

It can be established that, for main minors of the determinant, the following recurrent equation is valid [177]

$$\Delta_k = 2\nu\Delta_{k-1} - \Delta_{k-2}, \quad k = \overline{1, p},$$

with boundary conditions $\Delta_{-1} = 0,\ \Delta_0 = 1$. In the cases that are of interest, $|\nu| < 1$. Under this condition, this equation has the following solution:

$$\Delta_k = \frac{\sin(k+1)\theta}{\sin\theta}, \quad \theta = \arccos\nu.$$

Consider polynomial $P(\nu) = \det \mathbf{A}_n$. Expanding the determinant of the matrix on the first, and then on the last line, we obtain the expression of the desired polynomial:

$$P(\nu) = (2\nu + \alpha)(2\nu + \beta)\Delta_{p-2} - (4\nu + \alpha + \beta)\Delta_{p-3} + \Delta_{p-4}.$$

Taking into account the recurrence equation, the polynomial is simplified:

$$P(\nu) = \Delta_p + (\alpha + \beta)\Delta_{p-1} + \alpha\beta\Delta_{p-2}.$$

If we assume in this equation that $\nu = 1 - \lambda/2$, then $P(\nu) \equiv P(\lambda)$ is the characteristic polynomial of the matrix, and $P(\lambda) = 0$ is its characteristic equation. Let us consider several cases of parameter values.

1) $\alpha = -1$, $\beta = 1$. In this case,

$$P(\nu) = \Delta_p - \Delta_{p-2} = \frac{\sin(p+1)\theta - \sin(p-1)\theta}{\sin\theta} = 2\cos p\theta.$$

The characteristic equation has the form

$$\cos p\theta = 0.$$

By solving it, we obtain the eigenvalues of the matrix:

$$\lambda_j = 4\sin^2\frac{\pi + 2\pi j}{4p}, \quad j = \overline{0, p-1}.$$

2) $\alpha = -1$, $\beta = 0$. In this case, we obtain the following characteristic equation:

$$P(\nu) = \Delta_p - \Delta_{p-1} = \frac{\cos(p + 1/2)\theta}{\cos\theta/2} = 0.$$

By solving it, we obtain the eigenvalues of the matrix:

$$\lambda_j = \frac{4\sin^2(\pi + 2\pi j)}{2(2p+1)}, \quad j = \overline{0, p-1}.$$

3) $\alpha = 0,\ \beta = 0.$ In this case, $P(\nu) = \Delta_p = \frac{\sin(p+1)\theta}{\sin\theta}$. By solving it, we obtain the eigenvalues of the matrix:

$$\lambda_j = \frac{4\sin^2 \pi j}{2(p+1)}, \quad j = \overline{1, p}.$$

REFERENCES

1. H. Poincaré, Mémoire sur les courbes définies par une équation différentielle (I) Journal de mathématiques pures et appliquées 3e série, tome 7 (1881), p. 375-422.

2. Lyapunov A.M. General problem of motion stability. in V volumes. – M.-L.: GITTL, 1952. (in Russian)

3. Van der Pol B. Forced oscillation in circuit with non-linear resistance // Philos. Mag. Ser. 7. 1927. Vol. 3, N 13. P. 65–80.

4. Andronov A.A., Vitt A.A. To the mathematical theory of capture // Journal of Applied Physics. 1930. V. 7. Issue 4. P. 3–20. (in Russian)

5. Mandelstam L.I., Papaleksi N.D. On the phenomena of resonance of the n-th kind // Collection of works of L. I. Mandelstam. V. 2. – M.: AN SSSR, 1947. (in Russian)

6. Teodorchik K.F. To the theory of synchronization of self-oscillating relaxation systems // J. of Phys. 1945. V. 9, № 2. P. 139. (in Russian)

7. Teodorchik K.F., Khaikin S.E. Acoustic capture // ZhTF. 1932. V. 2. Issue 1. (in Russian)

8. Lyon W.V., Edgerton H.E. Transient torque-angle characteristics of synchronous machines // Transactions of the American IEE. 1930. Vol. 49, N 2. P. 689.

9. Goldstein L.D. On a complex effect on a self-oscillating system // Scientific and technical collection of the Leningrad Institute of Communica-

tions. 1934. Issue 15, № 4. (in Russian)

10. Andronov A.A., Vitt A.A. To the mathematical theory of self-oscillatory systems with two degrees of freedom // ZhTF. 1934. V. 4, № 1. P. 122–143. (in Russian)

11. Andronov, A.A., Vitt, A.A., and Khaikin, S.E. Theory of Oscillators. Dover Publications, New York, 1987.

12. Mayer A.G. Rough transformation of a circle // Uchenye zapiski GGU. 1939. Issue 12. P. 215–230. (in Russian)

13. Bautin N.N., Leontovich E.A., Methods and means for a qualitative investigation of dynamical systems on the plane, Moscow, 1990 (in Russian).

14. Neimark Yu.I., The method of point mappings in the theory of nonlinear oscillations, Moscow, 1972, (in Russian).

15. Butenin N.V., Neimark Yu.I., and Fufaev N.A., Introduction to the Theory of Nonlinear. Oscillations, Nauka, Moscow, 1976 (in Russian).

16. Krylov N.M., Bogolyubov N.N., Introduction to non-linear mechanics, Princeton Univ. Press, 1947, (translated from Russian).

17. Bogolyubov N.N., Mitropol'skiy Yu.A. Asymptotic methods in the theory of nonlinear oscillations. Gordon and Breach; Second Edition-Revised (January 1, 1961).

18. Mitropolsky Yu.A. and Lykova O.V., Integral Manifolds in Nonlinear Mechanics, Nauka, Moscow, 1973 (in Russian).

19. Hale J.K. Oscillations in nonlinear systems. – NewYork: McGrawHill, 1963.

20. Volosov V.M., Morgunov B.I., Averaging methods in the theory of non-linear oscillatory systems, Moscow, 1971 (in Russian).

21. Moiseev N.N. Asymptotic methods in nonlinear mechanics. – Moscow: Nauka, 1981. (in Russian)

22. Blekhman I.I. Synchronization of dynamical systems, Nauka, Moscow, 1971 (in Russian).

23. Blekhman I.I., Indeytsev D.A., Fradkov A.L. Slow motions in systems with inertial excitation of oscillations // Problems of mechanical engineering and machine reliability. 2008. № 1. P. 25–32. (in Russian)

24. Khokhlov R.V. To the theory of synchronization on untertons // Vestnik MGU. Ser. fiz-mat. i estestv. nauk. 1954. Issue 8, № 12. P. 33. (in Russian)

25. Utkin G.M. Mutual synchronization of generators at multiple frequencies // Radio Engineering and Electronics. 1957. V. 2, № 1. P. 44. (in Russian)

26. Landa P.S. Self-oscillations in systems with a finite number of degrees of freedom. / M.: Nauka, 1980. (in Russian)

27. Korolev V.I., Postnikov L.V. To the theory of synchronization of the generator of self-oscillations. Parts I, II // Izv. VUZov. Ser. Radiophysica.1969. V. 12. Issue 3. P. 406; Issue 11. P. 1710. (in Russian)

28. Migulin V.V., Medvedev V.I., Mustel E.R., Parygin V.N. Foundations of the oscillation theory / M.: Nauka, 1978. (in Russian)

29. Minakova I.I., Teodorchik K.F. To the theory of synchronization of self-oscillations of arbitrary shape // DAN SSSR. 1956. V. 106. Issue 4. P. 658. (in Russian)

30. Romanovskii, Yu.M., On the mutual synchronization of many auto-oscillatory systems coupled through a common medium // Izv. VUZov. Ser. Radiophysica 1972. V. 15, № 5. P. 718. (in Russian)

31. Dimentberg M.F. Nonlinear stochastic problems of mechanical vibrations // M.: Nauka, 1980. (in Russian)

32. L. Cesari, Asymptotic Behavior and Stability Problems in Ordinary Differential Equations / Springer-Verlag Berlin Heidelberg, 1971.

33. Levinson N. Small periodic perturbations of on autonomous system with a stable orbit // Annals of Math. 1950. Vol. 52, N 3.

34. Afraimovich V.S., Shilnikov L.P., Invariant tori, their breakdown and stochastisity // Amer. Math. Soc. Transl. 1991. Vol. 149. P. 201 - 211.

35. Afraimovich V.S., Shil'nikov L.P. Invariant tori, their breakdown and stochastisity // Amer. Math. Soc. Translations. 1991. Vol. 149. P. 201–211.

36. Results of Science and Technology. Modern problems of mathematics. Fundamental directions. T. 5 / Ed. R. V. Gamkrelidze, D. V. Anosov, V. I. Arnold., M.: VINITI, 1986. (in Russian)

37. Patent application № 62595 from 26.03.1930. Method for stabilizing the frequency of the generator / Terentyev B.P. (in Russian)

38. De Bellescize H. La Reseption Synchrone // Onde electr. 1932. Vol. 11. P. 230–240.

39. Tricomi F. Integratione di unequatione differentiable presentatasi in elecrotechnica // Annali della Roma Schuola Normale Superiore de Piza Scienza Physiche e Matematiche. 1933. Vol. 30. P. 1.

40. Travis C. Automatic frequency control // Proc. IRE. 1935. Vol. 23. P.

1125–1141.

41. Shakhgildyan V.V., Lyakhovkin A.A. Systems of phase-locked loop frequency / M.: Svyaz’, 1972. (in Russian)

42. V.N. Akimov, L.N. Belyustina, V.N. Belykh, et al., Phase synchronization systems, (Radio Svyaz', Moscow), 1982, (in Russian).

43. Lindsey W. C. Synchronization systems in communication control. – New Jersey: Prentice-Hall, Inc., EnglewoodCliffs, 1972.

44. Kapranov M.V., Kuleshov V.N., Utkin G.M. The theory of oscillations in radio engineering / M.: Nauka, 1984. (in Russian)

45. Likharev K.K., Introduction to the dynamics of Josephsonjunctions / M.: Nauka, 1985. (in Russian)

46. Barone A., Paterno G. Physics and Applications of the Josephson Effect. – NewYork: Wiley, 1982.

47. Magnus K., Schwingungen. – Stuttgart: Teubner, 1976.

48. Gorev A.A. Selected works on questions of the stability of electric systems, Moscow, Gosenergoizdat, 1960 (in Russian).

49. Korolev V.I., Fufaev N.A., and Chesnokova R.A., Correctness of approximate study of rotor vibration. in a synchronous machine, Applied Mathematics and Mechanics, 37, v.6, pp.1007-1014, 1973 (in Russian).

50. Kononenko V.O., Vibrating systems with a limited power supply, Iliffe Books, London, 1969.

51. Blekhman I.I., Vibrations in engineering, V.2. Vibrations of nonlinear mechanical systems, Moscow: Mashinostroenie, 1979 (in Russian).

52. Alifov A.A., Frolov K.V., Interaction of non-linear oscillatory systems

with energy sources, Taylor & Francis, 1990.

53. Dimentberg F.M. Bending vibrations of rotating shafts / M.: AN SSSR, 1959. (in Russian)

54. Filippov A.P., Vibrations of Deformable Systems, Mashinostroenie, Moscow, 1970 (in Russian).

55. Lurie A.I. Some nonlinear problems of the theory of automatic control / M.: Gostekhizdat, 1951. (in Russian)

56. Barbashin E.A., Krasovskii N.N. On stability of motion in general // Dokl. AN SSSR. 1952. V. 86, № 3. (in Russian)

57. Barbashin E.A. and Tabueva V.A., Dynamic Systems with a Cylindrical Phase Space, Nauka, Moscow (1969) (in Russian).

58. Popov V. M. Criterii de stabilitate pentru sistemele nonlineare de reglage automata bazata pe utilizarea transformanei Laplace // Studii si ceccetar tari de energetic. 1959. Vol. IX, N 1.

59. Leonov G.A. On the stability of phase systems // Sib. matem. zhurnal. 1974. № 3. (in Russian)

60. Gelig A. Kh., Leonov G. A., Yakubovich V. A. Stability of non-linear systems with a non-unique equilibrium / M.: Nauka, 1978. (in Russian)

61. Shakhgildyan V.V., Savvateev Yu.N. On the investigation of stability conditions for two-loop phase synchronization systems // Izv. VUZov. Ser. Radiophysics. 1971. V. 14, № 7. (in Russian)

62. Bakaev Yu.N. Synchronizing properties of the phase automatic frequency control of the third order // Radiotekhnika i Electronica.1965. V. 10, № 1. (in Russian)

63. Belykh V.N. and Nekorkin V.I., Qualitative study of a system of three

differential equations in the. theory of phase synchronization, Applied Mathematics and Mechanics, 39, No. 4, 642, 1975.

64. Belykh V.N. and Nekorkin V.I., On a qualitative study of a multidimensional phase system, Siberian Math. Journal. 1977. V. 18, № 4. (in Russian)

65. Afraimovich V.S., Nekorkin V.I., Osipov G.V., Shalfeev V.D., Stability, structures and chaos in nonlinear synchronization networks / Ed. A.V. Gaponov-Grekhov and M.I. Rabinovich. - Gorky: IPF Academy of Sciences of the USSR, 1989 (in Russian).

66. Belyustina L.N., Belykh V.N., Shalfeev V.D. On the capture in the PLL system under the action of additive harmonic noise // Theory of oscillations, applied mathematics and cybernetics. 1975. Issue. 1, pp. 94-101. (in Russian)

67. Yamada T., Fujisaka H. Stability theory of synchronized motion in coupled-oscillator systems // Prog. Theor. Phys. 1983. Vol. 70. P. 1240–1248.

68. Afraimovich V.S., Verichev N.N., Rabinovich M.I., Stochastic synchronization of oscillation in dissipative systems. Radiophysics and Quantum Electron 1986; 29: 795–803.

69. Dmitriev A.S., Panas A.I., Starkov S.O. Dynamic chaos as a paradigm of modern communication systems // Foreign Radioelectronics. Advances in Modern Radioelectronics, 1997, No. 10, pp.4-26 (in Russian)

70. Kocarev L., Halle K. S., Eckert K., Chua L., Parlitz U. Experimental demonstration of secure communication via chaotic synchronization // Int. J. Bifurcation and Chaos. 1992. Vol. 2, 3. P. 709.

71. Dedieu H., Kennedy M., Hasler M. Chaos shift keying: modulation and demodulation of a chaotic carrier using self-synchronizing Chua's circuits // IEEE Trans. Circuits and systems. 1993. Vol. CAS-40, N 10. P. 634.

72. Matrosov V.V. Dynamics of two parallel coupled phase-controlled generators with low-inertia control circuits // Izv. VUZov Applied Nonlinear Dynamics. 2006. V. 14, № 1. P. 25–37. (in Russian)

73. Freeman W. J. Tutorial on neurobiology: from single neurons to brain chaos // Int. J. Bifurcation and Chaos. 1992. Vol. 2. P. 451–482.

74. Babloyntz A., Destexhe A. Low-dimensional chaos in an instance of epilepsy // Proc. National Acad. Sci. USA. 1986. Vol. 83. P. 3513.

75. Abarbanel H.D., Rabinovich M.I., Selverston A., Bazhenov M.V., Huerta R., Sushchik M.M., Rubchinskii L.L. Synchronisation in neural networks, UFN, 166:4 (1996), 363–390; Phys. Usp., 39:4 (1996), 337–362.

76. Borisyuk G.N., Borisyuk R.M. Kazanovich Ya.B., Ivanitskii G.R. Models of neural dynamics in brain information processing – the developments of the decade // Phys. Usp. 45 1073–1095, 2002 (in Russian).

77. Hodgkin A. L., Huxley A. F. A quantitative description of membrane current and its application to conduction and excitation in nerve // J. Physiol. 1952. Vol. 183. P. 500.

78. Fitz Hugh R. Impulses and physiological states in theoretical model of nerve membrane // Biophys. J. 1961. Vol. 1. P. 445.

79. Kolmogorov A.N., Petrovsky I.E., Piskunov N.S. Study of the diffusion equation with a source of matter and its applications to biological

problems // Voprosy kibernetiki. 1975. Issue. 12, P. 3. (in Russian)

80. Pecora L. M., Carroll T. L. Synchronization in chaotic systems // Phys. Rev. Lett. 1990. Vol. 64. P. 821.

81. Rulkov N. F., Volkovskii A. R., Rodriguez-Lozano A. Del Rio E., Velarde M.G. Mutual synchronization of chaotic self-oscillations with dissipative coupling // Int. J. Bifurcation Chaos Appl. Sci. Eng. 1992. Vol. 2. P. 669–676.

82. Ashwin P., Buescu J., Stewart I. Bubbling of attractors and synchronization of chaotic oscillators // Phys. Lett. A. 1994. Vol. 193. P. 126.

83. Venkataramani S. C., Hunt B. R., Ott E., Gaunthier D. J., Bienfang J. S. Transitions to bubbling of chaotic systems // Phys. Rev. Lett. 1996. Vol. 77. P. 5361–5364.

84. Venkataramani S. C., Hunt B. R., Ott E. Bubbling transitions // Phys. Rev. E. 1996. Vol. 54. P. 1346–1360.

85. A. Pikovsky, M. Rosenblum, J. Kurths. Synchronization. Fundamental Nonlinear Phenomenon / Tekhnosfera, Moscow, 2003 (in Russian)

86. Anischenko V.S. Complex oscillations in simple systems / M.: Nauka, 1990. (in Russian)

87. Prigogine I. Non-equilibrium statistical mechanics / M.: Mir, 1964. (in Russian)

88. Prigogine I., Stengers I. Order from chaos. Man’s new dialogue with nature / Bantam New Age Books, 1984.

89. Quastler H. The emergence of biological organization / Yale University Press, 1964.

90. Evdokimov Yu. M. Spatially ordered forms of DNA and its complexes – the basis for creating nanostructures for medicine and biotechnology // Russian nanotechnologies. 2006. T. 1, No. 1/2. P. 256-264. (in Russian)

91. Suzdalev I.P. Nanotechnology: Physicochemistry of Nanoclusters, Nanostructures and Nanomaterials / Moscow: KomKniga, 2006. (in Russian)

92. Potapov A.A., Fractals in Radiophysics and Electromagnetic Detections / Logos, Moscow, 2002.

93. Kornev V.K., Borisenko I.V., Ovsyannikov G.A. High-frequency electromagnetic interactions in multielement Josephson structures // Radio engineering and electronics. 2001. No. 46. P. 1029-1048. (in Russian)

94. Josic K. Invariant manifolds and synchronization of coupled dynamical systems // Phys. Rev. Lett. 1998. Vol. 80. P. 3053–3056.

95. Kaneko K. Relevance of clustering to biological networks // Physica. D. 1994. Vol. 75. P. 55–73.

96. Kaneko K. Clustering, coding, switching, hierarchical ordering, and control in a network of chaotic elements // Physica. D. 1990. Vol. 41. P. 137–72.

97. Georgiou I. T., Bajaj A. K., Corless M. Invariant manifolds and chaotic vibrations in singularly perturbed nonlinear oscillators // Int. J. Eng. Sci. 1998. Vol. 36. P. 431–58.

98. Belykh V. N., Belykh I. V., Hasler M. Hierarchy and stability of partially synchronous oscillations of diffusively coupled dynamical systems // Phys. Rev. E. 2000. Vol. 62. P. 6332–6345.

99. Belykh V. N., Belykh I. V., Mosekilde E. Cluster synchronization

modes in an ensemble of coupled chaotic oscillators // Phys. Rev. E. 2001. Vol. 63. P. 036216.

100. Belykh V. N., Belykh I. V., Hasler M., Nevidin K. Cluster synchronization in three-dimensional lattices of diffusively coupled oscillators // Int. J. Bifurcation and Chaos. 2003. Vol. 13. P. 755–779.

101. Okuda K. Variety and generality of clustering in globally coupled oscillators // Physica. D. 1993. Vol. 63. P. 424–436.

102. Lorenz E. N. Deterministic nonperiodic flow // J. Atoms. Sci. 1963. Vol. 20. P. 130–141.

103. Afraimovich V.S., Bykov V.V., and Shilnikov L.P. On structurally stable attracting limit sets of Lorenz-attractor type, Trudy Mosk. Mat. Obshch, 46 (1983), 153–216; English transl Trans. Moscow Math. Soc, 2, 1983. (in Russian)

104. Rabinovich M.I., Stochastic self-oscillations and turbulence // Usp. 1978. V. 1 25. 1. P. 123-168. (in Russian)

105. F. Moon, Chaotic Oscillations / Wiley-Interscience, New York, 1987.

106. Kuznetsov S.P. Dynamic chaos / M.: Fizmatlit, 2001.

107. Strange Attractors / Ed. Ya. G. Sinai and L. P. Shilnikov. / M.: Mir, 1981. (in Russian)

108. H. Haken, Advanced Synergetics: Instability Hierarchies of Self-Organizing Systems and Devices (Springer Series in Synergetics) / Springer, 2012.

109. Feigenbaum M. Quantitative universally for a class of nonlinear transformations // J. Stat. Phys. 1978. Vol. 19. P. 25–52.

110. Chua L. O., Komuro M., Matsumoto T. The double scroll family // IEEE Transaction on Circuits & Systems. 1986. Vol. CAS-33, N 11. P. 1073–1118.

111. Special issue on Chua's circuit // J. of Circuit, Systems, and Computers. 1993. Vol. 3, N 2.

112. Pikovskii, A.S. and Rabinovich, M.I. Simple self-oscillator with stochastic behavior // Dokl. 1978. V. 239, No. 2. P. 301–304. (in Russian)

113. Dmitriev A.S., Kislov V.Ya. Stochastic oscillations in a delf-oscillator with a first-order inertial delay // Radio engineering and electronics. 1984. V. 29, No. 12, P. 2389-2398. (in Russian)

114. Anishchenko V.S., Astakhov V.V. Experimental study of the mechanism of occurrence and structure of a strange attractor in a generator with inertial nonlinearity // Radiotekhnika i Electronica. 1983. V. 28, No. 6. P. 1109-1115. (in Russian)

115. Batalova Z.S., Bezdenezhnykh A.N., Neimark Yu.I., and Romashova I.B., On bifurcations leading to chaotization of rotor motions // Dinamika Sistem. 1980. Issue. 19. P. 110-125. (in Russian)

116. Belyustina L.N. and Belykh V.N. On a non-autonomous phase system of equations with a small parameter, containing invariant tori and rough homoclinic curves // Izv. VUZov. Ser. Radiophysics. 1972. V. XV, No. 7, P. 1039-1049. (in Russian)

117. Morozov A. D. Quasi-conservative systems: cycles, resonances and chaos // World Sci. 1998.

118. Gerasimov S.I., Erofeev V.I., Soldatov I.N. Wave processes in continuous media / Sarov: RFNC-VNIIEF, 2012. (in Russian)

119. Yu.I. Neimark, The method of the averaging from the point of view of the method of point-to-point mappings // Izv. VUZov. Ser. Radiophysics. 1963. V. 6, No. 5. (in Russian)

120. Mel'nikov, V.K. Center stability under time-periodic perturbations // Tr. Moscow mat. society. 1963, V. 12, P. 3-52. (in Russian)

121. Belykh V. N., Pedersen N. F., Soerensen O. H. Shunted Josephson junction model // Phys. Rev. B. 1988. Vol. 16, N 11. P. 4853–4871.

122. Watson G. A Treatise on the Theory of Bessel Functions / Cambridge University Press, 1995.

123. Uglov A. Mechanical vibrations: measurement, effects and control. – N.-Y.: Nova Sci. Publishers, 2009. P. 59–175.

124. N. Verichev, S. Verichev, V. Erofeev, Chaos, Synchronization and Structures in Dynamics of Systems with Cylindrical Phase Space, Springer 2020.

125. Shilnikov L.P. Theory of bifurcations of dynamical systems with homoclinic Poincare curves // VII Int. Conf. for Nonlinear Oscillations. Bd. 12. – Berlin: Akad-Verlag, 1977.

126. Sharkovsky A. N., Maistrenko Yu. A., Romanenko E. Yu. Difference equations and their applications / Kiev: Naukova Dumka, 1986. (in Russian)

127. Danilov Yu. A. Lectures on nonlinear dynamics. An elementary introduction / M.: Postmarket, 2001. (in Russian)

128. Pontryagin, L.S. Asymptotic behavior of solutions of systems of differential equations with a small parameter at the highest derivatives // Izv.

Academy of Sciences of the USSR. Gray Mathematical. 1957. T. 21, No. 4. (in Russian)

129. Palis J., Pugh C. Fifty problems in dynamical systems // Lect. Notes Math. 1975. Vol. 468. P. 345–353.

130. Shilnikov L. P., Turaev D. V. A new simple bifurcation of a periodic orbit of blue sky catastrophe type. Methods of qualitative theory of differential equations and related topics // Amer. Math. Soc. Transl. II Ser. 200. AMS, Providence, RI, 165-188, 2000.

131. Medvedev V.S. On a new type of bifurcations on manifolds, Mat. Sat 1980. T. 113, No. 3. S. 487-492. (in Russian)

132. Homoclinic touches: Sat. articles / Ed. S. V. Gonchenko, L. P. Shilnikova / Izhevsk: NITs RHD, 2007. (in Russian)

133. Belykh V.N., Verichev N.N. Dynamics of a rotator coupled with an oscillator, Radiophysics and Quantum Electronics 31(8), 1988, p. 657.

134. Bolshakov, V.M., Zeldin, E.S., Mints, R.M., and Fufaev, N.A., On the dynamics of the “oscillator – rotator” system / Izv. VUZov. Ser. Radiophysics. 1965. V. 8, No. 2.

135. Verichev N.N., Verichev S.N., Erofeyev V.I. Chaotic Dynamics of Simple Vibrational Systems, International Journal of Sound and Vibration, 310, 755–767, 2008.

136. Pechenev, A.V., On the motion of an oscillatory system with limited excitation near resonance, Dokl. 1986. V. 290, No. 1. P. 27-31. (in Russian)

137. Blekhman I.I., Indeitsev D.A., Fradkov A.L. Slow motions in systems with inertial excitation of oscillations // Problems of mechanical engineer-

ing and reliability of machines. 2008. No. 1. S. 25-42. (in Russian)

138. Levitsky N.I., The theory of mechanisms and machines / M.: Nauka, 1979 (in Russian)

139. Belykh V.N., Verichev N.N. On dynamics of coupled rotators. Izv. Vuzov Radiofizika, 1988, V.XXXI, N.6, P.688-697 (in Russian).

140. Belykh V.N., Verichev N.N. On the complex dynamics of an autonomous system with Josephson junctions // Radiotekhnika i Elektronika. 1987. Vol. 31, No. 1. P. 140 -147 (in Russian)

141. Shilnikov L.P., Shilnikov A.L., Turaev D.V. et al. Methods of qualitative theory in nonlinear dynamics. Part 1. / Izhevsk, NITs RHD, 2004. (in Russian)

142. Shilnikov L.P., Shilnikov A.L., Turaev D.V., Chua L., et al. Methods of qualitative theory in nonlinear dynamics. Part 2. / Izhevsk, NITs RHD, 2009. (in Russian)

143. Ito A. Successive Subharmonic Bifurcations and Chaos in a Nonlinear Mathieu Equation // Progress Theor. Phys. 1979. Vol. 61. P. 815.

144. Izrailev F. M., Rubinovich V. I., Ugodnikov A. D. Approximate description of three-dimensional dissipative systems with stochastic behaviour // Phys. Lett. 1981. Vol. 68A. P. 321.

145. Afraimovich, V.S., Rabinovich, M.I., and Ugodnikov, A.D., On The Birth OF A Strange Attractor In Ssystems Close To Hamiltonian Ones // Izv. VUZov. Ser. Radiophysics. 1984. T. 27, No. 10, P. 1346. (in Russian)

146. Ashwin P., Buescu J., Stewart I. Bubbling of attractors and synchronisation of chaotic oscillators // Phys. Lett. A. 1994. Vol. 193. P. 126.

147. Heagy J. F., Carroll T. L., Pecora L. M. Desynchronization by periodic orbits, // Phys. Rev. E. 1995. Vol. 52. P. 1253.

148. Gerasimov S.I., Erofeev V.I., Problems of the Wave Dynamics of Structures / Sarov: RFNC-VNIIEF, 2016. (in Russian)

149. Rulkov N. F., Afraimovich V. S., Lewis C. T., Chazottes J.-R., Cordonet A. Multi-valued in generalized chaos synchronization // Phys. Rev. E. 2001. Vol. 64. P. 016217.

150. Verichev N. N., Maksimov A. G. Synchronization of stochastic oscillations of parametrically excited nonlinear oscillators // Radiophys. and Quantum Electronics. 1989. Vol. 32, N 8. P. 713–716.

151. Rulkov N. F., Suschik M. M., Tsimring L. S., Abarbanel H. D. Generalized synchronization of chaos in directionally coupled chaotic systems // Phys. Rev. E. 1995. Vol. 51. P. 980.

152. Abarbanel H. D., Rulkov N. F., Suschik M. M. Generalized synchronization of chaos: The auxiliary system approach // Phys. Rev. E. 1996. Vol. 53. P. 4528.

153. Kocarev L., Parlitz U. Generalized synchronization, predictability, and equivalence of unidirectionally coupled dynamical systems // Phys. Rev. Lett. 1996. Vol. 76. P. 1816.

154. Rosenblum M. G., Pikovsky A. S., Kurths J. Phase synchronization of chaotic oscillators // Ibid. P. 1804.

155. Rosenblum M. G., Pikovsky A. S., Kurths J. From Phase to Lag Synchronization in Coupled Chaotic Oscillators // Phys. Rev. Lett. 1997. Vol. 78. P. 4193.

156. Alexander J. C., Yorke J. A., You Z., Kan I. Riddled basins // Int. J.

Bifurcation Chaos Appl. Sci. Eng. 1992. Vol. 2. P. 795.

157. Alexander J. C., Hant B. R., Kan I., Yorke J. A. Intermingled basins for the triangle map // Ergod. Th. Dyn. Syst. 1996. Vol. 16. P. 651.

158. Lai Y.-C., Grebogi C. Riddling Bifurcation in Chaotic Dynamical Systems // Phys. Rev. Lett. 1996. Vol. 77. P. 5047.

159. Lai Y.-C., Andrade V. Catastrophic bifurcation from riddled to fractal basins // Phys. Rev. E. 2001. Vol. 64. P. 056228.

160. Yu L., Ott E., Chen Q. // Physica. D. 1992. Vol. 53. P. 102.

161. Platt N., Spiegel E. A., Tresser C. On-off intermittency: A mechanism for bursting // Phys. Rev. Lett. 1993. Vol. 70. P. 279.

162. Lai Y.-C., Grebogi C. Intermingled basins and two-state on-off intermittency // Phys. Rev. E. 1995. Vol. 52. P. 3313.

163. Pliss V.A., Integral sets of periodic systems of differential equations / M.: Nauka, 1997. (in Russian)

164. Belykh I. V., Verichev N. N. Global synchronization of the regular and chaotic self oscillatory coupled systems with superconducting junctions // Proc. of the 5th Int. Specialist Workshop Nonlinear Dynamics of Electronic Systems. – Moscow, 1997. P. 145–149.

165. Anischenko V. Dynamical chaos: models and experiments: appearance and structure of chaos in simple dynamical systems // World Scientific on Nonlinear Science. Series A. 1995. Vol. 8.

166. Verichev N.N., Verichev S.N., Asymptotic theory of synchronization of chaotic oscillations of dissipatively coupled dynamic systems // N.E. Bauman Vestnik MGTU. Ser. Natural Sciences. 2007. No. 4. P. 77–97. (in Russian)

167. Verichev N. N., Verichev S. N., Wiercigroch M. Asymptotic theory of synchronization for dissipative-coupled dynamical systems // Chaos, Solitons & Fractals. 2009. Vol. 41, Issue 2. P. 752–763.

168. Verichev N. N. On a theory of stochastic synchronization of dissipative dynamic systems // Proc. of the Int. conf. dedicated to the 100th anniversary of A. A. Andronov “Progress in nonlinear science”. Vol. III. Nonlinear oscillations control and information. – Nizhniy Novgorod, 2002. P. 317–321.

169. Verichev S.N. and Verichev N.N., To the theory of stochastic synchronization // Proceedings of V International. conf. “Nonlinear vibrations of mechanical systems”. N. Novgorod, 1999. P. 45. (in Russian)

170. Van Dyck M. Album of fluid motion. / Parabolic Press, Inc., 1982.

171. Verichev N.N. Stability of structures in nonequilibrium systems // Computational mechanics of continuous media. V. 6(1). P. 23 - 33. 2013 (in Russian).

172. Verichev N. N., Verichev S. N., Wiercigroch M. C-oscillators and stability of stationary cluster structures in lattices of diffusively coupled oscillators // Chaos, Solitons and Fractals. 2009. Vol. 42, Issue 2. P. 686–701.

173. Lancaster P. Theory of Matrices / Academic Press, 1969.

174. Gantmacher F.R. The Theory of Matrices / Chelsea Pub. Co., 1960.

175. Belykh I.V., Verichev N.N. Global synchronization and strange attractors in coupled pendulum systems. Bulletin NNGU “Nonlinear dynamics and chaos”, 1997, V.2, P. 93 – 102 (in Russian).

176. Vasiliev V., Romanovsky Yu., Yakhno V. Autowave processes / M.:

Nauka, 1987. (in Russian)

177. Belykh V.N., Verichev N.N. Spatially homogeneous autowave processes in systems with transport and diffusion, Izv. universities. Ser. Radiophysics. 1996. Vol. 39, No. 5. P. 588-596 (in Russian).

178. Kolmogorov A.N., Petrovsky I.G., Piskunov N.S. // Problems of Cybernetics. 1975. Issue. 12, P. 3. (in Russian)

179. Tikhonov A.N., Samarskiy A.A. Equations of mathematical physics / M.: Nauka, 1977. (in Russian)

180. Belykh V. N., Verichev N. N., Kocarev L. J., Chua L. O. On chaotic synchronization in a linear array of Chua's circuits // J. of Circuits, Systems, and Computers. 1993. Vol. 3, N 2. P. 579–589.

181. Verichev N.N., Verichev S.N., Erofeev V.I. Cluster dynamics of a homogeneous chain of dissipatively coupled rotators // Applied Mathematics and Mechanics. 2008. T. 72, No. 6. P. 882 - 897.

182. Belykh V.N., Belykh I.V., Verichev N.N. Regular and chaotic spatially-homogeneous oscillations in a chain of coupled superconductive junctions. Izv. Vuzov Radiofizika, 1997, V.15, N7, P.912 – 924 (in Russian).

183. Afraimovich V.S., Rabinovich M.I., Sbitnev V.I. Attractor dimensions in the coupled generator chain // Letters in ZhTF. 1985. T. 6. P. 338 (in Russian).

184. Aranson I.S., Gaponov-Grekhov A.V., Rabinovich M.I. Starobinets I.M. Strange attractors and the spatial development of turbulence in flow systems // ZhETF. 1986. 90. P. 1707 (in Russian).

185. Anishchenko V.S., Aranson I.S., Postnov D.E., Rabinovich M.I. Spa-

tial synchronization and chaos developement bifurcations in a chain of coupled self-sustained oscillators // DAN SSSR. 1986. Vol. 286, No. 5. P. 628 (in Russian).

186. Aranson I.S. and Verichev N.N. Dynamics of quasiperiodic excitations in unidirectional chains of generators. // Izv. VUZov -Radiofizika, V. 31(1), P. 29-40, 1988 (in Russian).

187. Demidovich B.P. Lectures on the mathematical theory of stability / M.: Nauka, 1967. (in Russian)

188. Lifshits E.M., Pitaevsky L.P. Physical kinetics / M.: Nauka, 1979. (in Russian)

189. Gaponov-Grekhov A.V., Rabinovich M.I., Starobinets I.M. Dynamic model of the spatial development of turbulence // Letters to ZhTF. 1984. P. 39. P. 561 (in Russian).

190. Verichev N. N. C-oscillators and new outlook on cluster dynamics // J. of Phys. Conf. Ser. 2005. Vol. 23. P. 23–46.

191. Verichev N. N., Verichev S. N., Wiercigroch M. Physical interpretation and theory of existence of cluster structures in lattices of dynamical systems // Chaos, Solutions and Fractals. 2007. Vol. 34, Issue 4. P. 1082–1104.

192. Verichev N.N. Physics, existence and fusion of cluster structures of coupled dynamical systems // Nonlinear World. 2009. V. 7, No. 1. P. 28 – 45 (in Russian).

193. Potapov A.A., Gilmutdinov A.H., Ushakov P.A. Fractional-order radio-elements and radio-systems – Radiotechnika, 2009–200 p. (in Russian).

194. Vonsovski S.V. Modern scientific picture of the world / Publishing House of the RHD, 2006 (in Russian).

195. Osipov G.V., Sushchik M.M. Synchronized clusters and multistability in arrays of oscillators with different natural frequencies // Phys. Rev. E. 1998. Vol. 58. P. 7198.

196. Kanakov O.I, Osipov G.V., Chan C.-K., Kurths J. Cluster synchronization and spatio-temporal dynamics in networks of oscillatory and excitable Luo-Rudy cells // Chaos. 2007. Vol. 17. P. 015111.

197. Pecora L.M., Carroll T.L. Synchronization in chaotic systems // Phys. Rev. Lett. 1990. Vol. 64. P. 821.

198. Pecora L.M., Carroll T.L. Master Stability Functions for Synchronized Coupled Systems // Phys. Rev. Lett. 1998. Vol. 80. P. 2109–2112.

199. Rabinovich M.I., Trubetzkov D.I. Introduction in theory of oscillations and waves. Nauka, Moscow, 1984 (in Russian).

200. Mosekilde E., Maistrenko Y., Postnov D. Chaotic synchronization: applications to living systems. – Singapore: World Scientific, 2002.

201. Wang W., Kiss I.Z., Hudson J.L. Experiments on arrays of globally coupled chaotic electrochemical oscillators: Synchronization and clustering // Chaos. 2000. Vol. 10. P. 248.

202. Roy R., Thornburg K.S. Synchronization of chaotic lasers // Phys. Rev. Lett. 1994. Vol. 72. P. 2009.

203. Cuomo K.M., Oppenheim A.V. Circuit Implementation of Synchronized Chaos with Applications to Communications // Phys. Rev. Lett. 1993. Vol. 71. P. 65.

204. Verichev N.N., Verichev S.N., Erofeev V.I. C-oscillators in a homo-

geneous ring of diffusive-coupled dynamical systems: existence, stability, and fusion of cluster structures // Nonlinear World. 2008. V. 6, No. 56. P. 398 – 423 (in Russian).

205. Afraimovich V. S., Chow S.N., Hale J. K. Synchronization in lattices of coupled oscillators // Physica. D. 1997. Vol. 103, N 1–4. P. 442–451.

206. Chiu C.H., Lin W.W., Wang C.S. Synchronization in a lattice of coupled Van der Pol systems // Int. J. of Bifurcation and Chaos. 1998. Vol. 8, Issue 12. P. 2353–2373.

207. Liang Zhao, Aparecido F. Breve. Chaotic synchronization in 2D lattice for scene segmentation // Neurocomputing. 2008. Vol. 71, Issue 13–15. P. 2761–2771.

208. Hirokazu Fukuda, Hikaru Nagano, Shoichi Kai. Stochastic synchronization in two-dimensional coupled lattice oscillators in the Belousov-Zhabotinsky reaction // J. or the Japan Phys. Soc. 2003. Vol. 72. P. 487–490.

209. Moss F., Pierson D., O'Gorman D. Stochastic resonance: Tutorial and update // Int. J. Bifurcation Chaos. 1994. Vol. 4. P. 1383.

210. Guderian A., Dechert G., Zeyer K.P., Schneider F. W. Stochastic Resonance and time advance coding in chemical reactions // J. Phys. Chem. 1996. Vol. 100. P. 4437.

211. Kádár S., Wang J., Showalter K. Noise-supported travelling waves in sub-excitable media // Nature. 1998. Vol. 391. P. 770.

212. Collins J.J., Imhoff T.T. and Crigg P. Noise-enhanced tactile sensation // Nature. 1996. Vol. 383. P. 770.

213. Neiman A. B., Russell D. F., Pei X. et al. Stochastic synchronization

of electroreceptors in paddlefish // Int. J. Bifurcation Chaos. 2000. Vol. 10. P. 2499.

214. Shafranovsky I.I. Symmetry in nature / L.: Nedra, 1985. (in Russian)

215. Amritkar R. E., Jalan S., Hu C. K. Synchronized clusters in coupled networks. II. Stability analysis // Nonlinear oscillation. 2004. Vol. 5, N 3. P. 326–337.

216. Woochang Lim, Sang-Yoon Kimy. On the occurrence of partial synchronization in unidirectional coupled maps // J. of the Korean Phys. Soc. 2005. Vol. 46, N 3. P. 638–641.

217. Yanchuk S., Maistrenko Yu., Mosekilde E. Synchronization and Clustering in Ensembles of Coupled Chaotic Oscillators // Chaos. 2003. Vol. 13. P. 388.

218. Maistrenko Yu., Popovych O., Hasler M. On strong and weak chaotic partial synchronization // Int. J. Bifurcation Chaos Appl. Sci. Eng. 2000. Vol. 10. P.179.

219. Zing Y., Hu G., Cerdera H. A. et al. // Phys. Rev. E. 2001. Vol. 63. P. 026211.

220. Fujimoto K., Kaneko K. Noise-induced input dependence in a convective unstable dynamical system // Physica. D. 1999. Vol. 129. P. 203–222.

221. Kaneko K., Yomo T. Isologues diversification for Robust Development of Cell Society // J. Theor. Biol. 1999. Vol. 199. P. 243–256.

222. Pikovsky A., Rosenblum M., Kurths J. Synchronization. A universal concept in nonlinear sciences // Cambridge Nonlinear Sci. Series. 2001. Vol. 12.

223. Markov A.A. Selected Works / M.: Gostekhizdat, 1948. (in Russian)

224. Bylov F., Vinograd R.E., Grobman D.M. The theory of Lyapunov exponents and its applications to stability problems / Moscow: Nauka, 1966 (in Russian).

225. Myshkis A.D. Mathematics. Special courses / Moscow: Nauka, 1971 (in Russian).

About the Authors

Nikolai Verichev

Principal Researcher at Mechanical Engineering Research Institute of the Russian Academy of Sciences. Graduated from Nizhny Novgorod State University in 1975 (MSc in Radio Enfineering). Got his PhD Degree in Nizhny Novgorod State University (1985). Specializes in the field of the qualitative theory of dynamical systems, oscillation theory, nonlinear dynamics, dynamic chaos, and chaotic synchronization. He has discovered the effect of chaotic synchronization of non-identical systems (1985). Author/co-author of 44 papers, 4 books and 2 patents.

Email: nverichev@yandex.ru

Stanislav Verichev

Senior Researcher at Delft University of Technology, the Netherlands. Graduated from Nizhny Novgorod State University in 1998 (MSc in Physics). Got his PhD Degree in TU Delft (2002). Specializes in Nonlinear Dynamics as well as such practical fields as Dredging and Mining, Oil & Gas, Civil and Mechanical Engi-

neering, and Deep Sea Mining. Author/co-author of 36 papers, 5 books and 8 patents.

Email: s.verichev@mail.ru

Vadimir Erofeev

Profrssor, Director of Mechanical Engineering Research Institute of the Russian Academy of Sciences. Got his PhD/Dr. Habil. degrees in Nizhny Novgorod State University (1986, 1994). He has proposed new methods of non-destructive testing of materials and structures. Developed scientific foundations of vibration protection systems for machines and structures using inertia and dissipation of rheological media. Performed a series of studies on the chaotic dynamics of mechanical systems with energy sources of limited power, as well as on the existence and stability of stationary cluster structures in homogeneous chains of dissipative coupled rotators. Email: erof.vi@yandex.ru